# Direct-Interaction Approximation

## Principles and Applications

by

**Susumu GOTO**

DOCTOR OF PHILOSOPHY

Department of Fusion Science,
School of Mathematical and Physical Science,
The Graduate University for Advanced Studies

1998 (School Year)

# Abstract

It has been phenomenologically shown and widely supported by experiments that statistical properties in small scales of turbulence of incompressible fluids exhibit some universality irrespective of the kinds of fluids, boundary condition and the Reynolds number. On the other hand, this system is believed to be governed by the Navier-Stokes equations which consist of the equations of motion and of continuity. However, relationships between these equations and phenomenologies on statistical properties of small-scale motions have not been clearly understood primarily because such a statistical theory is hard to construct due to the nonlinearity of the basic equations. Since the nonlinearity causes an infinite hierarchy of moments, we never obtain a closed set of equations for a finite number of statistical quantities without any assumptions. This is the so-called closure problem in the statistical theory of turbulence. We adopt the direct-interaction approximation (DIA), which was originally proposed by Kraichnan (1959), to attack and solve the closure problem.

The DIA is an excellent approximation in the sense that the nonlinearity is never neglected and no adjustable parameter is introduced in the formulation. Unfortunately, however, it is known that a closed set of equations obtained by a naive application of DIA (Kraichnan 1959) to the Navier-Stokes system is inconsistent with experimental observation. Especially, it is $E(k) \propto k^{-3/2}$ that the closure equations predict as the energy spectrum $E(k)$ in the inertial range, where the $k^{-5/3}$ power law is observed by many experiments. This inconsistency implies incompleteness of the application of DIA to the Navier-Stokes system. Although Kraichnan (1965) improved the application method of DIA and succeeded in deriving the $k^{-5/3}$ power law, the formulations are too complicated to be justified. Moreover, in spite of its long history and important role in the field of the statistical theory of turbulence, the essence of DIA may have been misunderstood by many researchers. This is due to the fact that validity conditions and applicability of DIA were not clear.

We introduce a model equation, consisting of quadratic nonlinear and linear dissipative terms, which is simpler than the Navier-Stokes equation but still possesses its important mathematical structures. Then, it is shown that DIA is valid for such a system that has weak nonlinear couplings and large numbers of degrees of freedom even if nonlinearity of the system is strong (i.e., the nonlinear terms are larger than the linear ones in magnitude). Furthermore, we clarify similarities and differences between DIA and a Reynolds-number expansion so-called RRE (Reynolds-number reversed expansion). For some known systems, including the Navier-Stokes system and the present model, these two approximations yield an identical set of equations for the correlation and the response functions. Owing to this fact, these two approximations have sometimes been identified erroneously. It must be stressed, however, that DIA and RRE are based upon completely different ideas and work-

ing assumptions. Hence, we should distinguish these two theories. This is reasonable because the validity conditions of DIA depend on the strength of nonlinear couplings and the number of degrees of freedom, but not on the Reynolds number, while the validity of RRE depends crucially on magnitude of the Reynolds number.

We further investigate the validity condition of DIA and the relationships between DIA and RRE from a viewpoint of the strength of nonlinear couplings by extending the model equation. It is then shown that DIA is valid for systems such that the average number of direct interactions between a pair of modes is much smaller than the square root of the number of degrees of freedom, and that RRE may be regarded as an approximation under which the nonlinear terms are replaced by a joint-Gaussian random variables. The last approximation, called normal nonlinear term approximation, has the same validity conditions as DIA.

Small-scale motions of turbulence may be statistically homogeneous, and the number of degrees of freedom of this system increases in proportion to the 9/4 power of the Reynolds number. Hence, small-scale motions of turbulent fields at high Reynolds number satisfy the two validity conditions of DIA, i.e., weakness of nonlinear couplings and largeness of the degrees of freedom. This implies that DIA is applicable to this system. As mentioned above, however, when we apply DIA to the Eulerian velocity correlation function and the Eulerian velocity response function (Kraichnan 1959), we encounter the difficulty that the resultant closure equations are incompatible with experiments. Here, we instead apply DIA to the Lagrangian velocity correlation function and the Lagrangian response function with the help of the position function (Kaneda 1981), which is a map between the Eulerian and the Lagrangian fields. The resultant equations yield not only the well-known $k^{-5/3}$ power law predicted phenomenologically by Kolmogorov (1941) of the energy spectrum, but also the functional form in the entire universal range, which excellently agrees with experimental data.

We next apply DIA to passive scalar fields (temperature, particle concentration, smoke, and so on) advected by turbulence without affecting fluid motions. Then it is systematically shown that solutions to the resultant closure equations by DIA for the Lagrangian correlation and the response functions for the velocity and the passive scalar fields are completely consistent with the phenomenologies on the scalar spectrum by Obukhov (1949) and Corrsin (1951) in the inertial-advective range, Batchelor, Howells & Townsend (1959) in the inertial-diffusive range, and Batchelor (1959) in the viscous-advective range.

# Contents

# Chapter 1

# Introduction

## 1.1 Universality of turbulence

Let us start with Fig.1.1 which shows the well-known characteristics of incompressible fluid turbulence: Universality of statistics of small-scale structures.

In this figure, experimental data of the one-dimensional longitudinal energy spectrum $E_{\|}(k)$ defined by

$$E_{\|}(k) = \frac{1}{2\pi} \int \mathrm{d}r \, V_{\|}(r) \, \exp\Big[ -\mathrm{i}kr \Big] \tag{1.1}$$

with

$$V_{\|}(r) = \overline{u_1(\boldsymbol{x} + \boldsymbol{e}_1 r) \, u_1(\boldsymbol{x})} \tag{1.2}$$

in various kinds of turbulence are collected and shown by symbols. Here, $u_i(\boldsymbol{x}, t)$ is the $i(= 1, 2, 3)$ component of fluid velocity vector measured at position $\boldsymbol{x}$ at time $t$, $\boldsymbol{e}_i$ is the unit vector parallel to $i$ axis, $k$ is the wavenumber, and an overbar denotes an average. Such a remarkable coincidence in the large-wavenumber (small-scale) range of the spectrum from different data has been brought about by normalization of $k$ by the Kolmogorov wavenumber,

$$k_{\mathrm{K}} = \eta^{-1} = (\epsilon/\nu^3)^{1/4} \tag{1.3}$$

and of $E_{\|}$ by $(\epsilon\nu^5)^{1/4}$, where $\epsilon$ and $\nu$ are the mean rate of the energy dissipation per unit mass and the kinematic viscosity of fluid, respectively. It is these unique combinations of $\epsilon$ and $\nu$, i.e., $(\epsilon/\nu^3)^{1/4}$ and $(\epsilon\nu^5)^{1/4}$, that yield the dimensions of the wavenumber $[L^{-1}]$ and the energy spectrum $[L^3T^{-2}]$ because $\epsilon$ and $\nu$ have the dimensions of $[L^2T^{-3}]$ and $[L^2T^{-1}]$, respectively.

Both the idea of universality of small-scale fluctuations and the dimensional analysis in terms of $\epsilon$ and $\nu$ constitute the basis of the Kolmogorov theory [1]. He introduced a local spatiotemporal coordinate and a relative velocity field, and defined a notion of locally homogeneous isotropic turbulence, which is much wider than the notion of isotropic turbulence by Taylor [2, 3] (see also §1.5). Here,

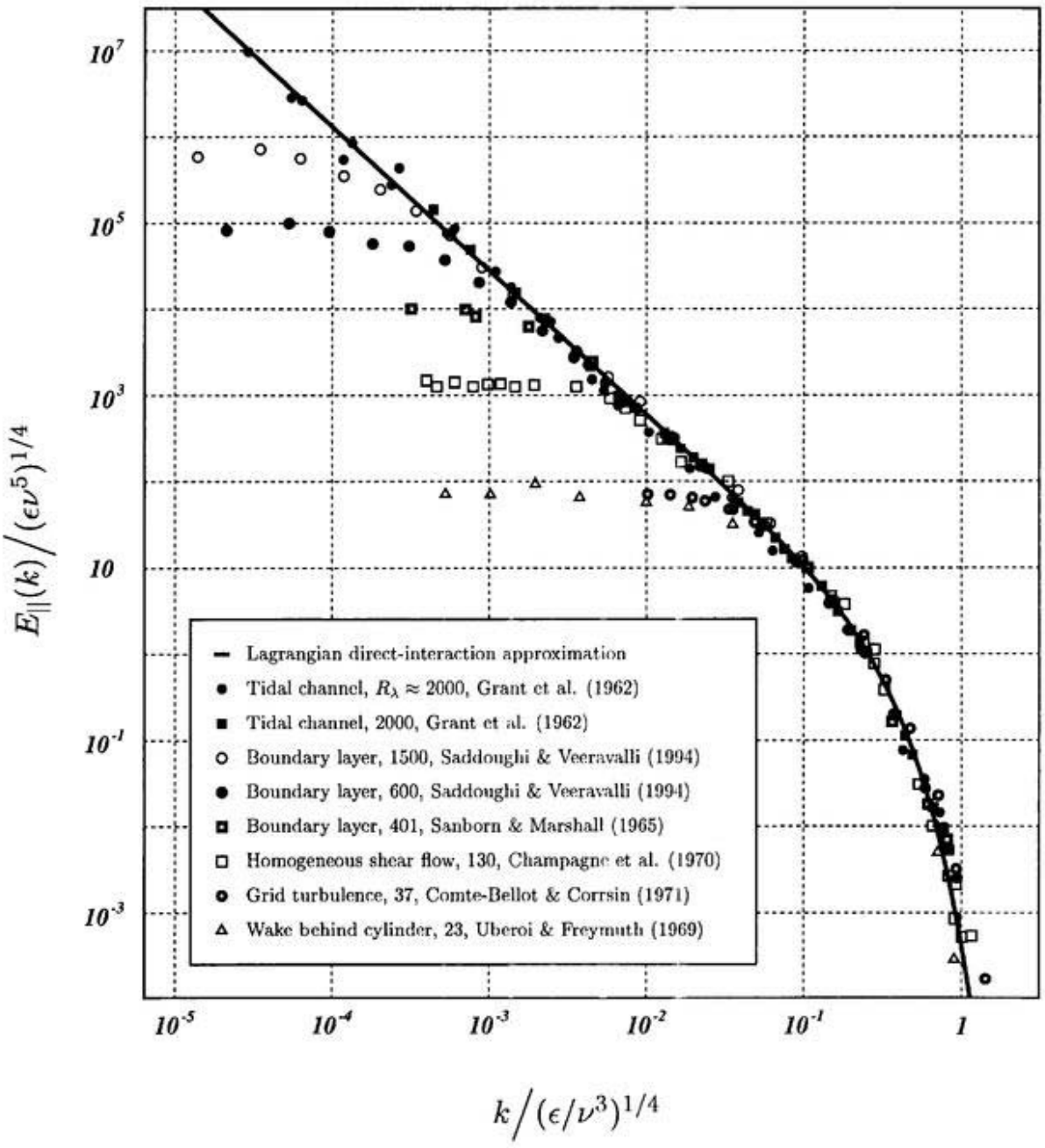


FIGURE 1.1 One-dimensional longitudinal energy spectrum defined by (1.1) in the universal range of statistically stationary turbulence. Symbols denote experimental data for various kinds of turbulence (taken from Chapman 1979, Grant et al. 1962 and Saddoughi & Veeravalli 1994). $R_\lambda$ is the Taylor microscale Reynolds number defined by (1.24).

the words homogeneity and isotropy are used in a statistical sense. In other words, even if a flow field is not globally statistically isotropic by the boundary condition or some other reasons, the field may be locally isotropic in small (precisely, much smaller than the integral scale (1.20)) domains far from the boundaries, when the Reynolds number, defined by (1.13), is sufficiently large. He then suggested a similarity hypothesis that the joint-probability distribution function of relative velocities in the local coordinate is uniquely determined by $\epsilon$ and $\nu$, if the system is locally homogeneous and isotropic. This is the first similarity hypothesis by Kolmogorov, and is the basis of the dimensional analysis. Incidentally, he further suggested, as the second hypothesis, that for length scale larger than the viscous scale $\eta$ (the Kolmogorov scale) the joint-probability distribution function is free from the viscosity $\nu$, and is determined only by $\epsilon$. This Kolmogorov second hypothesis yields the well-known $k^{-5/3}$ power law of the energy spectrum in the inertial range, i.e., over the length scales between the integral and the viscous scales (see §3.1.1).

We should refer, in passing, to a widely accepted understanding of the Kolmogorov theory by the use of the notion of the energy cascade to smaller scales. Energy inputed by large-scale motions is transfered down to small scales, and during this process information of the large-scale structure may be lost, and then the small-scale motions acquire a universality. However, it has been reported that the energy transfer between different scales is caused by strong non-local interactions (see e.g. Ref. [4] and also §3.4.4). This may call the above simple argument of the energy cascade into question. There does not seem to any definite reasons why turbulence has the universality in small scales. Notice that the energy dissipation rate $\epsilon$, which is employed in the dimensional analysis, is also equal to the energy input rate and to the energy flux in the energy cascading range of statistically stationary turbulence.

Throughout this thesis, we assume that the fluid motion is governed by the Navier-Stokes equation,

$$\frac{\partial}{\partial t} u_i(\boldsymbol{x},t) + u_j(\boldsymbol{x},t) \frac{\partial}{\partial x_j} u_i(\boldsymbol{x},t) = -\frac{1}{\rho} \frac{\partial}{\partial x_i} p(\boldsymbol{x},t) + \nu \frac{\partial^2}{\partial x_j \partial x_j} u_i(\boldsymbol{x},t) \quad (i=1,2,3) \tag{1.4}$$

and the equation of continuity,

$$\frac{\partial}{\partial x_i} u_i(\boldsymbol{x},t) = 0\,, \tag{1.5}$$

where $\rho$ is the (uniform) density and $p(\boldsymbol{x},t)$ is the pressure. Repeated subscripts are summed up over 1—3. Once we assume that the governing equation is common irrespective of the kind of flows, the validness of the universality of small-scale fluctuations may be trivial. We emphasize, however, that it is never easy to reveal the relationships between the universality of the small-scale motion and the basic equations (1.4) and (1.5) because of their nonlinearity. In the next section, we describe this problem.

## 1.2 Statistical theory — closure problem

It has been a common sense that the problem on turbulence is one of the most difficult unsolved scientific issues in the classical mechanics. A main difficulty seems to arise from its strong nonlinearity. In general, this property yields chaotic motion, which is one of the most typical characteristics

of turbulence, and makes the analysis of the system difficult. However, it is not necessarily disadvantageous because the randomness may permit us to treat the system statistically. In other words, one may describe the properties of the field in terms of the distribution function in a six dimensional phase space instead of the detailed spatiotemporal information of the field with an enormous number of degrees of freedom. Indeed, Hopf [5] succeeded in obtaining a functional integro-differential equation which describes the temporal evolution of the probability distribution of the velocity field. This contains complete information of the statistics of homogeneous isotropic turbulence. However, this functional equation is too difficult to solve. In this situation we are tempted to deal only with the lower order moments of the distribution function such as the mean velocity or the two-point velocity correlation function, which are usually more important than the higher order moments. By taking an average of the basic equation, we derive easily the governing equation for the mean velocity, which depends on second-order moments of the velocity field (or the Reynolds stress). Similarly, third-order moments generally appear in the evolution equation for the two-point velocity correlation function. These terms of higher-order correlation functions originate from the nonlinearity of the Navier-Stokes equation, and this hierarchy of moments continues infinitely. Hence, we have to impose some assumptions to obtain a closed set of equations for finite number of statistical quantities. This is the so-called closure problem in the statistical theory of turbulence. Although numerous studies for this problem have been proposed by many researchers, none of them seem to be successful. The quasi-normal approximation (QNA) [6–8], for example, is based upon the experimental evidence that the probability density function of the velocity is nearly Gaussian. Thanks to the mathematical property that even-order moments of joint-Gaussian random variables are expressed in terms of only its second-order moments, we obtain a closed set of equations for second-order correlation function of velocity field in the frame of QNA. However, this approximation leads to an unphysical result such as the negative energy spectrum [9]. Although a Markovianization [10,11] can avoid this realizability problem, it predicts $k^{-2}$ power law of the energy spectrum in the inertial range, which is inconsistent with both the Kolmogorov theory and observations. The eddy-dumped quasi-normal Markovian (EDQNM) theory proposed by Orszag [12] successfully predicts the $k^{-5/3}$ power law of the energy spectrum. However, EDQNM has a free parameter which cannot be determined in the framework of the theory itself, and which are adjusted for a better agreement with observations.

## 1.3 Weakness of the nonlinear couplings

As stated above, it is challenging to attack the closure problem in the statistical theory of turbulence. In the following, we restrict ourselves to homogeneous turbulence. As shown below, homogeneous turbulence possesses an important property: Weakness of the nonlinear couplings. This will serve as a small parameter, based upon which we shall develop a closure theory.

In order to make the analysis easier, we consider, first, the motion of a fluid confined in a periodic cube of side $L$, and later we shall take the limit $L \to \infty$. These procedures may be justified for small-scale motions of turbulence at very large Reynolds number. Thus, we expand the velocity field $u_i$ into the Fourier series as

$$u_i(\boldsymbol{x},t) = \left(\frac{2\pi}{L}\right)^3 \sum_{\boldsymbol{k}} \tilde{u}_i(\boldsymbol{k},t)\, \exp\Big[\, \mathrm{i}\boldsymbol{k}\cdot\boldsymbol{x}\,\Big], \tag{1.6}$$

where

$$\sum_{\boldsymbol{k}} = \sum_{n_1=-\infty}^{\infty} \sum_{n_2=-\infty}^{\infty} \sum_{n_3=-\infty}^{\infty} \tag{1.7}$$

with

$$\boldsymbol{k} = \frac{2\pi}{L}(n_1, n_2, n_3) \qquad (n_1, n_2, n_3 = 0, \pm 1, \pm 2, \cdots), \tag{1.8}$$

and rewrite (1.4) in terms of the Fourier components as

$$\left[\frac{\partial}{\partial t} + \nu k^2\right] \tilde{u}_i(\boldsymbol{k}, t) = -\frac{\mathrm{i}}{2}\left(\frac{2\pi}{L}\right)^3 \tilde{P}_{ijm}(\boldsymbol{k}) \sum_{\boldsymbol{p}} \sum_{\boldsymbol{q}} \tilde{u}_j(-\boldsymbol{p}, t)\, \tilde{u}_m(-\boldsymbol{q}, t)\,. \tag{1.9}$$
$$(\boldsymbol{k}+\boldsymbol{p}+\boldsymbol{q}=\boldsymbol{o})$$

Here, $k = |\boldsymbol{k}|$ and

$$\tilde{P}_{ijm}(\boldsymbol{k}) = k_m \tilde{P}_{ij}(\boldsymbol{k}) + k_j \tilde{P}_{im}(\boldsymbol{k}) \quad \text{and} \quad \tilde{P}_{ij}(\boldsymbol{k}) = \delta_{ij} - \frac{k_i k_j}{k^2}\,. \tag{1.10}$$

In the derivation of (1.9) we have used the incompressible condition $k_i \tilde{u}_i(\boldsymbol{k}) = 0$, which is equivalent to (1.5).

The right-hand side of (1.9) is composed of a summation of many products of Fourier modes. We choose arbitrarily a triplet of Fourier modes $\tilde{u}_i(\boldsymbol{k}_1)$, $\tilde{u}_i(\boldsymbol{k}_2)$ and $\tilde{u}_i(\boldsymbol{k}_3)$ $(\boldsymbol{k}_1 + \boldsymbol{k}_2 + \boldsymbol{k}_3 = \boldsymbol{o})$. Then, $\tilde{u}_i(\boldsymbol{k}_2)$ appears on the right-hand side of the governing equation (1.9) for $\boldsymbol{k}_1$ as a term,

$$-\mathrm{i}\left(\frac{2\pi}{L}\right)^3 \tilde{P}_{ijm}(\boldsymbol{k}_1)\, \tilde{u}_j(-\boldsymbol{k}_2, t)\, \tilde{u}_m(-\boldsymbol{k}_3, t)\,. \tag{1.11}$$

On the other hand, $\tilde{u}_i(\boldsymbol{k}_1)$ appears in the equation for $\tilde{u}_i(\boldsymbol{k}_2)$ as

$$-\mathrm{i}\left(\frac{2\pi}{L}\right)^3 \tilde{P}_{ijm}(\boldsymbol{k}_2)\, \tilde{u}_j(-\boldsymbol{k}_1, t)\, \tilde{u}_m(-\boldsymbol{k}_3, t)\,. \tag{1.12}$$

We call these nonlinear interactions, which explicitly show up in the governing equation, the direct interactions between $\tilde{u}_i(\boldsymbol{k}_1)$ and $\tilde{u}_i(\boldsymbol{k}_2)$ through $\tilde{u}_i(\boldsymbol{k}_3)$. Of course, these two modes nonlinearly interact with each other by a series of direct interactions between other modes, which is called the indirect interaction.

It must be emphasized that the condition of the summation on the right-hand side of (1.9) such that $\boldsymbol{k} + \boldsymbol{p} + \boldsymbol{q} = \boldsymbol{o}$ permits only a single direct interaction between any pair of Fourier modes; for example, as seen above, $\tilde{u}_i(\boldsymbol{k}_1)$ and $\tilde{u}_i(\boldsymbol{k}_2)$ interact only through $\tilde{u}_i(-\boldsymbol{k}_1 - \boldsymbol{p}_2)$. Incidentally, the number of direct interactions between a pair of modes in an $N$-mode quadratic nonlinear system is $O(N)$ in general. In this sense, the nonlinear couplings of the Navier-Stokes system (1.9) are quite weak even if the nonlinearity (ratio in magnitude of the nonlinear to the linear terms) is very strong.

## 1.4 Purpose of this thesis

The main purpose of this thesis is to reveal the relationships between the phenomenologies on small-scale statistics of turbulence and the basic equations. In other words, we aim at solving the closure

problem in the statistical theory of turbulence. It is the weakness of the nonlinear couplings of the Navier-Stokes system that is a key to attack this problem. Notice that phenomenologies such as Kolmogorov's can predict the existence of universality of statistical quantities, but not the functional forms (e.g. a solid line in Fig.1.1). On the other hand, the statistical theory based upon the basic equations should be able to make quantitative estimations of the universal forms. Therefore, an introduction of adjustable parameters reduces the value of the closure theory.

## 1.5 Fundamental quantities

Before moving on to the main task, we define here some fundamental quantities such as the Reynolds number. For saving space, we give a minimum amount of descriptions. For further details, see textbooks by Lamb [13] and Batchelor [14] for fundamentals of fluid mechanics, and by Batchelor [15], Rotta [16], Tennekes & Lumly [17], Leslie [18], Moin & Yaglom [19], McComb [20], Frisch [21], Lesieur [22] and so on for fluid turbulence.

Let $u_m$ and $L$ be the characteristic velocity and length scale, respectively. It is easy to show that the Navier-Stokes equation non-dimensionalized by $u_m$ and $L$ has only a non-dimensional parameter, the Reynolds number, defined by

$$Re = \frac{u_m L}{\nu} . \tag{1.13}$$

For isotropic turbulence (see below) the characteristic velocity $u_m$ is defined by

$$u_m^2 = \tfrac{1}{3}\,\overline{u_i(\boldsymbol{x})\,u_i(\boldsymbol{x})} \tag{1.14}$$

and the characteristic length scale is defined by (1.20). The Reynolds number represents the ratio between the magnitudes of the nonlinear and the linear terms, i.e., the strength of nonlinearity.

If the statistical quantities are independent of the absolute position, the system is called to be statistically homogeneous. For example, the two-point velocity correlation function defined by $V_{ij} = \overline{u_i(\boldsymbol{x},t)\,u_j(\boldsymbol{x}',t)}$ in a statistically homogeneous field depends only on the difference between the position vector $\boldsymbol{r} = \boldsymbol{x} - \boldsymbol{x}'$, and is expressed as

$$V_{ij}(\boldsymbol{r},t) = \overline{u_i(\boldsymbol{x},t)\,u_j(\boldsymbol{x}+\boldsymbol{r},t)} . \tag{1.15}$$

Furthermore, if statistical quantities of a system have rotational symmetry, we call that the system is statistically isotropic. The general form of an isotropic second-order tensor depending on a vector $\boldsymbol{r}$ is expressed as

$$V_{ij}(\boldsymbol{r},t) = \mathcal{A}(r,t)\,r_i r_j + \mathcal{B}(r,t)\,\delta_{ij} + \mathcal{C}(r,t)\,\epsilon_{ijk}\,r_k \tag{1.16}$$

(see e.g. Ref. [15]). If the system has a reflectional symmetry, the scalar $C$ vanishes. In the following, we use the word isotropic for those systems that have both rotational and reflectional symmetries. Therefore, in the statistically homogeneous isotropic field, $V_{ij}$ can be expressed in general in terms of only two scalar functions. Furthermore, if the velocity field is incompressible, then

$$\frac{\partial}{\partial r_i} V_{ij}(\boldsymbol{r},t) = \frac{\partial}{\partial r_j} V_{ij}(\boldsymbol{r},t) = 0 , \tag{1.17}$$

and $V_{ij}$ is expressed in terms of a scalar function $f(r)$ as

$$V_{ij}(\boldsymbol{r},t) = u_m^2 \left[ -\frac{\partial}{\partial r} f(r,t)\, \frac{r_i r_j}{2r} + \left[ f(r,t) + \frac{r}{2}\, \frac{\partial}{\partial r}\, f(r,t) \right] \delta_{ij} \right]. \tag{1.18}$$

Here, $f(r)$ is the longitudinal velocity correlation function defined by

$$u_m^2\, f(r,t) = \overline{u_1(\boldsymbol{x},t)\, u_1(r\boldsymbol{e}_1 + \boldsymbol{x},t)}\,. \tag{1.19}$$

Notice again that the two-point velocity correlation tensor in statistically homogeneous isotropic turbulence can be expressed by only one scalar function. This simplicity encourages us to attack the statistical theory of the system.

One of the most important statistical properties of turbulence is that there exist a few number of characteristic length scales. For example, there are only two characteristic length scales in the statistics of the incompressible turbulent velocity field. They are $L$ and $\eta$, which characterize the large and the small scale motions, respectively. Note that, as will be seen below, the ratio of $L$ to $\eta$ increases with the Reynolds number (see (1.26)). By the use of the longitudinal velocity correlation function (1.19), we can define the characteristic macroscale $L$ by

$$L = \int_0^\infty \mathrm{d}r\, f(r)\,, \tag{1.20}$$

which is sometimes called the integral scale. On the other hand, we often use the characteristic microscale defined by

$$\lambda = \left[ -\frac{\mathrm{d}^2}{\mathrm{d}r^2}\, f(r) \bigg|_{r=0} \right]^{-1/2}. \tag{1.21}$$

which is called the Taylor microscale. The ratio of $L$ to $\lambda$ increases with the Reynolds number as

$$\frac{L}{\lambda} \sim Re^{1/2}\,. \tag{1.22}$$

However, this microscale $\lambda$ is not appropriate to characterize the small-scale motion of turbulence. We should use the Kolmogorov length scale $\eta$ defined by (1.3) instead of $\lambda$. The ratio of $\eta$ to $\lambda$ is a function of the Reynolds number as

$$\frac{\lambda}{\eta} \sim Re^{1/4}\,. \tag{1.23}$$

The Kolmogorov $\eta$ is a scale at which the eddy turnover time and the viscous dissipation time scale are comparable, while the Taylor microscale has no such mathematical or physical meanings. Actually no characteristic features are seen at the microscale $\lambda$ in Fig.1.1, in which the wavenumber is normalized by the Kolmogorov wavenumber $k_\mathrm{K} = \eta^{-1}$. However, experimentalists prefer to the Reynolds number defined in terms of the Taylor microscale $\lambda$, which is easy to measure,

$$R_\lambda = \frac{u_m \lambda}{\nu}\,. \tag{1.24}$$

It is useful to remember that this Taylor microscale Reynolds number is expressed by the Reynolds number defined by (1.13) as

$$R_\lambda \sim Re^{1/2}\,. \tag{1.25}$$

Finally, let us consider the number of degrees of freedom of turbulence. Since the ratio of the macro and the micro scales is expressed by the Reynolds number as

$$\frac{L}{\eta} \sim Re^{3/4}, \tag{1.26}$$

the number of degrees of freedom $N$ of active components of motion may be estimated as

$$N \sim \left(\frac{L}{\eta}\right)^3 \sim Re^{9/4} \tag{1.27}$$

in a three dimensional flow. Note that (1.27) gives an upper bound of the number of degrees of freedom. Since small-scale structures in turbulence are known to be very localized, we may express turbulent field in terms of smaller number of components than $N$ by employing a more appropriate expansion instead of the Fourier. Although some attempts (e.g. Ref. [23]) to determine the actual number of degrees of freedom of turbulence by the use of notion of attractor in the phase space have been made, this problem is still open.

# Chapter 2

# Direct-Interaction Approximation

We introduce the direct-interaction approximation, which was originally proposed by Kraichnan [24], by the use of a model equation which is simpler than the Navier-Stokes equation but still retains its important properties. We show that this approximation is applicable for a system with a large number of degrees of freedom, clarify similarities and differences between this approximation and a so-called Reynolds-number reversed expansion [25], and point out importance of the strength of the nonlinear couplings.

## 2.1 Introduction

Although numerous attempts have been made on the closure problem (§1.2), little attention is paid to the important property of the Navier-Stokes equation (1.9) for homogeneous turbulence, that is, the weakness of the nonlinear couplings (§1.3). The direct-interaction approximation (DIA), which was originally introduced by Kraichnan [24], is a unique approximation which is founded on this property. Unfortunately, however, we encounter an additional problem in the choice of statistical variables (whether the Eulerian or the Lagrangian quantities), when we apply it to the Navier-Stokes turbulence. This additional problem will be considered in the next chapter. We focus here in this chapter to understanding of the essence and the applicability of DIA. It should be emphasized that in spite of its long history no systematic studies have ever been made to clarify the applicability of DIA.

Before moving on to the main task, it may be desirable to review that a closed set of integro-differential equations derived by DIA (called Eulerian DIA equations in this thesis) are also obtained by different kinds of approximations. For example, they are rederived by diagrammatic techniques developed by Wyld [26] and Martin et al. [27], and also by a method described in Leslie's textbook [18] as an explanation of DIA, which is a Reynolds-number expansion followed by a formal replacement of variables. This last method was justified in Ref. [25] by a kind of systematic expansion, which we

call here the Reynolds-number reversed expansion (RRE). This fact that the Eulerian DIA equations are derived by several methods has brought us some confusion. Especially, many researchers tend to regard mistakenly DIA as an approximation for low Reynolds number turbulence because RRE leads to the Eulerian DIA equations, and because RRE obviously works for small Reynolds numbers. In this chapter, in order to clarify this confusion we consider similarities and differences between DIA and RRE, and show that they have different parameter regions of applicability.

We shall introduce a model equation to explain DIA for understanding of its essence in detail. A large number of studies using model equations have already been made for this purpose. Among others, the random coupling model [28–30] and the spherical model [31,32] may be the most famous ones. These are known as such systems for which the DIA equations are exact in some limits. These models are, however, constructed as a coupling of the Navier-Stokes equations, and the physical meanings of couplings of equations are obscure. A model we deal with in this chapter is a dynamical system which is much simpler than the Navier-Stokes equation but still retains important ingredients of the latter. This model equation is a single equation for $N$ variables, and consists of quadratic-nonlinear, linear-viscous and random-forcing terms. It is the same as the ones introduced by Betchov [33] and Orszag [12] to explain the notion of DIA except that they do not have viscous and forcing terms. Incidentally, as long as the author knows, the article by Betchov [33] is one of the best explanations on DIA.

This chapter [1] is organized as follows. Our model equation is introduced by paying attention to the weakness of nonlinear couplings [2] of the Navier-Stokes equation and solved numerically as an initial value problem in §2.2 (an example of the concrete construction method of the model system is given in Appendix A). Then, DIA and RRE are formulated in §§2.3 and 2.4, respectively. Validity of all working assumptions introduced in DIA is confirmed numerically in §2.5. Section 2.6 is for the concluding remarks of this chapter.

## 2.2 Model equation

### 2.2.1 Model equation with weak nonlinear couplings

By noting the property of the nonlinear couplings of the Navier-Stokes equation (1.9) described in §1.3, we introduce a nonlinear model equation which is similar to (1.9). Let $X_i$ ( $i = 1, 2, \cdots, N$) be scalar real variables which correspond to the Fourier components $\tilde{\boldsymbol{u}}(\boldsymbol{k})$ in the Navier-Stokes system. Here, the subscript $i$ may be understood to represent the wavenumber $\boldsymbol{k}$, the three axial components,

[1] This chapter is based upon Ref. [34].

[2] We shall deal with the case of stronger nonlinear couplings in Chapter 5.

and the real and the imaginary parts of $\tilde{\boldsymbol{u}}(\boldsymbol{k})$. These real variables $X_i$ are governed by

$$\frac{\mathrm{d}}{\mathrm{d}t} X_i(t) = \sum_j \sum_k C_{ijk}\, X_j(t)\, X_k(t) - \nu_i\, X_i(t) + F_i(t) \qquad (i = 1, 2, \cdots, N)\,, \tag{2.1}$$

where $\sum_i$ stands for $\sum_{i=1}^{N}$. (The summation convention for repeated subscripts is not used throughout this chapter.) The coefficient, $\nu_i$, of the linear term is a positive constant, which is an analogue of the viscous effect in the Fourier representation of the Navier-Stokes equation. It can be assumed, without loss of generality, that the time-independent coefficients, $C_{ijk}$, of the quadratic-nonlinear terms should be symmetric with respect to the second and the third subscripts, i.e.,

$$C_{ijk} = C_{ikj} \qquad (i, j, k = 1, 2, \cdots, N)\,. \tag{2.2}$$

We further assume that

$$C_{ijk} + C_{jki} + C_{kij} = 0 \qquad (i, j, k = 1, 2, \cdots, N) \tag{2.3}$$

so that the sum of the energy of three modes $\frac{1}{2}(X_i^2 + X_j^2 + X_k^2)$ may be conserved through the direct interaction between them. This property of detailed balance of energy is analogous to the Navier-Stokes system, and guarantees the conservation of the total energy of the system $\mathcal{E} = \frac{1}{2}\sum_i X_i^2$ when the viscosity $\nu_i$ (and therefore $F_i$, see (2.4) below) vanishes. There is still an arbitrariness in the choice of the numerical values of the coefficients with the above properties. Here, notice that model equation (2.1) can be equivalent to a forced Navier-Stokes equation (1.9) if coefficients $C_{ijk}$ and $\nu_i$ are appropriately chosen. In the following we restrict ourselves to a much simpler system that

[1] $C_{ijk}$ satisfies conditions (2.2) and (2.3),

[2] the system is, for simplicity, symmetric with respect to $i$ (not only $\nu_i = \nu$ but also $C_{ijk}$ is homogeneous),

[3] the system have no self-interactions (i.e., $C_{ijk} = 0$ if $i = j$, $j = k$ or $k = i$),

[4] there is only a single, at the most, direct interaction between each pair of modes $\{X_i\}$.

A way of construction of the coefficients $C_{ijk}$ satisfying the above three properties is described in Appendix A. We emphasize the importance of the last property (weak nonlinear couplings). Figure 2.1 is drawn for an explanation on the direct interactions in the Navier-Stokes equation and this model. As discussed in §1.3, there is a unique direct interaction between each pair of Fourier modes, i.e., a property of the so-called triad interaction in the Navier-Stokes equation. The last condition [4] of the coefficient is reminiscent of it. This property of weakness of nonlinear couplings is essential in the formulation of DIA (see §2.3.1 and Chapter 5).

The inhomogeneous term $F_i(t)$ is a random driving force. It is piecewise constant in each time interval $\Delta t$, which is set to be equal to the time increment of the numerical simulations, and the amplitude obeys a Gaussian distribution of zero mean and of variance given by

$$\sigma^2 = \frac{2\,\nu}{N\,\Delta t}\,. \tag{2.4}$$

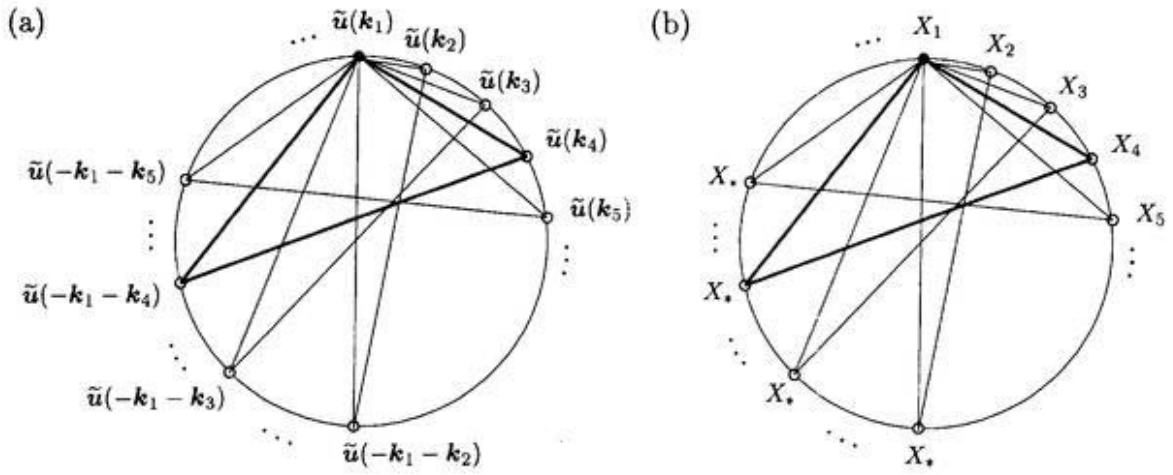


FIGURE 2.1 (a) Direct interactions between $\tilde{u}(k_1)$ and other modes in the Navier-Stokes equation (1.9). The direct interactions are expressed by triangles made by three points, which correspond to Fourier modes, placed on a circle drawn for the sake of convenience. As discussed in §1.3, there is a unique direct interaction between $\tilde{u}(k_1)$ and $\tilde{u}(k_4)$, for example. through $\tilde{u}(-k_1-k_4)$. This property is valid between an arbitrary pair of the Fourier modes. In other words, (1.9) is a dynamical system with weak nonlinear couplings. (b) Direct interactions between $X_1$ and other modes in the model equation (2.1) with the conditions ([1]—[4] in §2.2.1). This system is similar to (a) in the sense of weakness of the nonlinear couplings. The coefficients $C_{ijk}$ is constructed so that there is only a single direct interaction, at the most, between each pair of modes $\{X_i\}$.

The forcing at different time intervals or of different modes are assumed to be statistically independent of each other. Variance (2.4) has been chosen so that the averaged total energy be a half of unity,

$$\overline{\mathcal{E}} = \frac{1}{2}\sum_i \overline{X_i^2} = \frac{1}{2} \tag{2.5}$$

in the statistically stationary state [3]. The overbar stands for an ensemble average (or a long-term average in a single run of simulation).

### 2.2.2 Direct numerical simulation

Before developing formulation of closure equations, it may be useful to see the statistical property of model equation (2.1) by solving it numerically as the initial value problem.

The initial values of $X_i$ are given by random numbers under the constraint that $\sum_i X_i^2 = 1$. The fourth-order Runge-Kutta scheme is employed for the time integration. There are two control parameters which characterize the present system, that is, the degrees of freedom $N$ and the viscosity $\nu$. In

[3] By taking an ensemble average of equation (2.1) multiplied by $X_i$ and summed up over $1 \le i \le N$, we obtain the energy equation as

$$\nu \sum_i \overline{X_i^2} = \sum_i \overline{F_i X_i} = \frac{N}{2}\sigma^2 \Delta t\,,$$

in a statistically stationary state.

order to examine the dependence of the statistics of the system on these parameters we perform two series of simulations; $(N,\nu) = (7,100),(7,10),(7,1),(7,0)$ and $(N,\nu) = (7,0),(10,0),(20,0),(40,0)$. In the first series we examine the viscosity dependence, while in the second the dependence on the numbers of degrees of freedom. The time increment $\Delta t$ is taken as $5\times10^{-3}$, $2\times10^{-3}$, $10^{-3}$ and $10^{-4}$ for $N = 7$, 10, 20 and 40, respectively.

### 2.2.3 Correlation function

The two-time two-mode correlation function,

$$V_{in}(t,t') = \overline{X_i(t)\,X_n(t')} \qquad (t \geq t') \tag{2.6}$$

is one of the representative statistical quantities which characterize the dynamical system (2.1). The governing equations for it are derived from (2.1) as

$$\left[\frac{\partial}{\partial t} + \nu\right] V_{in}(t,t') = \sum_j \sum_k C_{ijk}\,\overline{X_j(t)\,X_k(t)\,X_n(t')} \qquad (t > t') \tag{2.7}$$

and

$$\left[\frac{\mathrm{d}}{\mathrm{d}t} + 2\nu\right] V_{in}(t,t) = \sum_j \sum_k C_{ijk}\,\overline{X_j(t)\,X_k(t)\,X_n(t)} + \overline{F_i(t)\,X_n(t)} + \ (i \leftrightarrow n)\,. \tag{2.8}$$

These equations cannot be solved because of the appearance of a higher-order (third-order) correlation function which originates from the nonlinearity of (2.1). This is the well-known closure problem. As closure theories to solve it, we consider DIA in §3 and RRE in §4.

For a later comparison with the statistical theories we show here the the auto-correlation function ($i = n$) obtained by the numerical simulations described in the preceding subsection. The viscosity dependence of the auto-correlation function is depicted in Fig.2.2(a) in which those for $\nu = 0$, 1, 10 and 100 are compared in the case of $N = 7$. The time is normalized by the viscous time-scale $1/\nu$ in Fig.2.2(b) (see (2.7)). We see that the characteristic time-scale of the velocity auto-correlation function changes in proportion to the viscous time for $\nu \gg 1$.

In Fig.2.3(a) we show the dependence on the number of degrees of freedom of the auto-correlation function, where those for $N = 7$, 10, 20 and 40 are compared in the inviscid case. The decaying time-scale of the function decreases as $N$ increases. The time is normalized by times-scale $\sqrt{N/c_1}$ of the nonlinear term in Fig.2.3(b) (see a paragraph below (2.76)).

## 2.3 Direct-interaction approximation

In this section we shall explain DIA by the use of the model equation (2.1). It should be emphasized again that the formulation for the model equation is essentially the same as one for the Navier-Stokes equation. It may be more understandable and useful for readers to see first the formulation for the simpler system.

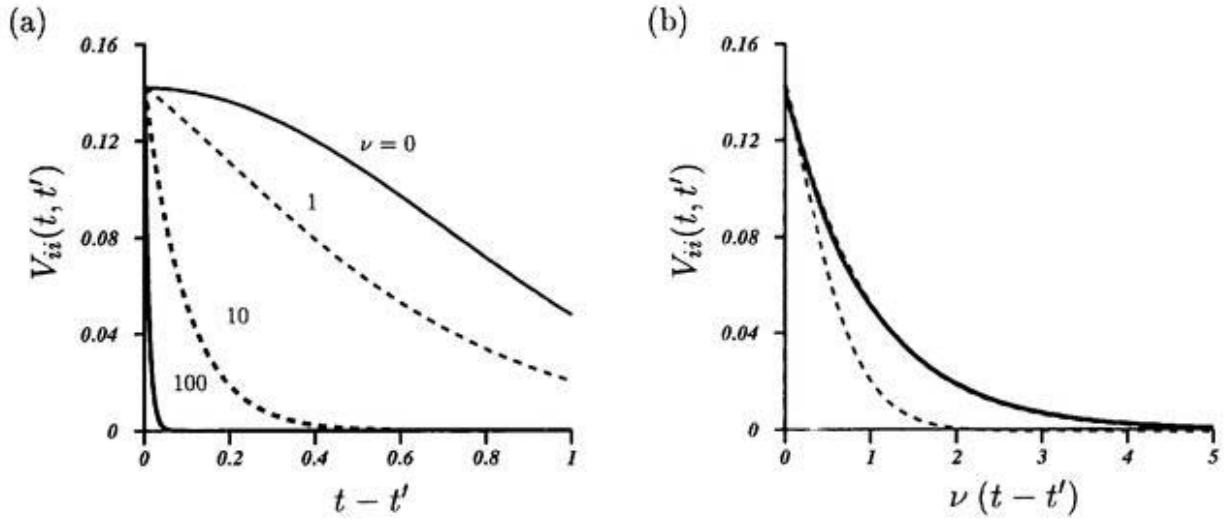


FIGURE 2.2 (a) Auto-correlation functions $V_{ii}(t,t') = \overline{X_i(t)X_i(t')}$ for $N = 7$ and $\nu = 0$ (thin solid line), 1 (thin broken line), 10 (thick broken line) and 100 (thick solid line). (b) Same as (a) but for a rescaled time.

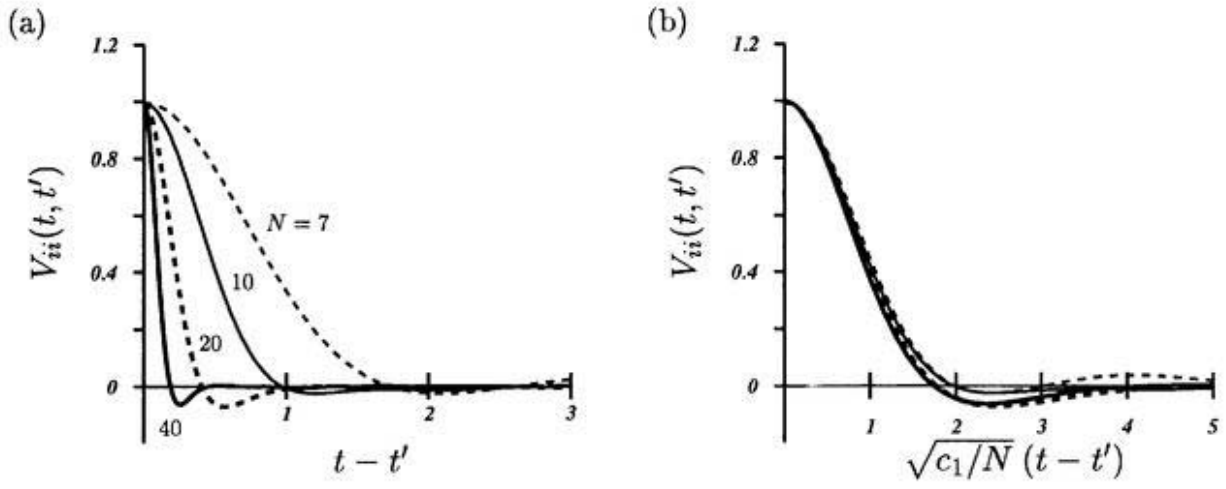


FIGURE 2.3 (a) Auto-correlation functions normalized by $V_{ii}(t,t)$ for $\nu = 0$. The degrees of freedom $N = 7$ (thin broken line), 10 (thin solid line), 20 (thick broken line) and 40 (thick solid line). (b) Same as (a) but for a rescaled time (see (2.74) for the definition of $c_1$).

First, for later use, we introduce a response function of $X_i$

$$G_{in}(t|t') = \frac{\delta X_i(t)}{\delta X_n(t')} \qquad (t \geq t') \,, \tag{2.9}$$

where $\delta$ stands for a functional derivative. The evolution equation of $G_{in}$ is derived from (2.1), by taking a functional derivative with respect to $X_n(t')$, as

$$\frac{\partial}{\partial t} G_{in}(t|t') = \sum_j \sum_k 2\, C_{ijk}\, X_j(t)\, G_{kn}(t|t') - \nu\, G_{in}(t|t') \qquad (t > t') \,. \tag{2.10}$$

The boundary condition is given by

$$G_{in}(t|t) = \delta_{in} \,, \tag{2.11}$$

where $\delta_{in}$ denotes Kronecker's delta. In the following we derive a closed set of equations for $V_{in}$ and $\overline{G}_{in}$ by the use of DIA from basic equation (2.1) and its products (2.7), (2.8), (2.10) and (2.11).

### 2.3.1 Direct-interaction decomposition

The DIA is formulated on the basis of the direct-interaction decomposition [24,35], in which the true field $X_i$ is decomposed into two fields, an NDI (Non-Direct-Interaction) field $X^{(0)}_{i/i_0j_0k_0}$ and a deviation field $X^{(1)}_{i/i_0j_0k_0}$, as

$$X_i(t) = X^{(0)}_{i/i_0j_0k_0}(t|t_0) + X^{(1)}_{i/i_0j_0k_0}(t|t_0) \quad (t \geq t_0) \,. \tag{2.12}$$

Here, $X^{(0)}_{i/i_0j_0k_0}(t|t_0)$ $(t \geq t_0)$ is defined as a fictitious field without the direct interaction between three particular modes $X_{i_0}$, $X_{j_0}$ and $X_{k_0}$, and $t_0$ denotes the time when the interaction is removed, i.e.,

$$X^{(0)}_{i/i_0j_0k_0}(t_0|t_0) = X_i(t_0) \qquad \text{and} \qquad X^{(1)}_{i/i_0j_0k_0}(t_0|t_0) = 0 \,. \tag{2.13}$$

For simplicity of notations, the argument $t_0$ in $X^{(0)}_{i/i_0j_0k_0}$ and $X^{(1)}_{i/i_0j_0k_0}$ will be omitted below. It should be noted that there is no direct interaction between the three modes $X^{(0)}_{i_0/i_0j_0k_0}$, $X^{(0)}_{j_0/i_0j_0k_0}$ and $X^{(0)}_{k_0/i_0j_0k_0}$ (see Fig.2.4). This property is originated from the the weakness of the nonlinear couplings of the system.

It follows from the definition that the NDI field obeys

$$\frac{\mathrm{d}}{\mathrm{d}t} X^{(0)}_{i/i_0j_0k_0}(t) = \sum_{\substack{j \\ \{i,j,k\} \neq \{i_0,j_0,k_0\}}} \sum_k C_{ijk}\, X^{(0)}_{j/i_0j_0k_0}(t)\, X^{(0)}_{k/i_0j_0k_0}(t) - \nu\, X^{(0)}_{i/i_0j_0k_0}(t) + F_i(t) \,. \tag{2.14}$$

Subtraction of the above equation from (2.1) leads to the equation for the deviation field as

$$\begin{aligned} \frac{\mathrm{d}}{\mathrm{d}t} X^{(1)}_{i/i_0j_0k_0}(t) = & \sum_{\substack{j \\ \{i,j,k\} \neq \{i_0,j_0,k_0\}}} \sum_k 2\, C_{ijk}\, X_j(t)\, X^{(1)}_{k/i_0j_0k_0}(t) - \nu\, X^{(1)}_{i/i_0j_0k_0}(t) \\ & + 2\,\delta_{ii_0}\, C_{i_0j_0k_0}\, X^{(0)}_{j_0/i_0j_0k_0}(t)\, X^{(0)}_{k_0/i_0j_0k_0}(t) \\ & + 2\,\delta_{ij_0}\, C_{j_0k_0i_0}\, X^{(0)}_{k_0/i_0j_0k_0}(t)\, X^{(0)}_{i_0/i_0j_0k_0}(t) \\ & + 2\,\delta_{ik_0}\, C_{k_0i_0j_0}\, X^{(0)}_{i_0/i_0j_0k_0}(t)\, X^{(0)}_{j_0/i_0j_0k_0}(t) \,, \end{aligned} \tag{2.15}$$

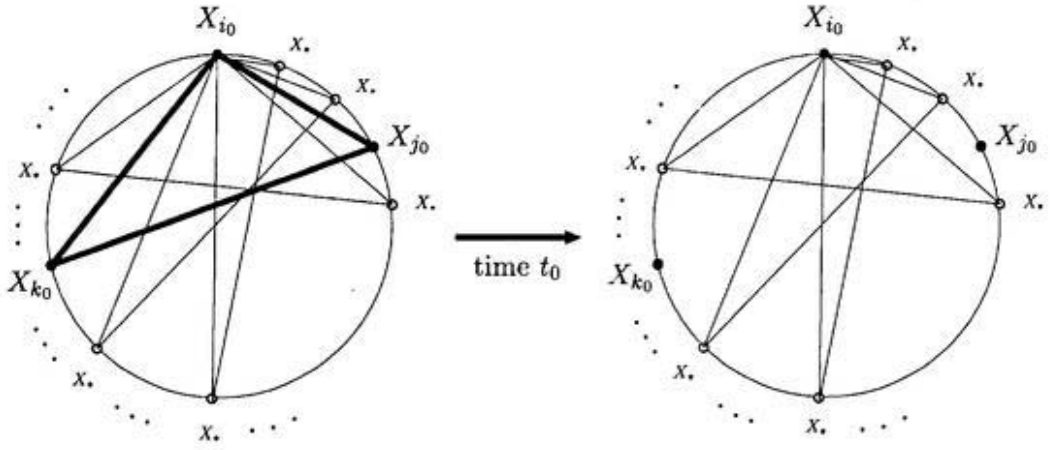


True field $X_i$ NDI field $X^{(0)}_{i/i_0j_0k_0}$

FIGURE 2.4 The direct-interaction decomposition. The NDI field $X^{(0)}_{i/i_0j_0k_0}$ is defined as an artificial field in which the direct interaction between $X_{i_0}$, $X_{j_0}$ and $X_{j_0}$ is absent for time $t \geq t_0$. Since there is only one, at the most, direct interaction between each pair of modes (the property of the weak nonlinear couplings), these three modes do not have any direct interaction between them in the NDI field.

where $X^{(1)}_i$ is assumed to be much smaller than $X^{(0)}_i$ in magnitude (see DIA assumption 1 below).

The response function $G_{in}$ is similarly decomposed as

$$G_{in}(t|t') = G^{(0)}_{in/i_0j_0k_0}(t|t') + G^{(1)}_{in/i_0j_0k_0}(t|t')\,, \tag{2.16}$$

where $G^{(0)}_{in/i_0j_0k_0}$ is governed by

$$\frac{\partial}{\partial t} G^{(0)}_{in/i_0j_0k_0}(t|t') = \sum_{\substack{j \\ \{i,j,k\}\neq\{i_0,j_0,k_0\}}} \sum_{k} 2\,C_{ijk}\,X_j(t)\,G^{(0)}_{kn/i_0j_0k_0}(t|t') - \nu\,G^{(0)}_{in/i_0j_0k_0}(t|t')\,. \tag{2.17}$$

Here, the direct-interaction decomposition has been made at $t'$. The evolution equation for the deviation field of the response function is then obtained from this equation and (2.10) as

$$\begin{aligned}
\frac{\partial}{\partial t} G^{(1)}_{in/i_0j_0k_0}(t|t') = & \sum_{\substack{j \\ \{i,j,k\}\neq\{i_0,j_0,k_0\}}} \sum_{k} 2\,C_{ijk}\,X_j(t)\,G^{(1)}_{kn/i_0j_0k_0}(t|t') - \nu\,G^{(1)}_{in/i_0j_0k_0}(t|t') \\
& + 2\,\delta_{ii_0}\,C_{i_0j_0k_0}\,X_{j_0}(t)\,G^{(0)}_{k_0n/i_0j_0k_0}(t|t') \\
& + 2\,\delta_{ii_0}\,C_{i_0j_0k_0}\,X_{k_0}(t)\,G^{(0)}_{j_0n/i_0j_0k_0}(t|t') \\
& + 2\,\delta_{ij_0}\,C_{j_0k_0i_0}\,X_{k_0}(t)\,G^{(0)}_{i_0n/i_0j_0k_0}(t|t') \\
& + 2\,\delta_{ij_0}\,C_{j_0k_0i_0}\,X_{i_0}(t)\,G^{(0)}_{k_0n/i_0j_0k_0}(t|t') \\
& + 2\,\delta_{ik_0}\,C_{k_0i_0j_0}\,X_{i_0}(t)\,G^{(0)}_{j_0n/i_0j_0k_0}(t|t') \\
& + 2\,\delta_{ik_0}\,C_{k_0i_0j_0}\,X_{j_0}(t)\,G^{(0)}_{i_0n/i_0j_0k_0}(t|t')\,,
\end{aligned} \tag{2.18}$$

where we have assumed that $|G^{(1)}_{in/i_0j_0k_0}| \ll |G^{(0)}_{in/i_0j_0k_0}|$ (see DIA assumption 1 below). The boundary conditions are written, from (2.11), as

$$G^{(0)}_{in/i_0j_0k_0}(t|t) = \delta_{in} \qquad \text{and} \qquad G^{(1)}_{in/i_0j_0k_0}(t|t) = 0\,. \tag{2.19}$$

Then, it follows from (2.13), (2.15), (2.17) and (2.19) that

$$\begin{aligned} X^{(1)}_{i/i_0j_0k_0}(t) = \int_{t_0}^{t} \mathrm{d}t' \Big[ & 2\, G^{(0)}_{ii_0/i_0j_0k_0}(t|t')\, C_{i_0j_0k_0}\, X^{(0)}_{j_0/i_0j_0k_0}(t')\, X^{(0)}_{k_0/i_0j_0k_0}(t') \\ & +2\, G^{(0)}_{ij_0/i_0j_0k_0}(t|t')\, C_{j_0k_0i_0}\, X^{(0)}_{k_0/i_0j_0k_0}(t')\, X^{(0)}_{i_0/i_0j_0k_0}(t') \\ & +2\, G^{(0)}_{ik_0/i_0j_0k_0}(t|t')\, C_{k_0i_0j_0}\, X^{(0)}_{i_0/i_0j_0k_0}(t')\, X^{(0)}_{j_0/i_0j_0k_0}(t') \Big], \end{aligned} \tag{2.20}$$

and, from (2.17)—(2.19), that

$$\begin{aligned} G^{(1)}_{in/i_0j_0k_0}(t|t') = \int_{t'}^{t} \mathrm{d}t'' \Big[ & 2\, G^{(0)}_{ii_0/i_0j_0k_0}(t|t'')\, C_{i_0j_0k_0}\, X_{j_0}(t'')\, G^{(0)}_{k_0n/i_0j_0k_0}(t''|t') \\ & +2\, G^{(0)}_{ii_0/i_0j_0k_0}(t|t'')\, C_{i_0j_0k_0}\, X_{k_0}(t'')\, G^{(0)}_{j_0n/i_0j_0k_0}(t''|t') \\ & +2\, G^{(0)}_{ij_0/i_0j_0k_0}(t|t'')\, C_{j_0k_0i_0}\, X_{k_0}(t'')\, G^{(0)}_{i_0n/i_0j_0k_0}(t''|t') \\ & +2\, G^{(0)}_{ij_0/i_0j_0k_0}(t|t'')\, C_{j_0k_0i_0}\, X_{i_0}(t'')\, G^{(0)}_{k_0n/i_0j_0k_0}(t''|t') \\ & +2\, G^{(0)}_{ik_0/i_0j_0k_0}(t|t'')\, C_{k_0i_0j_0}\, X_{i_0}(t'')\, G^{(0)}_{j_0n/i_0j_0k_0}(t''|t') \\ & +2\, G^{(0)}_{ik_0/i_0j_0k_0}(t|t'')\, C_{k_0i_0j_0}\, X_{j_0}(t'')\, G^{(0)}_{i_0n/i_0j_0k_0}(t''|t') \Big]. \end{aligned} \tag{2.21}$$

The deviation fields $X^{(1)}_{i/i_0j_0k_0}$ and $G^{(1)}_{in/i_0j_0k_0}$ are thus expressed in terms of the NDI and the true fields.

Before proceeding further, we summarize the assumptions employed in DIA, which are

**DIA assumption 1** The deviation field $X^{(1)}_{i/i_0j_0k_0}$ (or $G^{(1)}_{in/i_0j_0k_0}$) is much smaller in magnitude than the NDI field $X^{(0)}_{i/i_0j_0k_0}$ (or $G^{(0)}_{in/i_0j_0k_0}$), over the period of order of the decaying time-scale of the auto-correlation function.

**DIA assumption 2** (I) Three variables $X^{(0)}_{i/ijk}$, $X^{(0)}_{j/ijk}$ and $X^{(0)}_{k/ijk}$, between which the direct interaction is absent, are statistically independent of each other. (II) Similarly, $G^{(0)}_{in/ijk}$, $G^{(0)}_{jn/ijk}$ and $X_k$ are statistically independent of each other.

These assumptions may be reasonably accepted if the degrees of freedom $N$ of the system is large enough. Since there are a lot of direct interactions for $N \gg 1$, the influence of extracting only a single one should be negligible, and therefore the NDI field $X^{(0)}_i$ (or $G^{(0)}_{in}$) may approximate the true field $X_i$ (or $G_{in}$), which is DIA assumption 1. DIA assumption 2 is based upon the idea that the

correlation among three modes without direct interaction should be weak. This assumption may also be justified only in the case of $N \gg 1$. For example, the contribution to the dynamics of $X^{(0)}_{i_0/i_0j_0k_0}$ from $X^{(0)}_{j_0/i_0j_0k_0}$ or $X^{(0)}_{k_0/i_0j_0k_0}$ through the *indirect* interaction terms is not negligibly small unless $N \gg 1$. We will check in §5.2 the validity of these assumptions by making a comparison with direct numerical simulations.

### 2.3.2 Correlation function

The DIA is applied here to the governing equations (2.7) and (2.8) for the correlation functions. First, we consider the two-time correlation function. By substituting direct-interaction decomposition (2.12) into the nonlinear term of (2.7), we obtain

$$\begin{aligned}\sum_j \sum_k C_{ijk}\, \overline{X_j(t)\, X_k(t)\, X_n(t')} &= \sum_j \sum_k C_{ijk}\, \overline{X^{(0)}_{j/jkn}(t)\, X^{(0)}_{k/jkn}(t)\, X^{(0)}_{n/jkn}(t')} \\ &+ \sum_j \sum_k 2\, C_{ijk}\, \overline{X^{(0)}_{j/jkn}(t)\, X^{(1)}_{k/jkn}(t)\, X^{(0)}_{n/jkn}(t')} \\ &+ \sum_j \sum_k C_{ijk}\, \overline{X^{(0)}_{j/jkn}(t)\, X^{(0)}_{k/jkn}(t)\, X^{(1)}_{n/jkn}(t')}\,, \end{aligned} \tag{2.22}$$

where the higher-order terms of the deviation field have been neglected under DIA assumption 1. Notice that a different triplet of $(i_0, j_0, k_0)$ is chosen in each term in the summand on the right-hand side of the above equation, i.e., $(i_0, j_0, k_0) = (i, j, k)$.

Now we evaluate each term on the right-hand side of (2.22) in turn. It follows from DIA assumption 2(I) that

$$\text{(First term on r.h.s. of (2.22))} = 0\,. \tag{2.23}$$

For the second term, by substituting the solution (2.20) of the deviation field, we obtain

$$\begin{aligned}&\text{(Second term on r.h.s. of (2.22))} \\ &= 4 \sum_j \sum_k \int_{t_0}^{t} \mathrm{d}t''\, C_{ijk}\, C_{knj}\, \overline{G^{(0)}_{kk/jkn}(t|t'')\, X^{(0)}_{n/jkn}(t'')\, X^{(0)}_{n/jkn}(t')\, X^{(0)}_{j/jkn}(t)\, X^{(0)}_{j/jkn}(t'')} \\ &= 4 \sum_j \sum_k \int_{t_0}^{t} \mathrm{d}t''\, C_{ijk}\, C_{knj}\, \overline{G_{kk}(t|t'')}\, V_{nn}(\max\{t', t''\}, \min\{t', t''\})\, V_{jj}(t, t'')\,, \end{aligned} \tag{2.24}$$

where use has been made of DIA assumptions 1 and 2. The independency between $G^{(0)}_{in/ijk}$ and $X^{(0)}_{j/ijk}$ follows from the assumption that $X^{(0)}_{j/ijk} \approx X_j$ and DIA assumption 2(II). The third term is similarly calculated to be

$$\begin{aligned}&\text{(Third term on r.h.s. of (2.22))} \\ &\quad = 2 \sum_j \sum_k \int_{t_0}^{t'} \mathrm{d}t''\, C_{ijk}\, C_{njk}\, \overline{G_{nn}(t'|t'')}\, V_{jj}(t, t'')\, V_{kk}(t, t'')\,, \end{aligned} \tag{2.25}$$

by the use of (2.20). Thus the equation for the correlation function is written in terms of the correlation function itself and the response function $\overline{G}_{in}$ as

$$\left[\frac{\partial}{\partial t} + \nu\right] V_{in}(t, t')$$

$$= 4 \sum_j \sum_k \int_{t_0}^{t} \mathrm{d}t''\, C_{ijk}\, C_{knj}\, \overline{G_{kk}(t|t'')}\, V_{nn}(\max\{t', t''\}, \min\{t', t''\})\, V_{jj}(t, t'')$$

$$+2 \sum_j \sum_k \int_{t_0}^{t'} \mathrm{d}t''\, C_{ijk}\, C_{njk}\, \overline{G_{nn}(t'|t'')}\, V_{jj}(t, t'')\, V_{kk}(t, t'') \quad (t > t') \,. \tag{2.26}$$

For the one-time correlation function, the forcing term in (2.8) is rewritten as

$$\overline{F_i(t)\, X_n(t)} = \tfrac{1}{2}\, \Delta t\, \sigma^2\, \delta_{in} = \frac{\nu}{N}\, \delta_{in} \,, \tag{2.27}$$

and the nonlinear terms are calculated in a manner similar to the above. Then, we obtain

$$\left[ \frac{\mathrm{d}}{\mathrm{d}t} + 2\nu \right] V_{in}(t, t) = 4 \sum_j \sum_k \int_{t_0}^{t} \mathrm{d}t'\, C_{ijk}\, C_{knj}\, \overline{G_{kk}(t|t')}\, V_{nn}(t, t')\, V_{jj}(t, t')$$

$$+ 2 \sum_j \sum_k \int_{t_0}^{t} \mathrm{d}t'\, C_{ijk}\, C_{njk}\, \overline{G_{nn}(t|t')}\, V_{jj}(t, t')\, V_{kk}(t, t')$$

$$+ \frac{\nu}{N}\, \delta_{in} + (i \leftrightarrow n) \,. \tag{2.28}$$

### 2.3.3 Response function

An ensemble average of (2.10) for the response function is written as

$$\left[ \frac{\partial}{\partial t} + \nu \right] \overline{G_{in}(t|t')} = \sum_j \sum_k 2\, C_{ijk} \overline{X_j(t)\, G_{kn}(t|t')} \,. \tag{2.29}$$

The right-hand side of this equation may be calculated in the same way as in the preceding subsection. Substitution of direct-interaction decomposition (2.16) into the right-hand side leads to

$$\sum_j \sum_k 2\, C_{ijk} \overline{X_j(t)\, G_{kn}(t|t')} = \sum_j \sum_k 2\, C_{ijk} \overline{X_j(t)\, G^{(0)}_{kn/jkn}(t|t')}$$

$$+ \sum_j \sum_k 2\, C_{ijk} \overline{X_j(t)\, G^{(1)}_{kn/jkn}(t|t')} \,. \tag{2.30}$$

Thanks to DIA assumption 2(II), the first term on the right-hand side of (2.30) vanishes. By substituting expression (2.21) of the deviation field $G^{(1)}_{kn}$ and decomposition (2.12), we rewrite the second term as

$$\text{(Second term on r.h.s. of (2.30))}$$

$$= 4 \sum_j \sum_k \int_{t'}^{t} \mathrm{d}t''\; C_{ijk}\, C_{knj}\, V_{jj}(t, t'')\, \overline{G_{kk}(t|t'')}\, \overline{G_{nn}(t''|t')} \,, \tag{2.31}$$

where use has been made of DIA assumptions 1 and 2 and the assumption that $\overline{G^{(0)}_{ij/ijk}} = 0$. This last assumption follows from DIA assumption 2(I) and the approximation[4] that $G^{(0)}_{ij/i_0j_0k_0} \approx \delta X^{(0)}_{i/i_0j_0k_0}/\delta X^{(0)}_{j/i_0j_0k_0}$. The influence of $X^{(0)}_{i/ijk}(t')$ on $X^{(0)}_{j/ijk}(t)$ $(t > t')$ should be very small because there is no direct interaction between these modes. Thus, the temporal evolution of the response function is described by

$$\left[\frac{\partial}{\partial t} + \nu\right] \overline{G_{in}(t|t')} = 4 \sum_j \sum_k \int_{t'}^{t} \mathrm{d}t''\, C_{ijk}\, C_{knj}\, V_{jj}(t,t'')\, \overline{G_{kk}(t|t'')}\, \overline{G_{nn}(t''|t')}\,. \tag{2.32}$$

In summary, (2.26), (2.28) and (2.32) construct a closed set of equations for the correlation and the response functions. A closed system for the auto-correlation function $V_{ii}$ and the auto-response function $\overline{G}_{ii}$ follows by putting $i = n$ in these equations.

## 2.4 Reynolds-number reversed expansion

The reason why we explain here Reynolds-number reversed expansion (RRE), which is a kind of a Reynolds number expansion and is obviously an inappropriate approximation for large Reynolds number turbulence, is that we would like to clarify similarities and differences between RRE and DIA. As mentioned in the introduction of this chapter, these two approximations yield identical closed set of equations for some nonlinear systems including the model equation (2.1) (see §2.4.4). However, readers will see a clear difference between procedures of DIA and RRE. In addition, it will be shown in the next section that RRE is an approximation for small Reynolds number field, while DIA is applicable to a system with strong nonlinearity as long as its number of degrees of freedom is large enough. Incidentally, the number of degrees of freedom in the Navier-Stokes system increases with the Reynolds number.

Since we are considering the model equation (2.1) in the limit of weak nonlinearity in this section (§2.4), we start with the linearized equation and treat the nonlinear term as a perturbation. To make the formulation clearer, we introduce

$$\mathcal{R} = \frac{1}{\nu}\,, \tag{2.33}$$

which represents the ratio of the nonlinear to the viscous terms and will be called the Reynolds number on the analogy with the Navier-Stokes equation. Introducing a rescaled time,

$$\tilde{t} = \nu\, t\,, \tag{2.34}$$

[4]The evolution equation for $\widehat{G}^{(0)}_{ij/i_0j_0k_0} = \delta X^{(0)}_{i/i_0j_0k_0}/\delta X^{(0)}_{j/i_0j_0k_0}$ is derived from (2.1) as

$$\frac{\partial}{\partial t}\, \widehat{G}^{(0)}_{in/i_0j_0k_0}(t|t') = \sum_{\substack{j \\ \{i,j,k\}\neq\{i_0,j_0,k_0\}}} \sum_k 2\, C_{ijk}\, X^{(0)}_{j/i_0j_0k_0}(t)\, \widehat{G}^{(0)}_{kn/i_0j_0k_0}(t|t') - \nu\, \widehat{G}^{(0)}_{in/i_0j_0k_0}(t|t')\,.$$

A comparison between this equation and (2.17) may justify that $|\widehat{G}^{(0)}_{ij} - G^{(0)}_{ij}| \ll |G^{(0)}_{ij}|$ because $X_j(t) \approx X^{(0)}_{j/i_0j_0k_0}$.

we rewrite (2.1), (2.9)—(2.11) respectively as

$$\frac{\mathrm{d}}{\mathrm{d}\tilde{t}}\,\tilde{X}_i(\tilde{t}) = \mathcal{R}\sum_j\sum_k C_{ijk}\,\tilde{X}_j(\tilde{t})\,\tilde{X}_k(\tilde{t}) - \tilde{X}_i(\tilde{t}) + \tilde{F}_i(\tilde{t})\,, \tag{2.35}$$

$$\tilde{G}_{in}(\tilde{t}|\tilde{t}') = \frac{\delta\tilde{X}_i(\tilde{t})}{\delta\tilde{X}_n(\tilde{t}')} \qquad (\tilde{t}\geq\tilde{t}')\,, \tag{2.36}$$

$$\frac{\partial}{\partial\tilde{t}}\,\tilde{G}_{in}(\tilde{t}|\tilde{t}') = \mathcal{R}\sum_j\sum_k 2\,C_{ijk}\,\tilde{X}_j(\tilde{t})\,\tilde{G}_{kn}(\tilde{t}|\tilde{t}') - \tilde{G}_{in}(\tilde{t}|\tilde{t}') \qquad (\tilde{t}>\tilde{t}') \tag{2.37}$$

and

$$\tilde{G}_{in}(\tilde{t}|\tilde{t}) = \delta_{in}\,, \tag{2.38}$$

where $\tilde{X}_i(\tilde{t}) = X_i(t)$ and $\tilde{F}_i(\tilde{t}) = F_i(t)/\nu$. For simplicity of notations, we omit tildes on $\tilde{t}$, $\tilde{X}_i$, $\tilde{G}_{in}$ and $\tilde{F}_i$ in §§2.4.1—2.4.3.

### 2.4.1 Reynolds-number expansion

For small Reynolds numbers $\mathcal{R}\ll 1$ (i.e., $\nu\gg 1$) it may be legitimate to expand $X_i$ and $G_{in}$ in power series of $\mathcal{R}$ as

$$X_i(t) = X_i^{(0)}(t) + \mathcal{R}\,X_i^{(1)}(t) + O(\mathcal{R}^2) \tag{2.39}$$

$$G_{in}(t|t') = G_{in}^{(0)}(t|t') + \mathcal{R}\,G_{in}^{(1)}(t|t') + O(\mathcal{R}^2)\,. \tag{2.40}$$

By substituting these equations into (2.35) and (2.37), we obtain, at $O(1)$,

$$\frac{\mathrm{d}}{\mathrm{d}t}\,X_i^{(0)}(t) = -X_i^{(0)}(t) + F_i(t) \tag{2.41}$$

and

$$\frac{\partial}{\partial t}\,G_{in}^{(0)}(t|t') = -G_{in}^{(0)}(t|t')\,. \tag{2.42}$$

while, at $O(\mathcal{R})$,

$$\frac{\mathrm{d}}{\mathrm{d}t}\,X_i^{(1)}(t) = \sum_j\sum_k C_{ijk}\,X_j^{(0)}(t)\,X_k^{(0)}(t) - X_i^{(1)}(t) \tag{2.43}$$

and

$$\frac{\partial}{\partial t}\,G_{in}^{(1)}(t|t') = \sum_j\sum_k 2\,C_{ijk}\,X_j^{(0)}(t)\,G_{kn}^{(0)}(t|t') - G_{in}^{(1)}(t|t')\,. \tag{2.44}$$

The boundary conditions of response functions $G_{in}^{(0)}$ and $G_{in}^{(1)}$ are respectively written, from (2.38), as

$$G_{in}^{(0)}(t|t) = \delta_{in} \tag{2.45}$$

and

$$G_{in}^{(1)}(t|t) = 0\,. \tag{2.46}$$

It follows from (2.42), (2.43) and (2.45) that

$$X_i^{(1)}(t) = \sum_a\sum_b\sum_c \int_{t_0}^{t}\mathrm{d}t''C_{abc}\,G_{ia}^{(0)}(t|t'')\,X_b^{(0)}(t'')\,X_c^{(0)}(t'')\,, \tag{2.47}$$

and from (2.42) and (2.44)—(2.46) that

$$G_{in}^{(1)}(t|t') = \sum_a \sum_b \sum_c \int_{t'}^{t} \mathrm{d}t''\, 2\, C_{abc}\, G_{ia}^{(0)}(t|t'')\, X_b^{(0)}(t'')\, G_{cn}^{(0)}(t''|t')\,. \tag{2.48}$$

Here, we have assumed that

$$X_i^{(1)}(t_0) = 0\,. \tag{2.49}$$

### 2.4.2 Correlation function

The evolution equations for the correlation function (2.6) are derived from (2.35) as

$$\left[\frac{\partial}{\partial t} + 1\right] V_{in}(t,t') = \mathcal{R} \sum_j \sum_k C_{ijk}\, \overline{X_j(t)\, X_k(t)\, X_n(t')} \qquad (t > t') \tag{2.50}$$

and

$$\left[\frac{\mathrm{d}}{\mathrm{d}t} + 2\right] V_{in}(t,t) = \mathcal{R} \sum_j \sum_k C_{ijk}\, \overline{X_j(t)\, X_k(t)\, X_n(t)} + \frac{1}{N}\,\delta_{in} + (i \leftrightarrow n)\,. \tag{2.51}$$

Substitution of the Reynolds-number expansion (2.39) and (2.40) into the right-hand side of (2.50) leads to

$$\begin{aligned}
\mathcal{R} \sum_j \sum_k C_{ijk}\, \overline{X_j(t)\, X_k(t)\, X_n(t')} &= \mathcal{R} \sum_j \sum_k C_{ijk}\, \overline{X_j^{(0)}(t)\, X_k^{(0)}(t)\, X_n^{(0)}(t')} \\
&\quad + \mathcal{R}^2 \sum_j \sum_k 2\, C_{ijk}\, \overline{X_j^{(0)}(t)\, X_k^{(1)}(t)\, X_n^{(0)}(t')} \\
&\quad + \mathcal{R}^2 \sum_j \sum_k C_{ijk}\, \overline{X_j^{(0)}(t)\, X_k^{(0)}(t)\, X_n^{(1)}(t')}\,,
\end{aligned} \tag{2.52}$$

where the terms of $O(\mathcal{R}^3)$ are neglected under the assumption of small Reynolds number. Since $X_i^{(0)}$ is a solution to the linear equation (2.41) excited by a Gaussian random force, it obeys a joint normal probability distribution with vanishing covariance. This leads to

$$\text{(First term on r.h.s. of (2.52))} = 0\,. \tag{2.53}$$

The second term of (2.52) can be written, on substitution of the solution (2.47) of $X_i^{(1)}$, as

$$\begin{aligned}
&\text{(Second term on r.h.s. of (2.52))} \\
&= 2\mathcal{R}^2 \sum_j \sum_k \sum_a \sum_b \sum_c \int_{t_0}^{t} \mathrm{d}t''\, C_{abc}\, C_{ijk}\, \overline{G_{ka}^{(0)}(t|t'')\, X_j^{(0)}(t)\, X_n^{(0)}(t')\, X_b^{(0)}(t'')\, X_c^{(0)}(t'')} \\
&= 2\mathcal{R}^2 \sum_j \sum_k \sum_a \sum_b \sum_c \int_{t_0}^{t} \mathrm{d}t''\, C_{abc}\, C_{ijk}\, \overline{G_{ka}^{(0)}(t|t'')} \\
&\qquad \times \Big[\, \overline{X_j^{(0)}(t)\, X_n^{(0)}(t')}\ \overline{X_b^{(0)}(t'')\, X_c^{(0)}(t'')} \\
&\qquad + \overline{X_j^{(0)}(t)\, X_b^{(0)}(t'')}\ \overline{X_n^{(0)}(t')\, X_c^{(0)}(t'')}
\end{aligned}$$

$$+ \overline{X_j^{(0)}(t)\, X_c^{(0)}(t'')}\ \overline{X_n^{(0)}(t')\, X_b^{(0)}(t'')} \Big]$$

$$= 4\mathcal{R}^2 \sum_j \sum_k \int_{t_0}^{t} \mathrm{d}t''\, C_{knj}\, C_{ijk}\, \overline{G_{kk}^{(0)}(t|t'')}\ \overline{X_j^{(0)}(t)\, X_j^{(0)}(t'')}\ \overline{X_n^{(0)}(t')\, X_n^{(0)}(t'')}\,. \tag{2.54}$$

Here, we have used the relation,

$$G_{in}^{(0)}(t|t') = \delta_{in}\, G_{ii}^{(0)}(t|t') \tag{2.55}$$

and the assumption of independency between $X_i^{(0)}$ and $G_{in}^{(0)}$, both of which may be justified by the fact that $G_{in}^{(0)}$ is a solution to the linear equation (2.42) with the initial condition (2.45).

Now, we employ the procedure of so-called reversion to rewrite (2.54). Substitution of the Reynolds-number expansion (2.39) into the definition (2.6) of the correlation function gives

$$\begin{aligned} V_{in}(t,t') &= V_{in}^{(0)}(t,t') + \mathcal{R}\left[\overline{X_i^{(0)}(t)\, X_n^{(1)}(t')} + \overline{X_i^{(1)}(t)\, X_n^{(0)}(t')}\right] + O(\mathcal{R}^2) \\ &= V_{in}^{(0)}(t,t') + O(\mathcal{R})\,, \end{aligned} \tag{2.56}$$

where $V_{in}^{(0)}$ is defined by

$$V_{in}^{(0)}(t,t') = \overline{X_i^{(0)}(t)\, X_n^{(0)}(t')}\,. \tag{2.57}$$

For the response function, the ensemble average of (2.40) yields

$$\overline{G_{in}(t|t')} = \overline{G_{in}^{(0)}(t|t')} + O(\mathcal{R})\,. \tag{2.58}$$

The $O(\mathcal{R})$ and the higher-order terms in (2.56) and (2.58) can be expressed in terms of $V_{in}^{(0)}$ and $\overline{G_{in}^{(0)}}$ in principle (e.g. (2.47) and (2.48) for the $O(\mathcal{R})$ terms). We can then regard (2.56) and (2.58) as equations for $V_{in}^{(0)}$ and $\overline{G_{in}^{(0)}}$, the solution of which is written in power series of $\mathcal{R}$ as

$$V_{in}^{(0)}(t,t') = V_{in}(t,t') + O(\mathcal{R}) \tag{2.59}$$

$$\overline{G_{in}^{(0)}(t|t')} = \overline{G_{in}(t|t')} + O(\mathcal{R})\,. \tag{2.60}$$

This procedure is called the reversion [25], which the naming of the Reynolds-number reversed expansion (RRE) originates from. Equation (2.54) is then written in terms of the true field variables $V_{in}$ and $\overline{G_{in}}$ as

$$(2.54) = 4\mathcal{R}^2 \sum_j \sum_k \int_{t_0}^{t} \mathrm{d}t''\, C_{knj}\, C_{ijk}\, \overline{G_{kk}(t|t'')}\ V_{jj}(t,t'')\, V_{nn}(\max\{t',t''\}, \min\{t',t''\}) \tag{2.61}$$

at the leading order. The third term of (2.52) can be estimated in a similar manner as

$$\begin{aligned} &\text{(Third term on r.h.s. of (2.52))} \\ &\quad = 2\mathcal{R}^2 \sum_j \sum_k \int_{t_0}^{t'} \mathrm{d}t''\, C_{njk}\, C_{ijk}\, \overline{G_{nn}(t'|t'')}\ V_{jj}(t,t'')\, V_{kk}(t,t'')\,. \end{aligned} \tag{2.62}$$

Thus, a combination of (2.52), (2.53), (2.61) and (2.62) finally reduces the evolution equation for the two-time correlation function into

$$\left[\frac{\partial}{\partial t}+1\right] V_{in}(t,t') = 4\mathcal{R}^2 \sum_j \sum_k \int_{t_0}^{t} \mathrm{d}t''\, C_{knj}\, C_{ijk}\, \overline{G_{kk}(t|t'')}\; V_{jj}(t,t'')\, V_{nn}(\max\{t',t''\},\min\{t',t''\}) + 2\mathcal{R}^2 \sum_j \sum_k \int_{t_0}^{t'} \mathrm{d}t''\, C_{njk}\, C_{ijk}\, \overline{G_{nn}(t'|t'')}\; V_{jj}(t,t'')\, V_{kk}(t,t'') \,. \tag{2.63}$$

Equation (2.51) for the one-time correlation function is similarly derived as

$$\left[\frac{\mathrm{d}}{\mathrm{d}t}+2\right] V_{in}(t,t) = 4\mathcal{R}^2 \sum_j \sum_k \int_{t_0}^{t} \mathrm{d}t'\, C_{knj}\, C_{ijk}\, \overline{G_{kk}(t|t')}\; V_{jj}(t,t')\, V_{nn}(t,t') + 2\mathcal{R}^2 \sum_j \sum_k \int_{t_0}^{t} \mathrm{d}t'\, C_{njk}\, C_{ijk}\, \overline{G_{nn}(t|t')}\; V_{jj}(t,t')\, V_{kk}(t,t') + \frac{1}{N}\delta_{in} + (i \leftrightarrow n) \,. \tag{2.64}$$

### 2.4.3 Response function

The evolution equation for the ensemble average of the response function is

$$\left[\frac{\partial}{\partial t}+1\right] \overline{G_{in}(t|t')} = \mathcal{R} \sum_j \sum_k 2\, C_{ijk}\, \overline{X_j(t)\, G_{kn}(t|t')} \,, \tag{2.65}$$

which follows from (2.37). Substituting (2.39) and (2.40) into the right-hand side of this equation and discarding the terms of $O(\mathcal{R}^3)$, we obtain

$$\mathcal{R} \sum_j \sum_k 2\, C_{ijk}\, \overline{X_j(t)\, G_{kn}(t|t')} = \mathcal{R} \sum_j \sum_k 2\, C_{ijk}\, \overline{X_j^{(0)}(t)\, G_{kn}^{(0)}(t|t')} + \mathcal{R}^2 \sum_j \sum_k 2\, C_{ijk}\, \overline{X_j^{(1)}(t)\, G_{kn}^{(0)}(t|t')} + \mathcal{R}^2 \sum_j \sum_k 2\, C_{ijk}\, \overline{X_j^{(0)}(t)\, G_{kn}^{(1)}(t|t')} \,. \tag{2.66}$$

In the same way as in the preceding subsection we can write each term in this equation in terms of $\boldsymbol{V}$ and $\overline{\boldsymbol{G}}$. Then, (2.66) is converted into

$$\left[\frac{\partial}{\partial t}+1\right] \overline{G_{in}(t|t')} = 4\mathcal{R}^2 \sum_j \sum_k \int_{t'}^{t} \mathrm{d}t''\, C_{ijk}\, C_{knj}\, V_{jj}(t,t'')\, \overline{G_{kk}(t|t'')}\; \overline{G_{nn}(t''|t')} \,. \tag{2.67}$$

### 2.4.4 Equivalence of RRE and DIA equations

In the formulation made in the last three subsections the time was scaled as $\tilde{t} = \nu t = t/\mathcal{R}$ (see (2.33) and (2.34), and remember the omission of the tilde). If $\tilde{t}$ is transformed back to $t$ in the

resultant equations (2.63), (2.64) and (2.67), they become identical to (2.26), (2.28) and (2.32), respectively, which are derived by DIA. Incidentally a so-called bookkeeping parameter ($\mathcal{R} = 1$), which is sometimes introduced in this kind of expansion [36, 18, 12], plays a role similar to the time transformation such as (2.34).

The RRE described in the preceding subsections is based upon an idea developed by Kraichnan [25]. He showed it for the Navier-Stokes equation that those integro-differential equations derived by DIA (both in the Eulerian and the Lagrangian formulations) are also obtained by the use of RRE. Kaneda [36] applied this expansion (called the Lagrangian renormalized approximation by him) to the Lagrangian velocity field. The resultant integro-differential equations are again the same as those derived by DIA [35].

Now we know that the above two approximations lead to a same set of equations for the model equation (2.1) and the Navier-Stokes equation. The arguments on the differences between these approximations for the model equation, which will be made in the next section, is therefore expected to be applicable to the Navier-Stokes equation as well.

## 2.5 Applicability of DIA

### 2.5.1 Solution to DIA equations

In the preceding two sections we have shown that an identical system of equations is derived by two completely different approximations. It is quite obvious that RRE should be valid for small Reynolds numbers ($\nu \gg 1$), whereas the assumptions of DIA summarized in §2.3.1 be for the large degrees of freedom ($N \gg 1$). We expect, therefore, that the equations (hereafter, called the DIA-RRE equations) may give good predictions in such parameter ranges that $\nu \gg 1$ or $N \gg 1$. This expectation will be verified in the following by a series of direct numerical simulations of the model equation.

By construction (see (2.82)), the coefficients $C_{ijk}$ do not depend on the absolute value of the suffixes but only on their differences, and therefore the system can be statistically homogeneous (e.g., $V_{ii}$ can be independent of $i$). If the system is statistically stationary as well as homogeneous, the auto-correlation and the response functions are expressed as

$$V_{ii}(t,t') = \mathcal{V}(t-t')\,, \tag{2.68}$$

$$\overline{G_{ii}(t,t')} = \mathcal{G}(t-t')\,. \tag{2.69}$$

Then, the DIA-RRE equations (2.26), (2.28) and (2.32) for $i = n$ are respectively written as

$$\left[\frac{\mathrm{d}}{\mathrm{d}\tau} + \nu\right]\mathcal{V}(\tau) = -2c_1\int_0^\infty \mathrm{d}\tau'\,\mathcal{G}(\tau')\,\mathcal{V}(|\tau-\tau'|)\,\mathcal{V}(\tau') + 2c_1\int_\tau^\infty \mathrm{d}\tau'\,\mathcal{G}(\tau'-\tau)\,\mathcal{V}(\tau')\,\mathcal{V}(\tau') \qquad (\tau > 0)\,, \tag{2.70}$$

$$\mathcal{V}(0) = \frac{1}{N} \tag{2.71}$$

and

$$\left[\frac{\mathrm{d}}{\mathrm{d}\tau}+\nu\right]\mathcal{G}(\tau)=-2c_1\int_0^\tau \mathrm{d}\tau'\ \mathcal{V}(\tau')\,\mathcal{G}(\tau')\,\mathcal{G}(\tau-\tau')\ , \tag{2.72}$$

with boundary condition

$$\mathcal{G}(0)=1 \tag{2.73}$$

(see (2.11)). Here, the coefficient $c_1$ is defined by [5]

$$c_1=\sum_j\sum_k C_{ijk}\,C_{ijk}\ . \tag{2.74}$$

Notice here that the original upper bound $t-t_0$ of integrations in (2.70) has been replaced by the infinity. This will be justified a posteriori by taking it to be sufficiently larger than the decaying time-scale of $\mathcal{V}(\tau)$ and $\mathcal{G}(\tau)$ (see §2.5.2).

Equations (2.70)—(2.73) permit a solution such that

$$\mathcal{V}(\tau)=\mathcal{V}(0)\,\mathcal{G}(\tau) \tag{2.75}$$

and

$$\left[\frac{\mathrm{d}}{\mathrm{d}\tau}+\nu\right]\mathcal{G}(\tau)=-2c_1\,\mathcal{V}(0)\int_0^\tau \mathrm{d}\tau'\ \left[\mathcal{G}(\tau')\right]^2\mathcal{G}(\tau-\tau')\ . \tag{2.76}$$

Incidentally, this equation shows that the decaying time-scale of $\mathcal{G}(\tau)$ (and $\mathcal{V}(\tau)$) is inversely proportional to $\sqrt{c_1\,\mathcal{V}(0)}=\sqrt{c_1/N}$ in the inviscid limit (see Fig.2.3(b)).

Equation (2.76) with boundary condition (2.73) is solved numerically by an iterative method. The correlation function thus obtained are drawn in Figs.2.5 for various values of $N$ and $\nu$ together with the results by the direct numerical simulation. A case of small number of degrees of freedom is shown in Figs.2.5(a)—(c) for three different values of viscosity $\nu=10$, 1 and 0. It is seen that the agreement between the prediction by the DIA-RRE equation and the direct numerical simulation is better for larger values of $\nu$. The agreement seems perfect even at $\nu=1$ (see Fig.2.5(b)). We also compare them with a purely linear solution $\mathcal{V}(\tau)=\mathcal{V}(0)\ \exp[\,-\nu\tau\,]$ (shown with a dotted line). As seen in Fig.2.5(a), the three curves completely coincide with each other at $\nu=10$, which means that the nonlinear effects may be negligible at this value of viscosity. It is interesting however to see in Fig.2.5(b) that the purely linear solution deviates substantially from the results of both the DIA-RRE equation and the direct numerical simulation. This indicates that the nonlinear effects on the correlation function, even though they are not so large, are properly evaluated by the DIA-RRE equations. In Figs.2.5(c)—(f), we compare the results for various values of $N$ at vanishing viscosity (in the limit of large Reynolds number). It is seen that the agreement of the two improves as $N$ increases. In conclusion, the prediction by the DIA-RRE equation works well for small Reynolds numbers ($\nu\gg 1$) or for large degrees of freedom ($N\gg 1$).

[5] Notice the relation,

$$c_2=\sum_j\sum_k C_{ijk}\,C_{kij}\ =\sum_j\sum_k C_{ijk}\,(-C_{ijk}-C_{jki})=-c_1-\sum_j\sum_k C_{ikj}\,C_{jik}=-c_1-c_2\ ,$$

which implies that $c_2=-\frac{1}{2}\,c_1$, where use has been made of (2.2) and (2.3).

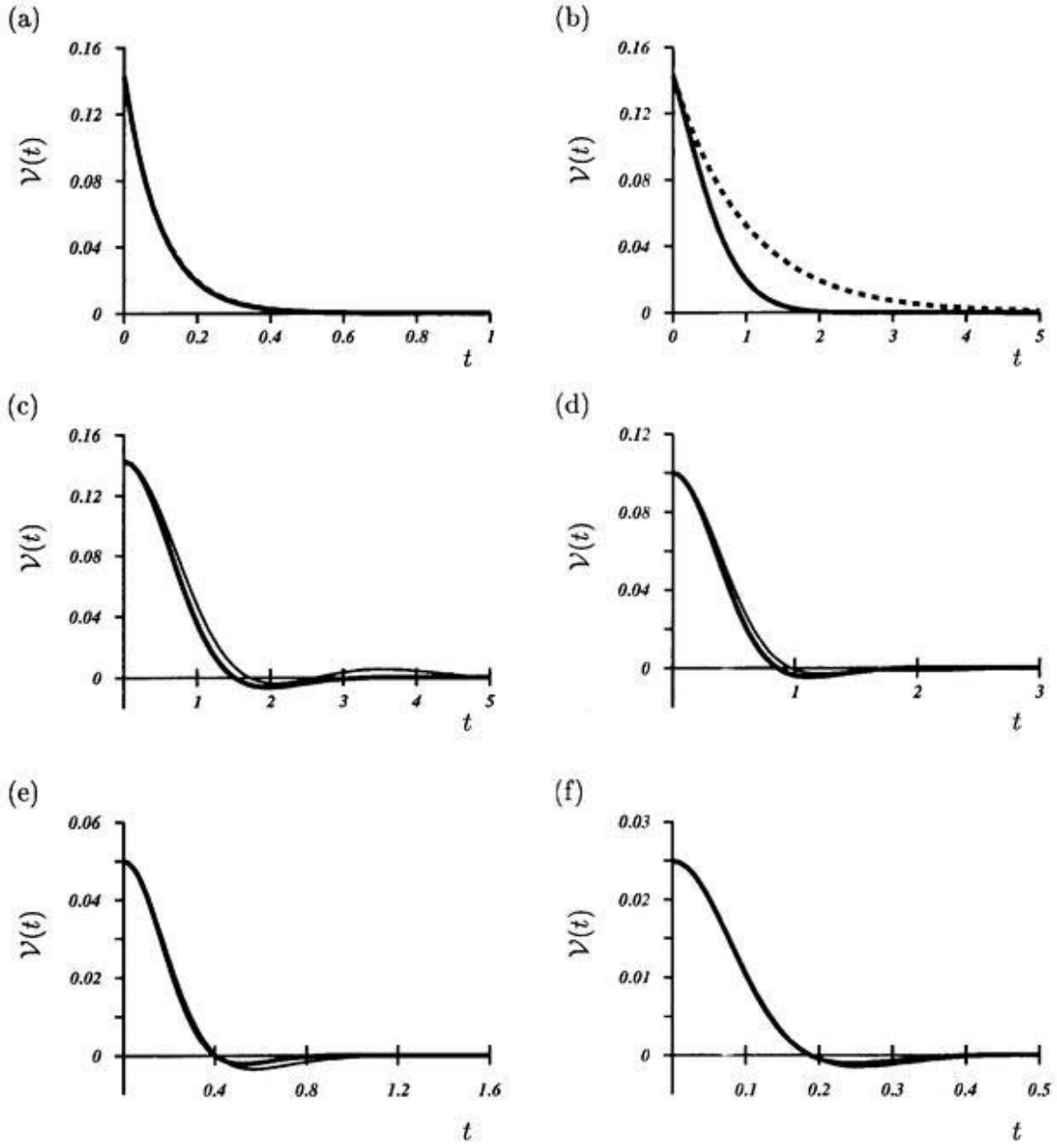


FIGURE 2.5 Comparisons between the predictions by the DIA-RRE equations (thick solid line) and the evaluations by the direct numerical simulation (thin solid line). The broken lines in (a) and (b) represent the linear solution $\mathcal{V}(\tau) = \mathcal{V}(0)\ \exp[\,-\nu\tau\,]$. (a) $(N, \nu) = (7, 10)$. (b) $(7, 1)$. (c) $(7, 0)$. (d) $(10, 0)$. (e) $(20, 0)$. (f) $(40, 0)$. The agreements are excellent in the cases of $\nu \gg 1$ or $N \gg 1$.

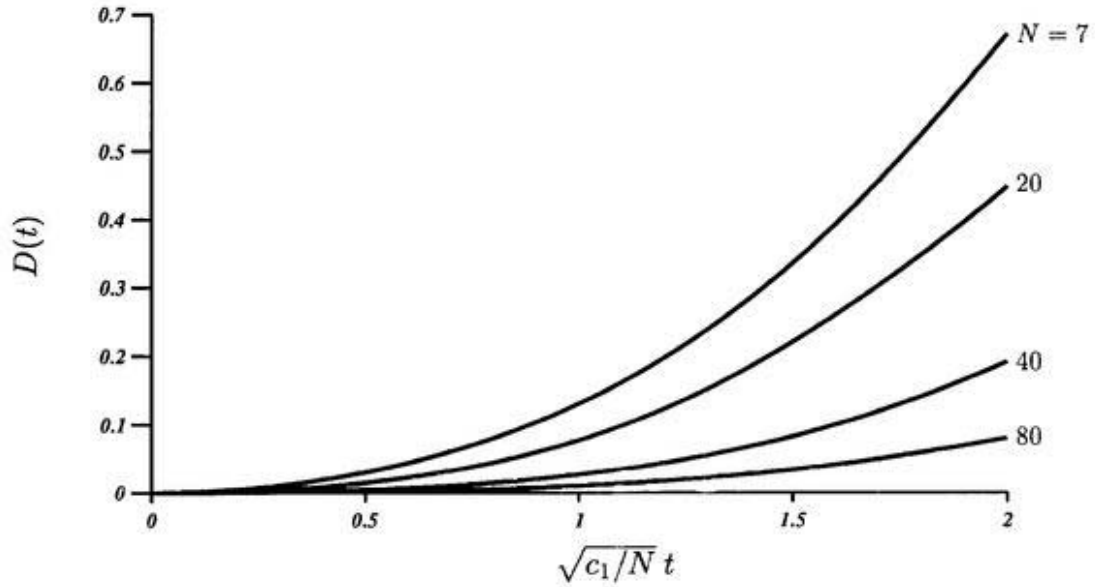


FIGURE 2.6 Magnitude of the deviation field with $(i_0, j_0, k_0) = (1, 2, 4)$ in the case of $\nu = 0$. The horizontal axis represents the time normalized by decaying time-scale of the auto-correlation function $V_{ii}(t, t')$ (cf. Fig.2.3(b)). Four different numbers of degrees of freedom ($N = 7, 20, 40$ and 80) are compared. As the number of degrees of freedom increases, DIA assumption 1 is satisfied better.

### 2.5.2 Validity of DIA assumptions

It was shown in the preceding subsection that the DIA-RRE equations give an excellent prediction of the auto-correlation function in the case of $N \gg 1$ or $\nu \gg 1$. This is quite reasonable because DIA and RRE are formulated for $N \gg 1$ and $\nu \gg 1$, respectively. Here we demonstrate it numerically that the assumptions of DIA summarized in §3.1 are actually satisfied for $N \gg 1$.

First, in order to examine DIA assumption 1 that the deviation field is much smaller in magnitude than the NDI field during the decaying time-scale of the auto-correlation function, we compare, in Fig.2.6, the temporal evolution of the magnitude of the deviation field,

$$D(t) = \left\langle \sum_i \left[ X^{(1)}_{i/i_0 j_0 k_0}(t|0) \right]^2 \right\rangle \tag{2.77}$$

for four different values of $N$ in the inviscid case. Here $\langle \quad \rangle$ stands for an average over a sufficiently large number of runs starting with random initial conditions. The time in the horizontal axis is normalized by the decaying time-scale of the auto-correlation function (cf. Fig.2.3(b)). Indeed the deviation field develops in time, but it never exceeds the NDI field in magnitude within the correlation time, namely, $D(t) < \sum_i [X_i^{(0)}]^2 = 1$ for $\sqrt{c_1/N}\, t < 2$. Moreover, $D(t)$ decreases roughly in the inverse proportion to $N$. This concludes that DIA assumption 1 may be better for larger values of $N$.

A remark on the replacement of the upper bound of the integrations in (2.70) may be in order.

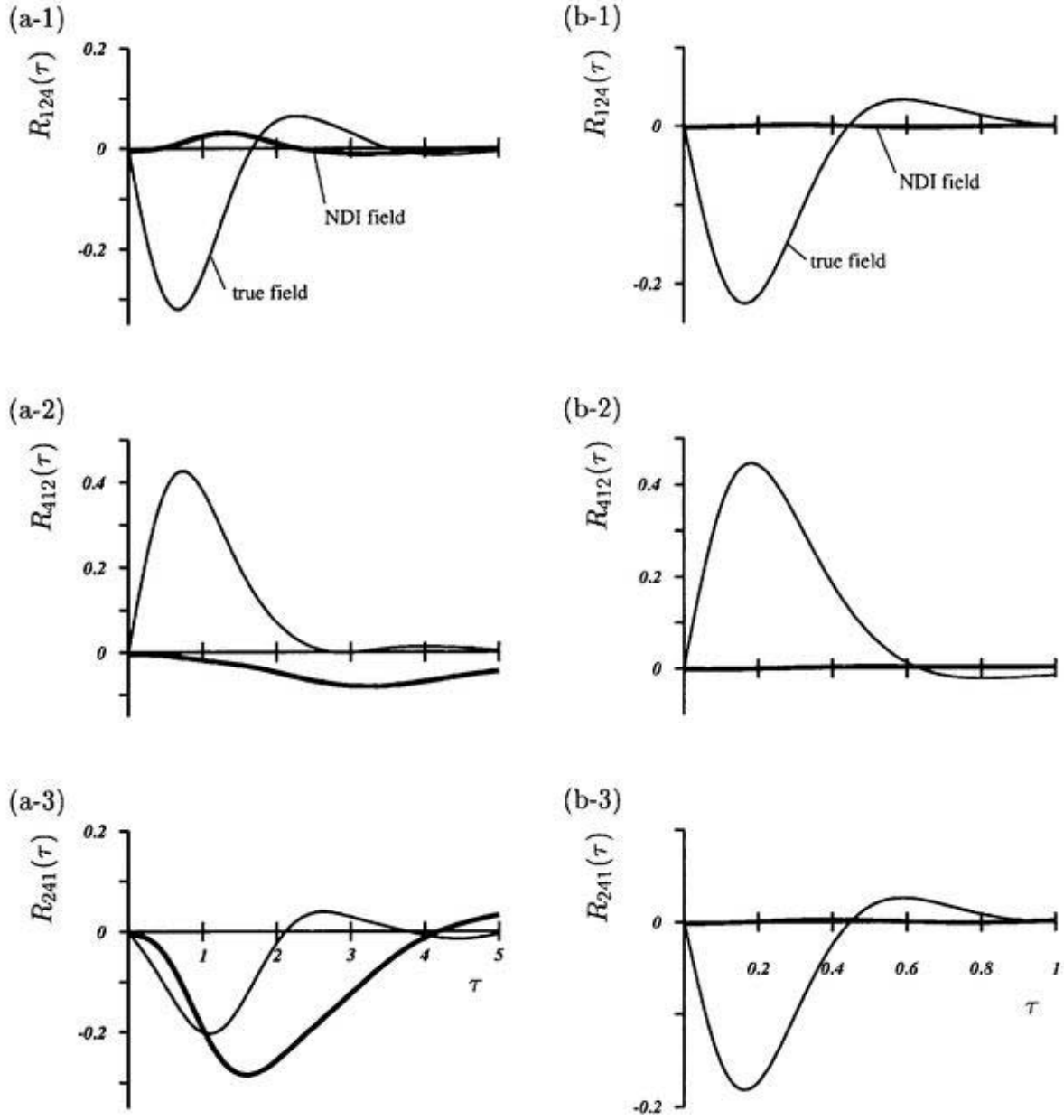


FIGURE 2.7 Triple correlation factor $R_{ijk}$ in the true field $X_i$ (thin line) and in the NDI field $X^{(0)}_{i/124}$ (thick line) in the weak nonlinear coupling case. (a) $(N, \nu) = (7, 0)$. (b) $(N, \nu) = (20, 0)$. DIA assumption 2(I) is satisfied well for $N = 20$, but not for $N = 7$.

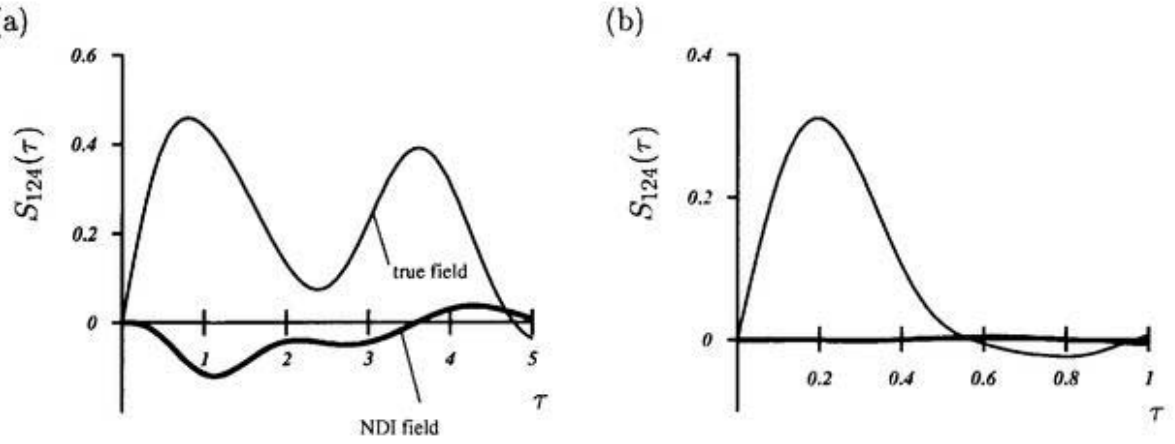


FIGURE 2.8 Correlation factor $S_{412}$ in the true field $G_{ij}$ (thin line) and in the NDI field $G^{(0)}_{ij/124}$ (thick line) in the weak nonlinear coupling case. (a) $(N,\nu) = (7,0)$. (b) $(N,\nu) = (20,0)$. DIA assumption 2(II) is satisfied well for $N = 20$, but not for $N = 7$.

Remember that the DIA-RRE equations are formulated under the assumption that the deviation fields are smaller in magnitude than the NDI fields (DIA assumption 1). The behavior of $D(t)$ shown in Fig.2.6 tells us that even if we choose the direct-interaction decomposition time $t_0$ so that $t - t_0$ is sufficiently larger than the correlation time, the assumption of smallness of the deviation fields is actually satisfied if $N \gg 1$. Then, thanks to the exponential decay of $\mathcal{G}(\tau)$ and $\mathcal{V}(\tau)$, we can replace $t - t_0$ by the infinity.

Next, we move to DIA assumption 2(I) on the independency between those modes without direct interactions. This assumption is used in the derivation of the DIA-RRE equations as

$$\overline{X^{(0)}_{i/ijk}(t)\, X^{(0)}_{j/ijk}(t)\, X^{(0)}_{k/ijk}(t')} = 0 \tag{2.78}$$

(see (2.23)). In order to assess this assumption quantitatively, we calculate the triple correlation factor,

$$R_{ijk}(t-t') = \frac{\overline{X_i(t)\, X_j(t)\, X_k(t')}}{\sqrt{\overline{X_i(t)^2}\;\overline{X_j(t)^2}\;\overline{X_k(t)^2}}}\,, \tag{2.79}$$

for the true field and for the NDI field (where $X_i(t)$ is replaced by $X^{(0)}_{i/ijk}$). In Figs.2.7, we plot the results for $\{i,j,k\} = \{1,2,4\}$ for (a) $N = 7$ and (b) 20 in the inviscid case. It is clear from Figs.2.7(b) that the triple correlation factor for the NDI field is drastically reduced for larger $N$. This gives a strong support of the validity of (2.78) for $N \gg 1$. As seen in Figs.2.7(a), on the other hand, it does not well behave for smaller $N$. This failure in the small-$N$ case is due to the indirect interactions.

Finally, we consider DIA assumption 2(II) that $G^{(0)}_{in/ijk}$, $G^{(0)}_{jn/ijk}$ and $X_k$ are statistically independent of each other. This is based on the fact that these three variables do not have direct nonlinear interaction between them (see e.g. (2.17)). This assumption is used, for example, as

$$\overline{G^{(0)}_{ij/ijk}(t|t')\, X_k(t)} = 0 \tag{2.80}$$

in the derivation of the DIA-RRE equations (see a paragraph below (2.30)). To check it we calculate a covariance factor,

$$S_{ijk}(t-t') = \frac{\overline{G_{ij}(t|t')\, X_k(t)}}{\sqrt{\overline{X_k(t)^2}}}, \tag{2.81}$$

for the true field and for the NDI field (where $G_{ij}$ is replaced by $G^{(0)}_{ij/ijk}$). Notice that the assumption requires that this factor should vanish for the NDI field. In Figs.2.8, we plot the results of $S_{412}$ for (a) $N = 7$ and (b) 20 in the inviscid case. Other factors such as $S_{214}$ show similar behavior to $S_{412}$ (figures are omitted). It is seen that $S_{412}$ tends to vanish for larger $N$ like $R_{ijk}$ (see Figs.2.7). In conclusion, DIA assumption 2(II) is also satisfied for $N \gg 1$.

## 2.6 Concluding remarks

One of the main purposes of this chapter is to remove a possible misunderstanding caused by the fact that the Eulerian DIA equations are derived by several kinds of different approximations. The DIA is a quite interesting approximation, in which the nonlinearity of the system is not totally neglected and any adjustable parameter is not introduced. The author would like to emphasize again that this approximation is based upon the weakness of the nonlinear couplings of the system, and that it is different from any other approximations dealing with the nonlinear term as a perturbation. Especially we have given a numerical evidence for a dynamical system that DIA and RRE have different parameter regions of validity although they lead to an identical set of equations for the correlation and the response functions. The RRE is applicable to a system with weak nonlinearity, whereas DIA is to that with a large number of degrees of freedom. Figure 2.9 shows schematically this situation. It should be stressed that we have checked this applicability of DIA by two means: Comparisons between the predictions by the DIA-RRE equations and the direct numerical simulations (see Fig.2.5) and direct confirmations of the DIA assumptions (see Figs.2.6—2.8).

We have to mention, however, that in the above discussions we restrict ourselves to weak nonlinear coupling cases. Intuitively, for stronger coupling systems DIA does not work well because the DIA assumption 2 (see §2.3.1) may be violated. In Chapter 5, we shall discuss this important problem on DIA for systems with stronger couplings by the use of the model equation introduced in this chapter.

As stressed in §§1.3 and 2.2.1, the weakness of the nonlinear couplings is one of the most important properties of the Navier-Stokes equation (1.9). It is shown that DIA is applicable to a weak nonlinear coupling system with large degrees of freedom, even if the nonlinearity is strong. The number of degrees of freedom in the Navier-Stokes turbulence is proportional to $Re^{9/4}$ (see §1.5), and therefore high Reynolds number homogeneous turbulence is a system with large degrees of freedom and strong nonlinearity of weak couplings. Hence, it seems likely that DIA is applicable to the Navier-Stokes turbulence at very high Reynolds number. In the next chapter, we shall examine this application of DIA.

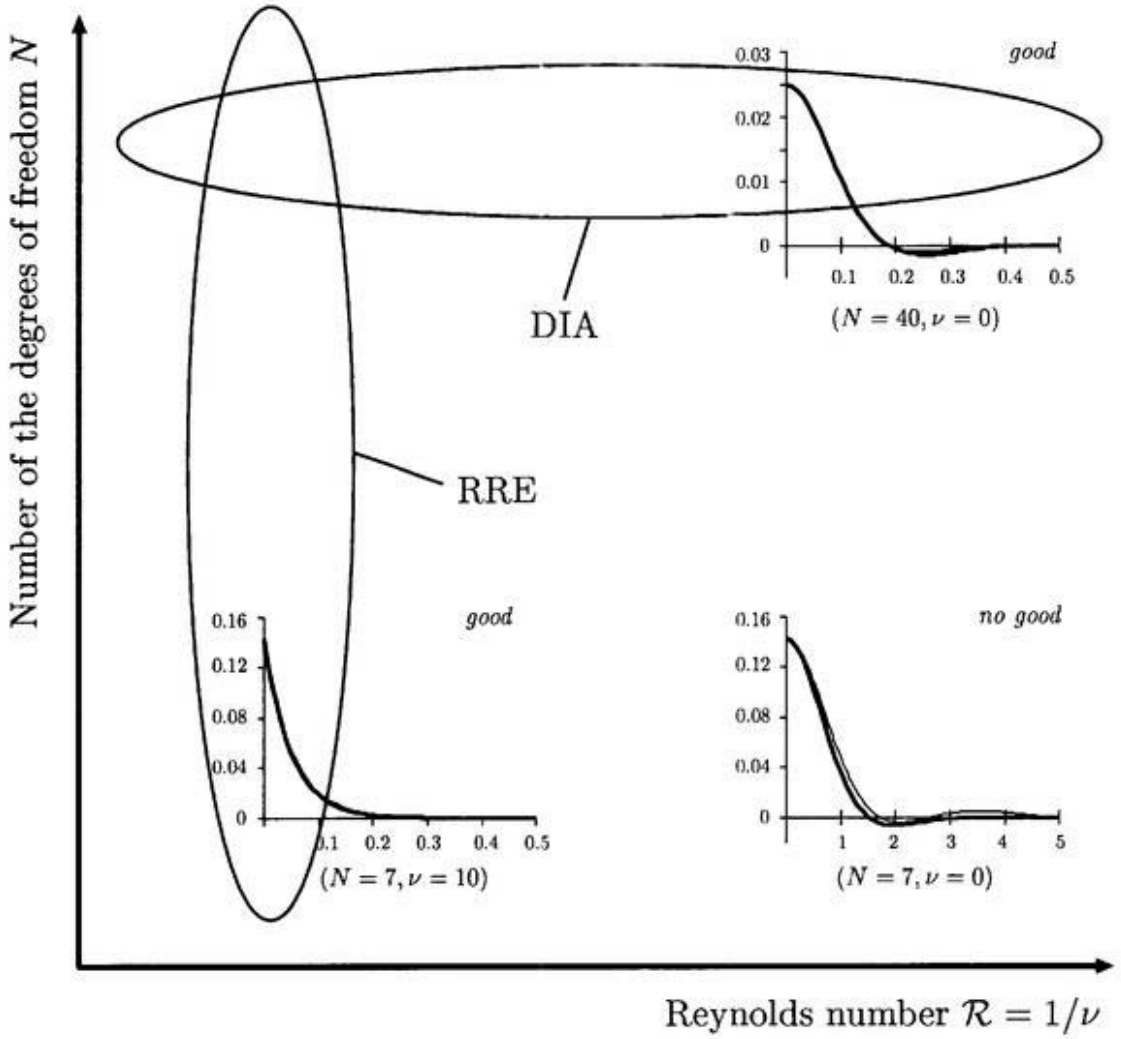


FIGURE 2.9 Applicability of DIA and RRE for systems with weak nonlinear couplings. The DIA is valid for a system with large degrees of freedom even if the nonlinearity is strong, whereas RRE is an approximation for small Reynolds number. The figures included are taken from Fig.2.5. Although the coincidence between the prediction by the DIA-RRE equation (thick line) and the direct numerical simulation (thin line) is not so bad even in the case $(N, \nu) = (7, 0)$, it is much more excellent in the cases $(N, \nu) = (40, 0)$ (large degrees of freedom) and $(N, \nu) = (7, 10)$ (small Reynolds number).

| $N$ | $(a_n, b_n, c_n)$ |
|---|---|
| 7 | $(1,2,4)$ |
| 10 | $(1,2,7)$ |
| 20 | $(1,2,17), (4,5,11)$ |
| 40 | $(1,2,37), (4,5,31). (6,7,27), (8,10,22), (11,12,17)$ |

TABLE 2.1 Triplets $(a_n, b_n, c_n)$ adopted in the present numerical simulation.

# Appendix A

We describe here an example of constructions of the coefficients $C_{ijk}$ which satisfy the three conditions in §2.2.1. The coefficients are specified as follows. For the sake of explanation, we introduce a circle of circumference $N$ and assign $N$ points with equal distance apart on it (Fig.2.10). For any triplets of integers, $i$, $j$ and $k$, we introduce $a$, $b$ and $c$ as three arc lengths divided by these three points in such a way that the point $i$ is sandwiched by $a$ and $c$, and that $a$, $b$ and $c$ are placed counterclockwise. Here, we choose a series of triplets of natural numbers $(a_n, b_n, c_n)$ $(a_n + b_n + c_n = N;\ n = 1, 2, 3, \cdots)$ so that there is no common element in a set $\{x | x = a_n, b_n, c_n, N - a_n, N - b_n, N - c_n;\ n = 1, 2, 3, \cdots\}$. (Note that the choice of $a_n$, $b_n$ and $c_n$ is not unique, and one adopted in the present paper is shown in Table 2.1.)

The coefficients $C_{ijk}$ are then defined by

$$C_{ijk} = \begin{cases} \frac{1}{3} N - b & (\text{ if } \exists n \text{ such that } (a,b,c) \equiv (a_n, b_n, c_n)\ ) \\ 0 & (\text{ otherwise }) \end{cases} \tag{2.82}$$

where $(a,b,c) \equiv (a',b',c')$ implies that $(a,b,c)$ is equal to $(a',b',c')$ itself or its cyclic permutations.

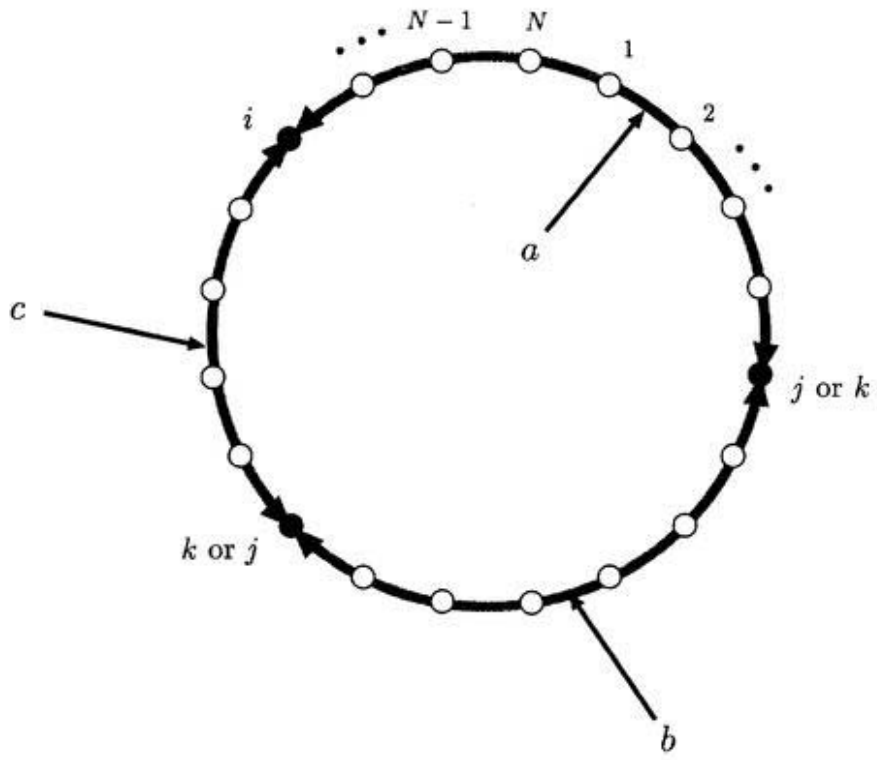


FIGURE 2.10 Definitions of $a$, $b$ and $c$. $N$ points are assigned with equal distance apart on a circle of circumference $N$. The arc lengths $a$, $b$ and $c$ between points $i$, $j$ and $k$ are defined in such a way that point $i$ is located between $a$ and $c$, and that $a$, $b$ and $c$ are placed counterclockwise.

# Chapter 3

# Lagrangian DIA for Homogeneous Isotropic Turbulence

We apply DIA, explained in detail in the preceding chapter by using a model equation, to homogeneous isotropic turbulence governed by the Navier-Stokes equation. Since it is known that DIA for the Eulerian field does not work well (this approximation is inconsistent with Kolmogorov's phenomenology), we shall propose a new Lagrangian version of DIA. It should be stressed that the present formulation is different from Kraichnan's so-called Lagrangian history DIA [37], and that the former is much simpler than the latter. We make a bridge to connect the basic equations and the Kolmogorov phenomenology. Namely, it is shown that Kolmogorov's universal function of the energy spectrum evaluated based upon the basic equations under the present Lagrangian DIA is in an excellent agreement with measurements and experimental data without any adjustable parameters. The Kolmogorov constant and the skewness factor of longitudinal derivative of velocity are determined as 1.722 and $-0.66$, respectively. Energy transfer and flux functions in the wavenumber space in stationary turbulence are evaluated. Universality and time independency of the large-scale structure in freely decaying turbulence are also considered, and it is shown that the Birkhoff invariance [38] does hold but not the Loitsiansky [39].

## 3.1 Introduction

As discussed in Chapter 2, DIA is valid for a nonlinear system with weak nonlinear couplings and a large number of degrees of freedom. Homogeneous turbulence at large Reynolds number satisfies these conditions because this nonlinear system, which is governed by the Navier-Stokes equation (1.9), has weak couplings as shown in Fig.2.1, and because the number of degrees of freedom is proportional to the power 9/4 of the Reynolds number as seen in §1.5. Then, in this chapter, we shall apply DIA to homogeneous turbulence to solve the closure problem in the statistical theory of turbulence described in §1.2.

This chapter [1] is organized as follows. In the rest of this introduction, we review phenomenologies and classical analytical theories on the universality of the small-scale (§3.1.1) and the large-scale (§3.1.2) structures, and summarize a history of DIA (§3.1.3). Then, in the next section, we introduce several basic quantities which are necessary in the subsequent analysis. The idea, the assumptions and the procedures of the present formulation of DIA are explained in §3.3, and we shall derive a closed set of equations for the Lagrangian velocity correlation and response functions. We then solve the resultant closure equations for a stationary case in §3.4. The skewness of the velocity derivative, the energy transfer and the flux functions and the wavenumber dependence of the eddy viscosity are also calculated. A freely decaying case is treated in §3.5. The shape of the energy spectrum and its time development are determined in a similarly evolving form. Section 3.6 is devoted to concluding remarks of this chapter. Details of some calculations are given in Appendices.

### 3.1.1 Kolmogorov theory

We describe Kolmogorov's phenomenology [1] in terms of the energy spectrum function defined by (3.45) below. As for the first similarity hypothesis, in the universal range (in which the length scale is much smaller than the integral scale $L$, i.e., $k \gg 1/L$) the turbulent field is locally isotropic and its statistics are determined by the wavenumber $k$, the mean rate of the energy dissipation per unit mass $\epsilon$ and the kinematic viscosity of fluid $\nu$. By employing a dimensional analysis, we can derive a similarity form,

$$E(k,t) = \nu^{5/4}\,\epsilon(t)^{1/4}\,F(k/k_{\mathrm{K}}) \tag{3.1}$$

with

$$k_{\mathrm{K}} = (\epsilon(t)/\nu^3)^{1/4}\,. \tag{3.2}$$

Figure 1.1 tells us that this universality of the energy spectrum is well supported by many kinds of turbulence. As for the second similarity hypothesis, in the inertial range (in which the length scale is much smaller than $L$ but much larger than the viscous scale $\eta = (\epsilon(t)^{-1}\nu^3)^{1/4}$, i.e., $1/L \ll k \ll k_{\mathrm{K}}$) the statistics are free from the viscous effect, and therefore the spectrum takes a power form as

$$E(k,t) = K\,\epsilon(t)^{\frac{2}{3}}\,k^{-\frac{5}{3}}\,, \tag{3.3}$$

where $K$ is the Kolmogorov constant, which is evaluated experimentally to be $1.62 \pm 0.17$ [40]. One of our main objects in this chapter is to determine the universal function $F$ with resort to the Navier-Stokes equation.

### 3.1.2 Large-scale structure of decaying turbulence

Since the statistical stationarity requires an energy supply by large-scale motions which depend on the kind of flows (e.g., the boundary condition), no universality may be expected in large scales. On

[1] This chapter is based upon Ref. [35].

the other hand, freely decaying isotropic turbulence may have universality of the large-scale structure as well as the small-scale. We review briefly several theories on this issue.

By making use of (1.18), the energy spectrum $E(k,t)$ defined by (3.45) below is expressed in terms of the velocity correlation function $f(r,t)$ as

$$E(k,t) = \frac{u_m^2}{\pi} \int_0^\infty \mathrm{d}r \left[ 3f(r,t) + r \frac{\partial}{\partial r} f(r,t) \right] kr \, \sin(kr) \,, \tag{3.4}$$

which is rewritten in the limit $k \to 0$ as

$$E(k,t) = \left[ \frac{u_m^2}{\pi} \lim_{r\to\infty} r^3 f(r,t) \right] k^2 + \left[ \frac{u_m^2}{3\pi} \int_0^\infty \mathrm{d}r \, r^4 f(r,t) - \frac{u_m^2}{3\pi} \lim_{r\to\infty} r^5 f(r,t) \right] k^4 + O(k^6) \,. \tag{3.5}$$

In order to examine the large-scale structure in terms of the energy spectrum, we introduce an index $\zeta$ which expresses the behavior of $E(k,t)$ in the vicinity of the wavenumber origin as

$$E(k,t) = \widehat{E}_\zeta^{(0)}(t) \, k^\zeta \qquad (\text{as } k \to 0) \tag{3.6}$$

with

$$0 < \widehat{E}_\zeta^{(0)}(t) < \infty \,. \tag{3.7}$$

In the rest of this subsection, we shall consider the existence and the temporal invariance conditions of $\widehat{E}_\zeta^{(0)}$. The results are summarized in Table.3.1.

Although there is no universality of $\zeta$, this index is limited as $\zeta \le 4$ because the coefficient of the $k^4$ term in (3.5) does not vanish in general. On the other hand, if $\zeta$ is less than 2 the Fourier component of the velocity correlation tensor $V_{ij}(\boldsymbol{k},t,t')$ diverges at the origin. Therefore, we restrict ourselves to the cases

$$2 \le \zeta \le 4 \,, \tag{3.8}$$

and consider the behavior of $\widehat{E}_\zeta^{(0)}$ separately in three cases, that is, $\zeta = 2$, 4 and $2 < \zeta < 4$. For $\zeta = 2$, (3.5) requires that $f(r,t) \propto r^{-3}$ as $r \to \infty$, and then $\widehat{E}_2^{(0)}$ is expressed as

$$\widehat{E}_2^{(0)}(t) = \frac{u_m^2}{\pi} \lim_{r\to\infty} r^3 f(r,t) \,. \tag{3.9}$$

In the case $2 < \zeta < 4$, (3.4) yields

$$\widehat{E}_\zeta^{(0)}(t) = \lim_{k\to 0} k^{1-\zeta} \frac{u_m^2}{\pi} \lim_{r\to\infty} r^2 f(r,t) \, \sin(kr) \qquad (2 < \zeta < 4) \,, \tag{3.10}$$

which requires, by the condition (3.7), that $f(r,t) \propto r^{-\zeta-1}$ as $r \to \infty$. Thus, we obtain

$$\widehat{E}_\zeta^{(0)}(t) = \frac{u_m^2}{\pi} \lim_{r\to\infty} r^{\zeta+1} f(r,t) \qquad (2 < \zeta < 4) \,. \tag{3.11}$$

Therefore, the two cases $\zeta = 2$ and $2 < \zeta < 4$ can be considered together (see (3.9) and (3.11)). As for the case $\zeta = 4$, on the other hand, it is easy to show from (3.5) that $f(r,t)$ must decay faster than $r^{-5}$ as $r \to \infty$, and then $\widehat{E}_4^{(0)}$ is expressed as

$$\widehat{E}_4^{(0)}(t) = \frac{u_m^2}{3\pi} \int_0^\infty \mathrm{d}r \, r^4 f(r,t) \,. \tag{3.12}$$

| | $2 \leq \zeta < 4$ | $\zeta = 4$ |
|---|---|---|
| $\widehat{E}_\zeta^{(0)}(t)$ | $\frac{u_m^2}{\pi} \lim_{r\to\infty} r^{\zeta+1} f(r,t)$ | $\frac{u_m^2}{3\pi} \int_0^\infty \mathrm{d}r\, f(r,t)\, r^4$ |
| Existence condition of $\widehat{E}_\zeta^{(0)}(t)$ | $f(r,t) \propto r^{-\zeta-1}$ as $r \to \infty$. | $f(r,t)$ decays faster than $r^{-5}$. |
| Invariance condition of $\widehat{E}_\zeta^{(0)}(t)$ | $h(r,t)$ decays faster than $r^{-\zeta}$. | $h(r,t)$ decays faster than $r^{-4}$. |

TABLE 3.1 Summary of §3.1.2. Parameter $\zeta$ represents the behavior of the energy spectrum $E(k,t)$ at the vicinity of the origin as $E(k,t) = \widehat{E}_\zeta^{(0)}(t)\, k^\zeta$ $(k \to 0)$.

Next, we consider temporal invariance of large-scale structure in terms of $\widehat{E}_\zeta^{(0)}(t)$ by the use of the Kármán-Howarth equation [41],

$$u_m^2 \frac{\partial}{\partial t} f(r,t) = u_m^3 \left[ \frac{\partial}{\partial r} h(r,t) + 4 \frac{h(r,t)}{r} \right] + 2\nu\, u_m^2 \left[ \frac{\partial^2}{\partial r^2} f(r,t) + \frac{4}{r} \frac{\partial}{\partial r} f(r,t) \right], \tag{3.13}$$

where $h(r,t)$ is the two-point triple velocity correlation function defined by

$$u_m^3\, h(r,t) = \overline{u_1(\boldsymbol{x},t)^2\, u_1(\boldsymbol{x}+\boldsymbol{r},t)}\,. \tag{3.14}$$

By taking the limit $r \to \infty$ of (3.13) multiplied by $r^{\zeta+1}/\pi$, we obtain

$$\frac{\mathrm{d}}{\mathrm{d}t} \widehat{E}_\zeta^{(0)}(t) = \frac{C_\zeta}{\pi} u_m^3 \lim_{r\to\infty} \left[ r^{\zeta-3} \frac{\partial}{\partial r} \left( r^4\, h(r,t) \right) \right] \qquad (2 \leq \zeta < 4)\,. \tag{3.15}$$

Hence, if $h(r,t)$ decays faster than $r^{-\zeta}$ as $r \to \infty$, $E_\zeta^{(0)}$ does not vary in time. On the other hand, for $\zeta = 4$, we multiply $r^4/(3\pi)$ to (3.13), and integrate from 0 to $\infty$ with respect to $r$ to obtain

$$\frac{\mathrm{d}}{\mathrm{d}t} \widehat{E}_4^{(0)}(t) = \frac{u_m^3}{3\pi} \lim_{r\to\infty} r^4\, h(r,t)\,. \tag{3.16}$$

The time invariance of $\widehat{E}_4^{(0)}$ requires that $h(r,t)$ decays faster than $r^{-4}$. Batchelor & Proudman [42] pointed out a case that $\widehat{E}_4^{(0)}$ does exist but is not invariant in time. We call $\widehat{E}_2^{(0)}$ and $\widehat{E}_4^{(0)}$ the Birkhoff constant [38] and the Loitsiansky integral [39], respectively.

### 3.1.3 Review of DIA family

Since the introduction of DIA by Kraichnan [24], many versions of application methods of DIA to the Navier-Stokes turbulence have been proposed. We review here the history briefly. A closed set of integro-differential equations for the correlation and the response functions of the Eulerian velocity $u_i(\boldsymbol{x},t)$, which represents the fluid velocity at a fixed position $\boldsymbol{x}$ at time $t$, are formulated

in the original DIA [24]. We call this kind of the direct-interaction approximation the Eulerian DIA. Although the Eulerian DIA seems to be the most naive application of DIA, it unfortunately predicts the $k^{-3/2}$ energy spectrum in the inertial range, which is inconsistent with the Kolmogorov phenomenology (3.3). This failure may be related to the fact the Eulerian statistical quantities violate the Galilean invariance [37, 12], which is one of the important symmetries inherent in the Navier-Stokes turbulence [21]. The closure equations by the Eulerian DIA are also derived by many kinds of different approximations [18, 25–27]. It should be stressed again (see Chapter 2 for detailed discussions) that although these approximations yield identical closure equations to those by the Eulerian DIA, they are based upon completely different idea and working assumptions. Hence, we have to distinguish these approximations from the DIA.

There have been proposed several closure theories to solve the misprediction of the $k^{-5/3}$ power law of the energy spectrum by the Eulerian DIA. McComb and his coworkers [43–46] developed the local energy transfer (LET) theory, in which the closure equation for the Eulerian velocity correlation function is identical to that by the Eulerian DIA, while the fluctuation-dissipation relation,

$$Q^{(E)}(\boldsymbol{k}, t, t') = Q^{(E)}(\boldsymbol{k}, t, t)\, G^{(E)}(\boldsymbol{k}, t, t')\,, \tag{3.17}$$

where $Q^{(E)}$ and $G^{(E)}$ are respectively the correlation and the response (called propagator by them) functions of the Eulerian velocity, is introduced instead of the Eulerian DIA equation for the response function. The LET theory is consistent with the Kolmogorov phenomenology and yields the $k^{-5/3}$ power law spectrum in the inertial range with the Kolmogorov constant $K \approx 2.3$ [44]. On the other hand, Kraichnan [37] proposed Lagrangian versions of DIA, in which closure equations for the correlation and the response functions of the Lagrangian velocity $v_i(t|\boldsymbol{x}, s)$, which represents the velocity at time $t$ of a fluid particle passing $\boldsymbol{x}$ at time $s$. There are two versions of Kraichnan's Lagrangian DIA, i.e., the abridged Lagrangian history DIA (ALHDIA) and the strain-based abridged Lagrangian history DIA (SBALHDIA) [47]. Although these abridged Lagrangian DIAs are shown to be consistent with the Kolmogorov spectrum in the inertial range (the Kolmogorov constant is evaluated as $K \approx 1.77$ by ALHDIA [48] and 2.0 by SBALHDIA [49]), it is difficult for the author to understand their formulations because they have an intuitive procedure called the abridgment.

We shall propose another Lagrangian DIA in the present chapter, which is much simpler than the ALHDIAs. Although we shall also construct a closed set of integro-differential equations for the Lagrangian velocity correlation and the response functions, the definition of the correlation function is different from the one employed in ALHDIA. In our formulation, the correlation function depends on only two times; the measuring time $t$ and the labeling time $s$, while it has three times $t$, $t'$ and $s$ in ALHDIAs. Hence, we need not employ the abridgment. The resultant equations in our formulation of Lagrangian DIA are identical to those derived by RRE (§2.4) proposed by Kaneda [36], which is called the Lagrangian renormalized approximation (LRA). Hence, we name the resultant closure equations the LRA-DIA equations. As discussed in Chapter 2, DIA and RRE are based upon completely different working assumptions and have different parameter range of validity. Therefore, the fact that they yield identical closure equation may imply its wide applicability. The properties of the LRA-DIA equations have been examined by Kaneda and his coworkers [36, 50–52]. It has been shown that the LRA-DIA equations yield the Kolmogorov spectrum (3.3) in the inertial range with $K \approx 1.722$ [50], which is in good agreement with measurements (see Ref. [40]).

## 3.2 Preparations

### 3.2.1 Basic equations

As mentioned in Chapter 1, we assume that the motion of an incompressible (Newtonian) viscous fluid is described by the Navier-Stokes equation,

$$\frac{\partial}{\partial t} u_i(\boldsymbol{x},t) + u_j(\boldsymbol{x},t) \frac{\partial}{\partial x_j} u_i(\boldsymbol{x},t) = -\frac{1}{\rho} \frac{\partial}{\partial x_i} p(\boldsymbol{x},t) + \nu \frac{\partial^2}{\partial x_j \partial x_j} u_i(\boldsymbol{x},t) \quad (i=1,2,3) \tag{3.18}$$

and the equation of continuity,

$$\frac{\partial}{\partial x_i} u_i(\boldsymbol{x},t) = 0\,. \tag{3.19}$$

Here, we employ, in contrast with Chapter 2, the summation convention for a repeated subscript.

### 3.2.2 Lagrangian velocity correlation function

In manipulation of Lagrangian quantities, the Lagrangian position function,

$$\psi(\boldsymbol{x},t|\boldsymbol{x}',t') = \delta^3(\boldsymbol{x} - \boldsymbol{y}(t|\boldsymbol{x}',t')) \tag{3.20}$$

plays an important role [36]. Here, $\boldsymbol{y}(t|\boldsymbol{x}',t')$ stands for the Lagrangian coordinate (i.e., the position of a fluid element at time $t$ which passed position $\boldsymbol{x}'$ at time $t'\,(<t)$), and $\delta^3$ is Dirac's delta function. The position function obeys

$$\frac{\partial}{\partial t} \psi(\boldsymbol{x},t|\boldsymbol{x}',t') = -u_j(\boldsymbol{x},t) \frac{\partial}{\partial x_j} \psi(\boldsymbol{x},t|\boldsymbol{x}',t') \tag{3.21}$$

with initial condition,

$$\psi(\boldsymbol{x},t'|\boldsymbol{x}',t') = \delta^3(\boldsymbol{x} - \boldsymbol{x}')\,. \tag{3.22}$$

The Lagrangian velocity $v_i(t|\boldsymbol{x}',t') = u_i(\boldsymbol{y}(t|\boldsymbol{x}',t'),t)$ and the Eulerian velocity are related with each other as

$$v_i(t|\boldsymbol{x}',t') = \int \mathrm{d}^3\boldsymbol{x}\; u_i(\boldsymbol{x},t)\; \psi(\boldsymbol{x},t|\boldsymbol{x}',t')\,, \tag{3.23}$$

$$u_i(\boldsymbol{x},t) = \int \mathrm{d}^3\boldsymbol{x}'\; v_i(t|\boldsymbol{x}',t')\; \psi(\boldsymbol{x},t|\boldsymbol{x}',t')\,. \tag{3.24}$$

A main purpose of this chapter is to construct a system of equations for the Lagrangian velocity correlation function which is defined by

$$V_{ij}(\boldsymbol{r},t,t') = \overline{v_i(t|\boldsymbol{x}+\boldsymbol{r},t')\, v_j(t'|\boldsymbol{x},t')} = \overline{v_i(t|\boldsymbol{x}+\boldsymbol{r},t')\, u_j(\boldsymbol{x},t')}\,. \tag{3.25}$$

Here and below, an overbar denotes an ensemble average. We have assumed that the velocity field is statistically homogeneous, so that $V_{ij}$ is independent of position vector $\boldsymbol{x}$.

### 3.2.3 Fourier decomposition

For simplicity of description, we consider the motion of a fluid confined in a periodic cube of side $L$. Then we can expand $u_i$, $v_i$, $\psi$ and $V_{ij}$ in Fourier series as

$$u_i(\boldsymbol{x},t) = \left(\frac{2\pi}{L}\right)^3 \sum_{\boldsymbol{k}} \tilde{u}_i(\boldsymbol{k},t)\, \exp\Big[\mathrm{i}\boldsymbol{k}\cdot\boldsymbol{x}\Big], \tag{3.26}$$

$$v_i(t|\boldsymbol{x}',t') = \left(\frac{2\pi}{L}\right)^3 \sum_{\boldsymbol{k}} \tilde{v}_i(t|\boldsymbol{k},t')\, \exp\Big[\mathrm{i}\boldsymbol{k}\cdot\boldsymbol{x}'\Big], \tag{3.27}$$

$$\psi(\boldsymbol{x},t|\boldsymbol{x}',t') = \left(\frac{2\pi}{L}\right)^6 \sum_{\boldsymbol{k}}\sum_{\boldsymbol{k}'} \tilde{\psi}(\boldsymbol{k},t|\boldsymbol{k}',t')\, \exp\Big[\mathrm{i}\,(\boldsymbol{k}\cdot\boldsymbol{x}+\boldsymbol{k}'\cdot\boldsymbol{x}')\Big] \tag{3.28}$$

and

$$V_{ij}(\boldsymbol{r},t,t') = \left(\frac{2\pi}{L}\right)^3 \sum_{\boldsymbol{k}} \tilde{V}_{ij}(\boldsymbol{k},t,t')\, \exp\Big[\mathrm{i}\boldsymbol{k}\cdot\boldsymbol{r}\Big], \tag{3.29}$$

respectively, where

$$\boldsymbol{k} = \frac{2\pi}{L}\,(n_1,n_2,n_3) \qquad (n_1,n_2,n_3 = 0,\pm1,\pm2,\cdots) \tag{3.30}$$

is the wavenumber vector. The summations are taken over triplets of integers $n_1$, $n_2$ and $n_3$. The Fourier inverse transformations are written as

$$\tilde{u}_i(\boldsymbol{k},t) = \left(\frac{1}{2\pi}\right)^3 \int \mathrm{d}^3\boldsymbol{x}\, u_i(\boldsymbol{x},t)\, \exp\Big[-\mathrm{i}\boldsymbol{k}\cdot\boldsymbol{x}\Big], \tag{3.31}$$

$$\tilde{v}_i(t|\boldsymbol{k},t') = \left(\frac{1}{2\pi}\right)^3 \int \mathrm{d}^3\boldsymbol{x}\, v_i(t|\boldsymbol{x}',t')\, \exp\Big[-\mathrm{i}\boldsymbol{k}\cdot\boldsymbol{x}'\Big], \tag{3.32}$$

$$\tilde{\psi}(\boldsymbol{k},t|\boldsymbol{k}',t') = \left(\frac{1}{2\pi}\right)^6 \int \mathrm{d}^3\boldsymbol{x} \int \mathrm{d}^3\boldsymbol{x}'\, \psi(\boldsymbol{x},t|\boldsymbol{x}',t')\, \exp\Big[-\mathrm{i}(\boldsymbol{k}\cdot\boldsymbol{x}+\boldsymbol{k}'\cdot\boldsymbol{x}')\Big] \tag{3.33}$$

and

$$\tilde{V}_{ij}(\boldsymbol{k},t,t') = \left(\frac{1}{2\pi}\right)^3 \int \mathrm{d}^3\boldsymbol{r}\, V_{ij}(\boldsymbol{r},t,t')\, \exp\Big[-\mathrm{i}\boldsymbol{k}\cdot\boldsymbol{r}\Big] = \left(\frac{2\pi}{L}\right)^3 \overline{\tilde{v}_i(t|\boldsymbol{k},t')\,\tilde{u}_j(-\boldsymbol{k},t')}\,, \tag{3.34}$$

respectively. In these equations, integrations are carried out over the periodic cube. Relations between Lagrangian velocity (3.23) and Eulerian velocity (3.24) are written, in the Fourier space, as

$$\tilde{v}_i(t|\boldsymbol{k},t') = \frac{(2\pi)^6}{L^3} \sum_{\boldsymbol{k}'} \tilde{u}_i(\boldsymbol{k}',t)\, \tilde{\psi}(-\boldsymbol{k}',t|\boldsymbol{k},t') \tag{3.35}$$

and

$$\tilde{u}_i(\boldsymbol{k},t) = \frac{(2\pi)^6}{L^3} \sum_{\boldsymbol{k}'} \tilde{v}_i(t|\boldsymbol{k}',t')\, \tilde{\psi}(\boldsymbol{k},t|-\boldsymbol{k}',t')\,, \tag{3.36}$$

respectively.

The governing equations of $\tilde{u}_i$ and $\tilde{\psi}$ are derived from (3.18), (3.19), (3.21) and (3.22) as

$$\left[\frac{\partial}{\partial t} + \nu\, k^2\right] \tilde{u}_i(\boldsymbol{k},t) = -\frac{\mathrm{i}}{2} \left(\frac{2\pi}{L}\right)^3 \tilde{P}_{ijm}(\boldsymbol{k}) \sum_{\substack{\boldsymbol{p}\\(\boldsymbol{k}+\boldsymbol{p}+\boldsymbol{q}=\boldsymbol{o})}} \sum_{\boldsymbol{q}} \tilde{u}_j(-\boldsymbol{p},t)\, \tilde{u}_m(-\boldsymbol{q},t)\,, \tag{3.37}$$

$$k_i\,\tilde{u}_i(\boldsymbol{k},t)=0\,, \tag{3.38}$$

and

$$\frac{\partial}{\partial t}\,\tilde{\psi}(\boldsymbol{k},t|\boldsymbol{k}',t')=-\mathrm{i}\,k_j\left(\frac{2\pi}{L}\right)^3\sum_{\substack{\boldsymbol{p}\\(\boldsymbol{k}+\boldsymbol{p}+\boldsymbol{q}=\boldsymbol{o})}}\sum_{\boldsymbol{q}}\tilde{u}_j(-\boldsymbol{p},t)\,\tilde{\psi}(-\boldsymbol{q},t|\boldsymbol{k}',t') \tag{3.39}$$

with initial condition

$$\tilde{\psi}(\boldsymbol{k},t'|\boldsymbol{k}',t')=\frac{L^3}{(2\pi)^6}\,\delta^3_{\boldsymbol{k}+\boldsymbol{k}'}\,. \tag{3.40}$$

Here,

$$\tilde{P}_{ijm}(\boldsymbol{k})=k_m\,\tilde{P}_{ij}(\boldsymbol{k})+k_j\,\tilde{P}_{im}(\boldsymbol{k})\,,\quad \tilde{P}_{ij}(\boldsymbol{k})=\delta_{ij}-\frac{k_ik_j}{k^2}\,, \tag{3.41}$$

where $\delta^3_{\boldsymbol{k}}$ and $\delta_{ij}$ are Kronecker's deltas ($\delta^3_{\boldsymbol{k}}=0(\boldsymbol{k}\neq\boldsymbol{o})$, $\delta^3_{\boldsymbol{k}}=1(\boldsymbol{k}=\boldsymbol{o})$, $\delta_{ij}=0(i\neq j)$, $\delta_{ij}=1(i=j)$). The time derivative of (3.35) then yields

$$\begin{aligned}\frac{\partial}{\partial t}\,\tilde{v}_i(t|\boldsymbol{k}',t')=&-\frac{(2\pi)^6}{L^3}\,\nu\sum_{\boldsymbol{p}}p^2\,\tilde{u}_i(\boldsymbol{p},t)\,\tilde{\psi}(-\boldsymbol{p},t|\boldsymbol{k}',t')\\&-\mathrm{i}\,\frac{(2\pi)^9}{L^6}\sum_{\substack{\boldsymbol{p}\\(\boldsymbol{p}+\boldsymbol{q}+\boldsymbol{r}=\boldsymbol{o})}}\sum_{\boldsymbol{q}}\sum_{\boldsymbol{r}}\frac{r_ir_mr_n}{r^2}\,\tilde{u}_m(\boldsymbol{p},t)\,\tilde{u}_n(\boldsymbol{q},t)\,\tilde{\psi}(\boldsymbol{r},t|\boldsymbol{k}',t')\,,\end{aligned} \tag{3.42}$$

where use has been made of (3.37) and (3.39). By using (3.34), (3.37) and (3.42), we can derive the governing equations of the two-point Lagrangian velocity correlation function for a single time as

$$\begin{aligned}\left[\frac{\partial}{\partial t}+2\nu k^2\right]\tilde{V}_{ij}(\boldsymbol{k},t,t)=&-\frac{\mathrm{i}}{2}\left(\frac{2\pi}{L}\right)^6\tilde{P}_{imn}(\boldsymbol{k})\sum_{\substack{\boldsymbol{p}\\(\boldsymbol{k}+\boldsymbol{p}+\boldsymbol{q}=\boldsymbol{o})}}\sum_{\boldsymbol{q}}\overline{\tilde{u}_m(-\boldsymbol{p},t)\,\tilde{u}_n(-\boldsymbol{q},t)\,\tilde{u}_j(-\boldsymbol{k},t)}\\&+(i\leftrightarrow j\,,\ \boldsymbol{k}\to-\boldsymbol{k})\end{aligned} \tag{3.43}$$

and for two times as

$$\begin{aligned}\frac{\partial}{\partial t}\,\tilde{V}_{ij}(\boldsymbol{k},t,t')=&-\frac{(2\pi)^9}{L^6}\,\nu\sum_{\boldsymbol{p}}p^2\,\overline{\tilde{u}_i(\boldsymbol{p},t)\,\tilde{\psi}(-\boldsymbol{p},t|\boldsymbol{k},t')\,\tilde{u}_j(-\boldsymbol{k},t')}\\&-\mathrm{i}\,\frac{(2\pi)^{12}}{L^9}\sum_{\substack{\boldsymbol{p}\\(\boldsymbol{p}+\boldsymbol{q}+\boldsymbol{r}=\boldsymbol{o})}}\sum_{\boldsymbol{q}}\sum_{\boldsymbol{r}}\frac{r_ir_mr_n}{r^2}\,\overline{\tilde{u}_m(\boldsymbol{p},t)\,\tilde{u}_n(\boldsymbol{q},t)\,\tilde{\psi}(\boldsymbol{r},t|\boldsymbol{k},t')\,\tilde{u}_j(-\boldsymbol{k},t')}\,.\end{aligned} \tag{3.44}$$

The higher-order correlation functions on the right-hand side of (3.43) and (3.44) are the origin of the closure problem (§1.2) of the Navier-Stokes turbulence. Based upon the idea of DIA, we shall attack this problem in the next section.

For later convenience, we define here the energy spectrum,

$$E(k,t)=\frac{1}{2}\,k^2\oint\mathrm{d}\Omega\,\tilde{V}_{ii}(\boldsymbol{k},t,t)\,, \tag{3.45}$$

where $\oint\mathrm{d}\Omega$ denotes a solid angle integration in the Fourier space, and the incompressible part of the Lagrangian velocity correlation,

$$\tilde{Q}_{ij}(\boldsymbol{k},t,t')=\tilde{P}_{im}(\boldsymbol{k})\,\tilde{V}_{mj}(\boldsymbol{k},t,t')\,. \tag{3.46}$$

### 3.2.4 Response function

The response functions of the velocity and the position functions [24] play a key role in the present formulation. The Eulerian velocity response function,

$$\widetilde{G}_{ij}^{(E)}(\boldsymbol{k},t|\boldsymbol{k}',t') = \frac{\delta\widetilde{u}_i(\boldsymbol{k},t)}{\delta\widetilde{u}_j(\boldsymbol{k}',t')} \tag{3.47}$$

expresses the influence on $\widetilde{u}_i(\boldsymbol{k},t)$ at time $t$ due to an infinitesimal disturbance for $\widetilde{u}_j(\boldsymbol{k}',t')$ $(t' \le t)$, where $\delta$ denotes a functional derivative. By taking a functional derivative of (3.37), we obtain the governing equation for this function as

$$\left[\frac{\partial}{\partial t} + \nu k^2\right]\widetilde{G}_{ij}^{(E)}(\boldsymbol{k},t|\boldsymbol{k}',t') = -\mathrm{i}\left(\frac{2\pi}{L}\right)^3 \widetilde{P}_{imn}(\boldsymbol{k}) \sum_{\substack{\boldsymbol{p}\\(\boldsymbol{k}+\boldsymbol{p}+\boldsymbol{q}=\boldsymbol{o})}}\sum_{\boldsymbol{q}} \widetilde{u}_m(-\boldsymbol{p},t)\,\widetilde{G}_{nj}^{(E)}(-\boldsymbol{q},t|\boldsymbol{k}',t')\,. \tag{3.48}$$

The initial condition is given by

$$\widetilde{G}_{ij}^{(E)}(\boldsymbol{k},t'|\boldsymbol{k}',t') = \frac{L^3}{(2\pi)^6}\,\delta_{ij}\,\delta^3_{\boldsymbol{k}+\boldsymbol{k}'}\,. \tag{3.49}$$

Similarly, the governing equations of the Lagrangian velocity response function,

$$\widetilde{G}_{ij}^{(L)}(t|\boldsymbol{k},\boldsymbol{k}',t') = \frac{\delta\widetilde{v}_i(t|\boldsymbol{k},t')}{\delta\widetilde{u}_j(\boldsymbol{k}',t')} \tag{3.50}$$

and the position response function,

$$\widetilde{\Psi}_i(\boldsymbol{k},t|\boldsymbol{k}',\boldsymbol{k}'',t') = \frac{\delta\widetilde{\psi}(\boldsymbol{k},t|\boldsymbol{k}',t')}{\delta\widetilde{u}_i(\boldsymbol{k}'',t')} \tag{3.51}$$

are obtained from (3.42) and (3.39), respectively, as

$$\begin{aligned}
&\frac{\partial}{\partial t}\widetilde{G}_{ij}^{(L)}(t|\boldsymbol{k},\boldsymbol{k}',t') = \\
&\quad -\nu\frac{(2\pi)^6}{L^3}\sum_{\boldsymbol{k}''} k''^2\left[\widetilde{G}_{ij}^{(E)}(\boldsymbol{k}'',t|\boldsymbol{k}',t')\,\widetilde{\psi}(-\boldsymbol{k}'',t|\boldsymbol{k},t') + \widetilde{u}_i(\boldsymbol{k}'',t)\,\widetilde{\Psi}_j(-\boldsymbol{k}'',t|\boldsymbol{k},\boldsymbol{k}',t')\right] \\
&\quad -\mathrm{i}\frac{(2\pi)^9}{L^6}\sum_{\substack{\boldsymbol{p}\\(\boldsymbol{p}+\boldsymbol{q}+\boldsymbol{r}=\boldsymbol{o})}}\sum_{\boldsymbol{q}}\sum_{\boldsymbol{r}}\frac{r_i r_m r_n}{r^2}\left[2\widetilde{u}_m(\boldsymbol{p},t)\,\widetilde{G}_{nj}^{(E)}(\boldsymbol{q},t|\boldsymbol{k}',t')\,\widetilde{\psi}(\boldsymbol{r},t|\boldsymbol{k},t')\right. \\
&\qquad\qquad \left. +\widetilde{u}_m(\boldsymbol{p},t)\,\widetilde{u}_n(\boldsymbol{q},t)\,\widetilde{\Psi}_j(\boldsymbol{r},t|\boldsymbol{k},\boldsymbol{k}',t')\right]
\end{aligned} \tag{3.52}$$

with initial condition,

$$\widetilde{G}_{ij}^{(L)}(t'|\boldsymbol{k},\boldsymbol{k}',t') = \frac{L^3}{(2\pi)^6}\,\delta_{ij}\,\delta^3_{\boldsymbol{k}+\boldsymbol{k}'}\,, \tag{3.53}$$

and

$$\begin{aligned}
&\frac{\partial}{\partial t}\widetilde{\Psi}_i(\boldsymbol{k},t|\boldsymbol{k}',\boldsymbol{k}'',t') = \\
&\quad -\mathrm{i}\,k_a\left(\frac{2\pi}{L}\right)^3\sum_{\substack{\boldsymbol{p}\\(\boldsymbol{k}+\boldsymbol{p}+\boldsymbol{q}=\boldsymbol{o})}}\sum_{\boldsymbol{q}}\left[\widetilde{u}_a(-\boldsymbol{p},t)\,\widetilde{\Psi}_i(-\boldsymbol{q},t|\boldsymbol{k}',\boldsymbol{k}'',t') + \widetilde{G}_{ai}^{(E)}(-\boldsymbol{p},t|\boldsymbol{k}'',t')\,\widetilde{\psi}(-\boldsymbol{q},t|\boldsymbol{k}',t')\right]
\end{aligned} \tag{3.54}$$

with initial condition,

$$\widetilde{\Psi}_i(\boldsymbol{k}, t'|\boldsymbol{k}', \boldsymbol{k}'', t') = 0\,. \tag{3.55}$$

A functional derivative of (3.36) gives a relation among the Eulerian velocity response, the Lagrangian velocity response and the position response functions as

$$\begin{aligned}\widetilde{G}^{(E)}_{ij}(\boldsymbol{k}, t|\boldsymbol{k}', t') = {} & \frac{(2\pi)^6}{L^3} \sum_{\boldsymbol{k}''} \widetilde{G}^{(L)}_{ij}(t|\boldsymbol{k}'', \boldsymbol{k}', t')\, \widetilde{\psi}(\boldsymbol{k}, t| - \boldsymbol{k}'', t') \\ & + \frac{(2\pi)^{12}}{L^6} \sum_{\boldsymbol{k}''} \sum_{\boldsymbol{k}'''} \widetilde{u}_i(\boldsymbol{k}''', t)\, \widetilde{\psi}(-\boldsymbol{k}''', t|\boldsymbol{k}'', t')\, \widetilde{\Psi}_j(\boldsymbol{k}, t| - \boldsymbol{k}'', \boldsymbol{k}', t')\,. \end{aligned} \tag{3.56}$$

For later use, we define here the incompressible part of the Lagrangian velocity response function by

$$\widetilde{G}_{ij}(\boldsymbol{k}, t, t') = \frac{(2\pi)^6}{L^3}\, \overline{\widetilde{G}^{(L)}_{im}(t|\boldsymbol{k}, -\boldsymbol{k}, t')}\, \widetilde{P}_{mj}(\boldsymbol{k})\,. \tag{3.57}$$

## 3.3 Lagrangian direct-interaction approximation

### 3.3.1 Direct-interaction decomposition

The DIA, discussed in Chapter 2, is applied to the Navier-Stokes turbulence to construct a closed set of equations for the Lagrangian velocity correlation and the response functions. The assumptions and procedures employed here, which will be summarized in the next section, and those in Chapter 2 are the same, except for treatments of the position function. Similarly to $X_i$ in the model equation (2.1), we first introduce the direct-interaction decomposition for the Fourier component of the Eulerian velocity $\widetilde{u}_i$ governed by (3.37).

Recall that the right-hand side of the Navier-Stokes equation (3.37) is composed of a sum of an infinite number of quadratic nonlinear terms, each of which represents direct-interactions between three Fourier components with wavenumbers $\boldsymbol{k}$, $\boldsymbol{p}$ and $\boldsymbol{q}$ which construct a triangle ($\boldsymbol{k} + \boldsymbol{p} + \boldsymbol{q} = \boldsymbol{o}$). We choose arbitrarily a triangular triplet of wavenumbers, say $\boldsymbol{k}_0$, $\boldsymbol{p}_0$ and $\boldsymbol{q}_0$ ($\boldsymbol{k}_0 + \boldsymbol{p}_0 + \boldsymbol{q}_0 = \boldsymbol{o}$), and imagine a fictitious field which does not contain the direct interactions between these three wavenumbers. This fictitious field is called the NDI field (non-direct-interaction field), and is denoted by $\widetilde{u}^{(0)}_i(\boldsymbol{k}, t\|\boldsymbol{k}_0, \boldsymbol{p}_0, \boldsymbol{q}_0)$. Furthermore, we define the deviation field $\widetilde{u}^{(1)}_i(\boldsymbol{k}, t\|\boldsymbol{k}_0, \boldsymbol{p}_0, \boldsymbol{q}_0)$ by the difference between the true field and the NDI field, namely,

$$\widetilde{u}_i(\boldsymbol{k}, t) = \widetilde{u}^{(0)}_i(\boldsymbol{k}, t\|\boldsymbol{k}_0, \boldsymbol{p}_0, \boldsymbol{q}_0) + \widetilde{u}^{(1)}_i(\boldsymbol{k}, t\|\boldsymbol{k}_0, \boldsymbol{p}_0, \boldsymbol{q}_0). \tag{3.58}$$

This decomposition is made at time $t_0$, the initial condition of the deviation field $\widetilde{u}^{(1)}_i$ is, therefore, expressed as

$$\widetilde{u}^{(1)}_i(\boldsymbol{k}, t_0\|\boldsymbol{k}_0, \boldsymbol{p}_0, \boldsymbol{q}_0) = 0\,. \tag{3.59}$$

By definition, the governing equation for $\tilde{u}_i^{(0)}$ is written as

$$\left[\frac{\partial}{\partial t}+\nu k^2\right]\tilde{u}_i^{(0)}(\boldsymbol{k},t\|\boldsymbol{k}_0,\boldsymbol{p}_0,\boldsymbol{q}_0)$$
$$=-\frac{\mathrm{i}}{2}\left(\frac{2\pi}{L}\right)^3\tilde{P}_{ijm}(\boldsymbol{k})\sum_{\substack{\boldsymbol{p}\\(\boldsymbol{k}+\boldsymbol{p}+\boldsymbol{q}=\boldsymbol{o})}}\sum_{\boldsymbol{q}}{}'\,\tilde{u}_j^{(0)}(-\boldsymbol{p},t\|\boldsymbol{k}_0,\boldsymbol{p}_0,\boldsymbol{q}_0)\tilde{u}_m^{(0)}(-\boldsymbol{q},t\|\boldsymbol{k}_0,\boldsymbol{p}_0,\boldsymbol{q}_0)\,, \quad (3.60)$$

where $\Sigma\Sigma'$ stands for summation without the interactions among chosen three wavenumbers $\boldsymbol{k}_0$, $\boldsymbol{p}_0$ and $\boldsymbol{q}_0$. Subtracting the above equation from the Navier-Stokes equation (3.37), we obtain the time-evolution equation of the deviation field as

$$\left[\frac{\partial}{\partial t}+\nu k^2\right]\tilde{u}_i^{(1)}(\boldsymbol{k},t\|\boldsymbol{k}_0,\boldsymbol{p}_0,\boldsymbol{q}_0)$$
$$=-\mathrm{i}\left(\frac{2\pi}{L}\right)^3\tilde{P}_{ijm}(\boldsymbol{k})\sum_{\substack{\boldsymbol{p}\\(\boldsymbol{k}+\boldsymbol{p}+\boldsymbol{q}=\boldsymbol{o})}}\sum_{\boldsymbol{q}}{}'\,\tilde{u}_j(-\boldsymbol{p},t)\tilde{u}_m^{(1)}(-\boldsymbol{q},t\|\boldsymbol{k}_0,\boldsymbol{p}_0,\boldsymbol{q}_0)$$
$$-\delta^3_{\boldsymbol{k}-\boldsymbol{k}_0}\,\mathrm{i}\left(\frac{2\pi}{L}\right)^3\tilde{P}_{ijm}(\boldsymbol{k}_0)\;\tilde{u}_j^{(0)}(-\boldsymbol{p}_0,t|\boldsymbol{k}_0,\boldsymbol{p}_0,\boldsymbol{q}_0)\,\tilde{u}_m^{(0)}(-\boldsymbol{q}_0,t|\boldsymbol{k}_0,\boldsymbol{p}_0,\boldsymbol{q}_0)$$
$$+\delta^3_{\boldsymbol{k}+\boldsymbol{k}_0}\,\mathrm{i}\left(\frac{2\pi}{L}\right)^3\tilde{P}_{ijm}(\boldsymbol{k}_0)\,\tilde{u}_j^{(0)}(\boldsymbol{p}_0,t|\boldsymbol{k}_0,\boldsymbol{p}_0,\boldsymbol{q}_0)\,\tilde{u}_m^{(0)}(\boldsymbol{q}_0,t|\boldsymbol{k}_0,\boldsymbol{p}_0,\boldsymbol{q}_0)$$
$$+(\boldsymbol{p}_0\to\boldsymbol{q}_0\to\boldsymbol{k}_0\to\boldsymbol{p}_0)\,, \quad (3.61)$$

where we have neglected the higher-order terms of $\tilde{u}^{(1)}$ (Assumption 1 written in the next subsection). The direct-interaction decompositions for the Eulerian velocity response function (3.48), the position function (3.39) and the position response function (3.54) are performed similarly (Appendix A).

By comparing (3.61) with (3.163) in Appendix A, we find that $\tilde{G}_{ij}^{(E0)}$ serves as Green's function of $\tilde{u}_i^{(1)}$. A solution to (3.61) is therefore expressed in terms of $\tilde{G}_{ij}^{(E0)}$ and $\tilde{u}_i^{(0)}$ as

$$\tilde{u}_i^{(1)}(\boldsymbol{k},t\|\boldsymbol{k}_0,\boldsymbol{p}_0,\boldsymbol{q}_0)=\mathrm{i}\,\frac{(2\pi)^9}{L^6}\,\tilde{P}_{abc}(\boldsymbol{k})\int_{t_0}^{t}\mathrm{d}t'\,\tilde{G}_{ia}^{(E0)}(\boldsymbol{k},t|-\boldsymbol{k},t'\|\boldsymbol{k}_0,\boldsymbol{p}_0,\boldsymbol{q}_0)$$
$$\times\Big[-\delta^3_{\boldsymbol{k}-\boldsymbol{k}_0}\,\tilde{u}_b^{(0)}(-\boldsymbol{p}_0,t'|\boldsymbol{k}_0,\boldsymbol{p}_0,\boldsymbol{q}_0)\,\tilde{u}_c^{(0)}(-\boldsymbol{q}_0,t'|\boldsymbol{k}_0,\boldsymbol{p}_0,\boldsymbol{q}_0)$$
$$-\delta^3_{\boldsymbol{k}+\boldsymbol{k}_0}\,\tilde{u}_b^{(0)}(\boldsymbol{p}_0,t'|\boldsymbol{k}_0,\boldsymbol{p}_0,\boldsymbol{q}_0)\,\tilde{u}_c^{(0)}(\boldsymbol{q}_0,t'|\boldsymbol{k}_0,\boldsymbol{p}_0,\boldsymbol{q}_0)$$
$$+(\boldsymbol{p}_0\to\boldsymbol{q}_0\to\boldsymbol{k}_0\to\boldsymbol{p}_0)\Big] \quad (3.62)$$

under the initial condition (3.59). The deviation fields of other quantities are similarly represented in terms of the NDI fields (see Appendix B).

### 3.3.2 Assumptions and procedures

For the purpose of easy reference, we summarize here assumptions and procedures to construct a system of equations for the Lagrangian velocity correlation and the response functions. We choose a coordinate system with zero mean velocity and make the following three assumptions [24]:

**Assumption 1** $\widetilde{X}^{(1)}$ is much smaller than $\widetilde{X}^{(0)}$ in magnitude, hence we can neglect their higher-order terms. Here, $\widetilde{X}$ stands for any physical quantity (for example $\widetilde{u}_i$).

**Assumption 2** $\widetilde{u}_i^{(0)}(\boldsymbol{k}_0, t||\boldsymbol{k}_0, \boldsymbol{p}_0, \boldsymbol{q}_0)$, $\widetilde{u}_j^{(0)}(\boldsymbol{p}_0, t'||\boldsymbol{k}_0, \boldsymbol{p}_0, \boldsymbol{q}_0)$ and $\widetilde{u}_k^{(0)}(\boldsymbol{q}_0, t''||\boldsymbol{k}_0, \boldsymbol{p}_0, \boldsymbol{q}_0)$ are statistically independent of each other.

**Assumption 3** $\{\widetilde{u}\}$, $\{\widetilde{G}\}$, $\{\widetilde{\psi}\}$ and $\{\widetilde{\Psi}\}$ are statistically independent of each other.

We construct a set of integro-differential equations for the Lagrangian quantities by employing the following four procedures:

**Procedure 1** Substitute the direct-interaction decompositions, (3.58) and (3.160)—(3.162), into the right-hand side of the governing equations of statistical quantities. Thanks to Assumption 1, we can neglect higher-order terms of the deviation field.

**Procedure 2** Eliminate the deviation field by making use of (3.62), (3.175), (3.176) and (3.177).

**Procedure 3** Eliminate $\overline{\widetilde{G}_{ij}^{(E0)}}$, $\overline{\widetilde{\psi}^{(0)}}$ and $\overline{\widetilde{\Psi}_i^{(0)}}$ respectively by making use of

$$\overline{\widetilde{G}_{ij}^{(E0)}(\boldsymbol{k}, t|\boldsymbol{k}', t'||\boldsymbol{k}_0, \boldsymbol{p}_0, \boldsymbol{q}_0)} = \overline{\widetilde{G}_{ij}^{(L0)}(t|\boldsymbol{k}, \boldsymbol{k}', t'||\boldsymbol{k}_0, \boldsymbol{p}_0, \boldsymbol{q}_0)}\,, \tag{3.63}$$

$$\overline{\widetilde{\psi}^{(0)}(\boldsymbol{k}, t|\boldsymbol{k}', t'||\boldsymbol{k}_0, \boldsymbol{p}_0, \boldsymbol{q}_0)} = \frac{L^3}{(2\pi)^6}\,\delta^3_{\boldsymbol{k}+\boldsymbol{k}'} \tag{3.64}$$

and

$$\overline{\widetilde{\Psi}_i^{(0)}(\boldsymbol{k}, t|\boldsymbol{k}', \boldsymbol{k}'', t'||\boldsymbol{k}_0, \boldsymbol{p}_0, \boldsymbol{q}_0)} = -\frac{\mathrm{i}\,k_a}{(2\pi)^3}\int_{t'}^{t} \mathrm{d}t''\,\overline{\widetilde{G}_{ai}^{(L0)}(t''|\boldsymbol{k}+\boldsymbol{k}', \boldsymbol{k}'', t'||\boldsymbol{k}_0, \boldsymbol{p}_0, \boldsymbol{q}_0)}\,. \tag{3.65}$$

**Procedure 4** Replace $\overline{\widetilde{u}_i^{(0)}\widetilde{u}_j^{(0)}}$ and $\overline{\widetilde{G}_{im}^{(L0)}}$ by $\widetilde{Q}_{ij}$ and $\widetilde{G}_{ij}$ through

$$\overline{\widetilde{u}_i^{(0)}(\boldsymbol{k}, t||\boldsymbol{k}_0, \boldsymbol{p}_0, \boldsymbol{q}_0)\,\widetilde{u}_j^{(0)}(-\boldsymbol{k}, t'||\boldsymbol{k}_0, \boldsymbol{p}_0, \boldsymbol{q}_0)} = \left(\frac{L}{2\pi}\right)^3 \widetilde{Q}_{ij}(\boldsymbol{k}, t, t') \tag{3.66}$$

and

$$\frac{(2\pi)^6}{L^3}\,\overline{\widetilde{G}_{im}^{(L0)}(t|\boldsymbol{k}, -\boldsymbol{k}, t'||\boldsymbol{k}_0, \boldsymbol{p}_0, \boldsymbol{q}_0)}\;\widetilde{P}_{mj}(\boldsymbol{k}) = \widetilde{G}_{ij}(\boldsymbol{k}, t, t')\,, \tag{3.67}$$

which follows from (3.57) under Assumption 1. For derivations of relations (3.63)—(3.66), see Appendix C.

The third assumption and the third procedure are different from those of DIA explained in Chapter 2 by the introduction of the position function and its response function. Assumption 3 may be ad hoc, and so strong that it makes the formulation of the closure drastically simple. There is room for argument on the implication of this assumption. Notice that this assumption yields (3.64), which physically implies that turbulent diffusion is not taken into account.

### 3.3.3 Closed system of equations for statistical quantities

Applying the methods of the Lagrangian DIA described in the preceding subsection, we can construct a system of equations for the statistical quantities. We start with the two-point one-time velocity correlation function. By substituting direct-interaction decomposition (3.58) into the right-hand side of (3.43), we obtain

$$\left[\frac{\partial}{\partial t}+2\nu k^2\right]\tilde{V}_{ij}(\boldsymbol{k},t,t) = -\frac{\mathrm{i}}{2}\left(\frac{2\pi}{L}\right)^6 \tilde{P}_{imn}(\boldsymbol{k}) \times \sum_{\substack{\boldsymbol{p}\\(\boldsymbol{k}+\boldsymbol{p}+\boldsymbol{q}=\boldsymbol{o})}}\sum_{\boldsymbol{q}} \Big[ \overline{\tilde{u}_m^{(0)}(-\boldsymbol{p},t\|\boldsymbol{k},\boldsymbol{p},\boldsymbol{q})\,\tilde{u}_n^{(0)}(-\boldsymbol{q},t\|\boldsymbol{k},\boldsymbol{p},\boldsymbol{q})\,\tilde{u}_j^{(0)}(-\boldsymbol{k},t\|\boldsymbol{k},\boldsymbol{p},\boldsymbol{q})} + 2\,\overline{\tilde{u}_m^{(0)}(-\boldsymbol{p},t\|\boldsymbol{k},\boldsymbol{p},\boldsymbol{q})\,\tilde{u}_n^{(1)}(-\boldsymbol{q},t\|\boldsymbol{k},\boldsymbol{p},\boldsymbol{q})\,\tilde{u}_j^{(0)}(-\boldsymbol{k},t\|\boldsymbol{k},\boldsymbol{p},\boldsymbol{q})} + \overline{\tilde{u}_m^{(0)}(-\boldsymbol{p},t\|\boldsymbol{k},\boldsymbol{p},\boldsymbol{q})\,\tilde{u}_n^{(0)}(-\boldsymbol{q},t\|\boldsymbol{k},\boldsymbol{p},\boldsymbol{q})\,\tilde{u}_j^{(1)}(-\boldsymbol{k},t\|\boldsymbol{k},\boldsymbol{p},\boldsymbol{q})} \Big] + (i\leftrightarrow j\,,\ \boldsymbol{k}\to-\boldsymbol{k})\,. \tag{3.68}$$

Here a set of removed wavenumbers has been selected as $(\boldsymbol{k}_0,\boldsymbol{p}_0,\boldsymbol{q}_0)=(\boldsymbol{k},\boldsymbol{p},\boldsymbol{q})$ in the summand on the right-hand side of the above equation, and higher-order terms of the deviation field have been neglected (Assumption 1). Applying Procedures 2—4 to (3.68), we obtain the temporal evolution equation for the velocity correlation function as

$$\left[\frac{\partial}{\partial t}+2\nu k^2\right]\tilde{Q}_{ij}(\boldsymbol{k},t,t) = \frac{1}{2}\left(\frac{2\pi}{L}\right)^3 \tilde{P}_{ia}(\boldsymbol{k}) \times\Bigg\{ \tilde{P}_{amn}(\boldsymbol{k}) \sum_{\substack{\boldsymbol{p}\\(\boldsymbol{k}+\boldsymbol{p}+\boldsymbol{q}=\boldsymbol{o})}}\sum_{\boldsymbol{q}} \int_{t_0}^{t}\mathrm{d}t'\,\tilde{Q}_{mb}(-\boldsymbol{p},t,t') \Big[ 2\Big(q_b\,\tilde{G}_{nc}(-\boldsymbol{q},t,t')+q_c\,\tilde{G}_{nb}(-\boldsymbol{q},t,t')\Big)\tilde{Q}_{jc}(-\boldsymbol{k},t,t') + \Big(k_b\,\tilde{G}_{jc}(-\boldsymbol{k},t,t')+k_c\,\tilde{G}_{jb}(-\boldsymbol{k},t,t')\Big)\tilde{Q}_{nc}(-\boldsymbol{q},t,t') \Big] + (a\leftrightarrow j\,,\ \boldsymbol{k}\to-\boldsymbol{k})\Bigg\}, \tag{3.69}$$

(see Appendix D for the derivation).

In a similar manner, we can express the governing equation for the two-point two-time Lagrangian velocity correlation function in terms of only the two-point Lagrangian velocity correlation and the response functions. Employing Procedures 1—4 for (3.44), we obtain

$$\left[\frac{\partial}{\partial t}+\nu k^2\right]\tilde{Q}_{ij}(\boldsymbol{k},t,t') = -2\left(\frac{2\pi}{L}\right)^3 \tilde{P}_{id}(\boldsymbol{k}) \sum_{\substack{\boldsymbol{p}\\(\boldsymbol{k}+\boldsymbol{p}+\boldsymbol{q}=\boldsymbol{o})}}\sum_{\boldsymbol{q}} \frac{q_aq_bq_cq_d}{q^2}\int_{t'}^{t}\mathrm{d}t''\,\tilde{Q}_{ab}(\boldsymbol{p},t,t'')\,\tilde{Q}_{cj}(\boldsymbol{k},t,t')\,. \tag{3.70}$$

Finally, for the Lagrangian velocity response function, it follows from (3.52) that

$$\left[\frac{\partial}{\partial t}+\nu k^2\right]\tilde{G}_{ij}(\boldsymbol{k},t,t') = -2\left(\frac{2\pi}{L}\right)^3 \sum_{\substack{\boldsymbol{p}\\(\boldsymbol{k}+\boldsymbol{p}+\boldsymbol{q}=\boldsymbol{o})}}\sum_{\boldsymbol{q}} \frac{k_ik_mk_n}{k^2}\int_{t'}^{t}\mathrm{d}t''\Big[q_b\tilde{G}_{nc}(-\boldsymbol{q},t,t')+q_c\tilde{G}_{nb}(-\boldsymbol{q},t,t')\Big]$$

$$\times \tilde{G}_{cj}(\boldsymbol{k},t'',t')\,\tilde{Q}_{mb}(-\boldsymbol{p},t,t'')$$

$$-2\left(\frac{2\pi}{L}\right)^3 \sum_{\substack{\boldsymbol{p}\\(\boldsymbol{k}+\boldsymbol{p}+\boldsymbol{q}=\boldsymbol{o})}}\sum_{\boldsymbol{q}} \frac{q_a q_b q_c q_i}{q^2} \int_{t'}^{t} \mathrm{d}t''\,\tilde{Q}_{ab}(\boldsymbol{p},t,t'')\,\tilde{G}_{cj}(\boldsymbol{k},t,t')\,. \tag{3.71}$$

Derivations of (3.70) and (3.71) will be given in Appendix E.

Equations (3.69)—(3.71) constitute a closed system of equations for the Lagrangian velocity correlation and the response functions. It should be remarked that this system of equations coincides exactly with that obtained before by the use of LRA [36]. Note that LRA can be regarded as a kind of RRE (§2.4) for the Lagrangian quantities. Relations between DIA and RRE have been discussed in Chapter 2 in detail. It should be mentioned that the fact that LRA and the present Lagrangian DIA yield the identical closure equations (we shall call them LRA-DIA equations hereafter) means that they have wide applicability (see Fig.2.9 in Chapter 2).

Equations (3.69)—(3.71) have been derived for homogeneous turbulence. If turbulence is isotropic as well as homogeneous, second-order tensors $\tilde{Q}_{ij}$ and $\tilde{G}_{ij}$ are represented by a single scalar as

$$\tilde{Q}_{ij}(\boldsymbol{k},t,t') = \tfrac{1}{2}\,\tilde{P}_{ij}(\boldsymbol{k})\,Q(k,t,t')\,, \tag{3.72}$$

and

$$\tilde{G}_{ij}(\boldsymbol{k},t,t') = \tilde{P}_{ij}(\boldsymbol{k})\,G(k,t,t') \tag{3.73}$$

by the use of their incompressible conditions (see Ref. [15] for example). Incidentally, the energy spectrum is represented by $Q$, from (3.45), (3.46) and (3.72), as

$$E(k,t) = 2\pi k^2\,Q(k,t,t)\,. \tag{3.74}$$

Then, (3.69)—(3.71) reduce to

$$\left[\frac{\partial}{\partial t} + 2\nu k^2\right] Q(k,t,t) = 2\pi \iint_{\triangle_k} \mathrm{d}p\mathrm{d}q\; kpq\,\hat{b}(k,p,q)$$

$$\times \int_{t_0}^{t} \mathrm{d}t'\,Q(q,t,t')\left[G(k,t,t')\,Q(p,t,t') - G(p,t,t')\,Q(k,t,t')\right], \tag{3.75}$$

$$\left[\frac{\partial}{\partial t} + \nu k^2 + \hat{\eta}(k,t,t')\right] Q(k,t,t') = 0\,, \tag{3.76}$$

$$\left[\frac{\partial}{\partial t} + \nu k^2 + \hat{\eta}(k,t,t')\right] G(k,t,t') = 0 \tag{3.77}$$

and

$$G(k,t,t) = 1 \tag{3.78}$$

respectively (for derivation, see Appendix F), where we have taken the limit $L \to \infty$, and

$$\iint_{\triangle_k} \mathrm{d}p\,\mathrm{d}q = \int_0^\infty \mathrm{d}p \int_{|k-p|}^{k+p} \mathrm{d}q\,, \tag{3.79}$$

(see Fig.3.1). Functions $\hat{b}(k,p,q)$ and $\hat{\eta}(k,t,t')$ in (3.75)—(3.77) are respectively defined by

$$\hat{b}(k,p,q) = \frac{1}{8k^4p^2q^2}\left[k^2-(p-q)^2\right]\left[(p+q)^2-k^2\right]\left[(2p^2-q^2)\,k^2-(p^2-q^2)\,q^2\right] \tag{3.80}$$

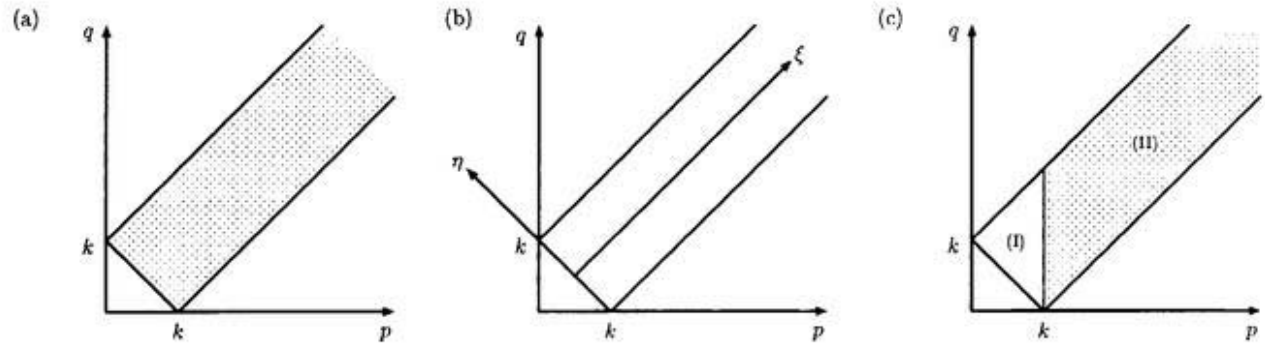


FIGURE 3.1 (a) Integral region represented by $\iint_{\triangle_k} \mathrm{d}p\mathrm{d}q$ (see (3.79)). (b) Variables of integration $\xi$ and $\eta$ are sometimes used instead of $p$ and $q$ (see Appendix C in Chapter 4). (c) It is convenient to remember that infinite region (II) is mapped onto (I) by changing variables of integration as $(k^2/p, kq/p) \to (p, q)$ (see e.g. (4.75)).

and

$$\widehat{\eta}(k,t,t') = \tfrac{4}{3}\,\pi\,k^5 \int_0^\infty \mathrm{d}p\, p^{\frac{10}{3}}\, J(p^{\frac{2}{3}}) \int_{t'}^t \mathrm{d}t''\, Q(kp,t,t'') \tag{3.81}$$

with

$$J(p) = \frac{3}{32p^5}\left[\frac{(1-p^3)^4}{2p^{\frac{3}{2}}}\,\log\frac{(1+p^{\frac{3}{2}})}{|1-p^{\frac{3}{2}}|} - \frac{1+p^3}{3}\,(3p^6-14p^3+3)\right]. \tag{3.82}$$

It follows from (3.76)—(3.78) that

$$Q(k,t,t') = Q(k,t',t')\,G(k,t,t')\,. \tag{3.83}$$

This fluctuation-dissipation relation between the correlation and the response functions may be important to express statistics of turbulence [46]. Once the single-time velocity correlation function $Q(k,t,t)$ and the response function $G(k,t,t')$ are determined, the two-time velocity correlation function $Q(k,t,t')$ follows from (3.83). In homogeneous isotropic turbulence, therefore, it is sufficient to deal with the system of equations for $Q(k,t,t)$ and $G(k,t,t')$. Using (3.75) and (3.83), we can write the equation for $Q(k,t,t)$ as

$$\begin{aligned}\left[\frac{\partial}{\partial t} + 2\nu k^2\right] Q(k,t,t) &= 2\pi \iint_{\triangle_k} \mathrm{d}p\mathrm{d}q\; kpq\,\widehat{b}(k,p,q) \\ &\times \int_{t_0}^t \mathrm{d}t'\, G(k,t,t')\,G(p,t,t')\,G(q,t,t')\,Q(q,t',t')\left[Q(p,t',t') - Q(k,t',t')\right].\end{aligned} \tag{3.84}$$

## 3.4 Stationary turbulence

In this section, we consider how the LRA-DIA equations (3.77) and (3.84) for isotropic turbulence behave under an additional assumption of stationarity. It is shown that $Q$ and $G$ depend only on the

difference between $t$ and $t'$, so that we put

$$Q(k,t,t') = \check{Q}(k,t-t')\,, \tag{3.85}$$

$$G(k,t,t') = \check{G}(k,t-t')\,. \tag{3.86}$$

Then, the single-time velocity correlation function is written as

$$Q(k,t,t) = \check{Q}(k,0)\,, \tag{3.87}$$

and (3.83) as

$$\check{Q}(k,t) = \check{Q}(k,0)\,\check{G}(k,t)\,. \tag{3.88}$$

Introduction of the above relations into (3.77) yields

$$\frac{\partial}{\partial t}\log\check{Q}(k,t) = -\nu k^2 - \frac{4}{3}\pi\,k^5\int_0^\infty \mathrm{d}p\,p^{\frac{10}{3}}\,J(p^{\frac{2}{3}})\int_0^t \mathrm{d}t'\,\check{Q}(kp,t')\,. \tag{3.89}$$

On the other hand, integration from $k_0$ to infinity with respect to $k$ of (3.84) multiplied by $2\pi k^2$ leads to

$$4\pi\nu\int_0^{k_0}\mathrm{d}k\,k^4\,\check{Q}(k,0) = \epsilon - 4\pi^2\int_{k_0}^\infty \mathrm{d}k\iint_{\triangle_k}\mathrm{d}p\mathrm{d}q\,k^3pq\,\widehat{b}(k,p,q) \times\int_0^\infty \mathrm{d}t'\,\check{Q}(k,t')\,\check{Q}(p,t')\,\check{Q}(q,t')\left[\check{Q}(k,0)^{-1}-\check{Q}(p,0)^{-1}\right], \tag{3.90}$$

where use has been made of

$$4\pi\nu\int_0^\infty \mathrm{d}k\,k^4\,\check{Q}(k,0) = \epsilon\,, \tag{3.91}$$

and the upper bound $t-t_0$ of the integration with respect to $t'$ is replaced by infinity. This last procedure may be justified by the exponential decay of $\check{Q}(k,t)$ with the second argument. It is interesting to observe the disappearance of the artificial time $t_0$ by such a reason. Equations (3.89) and (3.90) constitute the LRA-DIA equations for the stationary turbulence.

### 3.4.1 Kolmogorov constant

In order to examine the behavior of these equations in the inertial range, we take the limit $\nu\to 0$. Then, (3.89) and (3.90) are reduced respectively to

$$\frac{\partial}{\partial t}\log\check{Q}(k,t) = -\frac{4}{3}\pi\,k^5\int_0^\infty \mathrm{d}p\,p^{\frac{10}{3}}\,J(p^{\frac{2}{3}})\int_0^t \mathrm{d}t'\,\check{Q}(kp,t') \tag{3.92}$$

and

$$\epsilon = 4\pi^2\int_{k_0}^\infty \mathrm{d}k\iint_{\triangle_k}\mathrm{d}p\mathrm{d}q\,k^3pq\,\widehat{b}(k,p,q) \times\int_0^\infty \mathrm{d}t'\,\check{Q}(k,t')\,\check{Q}(p,t')\,\check{Q}(q,t')\left[\check{Q}(k,0)^{-1}-\check{Q}(p,0)^{-1}\right]. \tag{3.93}$$

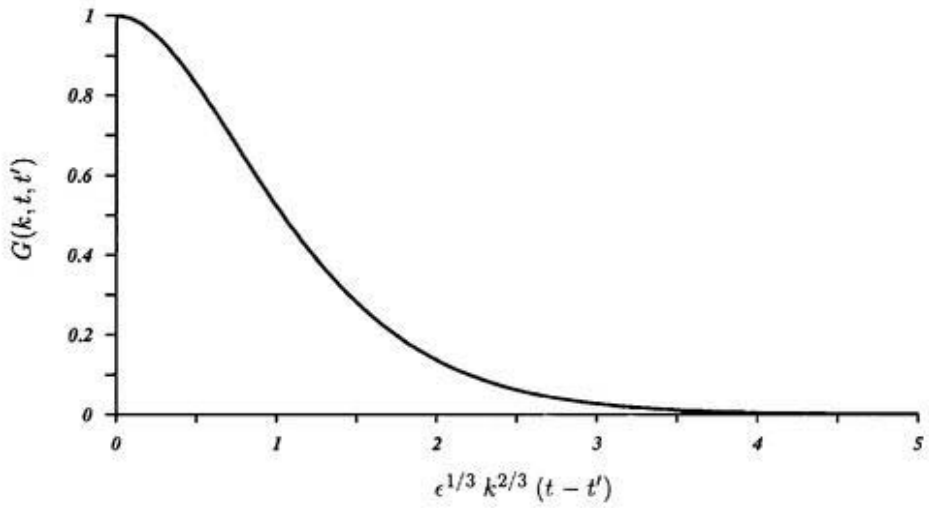


FIGURE 3.2 Lagrangian velocity response function for stationary turbulence.

These equations permit such a similar solution as

$$\check{Q}(k,t) = \frac{K}{2\pi}\,\epsilon^{\frac{2}{3}}\,k^{-\frac{11}{3}}\,\check{Q}^{\dagger}(K^{\frac{1}{2}}\epsilon^{\frac{1}{3}}k^{\frac{2}{3}}t)\,, \tag{3.94}$$

with

$$\check{Q}^{\dagger}(0) = 1\,. \tag{3.95}$$

In terms of $\check{Q}^{\dagger}$ we can rewrite (3.92) and (3.93) as

$$\frac{\mathrm{d}}{\mathrm{d}t}\,\log\check{Q}^{\dagger}(t) = -\int_0^{\infty}\mathrm{d}p\,J(p)\int_0^{t}\mathrm{d}t'\check{Q}^{\dagger}(pt') \tag{3.96}$$

and

$$K^{-\frac{3}{2}} = \int_1^{\infty}\mathrm{d}k\int_0^{1}\mathrm{d}p\int_{\max\{k-p,p\}}^{k+p}\mathrm{d}q\,k^3pq\int_0^{\infty}\mathrm{d}t\,\check{Q}^{\dagger}(k^{\frac{2}{3}}t)\,\check{Q}^{\dagger}(p^{\frac{2}{3}}t)\,\check{Q}^{\dagger}(q^{\frac{2}{3}}t)$$
$$\times\left\{\left[\widehat{b}(k,p,q)+\widehat{b}(k,q,p)\right](pq)^{-\frac{11}{3}}-\left[\widehat{b}(t,p,q)\,q^{-\frac{11}{3}}+\widehat{b}(t,q,p)\,p^{-\frac{11}{3}}\right]k^{-\frac{11}{3}}\right\}, \tag{3.97}$$

respectively. The energy spectrum is represented, from (3.74) and (3.87), by

$$E(k) = 2\pi k^2\,\check{Q}(k,0) = K\,\epsilon^{\frac{2}{3}}\,k^{-\frac{5}{3}}\,. \tag{3.98}$$

Hence, $K$ is actually the Kolmogorov constant (cf. (3.3)). We solved (3.96) numerically with boundary condition (3.95). The result is shown in Fig.3.2 (which is same as Fig.1 in Ref. [50]). Here, $G(k,t,t') = \check{Q}^{\dagger}(K^{\frac{1}{2}}\epsilon^{\frac{1}{3}}k^{\frac{2}{3}}(t-t'))$. By making use of (3.97) and the above numerical result for $\check{Q}^{\dagger}$, we can evaluate the Kolmogorov constant to be 1.722 [50].

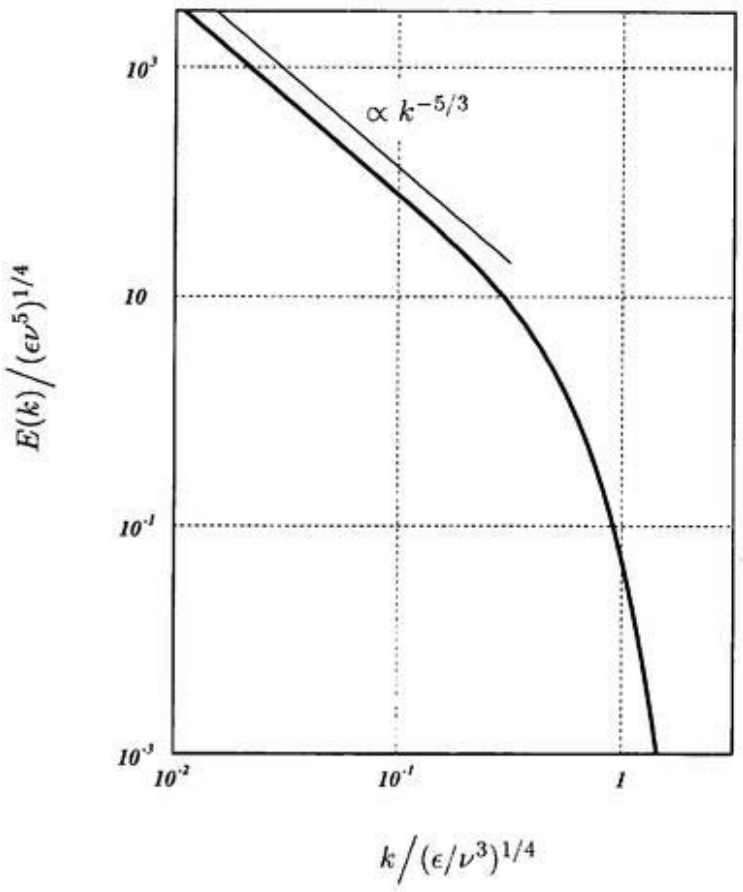


FIGURE 3.3 Three-dimensional energy spectrum in the universal range for stationary turbulence. The Kolmogorov scaling in the inertial range ($k \ll k_K = (\epsilon\nu^3)^{1/4}$) is well satisfied with the universal constant $K = 1.722$.

### 3.4.2 Energy spectrum

In order to solve (3.89) and (3.90) in the entire universal range, we express $\check{Q}$ in terms of non-dimensional functions $\check{Q}^\dagger$ of non-dimensional wavenumber $\kappa$ and time $\tau$ as

$$\check{Q}(k,t) = \frac{1}{2\pi} K \epsilon^{\frac{2}{3}} k^{-\frac{11}{3}} \check{Q}^\dagger(\kappa,\tau) \tag{3.99}$$

with

$$\check{Q}^\dagger(0,0) = 1\,, \tag{3.100}$$

where

$$\kappa = K^{-\frac{3}{8}} \epsilon^{-\frac{1}{4}} \nu^{\frac{3}{4}} k\,, \quad \tau = K^{\frac{1}{2}} \epsilon^{\frac{1}{3}} k^{\frac{2}{3}} t\,. \tag{3.101}$$

Then, (3.89) is converted into

$$\frac{\partial^2}{\partial\tau^2} \log \check{Q}^\dagger(\kappa,\tau) = -\int_0^\infty \mathrm{d}p\, J(p)\, \check{Q}^\dagger(\kappa p^{\frac{3}{2}}, \tau p) \tag{3.102}$$

with

$$\frac{\partial}{\partial\tau} \log \check{Q}^\dagger(\kappa,\tau)\Big|_{\tau=0} = -\kappa^{\frac{4}{3}}\,, \tag{3.103}$$

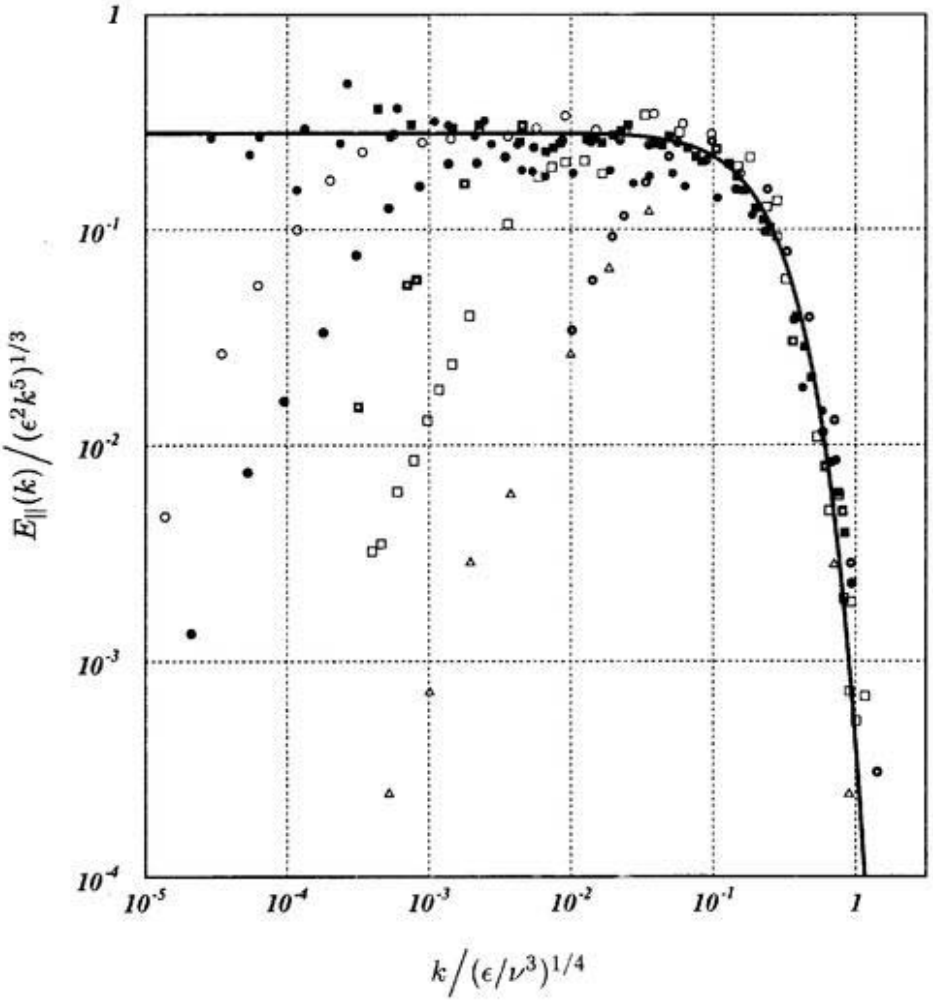


FIGURE 3.4 One-dimensional compensated longitudinal energy spectrum in the universal range for stationary turbulence. Solid line denotes the prediction by the Lagrangian DIA, and symbols show the same measurements as those in Fig.1.1.

while (3.90) is written as

$$\check{Q}^{\ddagger}(\kappa,0) = \frac{1}{2}\iint_{\triangle_\kappa} \mathrm{d}p\mathrm{d}q\,(pq)^{-\frac{8}{3}}\kappa^{-1}\,\widehat{b}(\kappa,p,q) \times \int_0^\infty \mathrm{d}t'\,\check{Q}^{\ddagger}(\kappa,\kappa^{\frac{2}{3}}t')\,\check{Q}^{\ddagger}(p,p^{\frac{2}{3}}t')\,\check{Q}^{\ddagger}(q,q^{\frac{2}{3}}t')\left[\kappa^{\frac{11}{3}}\,\check{Q}^{\ddagger}(\kappa,0)^{-1} - p^{\frac{11}{3}}\,\check{Q}^{\ddagger}(p,0)^{-1}\right]. \tag{3.104}$$

Note that the energy spectrum is expressed as

$$E(k) = K\epsilon^{\frac{2}{3}}k^{-\frac{5}{3}}\,\check{Q}^{\ddagger}(\kappa,0)\,. \tag{3.105}$$

Hence, by searching numerically [2] the solution of $\check{Q}^{\ddagger}$ which satisfies (3.102)—(3.104) and (3.100), the functional form of the energy spectrum $E(k)$ is determined uniquely through (3.105). The result is shown in Fig.3.3. In contrast with the three-dimensional energy spectrum, the one dimensional longitudinal energy spectrum $E_{\parallel}$ defined by (1.1) is relatively easy to measure in real flow turbulence. This spectrum $E_{\parallel}$, which is related with $E$ as [19]

$$E_{\parallel}(k) = \frac{1}{2}\int_k^{\infty} \mathrm{d}k' \left(1 - \frac{k^2}{k'^2}\right) \frac{E(k')}{k'}, \tag{3.106}$$

and the compensated one $E_{\parallel}(k)/(\epsilon^{2/3}k^{-5/3})$ are drawn in Figs.1.1 and 3.4, respectively. Here, a thick curve represents the solution to the LRA-DIA equations. An agreement in the universal range with measurements for various kinds of turbulence is excellent.

### 3.4.3 Skewness factor of velocity derivative

Although only the second-order moments are dealt with in the present closure theory, the skewness factor of the longitudinal derivative of the velocity, which is a third-order moment, can be calculated with the help of the the Kármán-Howarth equation (see e.g. [15]) as

$$S = \overline{\left(\frac{\partial u_1}{\partial x_1}\right)^3} \Big/ \overline{\left(\frac{\partial u_1}{\partial x_1}\right)^2}^{\frac{3}{2}} = -\frac{3\sqrt{30\nu}}{7} \int_0^{\infty} \mathrm{d}k\, k^4\, E(k) \Big/ \left(\int_0^{\infty} \mathrm{d}k\, k^2\, E(k)\right)^{\frac{3}{2}}. \tag{3.107}$$

Using the numerical solution of $\check{Q}^{\ddagger}$, we can perform the integrations on the right-hand side of (3.107) to find

$$S = -0.66, \tag{3.108}$$

which is in perfect agreement with the value obtained by a numerical integration of the Markovianized LRA equations for the decaying turbulence [52]. This agreement may be attributed to the fact that the structure of the energy spectrum in the universal range is the same for the stationary and the decaying cases (see Appendix G). Note that this factor is independent of the Reynolds number. Many turbulence measurements, on the contrary, show that it may increase in magnitude with Reynolds number which expresses the intermittency of turbulence, though it is not conclusive because fluctuations in the data are quite large. It varies from $-0.6$ to $-1$ in the range $10^3 < R_\lambda < 2 \times 10^4$ (see Ref. [53]). The present result (3.108) is consistent with observation within this range of the Reynolds number.

### 3.4.4 Energy transfer and flux functions

The scale locality of the nonlinear interactions is implicitly assumed in the Kolmogorov theory [1] (see §1.1). If the interactions between different scales are strong we may not expect the universality in small-scale structures of turbulence. In other words, the picture of the energy cascade requires the

[2] We have used an iterative method for (3.102) and (3.103), and the Newton-Raphson method for (3.104).

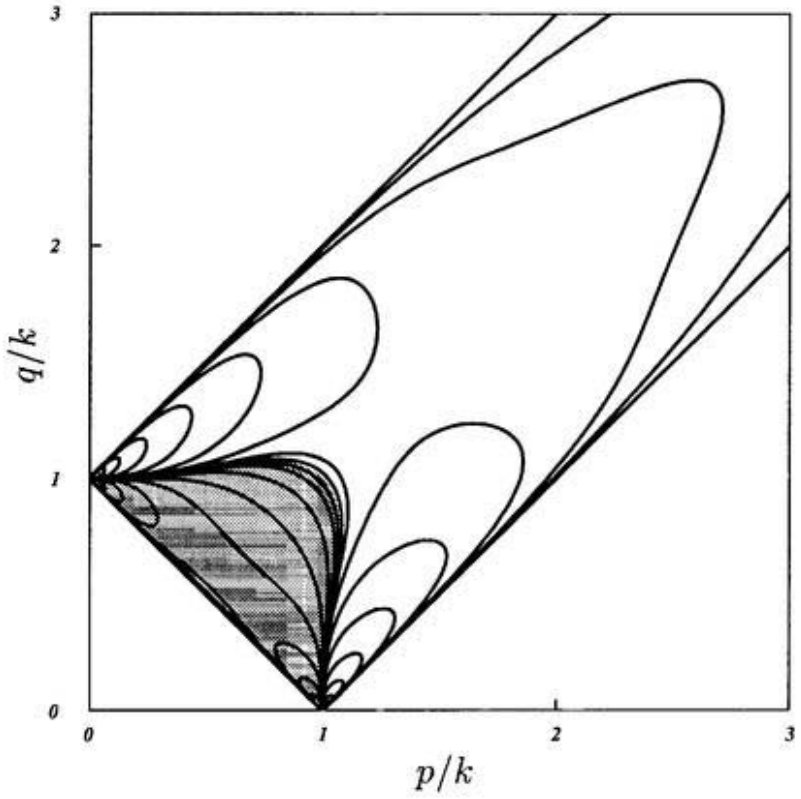


FIGURE 3.5 Triad energy transfer function $T^{(3)}(k,p,q)/(\epsilon k^3)$ in the inertial range for stationary turbulence. Contour levels are $0, \pm 10^{-1.5}, \pm 10^{-1}, \pm 10^{-0.5} \cdots, \pm 10^{2}$. Positive regions are shaded.

energies to transfer from large to small scales locally in the wavenumber space. This locality of the energy transfer has been investigated by the use of direct numerical simulations [54, 55, 4] and by a closure theory [56]. For discussions of the energy transfer in the wavenumber space it is convenient to rewrite the energy equation (3.84) as

$$\frac{\partial}{\partial t} E(k,t) = -2\nu k^2 E(k,t) + T(k,t)\,, \tag{3.109}$$

where

$$T(k,t) = \iint_{\triangle_k} \mathrm{d}p\, \mathrm{d}q\, T^{(3)}(k,p,q,t)\,, \tag{3.110}$$

and

$$\begin{aligned} T^{(3)}(k,p,q,t) = 2\pi^2 k^3 pq \int_{t_0}^{t} \mathrm{d}t'\, G(k,t,t')\, G(p,t,t')\, G(q,t,t') \\ \times \Big[ \Big( \widehat{b}(k,p,q) + \widehat{b}(k,q,p) \Big)\, Q(p,t',t')\, Q(p,t',t') \\ - \Big( \widehat{b}(k,p,q)\, Q(q,t',t') + \widehat{b}(k,q,p)\, Q(p,t',t') \Big)\, Q(k,t',t') \Big] \end{aligned} \tag{3.111}$$

is the triad energy transfer function. The first term on the right-hand side of (3.109) represents the dissipation of energy by molecular viscosity, and the second the energy transfer to the modal

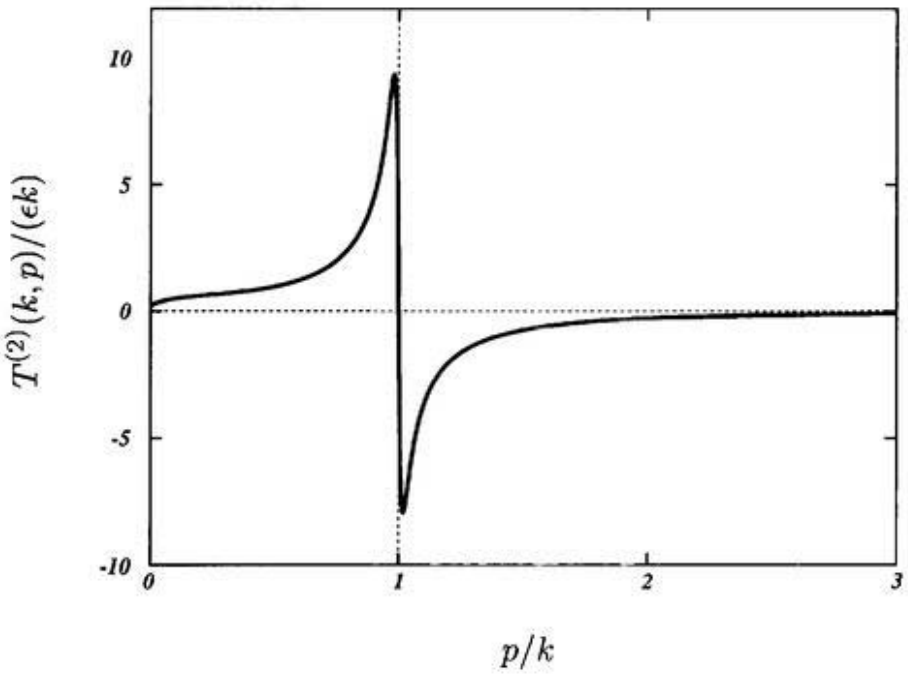


FIGURE 3.6 Two-component energy transfer function defined by (3.112) in the case that both wavenumbers $k$ and $p$ are within the inertial range.

energy of wavenumber $k$ from all the other modal energies through nonlinear interactions. Eddy viscosity is defined as the molecular viscosity counterpart when the contribution from the subgrid scale components is expressed like the first term of (3.109) (see (3.117) below). In Fig.3.5, we plot contours of the triad energy transfer function in the case that all of three wavenumbers, $k$, $p$ and $q$, are in the inertial range of stationary turbulence. Positive regions are shaded. Sharp peaks at the corners of the rectangular domain represent strong non-local triad interactions, which are also observed in the direct numerical simulation [55, 4]. This strength of the non-local interaction seems to be inconsistent with the picture of energy cascade in the wavenumber space in the context of the Kolmogorov theory [1]. However we should note that the non-local interactions do not necessarily cause the non-local energy transfer [55]. To see this, the two-component energy transfer function defined by

$$T^{(2)}(k,p,t) = \int_{|k-p|}^{k+p} \mathrm{d}q\, T^{(3)}(k,p,q,t) \tag{3.112}$$

is evaluated by integrating $T^{(3)}$ numerically (Fig.3.6). Since $T^{(2)}(k,p,t)$ expresses the energy transfer to the modal energy of wavenumber $k$ through the nonlinear interactions with the modes of wavenumber $p$, Fig.3.6 gives a strong support for the local energy transfers in the wavenumber space.

The locality of the energy transfer is also studied by examining how the triad transfer function $T^{(3)}$ contributes to the energy flux function,

$$\Pi(k) = \int_k^\infty \mathrm{d}k'\, T(k') \int_k^\infty \mathrm{d}k' = \int_k^\infty \mathrm{d}k' \iint_{\Delta_k'} \mathrm{d}p\, \mathrm{d}q\, T^{(3)}(k',p,q)\,, \tag{3.113}$$

which is independent of $k$ and equal to $\epsilon$ in the universal range. Defining a scale locality parameter

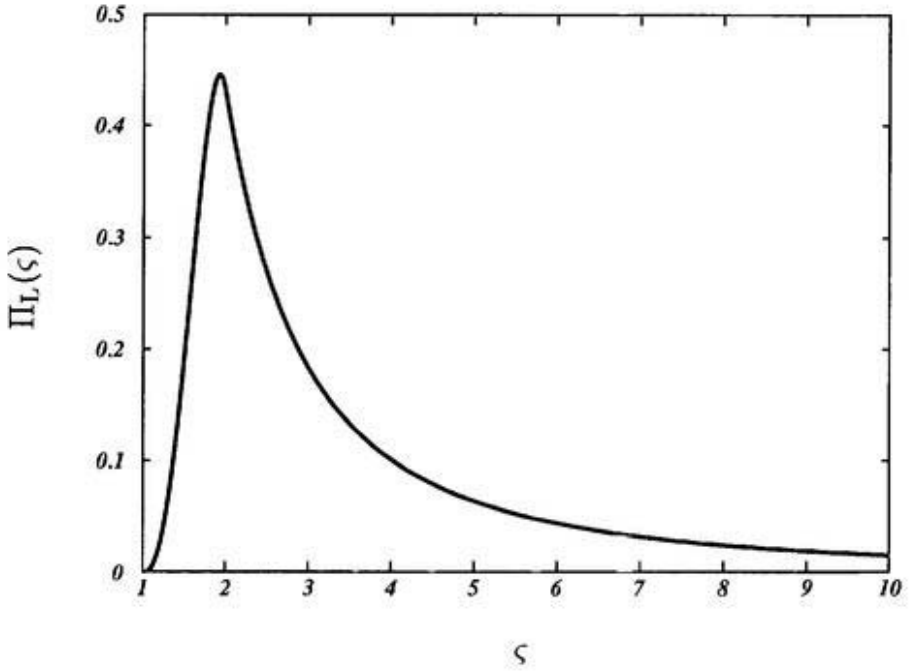


FIGURE 3.7 Local energy flux function in the inertial range. In spite of strong non-local interaction seen in Fig.3.5, the energy flux, which is expressed by the integration of the transfer function, occurs locally in the wavenumber space.

$\varsigma$ by

$$\varsigma = \frac{\max\{k,p,q\}}{\min\{k,p,q\}}\,, \tag{3.114}$$

we introduce the local energy flux function $\Pi_L(\varsigma)$, where $\Pi_L(\varsigma)d\varsigma$ represents the contribution from $T^{(3)}(k,p,q)$, whose scale locality parameter is lying between $\varsigma$ and $\varsigma + d\varsigma$, to the integral in (3.113). Noting the expression,

$$\Pi_L(\varsigma) = \begin{cases} \dfrac{2\log\varsigma}{\varsigma^2}\displaystyle\int_{1/\varsigma}^{1} dx\, T^{(3)}(1,x,1/\varsigma) - 2\int_{1/\varsigma}^{1} dx\, x\log x\, T^{(3)}(1,\varsigma x,x) & (\varsigma \le 2), \quad (3.115a) \\ \dfrac{2\log\varsigma}{\varsigma^2}\displaystyle\int_{(\varsigma-1)/\varsigma}^{1} dx\, T^{(3)}(1,x,1/\varsigma) - 2\int_{1/\varsigma}^{1/(\varsigma-1)} dx\, x\log x\, T^{(3)}(1,\varsigma x,x) & (\varsigma \ge 2) \quad (3.115b) \end{cases}$$

in the case that all of three arguments $k$, $p$ and $q$ of $T^{(3)}(k,p,q)$ are within the inertial range, we evaluate $\Pi_L(\varsigma)$ by the use of the numerical values of $T^{(3)}$ (Fig.3.5). The result is drawn in Fig.3.7. A peak near $\varsigma = 1.93$ in this figure again tells us that energy transfer in the inertial range is taking place locally in the wavenumber space. In summary, although the triad energy transfer function exhibits strong non-locality, the actual energy transfer occurs locally in the wavenumber space. This partly supports the Kolmogorov theory, i.e., the picture of energy cascade. However, the existence of strong non-local interactions raises a question on the universality of the small-scale structure of turbulence, although the strong non-local components of the triad energy transfer function may solely imply the sweeping effect by the large-scale structures without affecting the small-scale statistics.

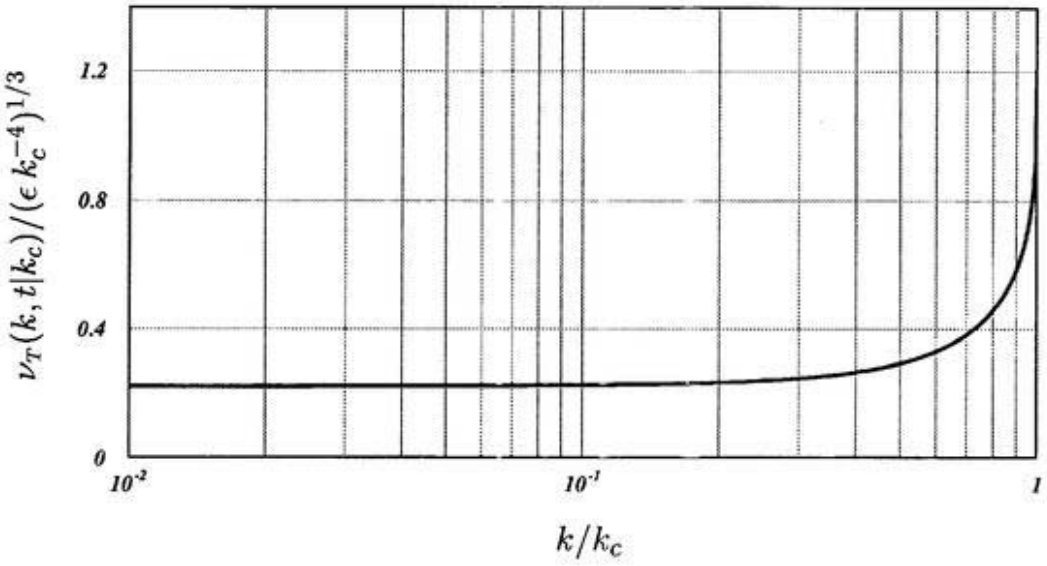


FIGURE 3.8 Wavenumber dependence of the eddy viscosity. It is nearly constant $\nu_T \approx 0.224\epsilon^{\frac{1}{3}}k_c^{-\frac{4}{3}}$ at small wavenumbers ($k \ll k_c$). The variation is less than 50% up to $k \approx 0.6k_c$. At cutoff wavenumber $k_c$, it is 5.7 times as large as that at small wavenumbers.

### 3.4.5 Eddy viscosity

One of the main difficulties in analyzing the structure of developed turbulence at high Reynolds numbers may be attributed to the enormously wide range of relevant scales of active motions. The ratio between the largest and smallest scales, that is, the energy-containing and the energy-dissipation scales, increases in proportion to the power 3/4 of the Reynolds number (see §1.5). It is hard to resolve the smallest excited scales of developed turbulence of practical interest even on a present-day supercomputer. The so-called large-eddy simulation (see Ref. [57] for a review) may be one of the most promising methods of analyzing the turbulence dynamics in which only large-scale components of motion are explicitly simulated, and the effects on the resolved-scale components of the subgrid-scale motions are implicitly taken into account as eddy viscosity. It is the purpose of the rest of this subsection to examine the property of the eddy viscosity in the framework of closure theories [58].

Let us denote by $k_c$ the cutoff wavenumber which is the reciprocal of the dividing length of the resolved and the subgrid scales (e.g., the mesh size in a numerical simulation of turbulence). We divide the energy transfer function $T(k,t)$, which is composed of many triad interactions, into two parts as

$$T(k,t) = T^{<}(k,t|k_c) + T^{>}(k,t|k_c), \tag{3.116}$$

where $T^{<}$ denotes the contribution from the resolved scales, i.e., an integral of (3.110) over $p$ and $q \le k_c$, and $T^{>}$ that from the subgrid scales, i.e. an integral for $p$ or $q > k_c$. If we write the second term of (3.116) formally as

$$T^{>}(k,t|k_c) = -2k^2\,\nu_T(k,t|k_c)\,E(k,t)\,, \tag{3.117}$$

then $\nu_T(k,t|k_c)$ may be regarded as the eddy viscosity since it is a molecular viscosity counterpart (cf. the first term of (3.109)). Notice that the eddy viscosity varies depending upon the relevant

wavenumber, contrary to the molecular viscosity. In the following we will estimate the wavenumber dependence of the eddy viscosity for both wavenumbers $k$ and $k_c$ lying in the inertial range of stationary turbulence. By making use of (3.111) and (3.117), we obtain

$$\nu_T(k,t|k_c) = K^{\frac{1}{2}} \epsilon^{\frac{1}{3}} k_c^{-\frac{4}{3}} I(k/k_c) \tag{3.118}$$

with

$$I(k/k_c) = -\frac{1}{3}(k/k_c)^{-\frac{4}{3}} \int_0^\infty \mathrm{d}t \int_{(k/k_c)^{-1}t}^\infty \mathrm{d}p \int_{p-t}^{p} \mathrm{d}q\, t^3 pq\, \check{Q}^\dagger(t^{\frac{2}{3}})\, \check{Q}^\dagger(p^{\frac{2}{3}})\, \check{Q}^\dagger(q^{\frac{2}{3}})$$
$$\times \left[ (pq)^{-\frac{11}{3}} \left( \widehat{b}(t,p,q) + \widehat{b}(t,q.p) \right) - (tp)^{-\frac{11}{3}}\, \widehat{b}(t,q,p) - (tq)^{-\frac{11}{3}}\, \widehat{b}(t,p,q) \right]. \tag{3.119}$$

Integration in (3.119) is carried out using the numerical solution of $\check{Q}^\dagger$ already obtained in §3.4.1. The eddy viscosity thus determined is shown in Fig.3.8. At two extreme values of $k/k_c$ we find $I(0) = 0.170$ and $I(1) = 0.970$. The eddy viscosity is nearly constant $\nu_T \approx 0.224\epsilon^{\frac{1}{3}} k_c^{-\frac{4}{3}}$ at wavenumbers much smaller than the cutoff wavenumber ($k \ll k_c$) [50]. The variation is less than 50% up to $k \approx 0.6k_c$. However, as the wavenumber concerned approaches the cutoff wavenumber, the eddy viscosity increases more and more rapidly. At the cutoff wavenumber it is 5.7 times as large as that at small wavenumbers. This sharp increase of the eddy viscosity near the cutoff wavenumber, which is caused by strong non-local triad interactions such as $p \ll k \approx q$ or $q \ll k \approx p$ (see Fig.3.5), is also observed in other closure theories [58], large-eddy simulations [59], and direct numerical simulations [60].

## 3.5 Decaying turbulence

We consider homogeneous isotropic freely decaying turbulence with the LRA-DIA equations (3.77) and (3.84). The initial value problem of these equations was solved numerically by Gotoh et al. [51]. We seek instead for solutions to these equations in a similarity form. It can be shown that there are in general no similar solutions with a single similarity law throughout the entire wavenumber range. Therefore, as was done by Kida [61] for the modified QNA, we seek similar solutions which obey different similarity laws in two wavenumber ranges. The energy spectrum is assumed to be characterized by total energy $\mathcal{E}(t)$ and energy dissipation rate $\epsilon(t)$ in the energy-containing range, and by $\epsilon(t)$ and $\nu$ in the universal range.

### 3.5.1 Similarity form in energy-containing range

It is easy to show that the similarity form of equations (3.77) and (3.84) in the universal range is the same for decaying and for stationary turbulence (see Appendix G). That in the energy-containing range, on the other hand, is derived as follows. We start by introducing a new variable $\widehat{E}_\zeta(k,t)$ by

$$E(k,t) = \widehat{E}_\zeta(k,t)\, k^\zeta\,, \tag{3.120}$$

where

$$0 < \widehat{E}_\zeta(0,t) < \infty\,. \tag{3.121}$$

Here, the index $\zeta$, which was introduced in §3.1.2, characterizes large-scale structure as

$$E(k,t) \propto k^{\zeta} \qquad \text{as} \quad k \to 0\,. \tag{3.122}$$

Then, (3.74) and (3.84) lead to

$$\left[\frac{\partial}{\partial t} + 2\nu k^2\right] \widehat{E}_\zeta(k,t) = \iint_{\triangle_k} \mathrm{d}p\mathrm{d}q\, k^{3-\zeta} p q^{\zeta-1}\, \widehat{b}(k,p,q) \\ \times \int_0^t \mathrm{d}t'\, G(k,t,t')\, G(p,t,t')\, G(q,t,t')\, \widehat{E}_\zeta(q,t') \left[ p^{\zeta-2}\, \widehat{E}_\zeta(p,t') - k^{\zeta-2}\, \widehat{E}_\zeta(k,t') \right], \tag{3.123}$$

where we have put $t_0 = 0$. Equation (3.77) for the response function is rewritten as

$$\left[\frac{\partial}{\partial t} + 2\nu k^2 + \frac{2}{3} k^{\zeta+3} \int_0^\infty \mathrm{d}p\, p^{\frac{4}{3}+\zeta}\, J(p^{\frac{2}{3}}) \int_{t'}^t \mathrm{d}t''\, \widehat{E}_\zeta(kp,t'')\, G(kp,t,t'')\right] G(k,t,t') = 0\,. \tag{3.124}$$

If we demand that turbulence in the energy-containing range is characterized only by $k$, $\mathcal{E}(t)$ and $\epsilon(t)$, functions $\widehat{E}_\zeta$ and $G$ may be written, from a dimensional analysis, as

$$\widehat{E}_\zeta(k,t) = \mathcal{E}(t)^{\frac{1}{2}(3\zeta+5)}\, \epsilon(t)^{-\zeta-1}\, E^\dagger{}_\zeta\Big(\mathcal{A}\mathcal{E}(t)^{\frac{3}{2}}\, \epsilon(t)^{-1}\, k\Big), \tag{3.125}$$

$$G(k,t,t') = G^\dagger\Big(\mathcal{A}\mathcal{E}(t)^{\frac{3}{2}}\, \epsilon(t)^{-1}\, k\,,\, \mathcal{A}\mathcal{E}(t')^{\frac{3}{2}}\, \epsilon(t')^{-1}\, k\Big), \tag{3.126}$$

where $\mathcal{A}$ is a non-dimensional constant, which will be determined later so that the final expression may be simple (see (3.137) below). By substituting these similarity forms into (3.123) and (3.124), we find that the viscous term is smaller than the time-derivative and the nonlinear terms by a factor $Re^{-1}$, where $Re$ is the Reynolds number ($Re = \mathcal{E}^2/\epsilon\nu$). Hence, in the limit of large Reynolds numbers, the viscous terms can be neglected.

By neglecting the viscous term and taking the limit of $k \to 0$ in (3.123), we obtain [3]

$$\frac{\mathrm{d}}{\mathrm{d}t}\, \widehat{E}_\zeta(0,t) = \begin{cases} 0 & (2 \le \zeta < 4), \qquad \text{(3.127a)} \\ \dfrac{14}{15} \displaystyle\int_0^\infty \mathrm{d}p \int_0^t \mathrm{d}t' \left[ p^3\, G(p,t,t')\, \widehat{E}_4(p,t') \right]^2 & (\zeta = 4). \qquad \text{(3.127b)} \end{cases}$$

For $2 \le \zeta \le 4$, substitution of similarity form (3.125) into (3.127a) leads to the power law,

$$\mathcal{E}(t) = \mathcal{E}_0\, t^{-\sigma}\,, \tag{3.128}$$

where

$$\sigma = \frac{2(\zeta+1)}{\zeta+3} \qquad (2 \le \zeta < 4)\,. \tag{3.129}$$

Here, we have used relation,

$$\epsilon(t) = -\frac{\mathrm{d}\mathcal{E}}{\mathrm{d}t}\,. \tag{3.130}$$

[3] This equation tells us that the Birkhoff constant [38], which is $\widehat{E}_2(0,t)$, is invariant in time, but the Loitsiansky integral [39], which is equal to $\widehat{E}_4(0,t)$, is not, as pointed out before in other closure theories of turbulence [61, 62].

For $\zeta = 4$, on the other hand, it may not be possible to prove that $\mathcal{E}(t)$ is a power function of $t$. However, if we assume (3.128), then $\sigma$ can be evaluated by

$$\frac{(2-\sigma)(10-7\sigma)}{2\,\sigma^2}\,E^{\dagger}{}_4(0) = \frac{28}{15}\,\mathcal{A}^{-7}\int_0^{\infty}\mathrm{d}p\int_0^1 \mathrm{d}t\,t^{(20-13\sigma)/(2-\sigma)}\left[p^3\,G^{\dagger}(p,pt)\,E^{\dagger}{}_4(pt)\right]^2 \qquad (\zeta=4)\,. \tag{3.131}$$

Inversely, it is easy to show that (3.128), (3.129) and (3.131) are sufficient conditions for the existence of similar solutions (3.125) and (3.126).

By making use of (3.128) and (3.130), we can rewrite (3.125) and (3.126) as

$$\widehat{E}_{\zeta}(k,t) = \mathcal{E}_0^{(\zeta+3)/2}\,\sigma^{-\zeta-1}\,t^{(-\sigma\zeta-3\sigma+2\zeta+2)/2}\,E^{\dagger}{}_{\zeta}\Big(\mathcal{A}\,\mathcal{E}_0^{\frac{1}{2}}\,\sigma^{-1}\,t^{-\frac{\sigma}{2}+1}k\Big), \tag{3.132}$$

$$G(k,t,t') = G^{\dagger}\Big(\mathcal{A}\,\mathcal{E}_0^{\frac{1}{2}}\,\sigma^{-1}\,t^{-\frac{\sigma}{2}+1}k\,,\,\mathcal{A}\,\mathcal{E}_0^{\frac{1}{2}}\,\sigma^{-1}\,t'^{-\frac{\sigma}{2}+1}k\Big). \tag{3.133}$$

In order to make the final equations simpler, we further replace $E^{\dagger}$, $G^{\dagger}$ and $\sigma$ with

$$E^{\dagger}{}_{\zeta}(x) = \mathcal{A}^{\zeta+3}\left(\frac{b}{2-3b}\right)^2 x^{-\zeta-\frac{5}{3}}\,E^{\ddagger}(x^{\frac{2}{3}})\,, \tag{3.134}$$

$$G^{\dagger}(x,x') = G^{\ddagger}(x^{\frac{2}{3}},x'^{\frac{2}{3}}) \tag{3.135}$$

and

$$\sigma = 2-3b\,, \tag{3.136}$$

respectively. If we choose

$$\mathcal{A} = \frac{2-3b}{\mathcal{E}_0^{\frac{1}{2}}\,b^{\frac{3}{2}}}\,, \tag{3.137}$$

then (3.132) and (3.133) are rewritten as

$$\widehat{E}_{\zeta}(k,t) = t^{2(b-1)}\,k^{-\zeta-\frac{5}{3}}\,E^{\ddagger}(b^{-1}t^b k^{\frac{2}{3}})\,, \tag{3.138}$$

$$G(k,t,t') = G^{\ddagger}(b^{-1}t^b k^{\frac{2}{3}},b^{-1}t'^b k^{\frac{2}{3}})\,, \tag{3.139}$$

and (3.123) and (3.124) as

$$\frac{\partial}{\partial t}\Big(t^{2-\frac{2}{b}}\,E^{\ddagger}(t)\Big) = t^{\frac{1}{b}-1}\iint_{\triangle_1}\mathrm{d}p\mathrm{d}q\,pq\,\widehat{b}(1,p,q)\int_0^t \mathrm{d}t'\,t'^{3-\frac{3}{b}}$$
$$\times\,G^{\ddagger}(t,t')\,G^{\ddagger}(p^{\frac{2}{3}}t,p^{\frac{2}{3}}t')\,G^{\ddagger}(q^{\frac{2}{3}}t,q^{\frac{2}{3}}t')\,q^{-\frac{11}{3}}\,E^{\ddagger}(q^{-\frac{11}{3}}t')\left[\,q^{-\frac{11}{3}}\,E^{\ddagger}(p^{-\frac{11}{3}}t')-E^{\ddagger}(t')\,\right] \tag{3.140}$$

and

$$\frac{\partial}{\partial t}\log G^{\ddagger}(t,t') = -t^{\frac{1}{b}-1}\int_0^{\infty}\mathrm{d}p J(p)\int_{t'}^t \mathrm{d}t''\,t''^{1-\frac{1}{b}}\,E^{\ddagger}(pt'')\,G^{\ddagger}(pt,pt'')\,, \tag{3.141}$$

respectively. Conditions (3.129) and (3.131) for $\sigma$ are also rewritten as

$$b = \begin{cases} \dfrac{4}{3(\zeta+3)} & (2\le\zeta<4), \quad \text{(3.142a)} \\[2ex] \left[\dfrac{21}{4}-\dfrac{7}{10\,E^{\ddagger}{}_0}\displaystyle\int_0^{\infty}\mathrm{d}k\,k^{-\frac{15}{2}}\int_0^1\mathrm{d}t\,t^{3-\frac{3}{b}}\left(G^{\dagger}(k,kt)\,Q^{\dagger}(kt)\right)^2\right]^{-1} & (\zeta=4). \quad \text{(3.142b)} \end{cases}$$

Here, $E^{\ddagger}{}_0$ is defined by

$$E^{\ddagger}(x) = E^{\ddagger}{}_0\,x^{\zeta+\frac{5}{3}} \qquad \text{as} \quad x\to 0\,, \tag{3.143}$$

which follows from (3.121) and (3.138).

Finally, we consider the boundary conditions for $E^\ddagger$ and $G^\ddagger$. Energy spectrum $E(k,t)$ is expressed, from (3.120) and (3.138), as

$$E(k,t) = t^{2(b-1)}\, k^{-\frac{5}{3}}\, E^\ddagger(b^{-1} t^b k^{\frac{2}{3}})\,. \tag{3.144}$$

If we demand that $E(k,t)$ at large wavenumbers in the inertial range be connected smoothly with the $k^{-5/3}$ spectrum which is realized at lower wavenumbers in the universal range, then $E^\ddagger$ must approach a constant, for which we can choose, without loss of generality, unity, i.e.,

$$E^\ddagger(\infty) = 1\,. \tag{3.145}$$

Then, we have

$$E(k,t) = k^{-\frac{5}{3}}\, t^{-2+2b} = \left(\mathcal{E}_0\,(2-3b)\right)^{-\frac{2}{3}} \epsilon(t)^{\frac{2}{3}}\, k^{-\frac{5}{3}} \quad \left(= K\,\epsilon(t)^{\frac{2}{3}}\, k^{-\frac{5}{3}}\,, \text{ say}\right) \quad \text{as } k \to \infty\,, \tag{3.146}$$

where use has been made of (3.128), (3.130), (3.136) and (3.144). Integration of (3.144) with respect to $k$ together with $\mathcal{E}(t) = \int_0^\infty \mathrm{d}k E(k,t)$ gives

$$\mathcal{E}_0 = \frac{3}{2b} \int_0^\infty \mathrm{d}x\, x^{-2}\, E^\ddagger(x)\,. \tag{3.147}$$

Hence, the Kolmogorov constant is expressed, from (3.146) and (3.147), as

$$K = \left[\frac{3}{2}\left(\frac{2}{b} - 3\right) \int_0^\infty \mathrm{d}x\, x^{-2}\, E^\ddagger(x)\right]^{-\frac{2}{3}}. \tag{3.148}$$

A boundary condition for $G^\ddagger$ follows from initial condition (3.78) as

$$G^\ddagger(x,x) = 1\,. \tag{3.149}$$

Thus, we have obtained a system of integro-differential equations (3.140)—(3.142) to be solved with boundary conditions (3.145) and (3.149).

### 3.5.2 Kolmogorov constant

In the limit $t' \to \infty$, equation (3.141) for the response function becomes

$$\frac{\partial}{\partial t} \log G^\ddagger(t,t') = -\int_0^\infty \mathrm{d}p\, J(p) \int_{t'}^t \mathrm{d}t''\, G^\ddagger(pt, pt'') \quad \text{as } t' \to \infty\,, \tag{3.150}$$

where use has been made of

$$\int_{t'}^t \mathrm{d}t''\, t''^{1-\frac{1}{b}}\, E^\ddagger(pt'')\, G^\ddagger(pt, pt'') = t^{1-\frac{1}{b}} \int_{t'}^t \mathrm{d}t''\, G^\ddagger(pt, pt'') \quad (\text{as } t' \to \infty)\,. \tag{3.151}$$

Equation (3.150) with (3.149) permits a solution such that

$$G^\ddagger(t,t') = G^\ddagger{}_\infty(t - t')\,, \tag{3.152}$$

where $G^{\ddagger}{}_{\infty}$ obeys

$$\frac{\mathrm{d}}{\mathrm{d}t}\log G^{\ddagger}{}_{\infty}(t) = -\int_0^{\infty}\mathrm{d}p\, J(p)\int_0^{t}\mathrm{d}t'\, G^{\ddagger}{}_{\infty}(pt')\,, \tag{3.153}$$

with boundary condition

$$G^{\ddagger}{}_{\infty}(0) = 1\,. \tag{3.154}$$

Notice that (3.153) is identical to (3.96). The functional form of $G^{\ddagger}{}_{\infty}$ does, therefore, coincide with that of $\check{Q}^{\dagger}$, which is the response function for the stationary case (Fig.3.2) [4].

The energy equation (3.140), on the other hand, is reduced to (see Appendix H for derivation)

$$\begin{aligned}
&\frac{3}{2}\left(\frac{2}{b}-3\right)\int_0^{\infty}\mathrm{d}x\, x^{-2}\, E^{\ddagger}(x) \\
&\quad = \int_1^{\infty}\mathrm{d}t\int_0^{1}\mathrm{d}p\int_{\max\{t-p,p\}}^{t+p}\mathrm{d}q\, t^3pq\int_0^{\infty}\mathrm{d}t'\, G^{\ddagger}{}_{\infty}(t^{\frac{2}{3}}t')\, G^{\ddagger}{}_{\infty}(p^{\frac{2}{3}}t')\, G^{\ddagger}{}_{\infty}(q^{\frac{2}{3}}t') \\
&\qquad \times\left\{\left[\widehat{b}(t,p,q)+\widehat{b}(t,q,p)\right](pq)^{-\frac{11}{3}} - \left[\widehat{b}(t,p,q)\, q^{-\frac{11}{3}}+\widehat{b}(t,q,p)\, p^{-\frac{11}{3}}\right]t^{-\frac{11}{3}}\right\}.
\end{aligned} \tag{3.155}$$

Hence, it follows from (3.148) and (3.155) that the Kolmogorov constant $K$ is written as

$$\begin{aligned}
K^{-\frac{3}{2}} &= \int_1^{\infty}\mathrm{d}t\int_0^{1}\mathrm{d}p\int_{\max\{t-p,p\}}^{t+p}\mathrm{d}q\, t^3pq\int_0^{\infty}\mathrm{d}t'\, G^{\ddagger}{}_{\infty}(t^{\frac{2}{3}}t')\, G^{\ddagger}{}_{\infty}(p^{\frac{2}{3}}t')\, G^{\ddagger}{}_{\infty}(q^{\frac{2}{3}}t') \\
&\quad\times\left\{\left[\widehat{b}(t,p,q)+\widehat{b}(t,q,p)\right](pq)^{-\frac{11}{3}} - \left[\widehat{b}(t,p,q)\, q^{-\frac{11}{3}}+\widehat{b}(t,q,p)\, p^{-\frac{11}{3}}\right]t^{-\frac{11}{3}}\right\}.
\end{aligned} \tag{3.156}$$

By remembering that $G^{\ddagger}{}_{\infty}$ is identical to $\check{Q}^{\dagger}$ and comparing (3.97) with (3.156), we can conclude that the Kolmogorov constant in decaying turbulence is same as that in stationary turbulence, i.e., $K = 1.722$.

### 3.5.3 Two-similarity-range solution

The LRA-DIA equations (3.140)—(3.142) for the energy-containing range are solved numerically under boundary conditions (3.145) and (3.149) for two extreme cases of index $\zeta$, i.e., $\zeta = 2$ and 4. In the case of $\zeta = 2$, (3.142a) gives $b = 4/15$. Equations (3.140) and (3.141) are then solved iteratively as described in Appendix I. The response function and the energy spectrum function thus obtained are plotted in Figs.3.9 (a) and 3.10 (a), respectively [5]. The almost equi-distance in the contours

[4] Note the difference in the arguments of $\check{Q}^{\dagger}$ and $G^{\ddagger}{}_{\infty}$. It is $K^{\frac{1}{2}}\epsilon^{\frac{1}{3}}k^{\frac{2}{3}}(t-t')$ in the former, while $K^{\frac{1}{2}}k^{\frac{2}{3}}(\epsilon(t)^{\frac{1}{3}}t - \epsilon(t')^{\frac{1}{3}}t')/b$ in the latter (see (3.94) and a footnote in §3.5.3). However, these two agree with each other in the limit $t' \to \infty$ because

$$K^{\frac{1}{2}}k^{\frac{2}{3}}(\epsilon(t)^{\frac{1}{3}}t - \epsilon(t')^{\frac{1}{3}}t')/b = k^{\frac{2}{3}}(t^b - t'^b)/b\,,$$

which is derived from (3.128), (3.130), (3.136) and (3.146).

[5] The response function and the energy spectrum function are respectively written in terms of solutions of (3.140) and (3.141) as

$$G(k,t,t') = G^{\ddagger}(\tau/b, \tau'/b)\,, \quad E(k,t)/(\mathcal{E}^{\frac{5}{2}}\epsilon^{-1}) = K\,(\mathcal{E}^{\frac{3}{2}}\epsilon^{-1}k)^{-\frac{5}{3}}\, E^{\ddagger}(K^{\frac{1}{2}}(2b^{-1}-3)(\mathcal{E}^{\frac{3}{2}}\epsilon^{-1}k)^{\frac{2}{3}})\,,$$

of logarithmic levels in Fig.3.9 (a) indicates that the response function decays exponentially with response time $\tau - \tau'$. The non-dimensional characteristic decay time $\tau - \tau'$ of the response function takes a non-zero finite value at initial time $\tau' = 0$ and decreases with $\tau'$. In the original physical time $t$, however, it is a monotonically increasing function of time starting zero at the initial instant (figures are omitted). The energy spectrum, shown in Fig.3.10 (a), has asymptotic forms, $\propto k^2$ and $\propto k^{-\frac{5}{3}}$, at small and large wavenumbers respectively as imposed as the boundary conditions.

In the case of $\zeta = 4$, on the other hand, parameter $b$ is not known a priori but to be determined iteratively together with $E^\ddagger$ and $G^\ddagger$ (cf. (3.142b)). We obtained numerically that

$$b = 0.207 \qquad (\text{for} \quad \zeta = 4)\,, \tag{3.157}$$

which gives, through (3.136), the power exponent of the energy decaying law,

$$\sigma = 1.38 \qquad (\text{for} \quad \zeta = 4)\,. \tag{3.158}$$

Interestingly, this value is exactly same as the one predicted by the EDQNM theory [62] as well as by the modified zero-fourth-order cumulant approximation [61]. As shown in Fig.3.9 (b) and Fig.3.10 (b), the shape of the response function and the energy spectrum function are qualitatively the same as for $\zeta = 2$.

As mentioned at the beginning of §3.5, there are in general no overall similarity solutions with a single similarity law valid over the entire wavenumber range. Instead, the energy spectrum obeys different similarity laws in the energy-containing range and in the universal range, and it is connected smoothly between them. It follows from (3.128) and (3.130) that the normalized energy and wavenumber depend on time, in the respective wavenumber ranges, as

$$\begin{cases} \dfrac{E(k,t)}{\mathcal{E}^{\frac{5}{2}}\epsilon^{-1}} \propto t^{\frac{3}{2}\sigma-1}\,, \quad \dfrac{k}{\mathcal{E}^{-\frac{3}{2}}\epsilon} \propto t^{-\frac{1}{2}\sigma+1} & (\text{in the energy-containing range})\,, \qquad (3.159a) \\ \dfrac{E(k,t)}{\epsilon^{\frac{1}{4}}\nu^{\frac{5}{4}}} \propto t^{\frac{1}{4}(\sigma+1)}\,, \quad \dfrac{k}{\epsilon^{\frac{1}{4}}\nu^{-\frac{1}{4}}} \propto t^{\frac{1}{4}(\sigma+1)} & (\text{in the universal range})\,. \qquad (3.159b) \end{cases}$$

Note that the two similarity laws coincide with each other only for $\sigma = 1$ for which the velocity correlation tensor $\widetilde{V}_{ij}(\boldsymbol{k}, t, t')$ diverges at zero wavenumber, or the three-dimensional energy spectrum behaves as $E(k,t) \propto k$ (as $k \to 0$). In this case, the total energy decreases in inverse proportion to time, which has been observed often in grid-generated turbulence (see Ref. [15]).

The time evolution of the energy spectrum with two similarity decay laws is depicted in the entire wavenumber range for cases $\zeta = 2$ (Fig.3.11(a)) and 4 (Fig.3.11(b)). In each figure, two inserted panels (which are identical to Figs.3.10 (a) and 3.3 for $\zeta = 2$, and 3.10 (b) and 3.3 for $\zeta = 4$) represent respectively the energy-containing and the universal ranges, which translate in time in the directions indicated by arrows. Notice that the direction of the arrow in the energy-containing range is exactly parallel to the asymptotic slope at the small wavenumber of the energy spectrum for the case $\zeta = 2$, which exhibits the invariance of the Birkhoff constant, whereas they are slightly inclined each other in the case $\zeta = 4$, which implies that the invariance of the Loitsiansky integral is slightly broken.

where use has been made of (3.101), (3.128), (3.130), (3.136), (3.139), (3.144) and (3.146). Here $\tau' = K^{\frac{1}{2}}\epsilon(t')^{\frac{1}{3}}k^{\frac{2}{3}}t'$.

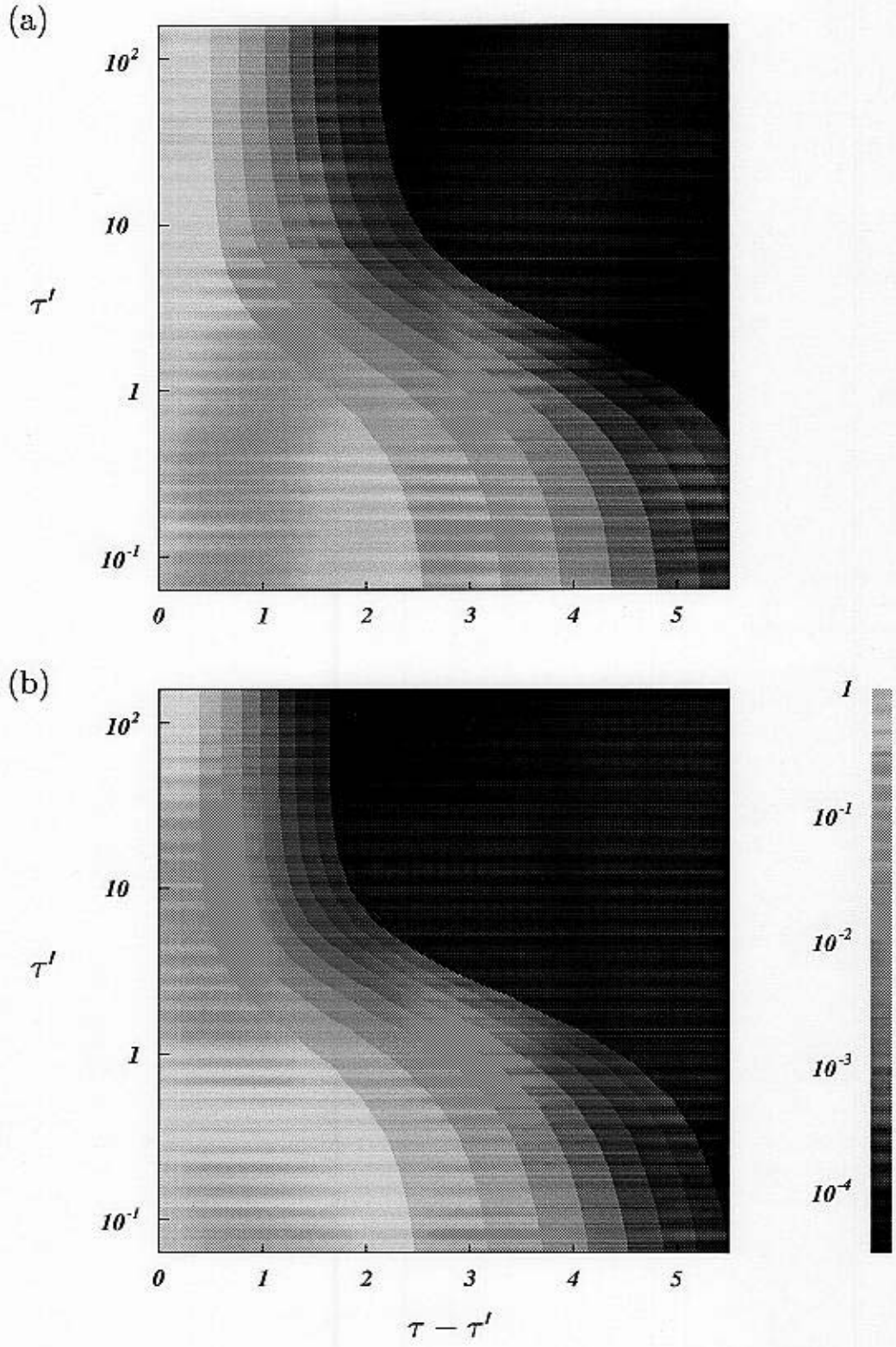


FIGURE 3.9 Similar solutions of the Lagrangian velocity response function $G(k, t, t')$ in the energy containing and the inertial ranges of freely decaying turbulence for (a) $\zeta = 2$ and (b) $\zeta = 4$. Here, $\tau = K^{\frac{1}{2}}\epsilon(t)^{\frac{1}{3}}k^{\frac{2}{3}}t$ and $\tau' = K^{\frac{1}{2}}\epsilon(t')^{\frac{1}{3}}k^{\frac{2}{3}}t'$. Contour levels are $10^x$ ($x = -0.5, -1, -1.5, \cdots, -4$).

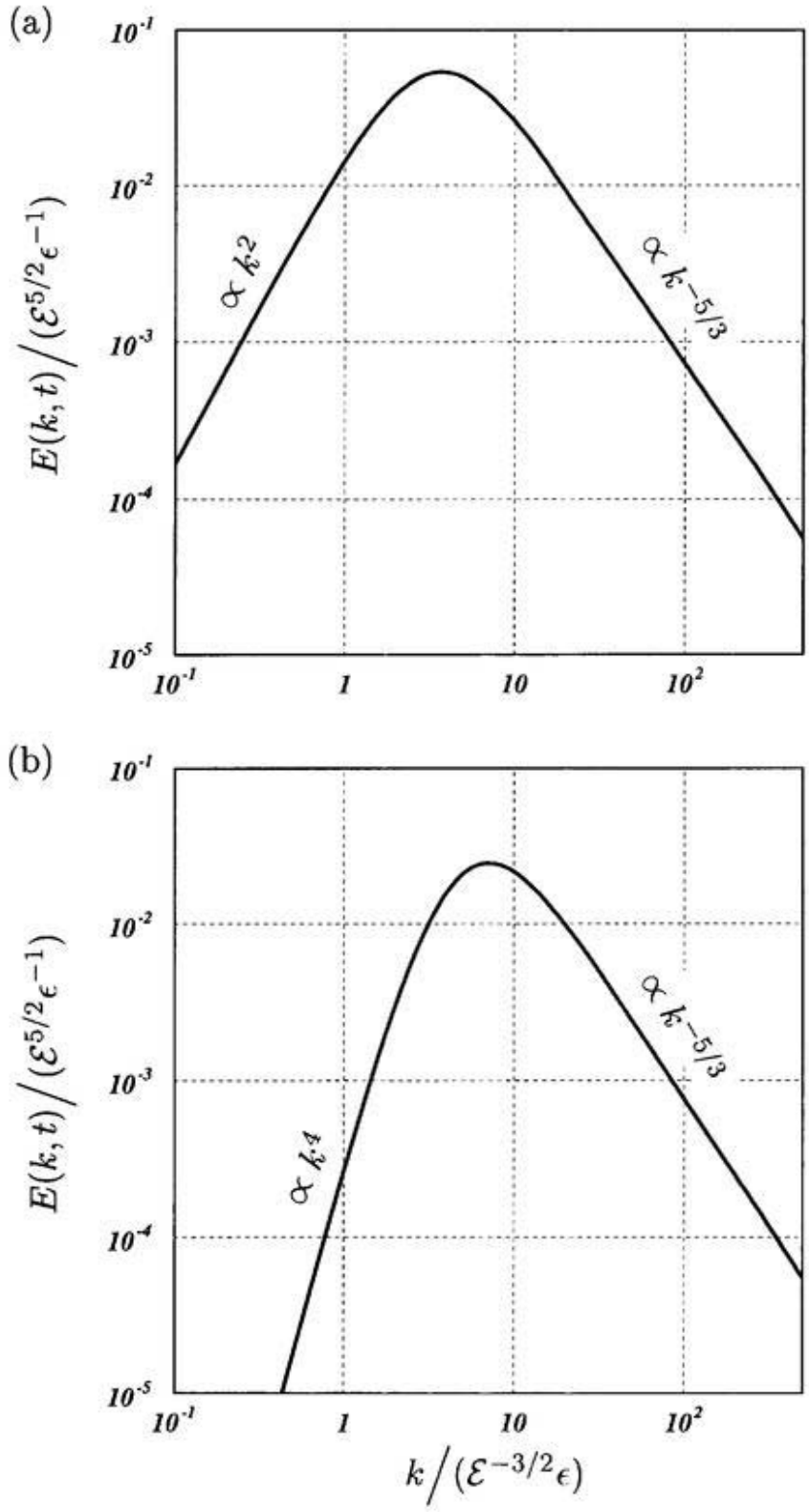


FIGURE 3.10 Similar solutions of the three-dimensional energy spectrum function in the energy containing and the inertial ranges of freely decaying turbulence for (a) $\zeta = 2$ and (b) $\zeta = 4$.

(a)

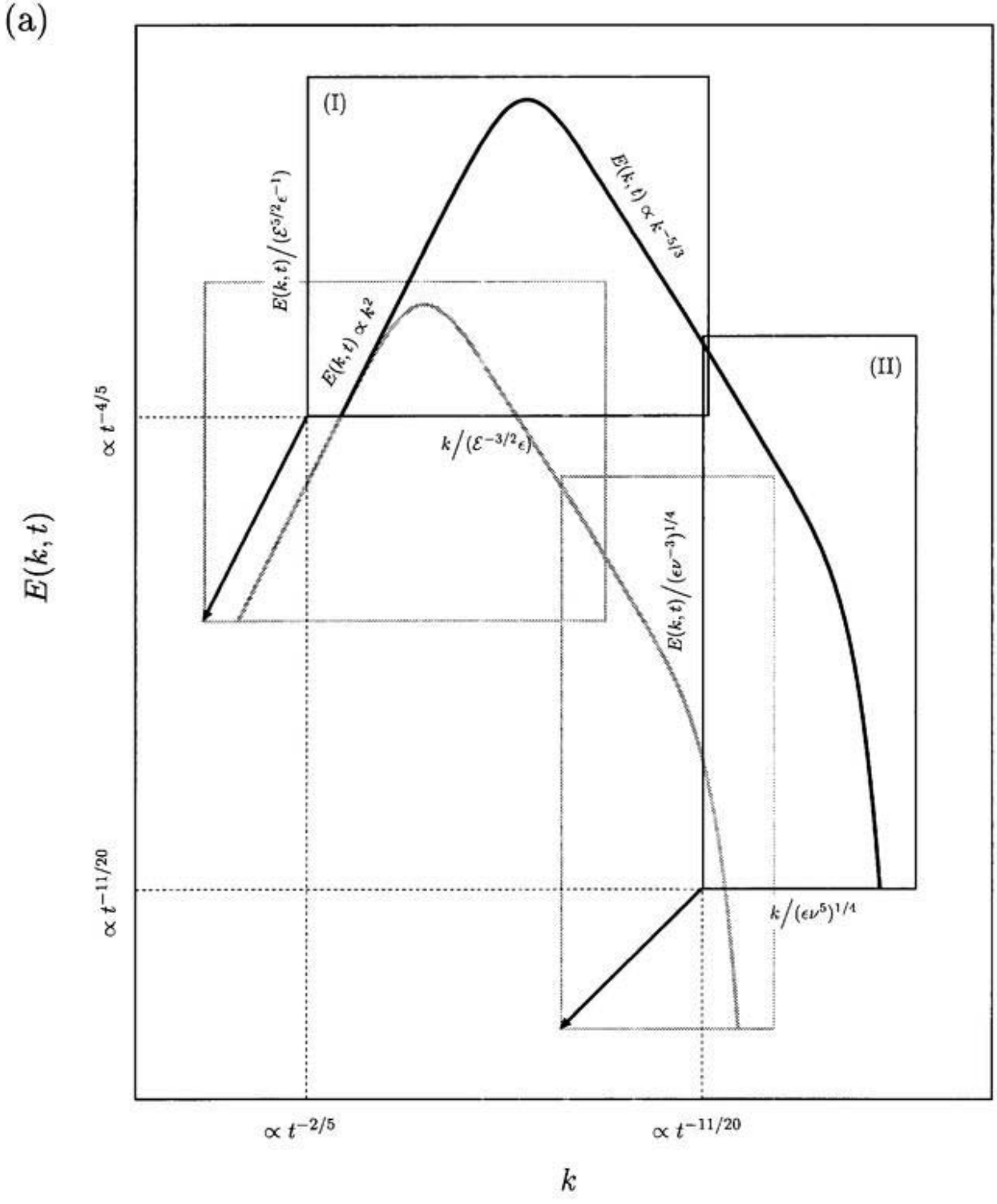
(I)
(II)
$E(k,t)/(\varepsilon^{3/2}\epsilon^{-1})$
$E(k,t) \propto k^{-5/3}$
$E(k,t) \propto k^2$
$k/(\varepsilon^{-3/2}\epsilon)$
$E(k,t)/(\epsilon\nu^{-3})^{1/4}$
$k/(\epsilon\nu^5)^{1/4}$
$\propto t^{-4/5}$
$\propto t^{-11/20}$
$\propto t^{-2/5}$
$\propto t^{-11/20}$
$E(k,t)$
$k$

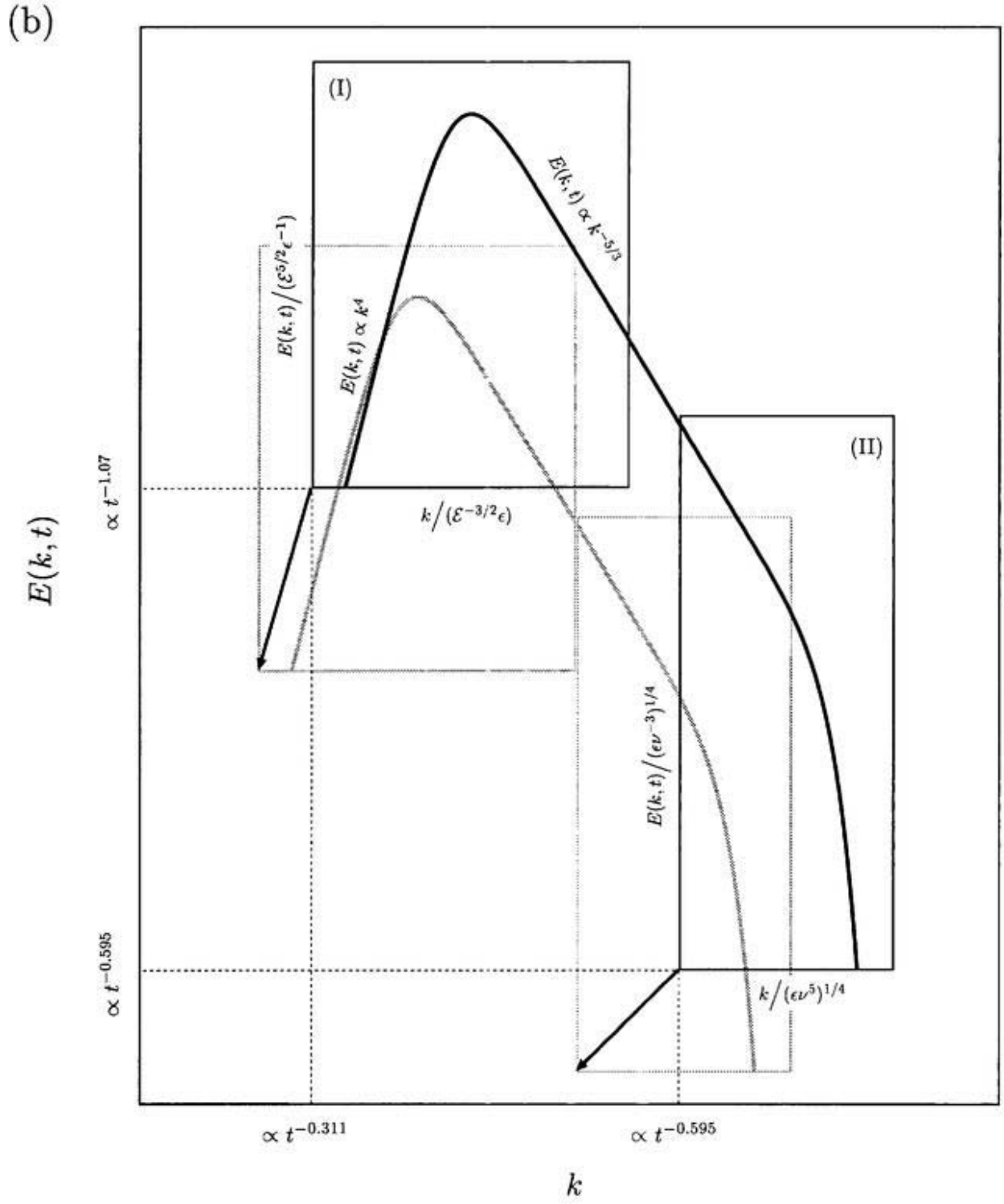


FIGURE 3.11 Time-evolution of the three-dimensional energy spectrum of freely decaying turbulence with two similarity laws for (a) $\zeta = 2$ and (b) $\zeta = 4$. Two kinds of inserted panels represent (I) the energy containing and the inertial ranges, and (II) the universal range, respectively. The energy spectra in these two ranges are connected smoothly in the inertial range between them. The two ranges move in this double logarithmic scale to the direction indicated by arrows according to the respective similarity laws.

## 3.6 Concluding remarks

We have shown that DIA is successfully applied to homogeneous turbulence governed by the Navier-Stokes equation. Employing the correlation and the response functions of the Lagrangian velocity field instead of the Eulerian field in the formulation of DIA, we can avoid a misprediction of the energy spectrum in the inertial range. Several useful findings obtained by the present Lagrangian DIA are summarized as follows. We have proved in the framework of the present closure that the form of the energy spectrum in the universal range is common between stationary and freely decaying turbulence if the energy spectrum and the wavenumber are appropriately normalized in terms of time-dependent energy dissipation rate. The universal form of the energy spectrum is in an excellent agreement with observations. The energy transfer occurs locally in the wavenumber space, which is consistent with the cascade picture used often for an explanation of the Kolmogorov theory [1]. Wavenumber dependence of the eddy viscosity [58], which is used in the large-eddy simulations [57] of turbulence, is estimated to give comparable results with other closure theories. The skewness factor of the velocity derivative is obtained to be equal to $-0.66$ and is independent of the Reynolds number. This value is consistent with available experimental data [53] in Reynolds number range $10^3 < R_\lambda < 2\times10^4$ though it is not conclusive whether there will appear a significant difference at larger Reynolds numbers. By considering two-similarity-range solutions for freely decaying turbulence, it is shown that the Birkhoff constant [38] is time independent, but the Loitsiansky integral [39] varies in time.

A closed system of equations for the Lagrangian velocity correlation and the response functions derived by the present Lagrangian DIA [35] is exactly same as those derived before by LRA [36], which is a kind of RRE. However, the importance of the difference between DIA and RRE cannot be overemphasized (see Chapter 2 for detailed discussions).

It is reasonable that DIA is applicable to homogeneous turbulence governed by the Navier-Stokes equation because the system possesses weak nonlinear couplings and the large number of degrees of freedom. It does not seem however to be totally understood why the Lagrangian DIA formulation does work but not the Eulerian, despite that there have been several suggestions based upon the Galilean invariance of the system (see [12]) and the sweeping effect (see [63]). This important question why we need Lagrangian formulation is still open. In order to clarify this problem, we shall discuss in the next chapter, the strong and weak points of the present Lagrangian DIA by applying it to a passive scalar field advected by isotropic turbulence.

# Appendix A

In §3.3.1, we introduced a direct-interaction decomposition for the Eulerian velocity field and constructed the governing equations for the NDI and the deviation fields of it. Here, we shall adopt this decomposition for the Eulerian velocity response function, the position function and the position response function, i.e.,

$$\tilde{G}_{ij}^{(E)}(\boldsymbol{k},t|\boldsymbol{k}',t') = \tilde{G}_{ij}^{(E0)}(\boldsymbol{k},t|\boldsymbol{k}',t'\|\boldsymbol{k}_0,\boldsymbol{p}_0,\boldsymbol{q}_0) + \tilde{G}_{ij}^{(E1)}(\boldsymbol{k},t|\boldsymbol{k}',t'\|\boldsymbol{k}_0,\boldsymbol{p}_0,\boldsymbol{q}_0)\,, \tag{3.160}$$

$$\tilde{\psi}(\boldsymbol{k},t|\boldsymbol{k}',t') = \tilde{\psi}^{(0)}(\boldsymbol{k},t|\boldsymbol{k}',t'\|\boldsymbol{k}_0,\boldsymbol{p}_0,\boldsymbol{q}_0) + \tilde{\psi}^{(1)}(\boldsymbol{k},t|\boldsymbol{k}',t'\|\boldsymbol{k}_0,\boldsymbol{p}_0,\boldsymbol{q}_0) \tag{3.161}$$

and

$$\widetilde{\Psi}_i(\boldsymbol{k},t|\boldsymbol{k}',\boldsymbol{k}'',t') = \widetilde{\Psi}_i^{(0)}(\boldsymbol{k},t|\boldsymbol{k}',\boldsymbol{k}'',t'\|\boldsymbol{k}_0,\boldsymbol{p}_0,\boldsymbol{q}_0) + \widetilde{\Psi}_i^{(1)}(\boldsymbol{k},t|\boldsymbol{k}',\boldsymbol{k}'',t'\|\boldsymbol{k}_0,\boldsymbol{p}_0,\boldsymbol{q}_0)\,. \tag{3.162}$$

Now, we write the governing equations for the six quantities defined by the above three decompositions. First, we can show from (3.48) and (3.49) that $\widetilde{G}_{ij}^{(E0)}$ obeys

$$\left[\frac{\partial}{\partial t} + \nu k^2\right] \widetilde{G}_{ij}^{(E0)}(\boldsymbol{k},t|\boldsymbol{k}',t'\|\boldsymbol{k}_0,\boldsymbol{p}_0,\boldsymbol{q}_0) = \\ -\mathrm{i}\left(\frac{2\pi}{L}\right)^3 \widetilde{P}_{imn}(\boldsymbol{k}) \sum_{\substack{\boldsymbol{p}\\(\boldsymbol{k}+\boldsymbol{p}+\boldsymbol{q}=\boldsymbol{o})}}\sum_{\boldsymbol{q}}{}' \widetilde{u}_m(-\boldsymbol{p},t)\, \widetilde{G}_{nj}^{(E0)}(-\boldsymbol{q},t|\boldsymbol{k}',t'\|\boldsymbol{k}_0,\boldsymbol{p}_0,\boldsymbol{q}_0) \tag{3.163}$$

with initial condition,

$$\widetilde{G}_{ij}^{(E0)}(\boldsymbol{k},t'|\boldsymbol{k}',t'\|\boldsymbol{k}_0,\boldsymbol{p}_0,\boldsymbol{q}_0) = \frac{L^3}{(2\pi)^6}\,\delta_{ij}\,\delta^3_{\boldsymbol{k}+\boldsymbol{k}'}\,, \tag{3.164}$$

whereas $\widetilde{G}_{ij}^{(E1)}$ obeys

$$\left[\frac{\partial}{\partial t} + \nu k^2\right] \widetilde{G}_{ij}^{(E1)}(\boldsymbol{k},t|\boldsymbol{k}',t'\|\boldsymbol{k}_0,\boldsymbol{p}_0,\boldsymbol{q}_0) = \\ -\mathrm{i}\left(\frac{2\pi}{L}\right)^3 \widetilde{P}_{imn}(\boldsymbol{k}) \sum_{\substack{\boldsymbol{p}\\(\boldsymbol{k}+\boldsymbol{p}+\boldsymbol{q}=\boldsymbol{o})}}\sum_{\boldsymbol{q}}{}' \widetilde{u}_m(-\boldsymbol{p},t)\, \widetilde{G}_{nj}^{(E1)}(-\boldsymbol{q},t|\boldsymbol{k}',t'\|\boldsymbol{k}_0,\boldsymbol{p}_0,\boldsymbol{q}_0) \\ -\delta^3_{\boldsymbol{k}-\boldsymbol{k}_0}\,\mathrm{i}\left(\frac{2\pi}{L}\right)^3 \widetilde{P}_{imn}(\boldsymbol{k}_0)\, \widetilde{u}_m^{(0)}(-\boldsymbol{p}_0,t\|\boldsymbol{k}_0,\boldsymbol{p}_0,\boldsymbol{q}_0)\, \widetilde{G}_{nj}^{(E0)}(-\boldsymbol{q}_0,t|\boldsymbol{k}',t'\|\boldsymbol{k}_0,\boldsymbol{p}_0,\boldsymbol{q}_0) \\ -\delta^3_{\boldsymbol{k}-\boldsymbol{k}_0}\,\mathrm{i}\left(\frac{2\pi}{L}\right)^3 \widetilde{P}_{imn}(\boldsymbol{k}_0)\, \widetilde{u}_m^{(0)}(-\boldsymbol{q}_0,t\|\boldsymbol{k}_0,\boldsymbol{p}_0,\boldsymbol{q}_0)\, \widetilde{G}_{nj}^{(E0)}(-\boldsymbol{p}_0,t|\boldsymbol{k}',t'\|\boldsymbol{k}_0,\boldsymbol{p}_0,\boldsymbol{q}_0) \\ +\delta^3_{\boldsymbol{k}+\boldsymbol{k}_0}\,\mathrm{i}\left(\frac{2\pi}{L}\right)^3 \widetilde{P}_{imn}(\boldsymbol{k}_0)\, \widetilde{u}_m^{(0)}(\boldsymbol{p}_0,t\|\boldsymbol{k}_0,\boldsymbol{p}_0,\boldsymbol{q}_0)\, \widetilde{G}_{nj}^{(E0)}(\boldsymbol{q}_0,t|\boldsymbol{k}',t'\|\boldsymbol{k}_0,\boldsymbol{p}_0,\boldsymbol{q}_0) \\ +\delta^3_{\boldsymbol{k}+\boldsymbol{k}_0}\,\mathrm{i}\left(\frac{2\pi}{L}\right)^3 \widetilde{P}_{imn}(\boldsymbol{k}_0)\, \widetilde{u}_m^{(0)}(\boldsymbol{q}_0,t\|\boldsymbol{k}_0,\boldsymbol{p}_0,\boldsymbol{q}_0)\, \widetilde{G}_{nj}^{(E0)}(\boldsymbol{p}_0,t|\boldsymbol{k}',t'\|\boldsymbol{k}_0,\boldsymbol{p}_0,\boldsymbol{q}_0) \\ +\ (\boldsymbol{p}_0 \to \boldsymbol{q}_0 \to \boldsymbol{k}_0 \to \boldsymbol{p}_0) \tag{3.165}$$

with initial condition,

$$\widetilde{G}_{ij}^{(E1)}(\boldsymbol{k},t'|\boldsymbol{k}',t'\|\boldsymbol{k}_0,\boldsymbol{p}_0,\boldsymbol{q}_0) = 0\,, \tag{3.166}$$

where higher-order terms of the deviation field have been neglected (Assumption 1). Next, the temporal evolution of the position function is derived from (3.39) and (3.40) as

$$\frac{\partial}{\partial t}\,\widetilde{\psi}^{(0)}(\boldsymbol{k},t|\boldsymbol{k}',t'\|\boldsymbol{k}_0,\boldsymbol{p}_0,\boldsymbol{q}_0) = -\mathrm{i}\,k_j\left(\frac{2\pi}{L}\right)^3 \sum_{\substack{\boldsymbol{p}\\(\boldsymbol{k}+\boldsymbol{p}+\boldsymbol{q}=\boldsymbol{o})}}\sum_{\boldsymbol{q}}{}' \widetilde{u}_j(-\boldsymbol{p},t)\, \widetilde{\psi}^{(0)}(-\boldsymbol{q},t|\boldsymbol{k}',t'\|\boldsymbol{k}_0,\boldsymbol{p}_0,\boldsymbol{q}_0) \tag{3.167}$$

with initial condition,

$$\widetilde{\psi}^{(0)}(\boldsymbol{k},t'|\boldsymbol{k}',t'\|\boldsymbol{k}_0,\boldsymbol{p}_0,\boldsymbol{q}_0) = \frac{L^3}{(2\pi)^6}\,\delta^3_{\boldsymbol{k}+\boldsymbol{k}'}\,, \tag{3.168}$$

and

$$\frac{\partial}{\partial t}\,\tilde{\psi}^{(1)}(\boldsymbol{k},t|\boldsymbol{k}',t'\|\boldsymbol{k}_0,\boldsymbol{p}_0,\boldsymbol{q}_0) =$$
$$-\mathrm{i}\,k_j\left(\frac{2\pi}{L}\right)^3 \sum_{\substack{\boldsymbol{p}\\(\boldsymbol{k}+\boldsymbol{p}+\boldsymbol{q}=\boldsymbol{o})}}\sum_{\boldsymbol{q}}{}' \tilde{u}_j(-\boldsymbol{p},t)\,\tilde{\psi}^{(1)}(-\boldsymbol{q},t|\boldsymbol{k}',t'\|\boldsymbol{k}_0,\boldsymbol{p}_0,\boldsymbol{q}_0)$$
$$-\delta^3_{\boldsymbol{k}-\boldsymbol{k}_0}\,\mathrm{i}\,k_{0j}\left(\frac{2\pi}{L}\right)^3 \tilde{u}^{(0)}_j(-\boldsymbol{p}_0,t\|\boldsymbol{k}_0,\boldsymbol{p}_0,\boldsymbol{q}_0)\,\tilde{\psi}^{(0)}(-\boldsymbol{q}_0,t|\boldsymbol{k}',t'\|\boldsymbol{k}_0,\boldsymbol{p}_0,\boldsymbol{q}_0)$$
$$-\delta^3_{\boldsymbol{k}-\boldsymbol{k}_0}\,\mathrm{i}\,k_{0j}\left(\frac{2\pi}{L}\right)^3 \tilde{u}^{(0)}_j(-\boldsymbol{q}_0,t\|\boldsymbol{k}_0,\boldsymbol{p}_0,\boldsymbol{q}_0)\,\tilde{\psi}^{(0)}(-\boldsymbol{p}_0,t|\boldsymbol{k}',t'\|\boldsymbol{k}_0,\boldsymbol{p}_0,\boldsymbol{q}_0)$$
$$+\delta^3_{\boldsymbol{k}+\boldsymbol{k}_0}\,\mathrm{i}\,k_{0j}\left(\frac{2\pi}{L}\right)^3 \tilde{u}^{(0)}_j(\boldsymbol{p}_0,t\|\boldsymbol{k}_0,\boldsymbol{p}_0,\boldsymbol{q}_0)\,\tilde{\psi}^{(0)}(\boldsymbol{q}_0,t|\boldsymbol{k}',t'\|\boldsymbol{k}_0,\boldsymbol{p}_0,\boldsymbol{q}_0)$$
$$+\delta^3_{\boldsymbol{k}+\boldsymbol{k}_0}\,\mathrm{i}\,k_{0j}\left(\frac{2\pi}{L}\right)^3 \tilde{u}^{(0)}_j(\boldsymbol{q}_0,t\|\boldsymbol{k}_0,\boldsymbol{p}_0,\boldsymbol{q}_0)\,\tilde{\psi}^{(0)}(\boldsymbol{p}_0,t|\boldsymbol{k}',t'\|\boldsymbol{k}_0,\boldsymbol{p}_0,\boldsymbol{q}_0)$$
$$+\ (\boldsymbol{p}_0\to\boldsymbol{q}_0\to\boldsymbol{k}_0\to\boldsymbol{p}_0)\,, \tag{3.169}$$

with initial condition,

$$\tilde{\psi}^{(1)}(\boldsymbol{k},t'|\boldsymbol{k}',t'\|\boldsymbol{k}_0,\boldsymbol{p}_0,\boldsymbol{q}_0) = 0\,. \tag{3.170}$$

Finally, for the position response function, we obtain, from (3.54) and (3.55), that

$$\frac{\partial}{\partial t}\,\tilde{\Psi}^{(0)}_i(\boldsymbol{k},t,|\boldsymbol{k}',\boldsymbol{k}'',t'\|\boldsymbol{k}_0,\boldsymbol{p}_0,\boldsymbol{q}_0) = -\,\mathrm{i}\,k_a\left(\frac{2\pi}{L}\right)^3 \sum_{\substack{\boldsymbol{p}\\(\boldsymbol{k}+\boldsymbol{p}+\boldsymbol{q}=\boldsymbol{o})}}\sum_{\boldsymbol{q}}{}' \tilde{u}_a(-\boldsymbol{p},t)\,\tilde{\Psi}^{(0)}_i(-\boldsymbol{q},t|\boldsymbol{k}',\boldsymbol{k}'',t'\|\boldsymbol{k}_0,\boldsymbol{p}_0,\boldsymbol{q}_0)$$
$$-\,\mathrm{i}\,k_a\left(\frac{2\pi}{L}\right)^3 \sum_{\substack{\boldsymbol{p}\\(\boldsymbol{k}+\boldsymbol{p}+\boldsymbol{q}=\boldsymbol{o})}}\sum_{\boldsymbol{q}} \tilde{G}^{(E)}_{ai}(-\boldsymbol{p},t|\boldsymbol{k}'',t')\,\tilde{\psi}(-\boldsymbol{q},t|\boldsymbol{k}',t') \tag{3.171}$$

with

$$\tilde{\Psi}^{(0)}_i(\boldsymbol{k},t'|\boldsymbol{k}',\boldsymbol{k}'',t'\|\boldsymbol{k}_0,\boldsymbol{p}_0,\boldsymbol{q}_0) = 0 \tag{3.172}$$

and

$$\frac{\partial}{\partial t}\,\tilde{\Psi}^{(1)}_i(\boldsymbol{k},t,|\boldsymbol{k}',\boldsymbol{k}'',t'\|\boldsymbol{k}_0,\boldsymbol{p}_0,\boldsymbol{q}_0) =$$
$$-\mathrm{i}\,k_a\left(\frac{2\pi}{L}\right)^3 \sum_{\substack{\boldsymbol{p}\\(\boldsymbol{k}+\boldsymbol{p}+\boldsymbol{q}=\boldsymbol{o})}}\sum_{\boldsymbol{q}}{}' \tilde{u}_a(-\boldsymbol{p},t)\,\tilde{\Psi}^{(1)}_i(-\boldsymbol{q},t|\boldsymbol{k}',\boldsymbol{k}'',t'\|\boldsymbol{k}_0,\boldsymbol{p}_0,\boldsymbol{q}_0)$$
$$-\delta^3_{\boldsymbol{k}-\boldsymbol{k}_0}\mathrm{i}\,k_{0a}\left(\frac{2\pi}{L}\right)^3 \tilde{u}^{(0)}_a(-\boldsymbol{p}_0,t\|\boldsymbol{k}_0,\boldsymbol{p}_0,\boldsymbol{q}_0)\,\tilde{\Psi}^{(0)}_i(-\boldsymbol{q}_0,t|\boldsymbol{k}',\boldsymbol{k}'',t'\|\boldsymbol{k}_0,\boldsymbol{p}_0,\boldsymbol{q}_0)$$
$$-\delta^3_{\boldsymbol{k}-\boldsymbol{k}_0}\mathrm{i}\,k_{0a}\left(\frac{2\pi}{L}\right)^3 \tilde{u}^{(0)}_a(-\boldsymbol{q}_0,t\|\boldsymbol{k}_0,\boldsymbol{p}_0,\boldsymbol{q}_0)\,\tilde{\Psi}^{(0)}_i(-\boldsymbol{p}_0,t|\boldsymbol{k}',\boldsymbol{k}'',t'\|\boldsymbol{k}_0,\boldsymbol{p}_0,\boldsymbol{q}_0)$$
$$+\delta^3_{\boldsymbol{k}+\boldsymbol{k}_0}\mathrm{i}\,k_{0a}\left(\frac{2\pi}{L}\right)^3 \tilde{u}^{(0)}_a(\boldsymbol{p}_0,t\|\boldsymbol{k}_0,\boldsymbol{p}_0,\boldsymbol{q}_0)\,\tilde{\Psi}^{(0)}_i(\boldsymbol{q}_0,t|\boldsymbol{k}',\boldsymbol{k}'',t'\|\boldsymbol{k}_0,\boldsymbol{p}_0,\boldsymbol{q}_0)$$
$$+\delta^3_{\boldsymbol{k}+\boldsymbol{k}_0}\mathrm{i}\,k_{0a}\left(\frac{2\pi}{L}\right)^3 \tilde{u}^{(0)}_a(\boldsymbol{q}_0,t\|\boldsymbol{k}_0,\boldsymbol{p}_0,\boldsymbol{q}_0)\,\tilde{\Psi}^{(0)}_i(\boldsymbol{p}_0,t|\boldsymbol{k}',\boldsymbol{k}'',t'\|\boldsymbol{k}_0,\boldsymbol{p}_0,\boldsymbol{q}_0)$$
$$+\ (\boldsymbol{p}_0\to\boldsymbol{q}_0\to\boldsymbol{k}_0\to\boldsymbol{p}_0) \tag{3.173}$$

with

$$\tilde{\Psi}^{(1)}_i(\boldsymbol{k},t'|\boldsymbol{k}',\boldsymbol{k}'',t'\|\boldsymbol{k}_0,\boldsymbol{p}_0,\boldsymbol{q}_0) = 0\,. \tag{3.174}$$

In derivation of (3.169) and (3.173), higher-order terms of the deviation field have been neglected (Assumption 1).

## Appendix B

In performing Procedure 2, the deviation fields must be represented in terms of the NDI fields. We shall give the expressions for $\widetilde{G}_{ij}^{(E1)}$, $\widetilde{\psi}^{(1)}$ and $\widetilde{\Psi}_i^{(1)}$.

First, by using (3.163) and (3.166), we can solve formally (3.165) to obtain

$$\begin{aligned}\widetilde{G}_{ij}^{(E1)}(\boldsymbol{k},t|\boldsymbol{k}',t'\|\boldsymbol{k}_0,\boldsymbol{p}_0,\boldsymbol{q}_0) = \mathrm{i}\,\frac{(2\pi)^9}{L^6}\,\widetilde{P}_{abc}(\boldsymbol{k})\int_{t'}^{t}\mathrm{d}t''\,\widetilde{G}_{ia}^{(E0)}(\boldsymbol{k},t|-\boldsymbol{k},t''\|\boldsymbol{k}_0,\boldsymbol{p}_0,\boldsymbol{q}_0)\\ \times\Big[-\delta_{\boldsymbol{k}-\boldsymbol{k}_0}^3\,\widetilde{u}_b^{(0)}(-\boldsymbol{p}_0,t''\|\boldsymbol{k}_0,\boldsymbol{p}_0,\boldsymbol{q}_0)\,\widetilde{G}_{cj}^{(E0)}(-\boldsymbol{q}_0,t''|\boldsymbol{k}',t'\|\boldsymbol{k}_0,\boldsymbol{p}_0,\boldsymbol{q}_0)\\ -\delta_{\boldsymbol{k}-\boldsymbol{k}_0}^3\,\widetilde{u}_b^{(0)}(-\boldsymbol{q}_0,t''\|\boldsymbol{k}_0,\boldsymbol{p}_0,\boldsymbol{q}_0)\,\widetilde{G}_{cj}^{(E0)}(-\boldsymbol{p}_0,t''|\boldsymbol{k}',t'\|\boldsymbol{k}_0,\boldsymbol{p}_0,\boldsymbol{q}_0)\\ -\delta_{\boldsymbol{k}+\boldsymbol{k}_0}^3\,\widetilde{u}_b^{(0)}(\boldsymbol{p}_0,t''\|\boldsymbol{k}_0,\boldsymbol{p}_0,\boldsymbol{q}_0)\,\widetilde{G}_{cj}^{(E0)}(\boldsymbol{q}_0,t''|\boldsymbol{k}',t'\|\boldsymbol{k}_0,\boldsymbol{p}_0,\boldsymbol{q}_0)\\ -\delta_{\boldsymbol{k}+\boldsymbol{k}_0}^3\,\widetilde{u}_b^{(0)}(\boldsymbol{q}_0,t''\|\boldsymbol{k}_0,\boldsymbol{p}_0,\boldsymbol{q}_0)\,\widetilde{G}_{cj}^{(E0)}(\boldsymbol{p}_0,t''|\boldsymbol{k}',t'\|\boldsymbol{k}_0,\boldsymbol{p}_0,\boldsymbol{q}_0)\\ +\ (\boldsymbol{p}_0\to\boldsymbol{q}_0\to\boldsymbol{k}_0\to\boldsymbol{p}_0)\Big]. \qquad (3.175)\end{aligned}$$

Next, it follows from (3.167), (3.169) and (3.170) that

$$\begin{aligned}\widetilde{\psi}^{(1)}(\boldsymbol{k},t|\boldsymbol{k}',t'\|\boldsymbol{k}_0,\boldsymbol{p}_0,\boldsymbol{q}_0) = \mathrm{i}\,k_j\,\frac{(2\pi)^9}{L^6}\int_{t'}^{t}\mathrm{d}t''\,\widetilde{\psi}^{(0)}(\boldsymbol{k},t|-\boldsymbol{k},t''\|\boldsymbol{k}_0,\boldsymbol{p}_0,\boldsymbol{q}_0)\\ \times\Big[-\delta_{\boldsymbol{k}-\boldsymbol{k}_0}^3\,\widetilde{u}_j^{(0)}(-\boldsymbol{p}_0,t''\|\boldsymbol{k}_0,\boldsymbol{p}_0,\boldsymbol{q}_0)\,\widetilde{\psi}^{(0)}(-\boldsymbol{q}_0,t''|\boldsymbol{k}',t'\|\boldsymbol{k}_0,\boldsymbol{p}_0,\boldsymbol{q}_0)\\ -\delta_{\boldsymbol{k}-\boldsymbol{k}_0}^3\,\widetilde{u}_j^{(0)}(-\boldsymbol{q}_0,t''\|\boldsymbol{k}_0,\boldsymbol{p}_0,\boldsymbol{q}_0)\,\widetilde{\psi}^{(0)}(-\boldsymbol{p}_0,t''|\boldsymbol{k}',t'\|\boldsymbol{k}_0,\boldsymbol{p}_0,\boldsymbol{q}_0)\\ -\delta_{\boldsymbol{k}+\boldsymbol{k}_0}^3\,\widetilde{u}_j^{(0)}(\boldsymbol{p}_0,t''\|\boldsymbol{k}_0,\boldsymbol{p}_0,\boldsymbol{q}_0)\,\widetilde{\psi}^{(0)}(\boldsymbol{q}_0,t''|\boldsymbol{k}',t'\|\boldsymbol{k}_0,\boldsymbol{p}_0,\boldsymbol{q}_0)\\ -\delta_{\boldsymbol{k}+\boldsymbol{k}_0}^3\,\widetilde{u}_j^{(0)}(\boldsymbol{q}_0,t''\|\boldsymbol{k}_0,\boldsymbol{p}_0,\boldsymbol{q}_0)\,\widetilde{\psi}^{(0)}(\boldsymbol{p}_0,t''|\boldsymbol{k}',t'\|\boldsymbol{k}_0,\boldsymbol{p}_0,\boldsymbol{q}_0)\\ +\ (\boldsymbol{p}_0\to\boldsymbol{q}_0\to\boldsymbol{k}_0\to\boldsymbol{p}_0)\Big]. \qquad (3.176)\end{aligned}$$

Finally, it is shown from (3.171), (3.173) and (3.174) that

$$\begin{aligned}\widetilde{\Psi}_i^{(1)}(\boldsymbol{k},t|\boldsymbol{k}',\boldsymbol{k}'',t'\|\boldsymbol{k}_0,\boldsymbol{p}_0,\boldsymbol{q}_0) = \mathrm{i}\,k_a\frac{(2\pi)^9}{L^6}\int_{t'}^{t}\mathrm{d}t''\,\widetilde{\psi}^{(0)}(\boldsymbol{k},t|-\boldsymbol{k},t''\|\boldsymbol{k}_0,\boldsymbol{p}_0,\boldsymbol{q}_0)\\ \times\Big[-\delta_{\boldsymbol{k}-\boldsymbol{k}_0}^3\,\widetilde{u}_a^{(0)}(-\boldsymbol{p}_0,t''\|\boldsymbol{k}_0,\boldsymbol{p}_0,\boldsymbol{q}_0)\,\widetilde{\Psi}_i^{(0)}(-\boldsymbol{q}_0,t''|\boldsymbol{k}',\boldsymbol{k}'',t'\|\boldsymbol{k}_0,\boldsymbol{p}_0,\boldsymbol{q}_0)\\ -\delta_{\boldsymbol{k}-\boldsymbol{k}_0}^3\,\widetilde{u}_a^{(0)}(-\boldsymbol{q}_0,t''\|\boldsymbol{k}_0,\boldsymbol{p}_0,\boldsymbol{q}_0)\,\widetilde{\Psi}_i^{(0)}(-\boldsymbol{p}_0,t''|\boldsymbol{k}',\boldsymbol{k}'',t'\|\boldsymbol{k}_0,\boldsymbol{p}_0,\boldsymbol{q}_0)\\ -\delta_{\boldsymbol{k}+\boldsymbol{k}_0}^3\,\widetilde{u}_a^{(0)}(\boldsymbol{p}_0,t''\|\boldsymbol{k}_0,\boldsymbol{p}_0,\boldsymbol{q}_0)\,\widetilde{\Psi}_i^{(0)}(\boldsymbol{q}_0,t''|\boldsymbol{k}',\boldsymbol{k}'',t'\|\boldsymbol{k}_0,\boldsymbol{p}_0,\boldsymbol{q}_0)\\ -\delta_{\boldsymbol{k}+\boldsymbol{k}_0}^3\,\widetilde{u}_a^{(0)}(\boldsymbol{q}_0,t''\|\boldsymbol{k}_0,\boldsymbol{p}_0,\boldsymbol{q}_0)\,\widetilde{\Psi}_i^{(0)}(\boldsymbol{p}_0,t''|\boldsymbol{k}',\boldsymbol{k}'',t'\|\boldsymbol{k}_0,\boldsymbol{p}_0,\boldsymbol{q}_0)\\ +\ (\boldsymbol{p}_0\to\boldsymbol{q}_0\to\boldsymbol{k}_0\to\boldsymbol{p}_0)\Big]. \qquad (3.177)\end{aligned}$$

# Appendix C

We derive here relations (3.63)—(3.66). First, by taking an ensemble average of (3.167) and using Assumption 3, we obtain

$$\frac{\partial}{\partial t}\,\overline{\tilde{\psi}^{(0)}(\boldsymbol{k},t|\boldsymbol{k}',t'\|\boldsymbol{k}_0,\boldsymbol{p}_0,\boldsymbol{q}_0)} = 0\,, \tag{3.178}$$

which leads to (3.64) under initial condition (3.168) of $\tilde{\psi}^{(0)}$. Next, an ensemble average of (3.56) gives, under Assumptions 1 and 3, that

$$\overline{\tilde{G}_{ij}^{(E0)}(\boldsymbol{k},t|\boldsymbol{k}',t'\|\boldsymbol{k}_0,\boldsymbol{p}_0,\boldsymbol{q}_0)} = \frac{(2\pi)^6}{L^3}\sum_{\boldsymbol{k}''}\overline{\tilde{G}_{ij}^{(L0)}(t|\boldsymbol{k}'',\boldsymbol{k}',t'\|\boldsymbol{k}_0,\boldsymbol{p}_0,\boldsymbol{q}_0)}\;\overline{\tilde{\psi}^{(0)}(\boldsymbol{k},t|-\boldsymbol{k}'',t'\|\boldsymbol{k}_0,\boldsymbol{p}_0,\boldsymbol{q}_0)}\,, \tag{3.179}$$

where $\tilde{G}_{ij}^{(L0)}$ denotes the NDI field of $\tilde{G}_{ij}^{(L)}$. By substituting (3.64) into the above equation, we obtain (3.63). As for (3.65), we take an ensemble average of (3.171) to obtain

$$\begin{aligned}&\frac{\partial}{\partial t}\,\overline{\tilde{\Psi}_i^{(0)}(\boldsymbol{k},t,|\boldsymbol{k}',\boldsymbol{k}'',t'\|\boldsymbol{k}_0,\boldsymbol{p}_0,\boldsymbol{q}_0)} = \\ &-\mathrm{i}\,k_a\left(\frac{2\pi}{L}\right)^3\sum_{\substack{\boldsymbol{p}\\(\boldsymbol{k}+\boldsymbol{p}+\boldsymbol{q}=\boldsymbol{o})}}\sum_{\boldsymbol{q}}\overline{\tilde{G}_{ai}^{(E0)}(-\boldsymbol{p},t|\boldsymbol{k}'',t'\|\boldsymbol{k}_0,\boldsymbol{p}_0,\boldsymbol{q}_0)}\;\overline{\tilde{\psi}^{(0)}(-\boldsymbol{q},t|\boldsymbol{k}',t'\|\boldsymbol{k}_0,\boldsymbol{p}_0,\boldsymbol{q}_0)}\,,\end{aligned} \tag{3.180}$$

where Assumptions 1 and 3 have been employed. Equation (3.65) follows by substituting (3.63) and (3.64) into (3.180) and integrating it under initial condition (3.172). Finally, in order to show (3.66) we note the identity that

$$\begin{aligned}&\overline{\tilde{u}_i^{(0)}(\boldsymbol{k},t\|\boldsymbol{k}_0,\boldsymbol{p}_0,\boldsymbol{q}_0)\,\tilde{u}_j^{(0)}(-\boldsymbol{k},t'\|\boldsymbol{k}_0,\boldsymbol{p}_0,\boldsymbol{q}_0)} = \\ &\tilde{P}_{ia}(\boldsymbol{k})\,\frac{(2\pi)^6}{L^3}\sum_{\boldsymbol{k}'}\overline{\tilde{v}_a^{(0)}(t|\boldsymbol{k}',t'\|\boldsymbol{k}_0,\boldsymbol{p}_0,\boldsymbol{q}_0)\,\tilde{\psi}^{(0)}(\boldsymbol{k},t|-\boldsymbol{k}',t'\|\boldsymbol{k}_0,\boldsymbol{p}_0,\boldsymbol{q}_0)\,\tilde{u}_j^{(0)}(-\boldsymbol{k},t'\|\boldsymbol{k}_0,\boldsymbol{p}_0,\boldsymbol{q}_0)}\,,\end{aligned} \tag{3.181}$$

which follows from relation (3.36) between $\tilde{u}_i$ and $\tilde{v}_j$ and continuity equation (3.38). Here, $\tilde{v}_a^{(0)}$ denotes the NDI field of the Lagrangian velocity. By substituting (3.64) and replacing $(\tilde{u}_i^{(0)},\,\tilde{v}_i^{(0)})$ by $(\tilde{u}_i,\,\tilde{v}_i)$ (Assumption 1), we obtain

$$\overline{\tilde{u}_i^{(0)}(\boldsymbol{k},t\|\boldsymbol{k}_0,\boldsymbol{p}_0,\boldsymbol{q}_0)\,\tilde{u}_j^{(0)}(-\boldsymbol{k},t'\|\boldsymbol{k}_0.\boldsymbol{p}_0,\boldsymbol{q}_0)} = \tilde{P}_{ia}(\boldsymbol{k})\,\overline{\tilde{v}_a(t|\boldsymbol{k},t')\,\tilde{u}_j(-\boldsymbol{k},t')}\,. \tag{3.182}$$

Then, (3.66) follows from (3.25) (3.46) and (3.182).

# Appendix D

A deduction of (3.69) from (3.68) is described here. The first term on the right-hand side of (3.68) vanishes because of Assumption 2. On substitution of

$$\begin{aligned}&\tilde{u}_n^{(1)}(-\boldsymbol{q},t\|\boldsymbol{k},\boldsymbol{p},\boldsymbol{q}) \\ &\quad=\mathrm{i}\frac{(2\pi)^9}{L^6}\,\tilde{P}_{abc}(\boldsymbol{q})\int_{t_0}^{t}\mathrm{d}t'\,\tilde{G}_{na}^{(E0)}(-\boldsymbol{q},t|\boldsymbol{q},t'\|\boldsymbol{k},\boldsymbol{p},\boldsymbol{q})\,\tilde{u}_b^{(0)}(\boldsymbol{p},t'\|\boldsymbol{k},\boldsymbol{p},\boldsymbol{q})\,\tilde{u}_c^{(0)}(\boldsymbol{k},t'\|\boldsymbol{k},\boldsymbol{p},\boldsymbol{q})\,,\end{aligned} \tag{3.183}$$

which is derived from (3.62), into the second term of (3.68), we obtain

$$\begin{aligned}
&\text{(Second term on r.h.s. of (3.68))} \\
&= \frac{(2\pi)^{15}}{L^{12}}\,\tilde{P}_{imn}(\boldsymbol{k}) \sum_{\substack{\boldsymbol{p}\\(\boldsymbol{k}+\boldsymbol{p}+\boldsymbol{q}=\boldsymbol{o})}}\sum_{\boldsymbol{q}} \tilde{P}_{abc}(\boldsymbol{q}) \int_{t_0}^{t} \mathrm{d}t'\, \overline{\tilde{G}^{(E0)}_{na}(-\boldsymbol{q},t|\boldsymbol{q},t'\|\boldsymbol{k},\boldsymbol{p},\boldsymbol{q})\times} \\
&\qquad \overline{\times\, \tilde{u}^{(0)}_m(-\boldsymbol{p},t\|\boldsymbol{k},\boldsymbol{p},\boldsymbol{q})\,\tilde{u}^{(0)}_b(\boldsymbol{p},t'\|\boldsymbol{k},\boldsymbol{p},\boldsymbol{q})\,\tilde{u}^{(0)}_j(-\boldsymbol{k},t\|\boldsymbol{k},\boldsymbol{p},\boldsymbol{q})\,\tilde{u}^{(0)}_c(\boldsymbol{k},t'\|\boldsymbol{k},\boldsymbol{p},\boldsymbol{q})}\ . \qquad (3.184)
\end{aligned}$$

Assumptions 2 and 3, (3.63) and (3.66) then convert (3.184) into

$$\begin{aligned}
&\text{(Second term on r.h.s. of (3.68))} \\
&= \frac{(2\pi)^{15}}{L^{12}}\,\tilde{P}_{imn}(\boldsymbol{k}) \sum_{\substack{\boldsymbol{p}\\(\boldsymbol{k}+\boldsymbol{p}+\boldsymbol{q}=\boldsymbol{o})}}\sum_{\boldsymbol{q}} \tilde{P}_{abc}(\boldsymbol{q}) \int_{t_0}^{t} \mathrm{d}t'\, \overline{\tilde{G}^{(E0)}_{na}(-\boldsymbol{q},t|\boldsymbol{q},t'\|\boldsymbol{k},\boldsymbol{p},\boldsymbol{q})} \\
&\qquad \times \overline{\tilde{u}^{(0)}_m(-\boldsymbol{p},t\|\boldsymbol{k},\boldsymbol{p},\boldsymbol{q})\,\tilde{u}^{(0)}_b(\boldsymbol{p},t'\|\boldsymbol{k},\boldsymbol{p},\boldsymbol{q})}\ \overline{\tilde{u}^{(0)}_j(-\boldsymbol{k},t\|\boldsymbol{k},\boldsymbol{p},\boldsymbol{q})\,\tilde{u}^{(0)}_c(\boldsymbol{k},t'\|\boldsymbol{k},\boldsymbol{p},\boldsymbol{q})} \\
&= \frac{(2\pi)^{9}}{L^{6}}\,\tilde{P}_{imn}(\boldsymbol{k}) \sum_{\substack{\boldsymbol{p}\\(\boldsymbol{k}+\boldsymbol{p}+\boldsymbol{q}=\boldsymbol{o})}}\sum_{\boldsymbol{q}} \tilde{P}_{abc}(\boldsymbol{q}) \int_{t_0}^{t} \mathrm{d}t'\, \overline{\tilde{G}^{(L0)}_{na}(t|-\boldsymbol{q},\boldsymbol{q},t'\|\boldsymbol{k},\boldsymbol{p},\boldsymbol{q})}\ \tilde{Q}_{mb}(-\boldsymbol{p},t,t')\,\tilde{Q}_{jc}(-\boldsymbol{k},t,t')\ . \qquad (3.185)
\end{aligned}$$

Similarly, the third term reduces to

$$\begin{aligned}
&\text{(Third term on r.h.s. of (3.68))} \\
&= \frac{1}{2}\,\frac{(2\pi)^{9}}{L^{6}}\,\tilde{P}_{imn}(\boldsymbol{k}) \sum_{\substack{\boldsymbol{p}\\(\boldsymbol{k}+\boldsymbol{p}+\boldsymbol{q}=\boldsymbol{o})}}\sum_{\boldsymbol{q}} \tilde{P}_{abc}(\boldsymbol{k}) \int_{t_0}^{t} \mathrm{d}t'\, \overline{\tilde{G}^{(L0)}_{ja}(t|-\boldsymbol{k},\boldsymbol{k},t'\|\boldsymbol{k},\boldsymbol{p},\boldsymbol{q})}\ \tilde{Q}_{mb}(-\boldsymbol{p},t,t')\,\tilde{Q}_{nc}(-\boldsymbol{q},t,t')\ . \qquad (3.186)
\end{aligned}$$

A combination of (3.185) and (3.186) leads to

$$\begin{aligned}
&\left[\frac{\partial}{\partial t}+\nu k^2\right]\tilde{V}_{ij}(\boldsymbol{k},t,t) = \frac{1}{2}\,\frac{(2\pi)^{9}}{L^{6}}\,\tilde{P}_{imn}(\boldsymbol{k}) \sum_{\substack{\boldsymbol{p}\\(\boldsymbol{k}+\boldsymbol{p}+\boldsymbol{q}=\boldsymbol{o})}}\sum_{\boldsymbol{q}} \int_{t_0}^{t} \mathrm{d}t'\, \tilde{Q}_{mb}(-\boldsymbol{p},t,t') \\
&\times\Big\{\, 2\tilde{P}_{abc}(\boldsymbol{q})\,\overline{\tilde{G}^{(L0)}_{na}(t|-\boldsymbol{q},\boldsymbol{q},t'|\boldsymbol{k},\boldsymbol{p},\boldsymbol{q})}\,\tilde{Q}_{jc}(-\boldsymbol{k},t,t') \\
&\qquad\qquad +\tilde{P}_{abc}(\boldsymbol{k})\,\overline{\tilde{G}^{(L0)}_{ja}(t|-\boldsymbol{k},\boldsymbol{k},t'\|\boldsymbol{k},\boldsymbol{p},\boldsymbol{q})}\,\tilde{Q}_{nc}(-\boldsymbol{q},t,t')\,\Big\} \\
&+\ (i\leftrightarrow j\,,\ \boldsymbol{k}\to-\boldsymbol{k})\,. \qquad (3.187)
\end{aligned}$$

Multiplying the above equation by $\tilde{P}_{\alpha i}(\boldsymbol{k})$, replacing suffixes appropriately and using (3.46) and (3.67), we obtain (3.69).

## Appendix E

We derive here evolution equations (3.70) and (3.71) for the two-point two-time Lagrangian velocity correlation and the response functions.

As for the Lagrangian velocity correlation function, the viscous term of (3.44) is expressed, under Assumption 1, as

$$\text{(Viscous term of (3.44))} = -\frac{(2\pi)^9}{L^6}\,\nu \sum_{\boldsymbol{p}} p^2\, \overline{\tilde{u}_i^{(0)}(\boldsymbol{p},t\|\boldsymbol{k}_0,\boldsymbol{p}_0,\boldsymbol{q}_0)\,\tilde{\psi}^{(0)}(-\boldsymbol{p},t|\boldsymbol{k},t'\|\boldsymbol{k}_0,\boldsymbol{p}_0,\boldsymbol{q}_0)\,\tilde{u}_j^{(0)}(-\boldsymbol{k},t'\|\boldsymbol{k}_0,\boldsymbol{p}_0,\boldsymbol{q}_0)}\ , \tag{3.188}$$

which is rewritten, using Assumption 3, (3.64) and (3.66), as

$$\text{(Viscous term of (3.44))} = -\nu k^2\,\tilde{Q}_{ij}(\boldsymbol{k},t,t')\,. \tag{3.189}$$

The nonlinear term of (3.44) is approximated, under Assumption 1, by

$$\begin{aligned}\text{(Nonlinear term of (3.44))} = -\mathrm{i}\frac{(2\pi)^{12}}{L^9}\sum_{\substack{\boldsymbol{p}\\(\boldsymbol{p}+\boldsymbol{q}+\boldsymbol{r}=\boldsymbol{o})}}\sum_{\boldsymbol{q}}\sum_{\boldsymbol{r}}\frac{r_i r_m r_n}{r^2}\\ \times\Bigg[\ \overline{\tilde{u}_m^{(0)}(\boldsymbol{p},t\|\boldsymbol{p},\boldsymbol{q},\boldsymbol{r})\,\tilde{u}_n^{(0)}(\boldsymbol{q},t\|\boldsymbol{p},\boldsymbol{q},\boldsymbol{r})\,\tilde{\psi}^{(0)}(\boldsymbol{r},t|\boldsymbol{k},t'\|\boldsymbol{p},\boldsymbol{q},\boldsymbol{r})\,\tilde{u}_j^{(0)}(-\boldsymbol{k},t'\|\boldsymbol{p},\boldsymbol{q},\boldsymbol{r})}\\ +2\overline{\tilde{u}_m^{(1)}(\boldsymbol{p},t\|\boldsymbol{p},\boldsymbol{q},\boldsymbol{r})\,\tilde{u}_n^{(0)}(\boldsymbol{q},t\|\boldsymbol{p},\boldsymbol{q},\boldsymbol{r})\,\tilde{\psi}^{(0)}(\boldsymbol{r},t|\boldsymbol{k},t'\|\boldsymbol{p},\boldsymbol{q},\boldsymbol{r})\,\tilde{u}_j^{(0)}(-\boldsymbol{k},t'\|\boldsymbol{p},\boldsymbol{q},\boldsymbol{r})}\\ +\overline{\tilde{u}_m^{(0)}(\boldsymbol{p},t\|\boldsymbol{p},\boldsymbol{q},\boldsymbol{r})\,\tilde{u}_n^{(0)}(\boldsymbol{q},t\|\boldsymbol{p},\boldsymbol{q},\boldsymbol{r})\,\tilde{\psi}^{(0)}(\boldsymbol{r},t|\boldsymbol{k},t'\|\boldsymbol{p},\boldsymbol{q},\boldsymbol{r})\,\tilde{u}_j^{(1)}(-\boldsymbol{k},t'\|\boldsymbol{p},\boldsymbol{q},\boldsymbol{r})}\\ +\overline{\tilde{u}_m^{(0)}(\boldsymbol{p},t\|\boldsymbol{p},\boldsymbol{q},\boldsymbol{r})\,\tilde{u}_n^{(0)}(\boldsymbol{q},t\|\boldsymbol{p},\boldsymbol{q},\boldsymbol{r})\,\tilde{\psi}^{(1)}(\boldsymbol{r},t|\boldsymbol{k},t'\|\boldsymbol{p},\boldsymbol{q},\boldsymbol{r})\,\tilde{u}_j^{(0)}(-\boldsymbol{k},t'\|\boldsymbol{p},\boldsymbol{q},\boldsymbol{r})}\ \Bigg]\,.\end{aligned} \tag{3.190}$$

The first term of the above equation vanishes because of (3.64) and Assumptions 2 and 3. It is easily shown that both of the second and third terms are proportional to $k_i$. By substituting (3.176) in the fourth term, and using Assumptions 2, 3, (3.64) and (3.66), we obtain

$$\text{(Fourth term of (3.190))} = -2\left(\frac{2\pi}{L}\right)^3\sum_{\substack{\boldsymbol{p}\\(\boldsymbol{k}+\boldsymbol{p}+\boldsymbol{q}=\boldsymbol{o})}}\sum_{\boldsymbol{q}}\frac{q_a q_m q_n q_i}{q^2}\int_{t'}^{t}\mathrm{d}t''\,\tilde{Q}_{ma}(\boldsymbol{p},t,t'')\,\tilde{Q}_{nj}(\boldsymbol{k},t,t')\,. \tag{3.191}$$

Therefore, (3.44) reduces to

$$\begin{aligned}\frac{\partial}{\partial t}\tilde{V}_{ij}(\boldsymbol{k},t,t') = &-\nu k^2\,\tilde{Q}_{ij}(\boldsymbol{k},t,t') - 2\left(\frac{2\pi}{L}\right)^3\sum_{\substack{\boldsymbol{p}\\(\boldsymbol{k}+\boldsymbol{p}+\boldsymbol{q}=\boldsymbol{o})}}\sum_{\boldsymbol{q}}\frac{q_a q_m q_n q_i}{q^2}\int_{t'}^{t}\mathrm{d}t''\,\tilde{Q}_{ma}(\boldsymbol{p},t,t'')\,\tilde{Q}_{nj}(\boldsymbol{k},t,t')\\ &+(\text{terms proportional to } k_i)\,.\end{aligned} \tag{3.192}$$

By multiplying the above equation by $\tilde{P}_{li}(\boldsymbol{k})$, and noting that $\tilde{P}_{li}(\boldsymbol{k})\,k_i = 0$ and (3.46), we arrive at (3.70).

For the Lagrangian velocity response function we have only to deal with an ensemble average of (3.52) for $\boldsymbol{k}' = -\boldsymbol{k}$, i.e.

$$\begin{aligned}&\frac{\partial}{\partial t}\overline{\tilde{G}_{ij}^{(L)}(t|\boldsymbol{k},-\boldsymbol{k},t')} =\\ &-\nu\frac{(2\pi)^6}{L^3}\sum_{\boldsymbol{k}''}k''^2\left[\overline{\tilde{G}_{ij}^{(E)}(\boldsymbol{k}'',t|-\boldsymbol{k},t')\,\tilde{\psi}(-\boldsymbol{k}'',t|\boldsymbol{k},t')} + \overline{\tilde{u}_i(\boldsymbol{k}'',t)\,\tilde{\Psi}_j(-\boldsymbol{k}'',t|\boldsymbol{k},-\boldsymbol{k},t')}\right]\end{aligned}$$

$$-\mathrm{i}\frac{(2\pi)^9}{L^6}\sum_{\substack{\boldsymbol{p}\\(\boldsymbol{p}+\boldsymbol{q}+\boldsymbol{r}=\boldsymbol{o})}}\sum_{\boldsymbol{q}}\sum_{\boldsymbol{r}}\frac{r_i r_m r_n}{r^2}\left[2\overline{\widetilde{u}_m(\boldsymbol{p},t)\,\widetilde{G}^{(E)}_{nj}(\boldsymbol{q},t|-\boldsymbol{k},t')\,\widetilde{\psi}(\boldsymbol{r},t|\boldsymbol{k},t')}\right.$$
$$\left.+\overline{\widetilde{u}_m(\boldsymbol{p},t)\,\widetilde{u}_n(\boldsymbol{q},t)\,\widetilde{\Psi}_j(\boldsymbol{r},t|\boldsymbol{k},-\boldsymbol{k},t')}\right], \tag{3.193}$$

because only this combination appears in the equations for the correlation function (3.69) and (3.70). The viscous term of this equation is calculated, using Assumptions 1 and 3, (3.63) and (3.64), to be

$$\begin{aligned}&\text{(Viscous term of (3.193))}\\&\quad=-\nu\frac{(2\pi)^6}{L^3}\sum_{\boldsymbol{k}''}k''^2\,\overline{\widetilde{G}^{(E0)}_{ij}(\boldsymbol{k}'',t|-\boldsymbol{k},t'\|\boldsymbol{k}_0,\boldsymbol{p}_0,\boldsymbol{q}_0)}\;\overline{\widetilde{\psi}^{(0)}(-\boldsymbol{k}'',t|\boldsymbol{k},t'\|\boldsymbol{k}_0,\boldsymbol{p}_0,\boldsymbol{q}_0)}\\&\quad=-\nu\,k^2\,\overline{\widetilde{G}^{(L0)}_{ij}(t|\boldsymbol{k},-\boldsymbol{k},t\|\boldsymbol{k}_0,\boldsymbol{p}_0,\boldsymbol{q}_0)}\,.\end{aligned} \tag{3.194}$$

The first term in the second brackets of (3.193) is rewritten as

$$\begin{aligned}&\text{(First term in the second brackets of (3.193))}=-2\mathrm{i}\frac{(2\pi)^9}{L^6}\sum_{\substack{\boldsymbol{p}\\(\boldsymbol{p}+\boldsymbol{q}+\boldsymbol{r}=\boldsymbol{o})}}\sum_{\boldsymbol{q}}\sum_{\boldsymbol{r}}\frac{r_i r_m r_n}{r^2}\\&\quad\times\left[\overline{\widetilde{u}^{(0)}_m(\boldsymbol{p},t\|\boldsymbol{p},\boldsymbol{q},\boldsymbol{r})\,\widetilde{G}^{(E0)}_{nj}(\boldsymbol{q},t|-\boldsymbol{k},t'\|\boldsymbol{p},\boldsymbol{q},\boldsymbol{r})\,\widetilde{\psi}^{(0)}(\boldsymbol{r},t|\boldsymbol{k},t'\|\boldsymbol{p},\boldsymbol{q},\boldsymbol{r})}\right.\\&\quad+\overline{\widetilde{u}^{(1)}_m(\boldsymbol{p},t\|\boldsymbol{p},\boldsymbol{q},\boldsymbol{r})\,\widetilde{G}^{(E0)}_{nj}(\boldsymbol{q},t|-\boldsymbol{k},t'\|\boldsymbol{p},\boldsymbol{q},\boldsymbol{r})\,\widetilde{\psi}^{(0)}(\boldsymbol{r},t|\boldsymbol{k},t'\|\boldsymbol{p},\boldsymbol{q},\boldsymbol{r})}\\&\quad+\overline{\widetilde{u}^{(0)}_m(\boldsymbol{p},t\|\boldsymbol{p},\boldsymbol{q},\boldsymbol{r})\,\widetilde{G}^{(E1)}_{nj}(\boldsymbol{q},t|-\boldsymbol{k},t'\|\boldsymbol{p},\boldsymbol{q},\boldsymbol{r})\,\widetilde{\psi}^{(0)}(\boldsymbol{r},t|\boldsymbol{k},t'\|\boldsymbol{p},\boldsymbol{q},\boldsymbol{r})}\\&\quad\left.+\overline{\widetilde{u}^{(0)}_m(\boldsymbol{p},t\|\boldsymbol{p},\boldsymbol{q},\boldsymbol{r})\,\widetilde{G}^{(E0)}_{nj}(\boldsymbol{q},t|-\boldsymbol{k},t'\|\boldsymbol{p},\boldsymbol{q},\boldsymbol{r})\,\widetilde{\psi}^{(1)}(\boldsymbol{r},t|\boldsymbol{k},t'\|\boldsymbol{p},\boldsymbol{q},\boldsymbol{r})}\right],\end{aligned} \tag{3.195}$$

where higher-order terms of the deviation field have been neglected (Assumption 1). Thanks to Assumption 3 and $\overline{\widetilde{u}^{(0)}_i}=0$, the first term of (3.195) vanishes. For the other terms, we employ the procedures described in §3.3.2. On substitution of (3.62) in the second term to eliminate $\widetilde{u}^{(1)}_m$, we can show that it vanishes because of Assumptions 2 and 3. For the third term, we use (3.175) to eliminate $\widetilde{G}^{(E1)}_{nj}$. Then, Assumption 3, (3.63), (3.64) and (3.66) reduce it to

$$\begin{aligned}&\text{(Third term of (3.195))}=-2\,\frac{(2\pi)^9}{L^6}\,\frac{k_i k_m k_n}{k^2}\sum_{\substack{\boldsymbol{p}\\(\boldsymbol{k}+\boldsymbol{p}+\boldsymbol{q}=\boldsymbol{o})}}\sum_{\boldsymbol{q}}\widetilde{P}_{abc}(\boldsymbol{q})\\&\quad\times\int_{t'}^{t}\mathrm{d}t''\,\overline{\widetilde{G}^{(L0)}_{na}(t|-\boldsymbol{q},\boldsymbol{q},t''\|\boldsymbol{k},\boldsymbol{p},\boldsymbol{q})}\;\overline{\widetilde{G}^{(L0)}_{cj}(t''|\boldsymbol{k},-\boldsymbol{k},t'\|\boldsymbol{k},\boldsymbol{p},\boldsymbol{q})}\;\widetilde{Q}_{mb}(-\boldsymbol{p},t,t'')\,.\end{aligned} \tag{3.196}$$

For the fourth term, (3.176) is used to eliminate $\widetilde{\psi}^{(1)}$. Then, we can rewrite it, using Assumptions 2 and 3, (3.63), (3.64) and (3.66), as

$$\begin{aligned}&\text{(Fourth term of (3.195))}=-2\left(\frac{2\pi}{L}\right)^3\sum_{\substack{\boldsymbol{p}\\(\boldsymbol{k}+\boldsymbol{p}+\boldsymbol{q}=\boldsymbol{o})}}\sum_{\boldsymbol{q}}\frac{q_i q_m q_n q_a}{q^2}\\&\quad\times\int_{t'}^{t}\mathrm{d}t''\,\overline{\widetilde{G}^{(L0)}_{nj}(t|\boldsymbol{k},-\boldsymbol{k},t'\|\boldsymbol{k},\boldsymbol{p},\boldsymbol{q})}\;\widetilde{Q}_{ma}(\boldsymbol{p},t,t'')\,.\end{aligned} \tag{3.197}$$

Finally, we calculate the second term in the second brackets of (3.193). By neglecting higher-order terms of the deviation field under Assumption 1, we obtain

$$\begin{aligned}(\text{Second term in the second brackets of (3.193)}) = -\mathrm{i}\,\frac{(2\pi)^9}{L^6}\sum_{\substack{\boldsymbol{p}\\(\boldsymbol{p}+\boldsymbol{q}+\boldsymbol{r}=\boldsymbol{o})}}\sum_{\boldsymbol{q}}\sum_{\boldsymbol{r}}\frac{r_i r_m r_n}{r^2}\\ \times\Bigg[\overline{\widetilde{u}_m^{(0)}(\boldsymbol{p},t\|\boldsymbol{p},\boldsymbol{q},\boldsymbol{r})\,\widetilde{u}_n^{(0)}(\boldsymbol{q},t\|\boldsymbol{p},\boldsymbol{q},\boldsymbol{r})\,\widetilde{\Psi}_j^{(0)}(\boldsymbol{r},t|\boldsymbol{k},-\boldsymbol{k},t'\|\boldsymbol{p},\boldsymbol{q},\boldsymbol{r})}\\ +2\,\overline{\widetilde{u}_m^{(1)}(\boldsymbol{p},t\|\boldsymbol{p},\boldsymbol{q},\boldsymbol{r})\,\widetilde{u}_n^{(0)}(\boldsymbol{q},t\|\boldsymbol{p},\boldsymbol{q},\boldsymbol{r})\,\widetilde{\Psi}_j^{(0)}(\boldsymbol{r},t|\boldsymbol{k},-\boldsymbol{k},t'\|\boldsymbol{p},\boldsymbol{q},\boldsymbol{r})}\\ +\overline{\widetilde{u}_m^{(0)}(\boldsymbol{p},t\|\boldsymbol{p},\boldsymbol{q},\boldsymbol{r})\,\widetilde{u}_n^{(0)}(\boldsymbol{q},t\|\boldsymbol{p},\boldsymbol{q},\boldsymbol{r})\,\widetilde{\Psi}_j^{(1)}(\boldsymbol{r},t|\boldsymbol{k},-\boldsymbol{k},t'\|\boldsymbol{p},\boldsymbol{q},\boldsymbol{r})}\Bigg]. \qquad (3.198)\end{aligned}$$

The first term of this equation vanishes because $\widetilde{u}_m^{(0)}(\boldsymbol{p}\|\boldsymbol{p},\boldsymbol{q},\boldsymbol{r})$ has no correlation with $\widetilde{u}_n^{(0)}(\boldsymbol{q}\|\boldsymbol{p},\boldsymbol{q},\boldsymbol{r})$ (Assumption 2). Next, we substitute (3.62) into the second term, and (3.177) into the third term to eliminate quantities of deviation field. Then, it is easy to show that these terms vanish under Assumptions 2 and 3. The second term of the second brackets of (3.193), therefore, does not contribute at all to the governing equation of Lagrangian velocity response function. A combination of (3.194), (3.196) and (3.197) converts (3.193) into

$$\begin{aligned}&\frac{\partial}{\partial t}\,\overline{\widetilde{G}_{ij}^{(L)}(t|\boldsymbol{k},-\boldsymbol{k},t')} + \nu\,k^2\,\overline{\widetilde{G}_{ij}^{(L0)}(t|\boldsymbol{k},-\boldsymbol{k},t\|\boldsymbol{k}_0,\boldsymbol{p}_0,\boldsymbol{q}_0)} =\\ &\quad -2\,\frac{(2\pi)^9}{L^6}\,\frac{k_i k_m k_n}{k^2}\sum_{\substack{\boldsymbol{p}\\(\boldsymbol{k}+\boldsymbol{p}+\boldsymbol{q}=\boldsymbol{o})}}\sum_{\boldsymbol{q}}\widetilde{P}_{abc}(\boldsymbol{q})\\ &\qquad\times\int_{t'}^{t}\mathrm{d}t''\,\overline{\widetilde{G}_{na}^{(L0)}(t|-\boldsymbol{q},\boldsymbol{q},t''\|\boldsymbol{k},\boldsymbol{p},\boldsymbol{q})}\;\overline{\widetilde{G}_{cj}^{(L0)}(t''|\boldsymbol{k},-\boldsymbol{k},t'\|\boldsymbol{k},\boldsymbol{p},\boldsymbol{q})}\;\widetilde{Q}_{mb}(-\boldsymbol{p},t,t'')\\ &\quad -2\left(\frac{2\pi}{L}\right)^3\sum_{\substack{\boldsymbol{p}\\(\boldsymbol{k}+\boldsymbol{p}+\boldsymbol{q}=\boldsymbol{o})}}\sum_{\boldsymbol{q}}\frac{q_i q_m q_n q_a}{q^2}\int_{t'}^{t}\mathrm{d}t''\,\overline{\widetilde{G}_{nj}^{(L0)}(t|\boldsymbol{k},-\boldsymbol{k},t'\|\boldsymbol{k},\boldsymbol{p},\boldsymbol{q})}\;\widetilde{Q}_{ma}(\boldsymbol{p},t,t'')\,. \qquad (3.199)\end{aligned}$$

By multiplying this equation by $\widetilde{P}_{j\alpha}(\boldsymbol{k})$ and using (3.67), we obtain (3.71).

## Appendix F

Under the assumption of isotropy, by noting (3.72) and (3.73), we rewrite (3.69) as follows. First, we put $i = j$ and take a summation with respect to $i$. Then, the left-hand side reduces to

$$(\text{l.h.s. of (3.69)}) = \left[\frac{\partial}{\partial t} + 2\nu k^2\right] Q(k,t,t)\,. \qquad (3.200)$$

As for the first and the second terms on the right-hand side, we obtain

$$\begin{aligned}&(\text{First term on r.h.s. of (3.69)})\\ &\quad=\frac{1}{4}\left(\frac{2\pi}{L}\right)^3\widetilde{P}_{cmn}(\boldsymbol{k})\sum_{\substack{\boldsymbol{p}\\(\boldsymbol{k}+\boldsymbol{p}+\boldsymbol{q}=\boldsymbol{o})}}\sum_{\boldsymbol{q}}\widetilde{P}_{nbc}(\boldsymbol{p})\,\widetilde{P}_{mb}(\boldsymbol{q})\int_{t_0}^{t}\mathrm{d}t'\,G(p,t,t')\,Q(k,t,t')\,Q(q,t,t')\end{aligned}$$

$$= -\frac{1}{2}\left(\frac{2\pi}{L}\right)^3 \sum_{\substack{\boldsymbol{p}\\(\boldsymbol{k}+\boldsymbol{p}+\boldsymbol{q}=\boldsymbol{o})}}\sum_{\boldsymbol{q}} k^2\,\widehat{b}(k,p,q)\int_{t_0}^{t} \mathrm{d}t'\,G(p,t,t')\,Q(k,t,t')\,Q(q,t,t') \tag{3.201}$$

and

$$\begin{aligned}&\text{(Second term on r.h.s. of (3.69))}\\ &= \frac{1}{8}\left(\frac{2\pi}{L}\right)^3 \widetilde{P}_{imn}(\boldsymbol{k})\,\widetilde{P}_{ibc}(\boldsymbol{k}) \sum_{\substack{\boldsymbol{p}\\(\boldsymbol{k}+\boldsymbol{p}+\boldsymbol{q}=\boldsymbol{o})}}\sum_{\boldsymbol{q}} \widetilde{P}_{mb}(\boldsymbol{p})\,\widetilde{P}_{nc}(\boldsymbol{q})\int_{t_0}^{t}\mathrm{d}t'\,G(k,t,t')\,Q(p,t,t')\,Q(q,t,t')\\ &= \frac{1}{2}\left(\frac{2\pi}{L}\right)^3 \sum_{\substack{\boldsymbol{p}\\(\boldsymbol{k}+\boldsymbol{p}+\boldsymbol{q}=\boldsymbol{o})}}\sum_{\boldsymbol{q}} k^2\,\widehat{b}(k,p,q)\int_{t_0}^{t}\mathrm{d}t'\,G(k,t,t')\,Q(p,t,t')\,Q(q,t,t')\,,\end{aligned} \tag{3.202}$$

respectively. Here, use has been made of formulae,

$$\widetilde{P}_{ijm}(\boldsymbol{k})\,\widetilde{P}_{jin}(\boldsymbol{p})\,\widetilde{P}_{mn}(\boldsymbol{q}) = -2k^2\,\widehat{b}(k,p,q) \tag{3.203}$$

and

$$\widetilde{P}_{ijm}(\boldsymbol{k})\,\widetilde{P}_{ibc}(\boldsymbol{k})\,\widetilde{P}_{jb}(\boldsymbol{p})\,\widetilde{P}_{mc}(\boldsymbol{q}) = 2k^2\left[\,\widehat{b}(k,p,q)+\widehat{b}(k,q,p)\,\right]. \tag{3.204}$$

Hence, we get

$$\begin{aligned}\left[\frac{\partial}{\partial t}+2\nu k^2\right]Q(k,t,t) &= \left(\frac{2\pi}{L}\right)^3 \sum_{\substack{\boldsymbol{p}\\(\boldsymbol{k}+\boldsymbol{p}+\boldsymbol{q}=\boldsymbol{o})}}\sum_{\boldsymbol{q}} k^2\,\widehat{b}(k,p,q)\\ &\quad\times\int_{t_0}^{t}\mathrm{d}t'\,Q(q,t,t')\left[\,G(k,t,t')\,Q(p,t,t')-G(p,t,t')\,Q(k,t,t')\,\right].\end{aligned} \tag{3.205}$$

By taking the limit $L\to\infty$ and noting the formula (see for example Ref. [18])

$$\left(\frac{2\pi}{L}\right)^3 \sum_{\substack{\boldsymbol{p}\\(\boldsymbol{k}+\boldsymbol{p}+\boldsymbol{q}=\boldsymbol{o})}}\sum_{\boldsymbol{q}} \longrightarrow \iint_{\triangle_k}\mathrm{d}p\,\mathrm{d}q\,\frac{2\pi pq}{k} \qquad (L\to\infty)\,, \tag{3.206}$$

we may convert (3.205) into (3.75).

Next, we rewrite (3.70) under the assumption of isotropy. By putting $i=j$ and taking a summation with respect to $i$, the left and right-hand sides of (3.70) are reduced respectively to

$$\text{(l.h.s. of (3.70))} = \left[\frac{\partial}{\partial t}+\nu k^2\right]Q(k,t,t') \tag{3.207}$$

and

$$\begin{aligned}\text{(r.h.s. of (3.70))} &= -\frac{1}{2}\left(\frac{2\pi}{L}\right)^3 \widetilde{P}_{ab}(\boldsymbol{k}) \sum_{\substack{\boldsymbol{p}\\(\boldsymbol{k}+\boldsymbol{p}+\boldsymbol{q}=\boldsymbol{o})}}\sum_{\boldsymbol{q}} \frac{q_a q_b q_c q_d}{q^2}\,\widetilde{P}_{cd}(\boldsymbol{p})\int_{t'}^{t}\mathrm{d}t''\,Q(p,t,t'')\,Q(k,t,t')\\ &= -\frac{1}{2}\left(\frac{2\pi}{L}\right)^3 \sum_{\substack{\boldsymbol{p}\\(\boldsymbol{k}+\boldsymbol{p}+\boldsymbol{q}=\boldsymbol{o})}}\sum_{\boldsymbol{q}} k^2\,\widehat{d}(k,p,q)\int_{t'}^{t}\mathrm{d}t''\,Q(p,t,t'')\,Q(k,t,t')\,.\end{aligned} \tag{3.208}$$

Here, $\widehat{d}(k,p,q)$ is defined by

$$\frac{q_a q_b q_c q_d}{q^2}\,\widetilde{P}_{ab}(\boldsymbol{k})\,\widetilde{P}_{cd}(\boldsymbol{p}) = k^2\left[\frac{1}{4k^2pq}\,(k+p+q)\,(k+p-q)\,(p+q-k)\,(q+k-p)\right]^2 = k^2\,\widehat{d}(k,p,q)\,. \tag{3.209}$$

We take the limit $L\to\infty$ and rewrite (3.208) as

$$(\text{r.h.s. of (3.70)}) = -\iint_{\triangle_k} \mathrm{d}p\,\mathrm{d}q\,\pi\,kpq\,\widehat{d}(k,p,q)\int_{t'}^{t}\mathrm{d}t''\,Q(p,t,t'')\,Q(k,t,t')\,. \tag{3.210}$$

Carrying out the integration with respect to $q$ and using the function $\widehat{\eta}$ define by (3.81), we obtain (3.76) from (3.207) and (3.210).

Finally, we reduce (3.71) to (3.77) under the assumption of isotropy. By putting $i=j$ and taking summation with respect to $i$, we rewrite (3.71) as

$$(\text{l.h.s. of (3.71)}) = 2\left[\frac{\partial}{\partial t}+\nu k^2\right]G(k,t,t')\,, \tag{3.211}$$

$$(\text{First term on r.h.s. of (3.71)}) = 0\,, \tag{3.212}$$

since $k_i\widetilde{P}_{ij}(\boldsymbol{k})=0$, and

$$\begin{aligned}&(\text{Second term on r.h.s. of (3.71)})\\ &\quad= -\left(\frac{2\pi}{L}\right)^3\widetilde{P}_{ab}(\boldsymbol{k})\sum_{\substack{\boldsymbol{p}\\(\boldsymbol{k}+\boldsymbol{p}+\boldsymbol{q}=\boldsymbol{o})}}\sum_{\boldsymbol{q}}\frac{q_aq_bq_cq_d}{q^2}\,\widetilde{P}_{cd}(\boldsymbol{p})\int_{t'}^{t}\mathrm{d}t''\,Q(p,t,t'')\,G(k,t,t')\\ &\quad= -\left(\frac{2\pi}{L}\right)^3\sum_{\substack{\boldsymbol{p}\\(\boldsymbol{k}+\boldsymbol{p}+\boldsymbol{q}=\boldsymbol{o})}}\sum_{\boldsymbol{q}}k^2\,\widehat{d}(k,p,q)\int_{t'}^{t}\mathrm{d}t''\,Q(p,t,t'')\,G(k,t,t')\,.\end{aligned} \tag{3.213}$$

Then, (3.211)—(3.213) tends to (3.77) at the limit $L\to\infty$.

## Appendix G

We assume that in the universal range of decaying turbulence $Q(k,t,t)$ is characterized by $k$, $\epsilon(t)$ and $\nu$, and therefore written as

$$Q(k,t,t) = \nu^{\frac{11}{4}}\,\epsilon(t)^{-\frac{1}{4}}\,\widehat{Q}(\mathcal{B}\,\nu^{\frac{4}{3}}\,\epsilon(t)^{-\frac{1}{4}}\,k)\,, \tag{3.214}$$

where $\mathcal{B}$ is a non-dimensional constant. Then, it can be shown, under the assumption of a power decay law (3.128) of energy, that the time-derivative term in (3.84) is smaller in magnitude than the viscous and the nonlinear terms by $Re^{-\frac{1}{2}}$. Hence, in the limit of $Re\to\infty$, $Q(k,t,t)$ is independent of time in this range, which also allows such a stationary form as $G(k,t,t')=\tilde{G}(k,t-t')$ in governing equation (3.77) of $G(k,t,t')$. In conclusion, the solution of decaying turbulence in this range is identical to that of stationary turbulence.

## Appendix H

Equation (3.155) is derived here. Successive changes of variables in (3.140), $t'$ to $tt'$, $t$ to $t^{\frac{2}{3}}$ and $(pt, qt)$ to $(p, q)$, lead to

$$t^{\frac{4}{3b}-2}\frac{\partial}{\partial t}\Big(\, t^{\frac{4}{3}-\frac{4}{3b}}\, E^{\ddagger}(t^{\frac{2}{3}})\,\Big) = \frac{2}{3}\, t^{3}\iint_{\triangle_t} \mathrm{d}p\mathrm{d}q\, pq\, \widehat{b}(t,p,q)\int_{0}^{1}\mathrm{d}t'\, t'^{3-\frac{3}{b}}$$
$$\times\, G^{\ddagger}(t^{\frac{2}{3}}, t^{\frac{2}{3}}t')\, G^{\ddagger}(p^{\frac{2}{3}}, p^{\frac{2}{3}}t')\, G^{\ddagger}(q^{\frac{2}{3}}, q^{\frac{2}{3}}t')\, q^{-\frac{11}{3}}\, E^{\ddagger}(q^{\frac{2}{3}}t')\left[\, p^{\frac{11}{3}}\, E^{\ddagger}(p^{\frac{2}{3}}t') - t^{\frac{11}{3}}\, E^{\ddagger}(t^{\frac{2}{3}}t')\,\right]. \tag{3.215}$$

By integrating the both sides of the above equation from 0 to infinity with respect to $t$, we obtain

$$\text{(l.h.s.)} = -\Big(\frac{2}{b}-3\Big)\int_{0}^{\infty}\mathrm{d}t\, t^{-2}\, E^{\ddagger}(t)\,, \tag{3.216}$$

$$\text{(r.h.s.)} = -\lim_{T\to\infty}\frac{2}{3}\, T^{\frac{2}{3}}\int_{1}^{\infty}\mathrm{d}t\int_{0}^{\infty}\mathrm{d}p\int_{\max\{t-p,p\}}^{t+p}\mathrm{d}q\, t^{3}pq\int_{0}^{1}\mathrm{d}t'\, t'^{3-\frac{3}{b}}$$
$$\times\, G^{\ddagger}((tT)^{\frac{2}{3}}, (tT)^{\frac{2}{3}}t')\, G^{\ddagger}((pT)^{\frac{2}{3}}, (pT)^{\frac{2}{3}}t')\, G^{\ddagger}((qT)^{\frac{2}{3}}, (qT)^{\frac{2}{3}}t')$$
$$\times\Big\{\Big[\,\widehat{b}(t,p,q)+\widehat{b}(t,q,p)\,\Big]\,(pq)^{-\frac{11}{3}}\, E^{\ddagger}((pT)^{\frac{2}{3}}t')\, E^{\ddagger}((qT)^{\frac{2}{3}}t')$$
$$-\Big[\,\widehat{b}(t,p,q)\, q^{-\frac{11}{3}}\, E^{\ddagger}((qT)^{\frac{2}{3}}t') + \widehat{b}(t,q,p)\, p^{-\frac{11}{3}}\, E^{\ddagger}((pT)^{\frac{2}{3}}t')\,\Big]\, t^{-\frac{11}{3}}\, E^{\ddagger}((tT)^{\frac{2}{3}}t')\,\Big\}. \tag{3.217}$$

By taking account of (3.145) and (3.152), we can calculate (3.217) to be

$$\text{(r.h.s.)} = -\frac{2}{3}\int_{1}^{\infty}\mathrm{d}t\int_{0}^{1}\mathrm{d}p\int_{\max\{t-p,p\}}^{t+p}\mathrm{d}q\, t^{3}pq\int_{0}^{\infty}\mathrm{d}t'\, G^{\ddagger}{}_{\infty}(t^{\frac{2}{3}}t')\, G^{\ddagger}{}_{\infty}(p^{\frac{2}{3}}t')\, G^{\ddagger}{}_{\infty}(q^{\frac{2}{3}}t')$$
$$\times\Big\{\Big[\,\widehat{b}(t,p,q)+\widehat{b}(t,q,p)\,\Big]\,(pq)^{-\frac{11}{3}} - \Big[\,\widehat{b}(t,p,q)\, q^{-\frac{11}{3}} + \widehat{b}(t,q,p)\, p^{-\frac{11}{3}}\,\Big]\, t^{-\frac{11}{3}}\,\Big\}. \tag{3.218}$$

Equation (3.155) follows from (3.216) and (3.218).

## Appendix I

For the purpose of numerical computation of (3.140)—(3.142), it is convenient to introduce $H$ by

$$G^{\ddagger}(t,t') = H(t-t',t')\,, \tag{3.219}$$

because the difference between two times in $G^{\ddagger}$ has more important meaning of the response time. Substituting (3.219) into (3.140) and (3.141), we obtain

$$E^{\ddagger}(t) = -\frac{9}{4}\, t^{-2+\frac{2}{b}}\int_{0}^{\infty}\mathrm{d}k\int_{2^{-2/3}}^{\infty}\mathrm{d}q\int_{|q^{\frac{3}{2}}-k^{\frac{3}{2}}|^{\frac{2}{3}}}^{q}\mathrm{d}p\int_{\max\{0,\frac{t-k}{k}\}}^{\infty}\mathrm{d}s\,(s+1)^{\frac{1}{b}-1}\, k^{8-\frac{2}{b}}\,(pq)^{2}$$

$$\times H(ks,k)\ H(ps,p)\ H(qs,q)$$
$$\times \Big[ E^{\ddagger}(p)\, E^{\ddagger}(q)\, (pq)^{-\frac{11}{2}} \Big\{ \widehat{b}(k^{\frac{3}{2}},p^{\frac{3}{2}},q^{\frac{3}{2}}) + \widehat{b}(k^{\frac{3}{2}},q^{\frac{3}{2}},p^{\frac{3}{2}}) \Big\}$$
$$- E^{\ddagger}(k)\, k^{-\frac{11}{2}} \Big\{ E^{\ddagger}(p)\, p^{-\frac{11}{2}}\, \widehat{b}(k^{\frac{3}{2}},q^{\frac{3}{2}},p^{\frac{3}{2}}) + E^{\ddagger}(q)\, q^{-\frac{11}{2}}\, \widehat{b}(k^{\frac{3}{2}},p^{\frac{3}{2}},q^{\frac{3}{2}}) \Big\} \Big] \tag{3.220}$$

and

$$H(t,t') = \exp\Big[ -\int_0^{\infty} \mathrm{d}t'' \int_0^{\frac{tt''}{t'}} \mathrm{d}s \int_{\frac{s+t''}{t+t'}}^{\frac{t''}{t'}} \mathrm{d}p\, J(p)\, p^{-2} \Big[ \frac{s}{t''} + 1 \Big]^{\frac{1}{b}-1} E^{\ddagger}(t'')\, H(s,t'') \Big], \tag{3.221}$$

respectively. Boundary condition (3.149) is written as

$$H(0,t') = 1\,, \tag{3.222}$$

while, asymptotic condition (3.152) at large time is represented by

$$H(t,t') \to {G^{\ddagger}}_{\infty}(t) \qquad (\text{as } t' \to \infty)\,. \tag{3.223}$$

Relation (3.142) between $b$ and $\zeta$ is rewritten as

$$b = \begin{cases} \dfrac{4}{3(\zeta+3)} & (2 \le \zeta < 4)\,, \\ \Big[ \dfrac{21}{4} - \dfrac{7}{10\, {E^{\ddagger}}_0} \displaystyle\int_0^{\infty} \mathrm{d}t \int_0^{\infty} \mathrm{d}k\, (k+t)^{\frac{3}{b}-\frac{23}{2}}\, t^{3-\frac{3}{b}} \Big( H(k,t)\, E^{\ddagger}(t) \Big)^2 \Big]^{-1} & (\zeta = 4)\,. \end{cases} \tag{3.224}$$

We solve numerically a set of integro-differential equations (3.220), (3.221) and (3.224) under boundary conditions (3.145) and (3.222), and asymptotic conditions (3.143) and (3.223). Equations (3.221) and (3.224) are solved by an iterative method, while (3.220) by the Newton-Raphson method.

# Chapter 4

# Lagrangian DIA for a Passive Scalar Field Advected by Turbulence

We apply the Lagrangian DIA introduced in the preceding chapter to a passive scalar field advected by isotropic turbulence. We derive a closed set of equations for the passive scalar correlation and the Lagrangian velocity correlation functions, and show that solutions to the resultant closure equations are completely consistent with the well-known scaling laws of the scalar spectrum, which were predicted phenomenologically by Obukhov [64], Corrsin [65], Batchelor, Howells & Townsend [66] and Batchelor [67]. The functional forms of the scalar spectrum in the statistically stationary state in the entire universal wavenumber range are evaluated by solving numerically the closure equations for each case of moderate, extremely large and small values of the Schmidt number. Schmidt number dependence of the mixed-derivative skewness factor of the velocity and the scalar fields is also evaluated, which is in a good agreement with a direct numerical simulation by Kerr [68].

## 4.1 Introduction

Encouraged by the successes of an application of the Lagrangian DIA to incompressible turbulent velocity field in the preceding chapter, we shall apply this closure theory to a scalar field, such as temperature, contaminant, particle concentration, dye, smoke and so on, which is advected by isotropic turbulence. It is assumed that dynamics of the velocity field is free from that of the scalar field, in other words, the scalar field is passively advected by turbulent velocity field. Similarly to the Kolmogorov theory on the velocity correlation function, several phenomenologies [64–67] on small-scale statistics of scalar field, especially, the two-point correlation function, have been proposed. The aim of this chapter is to make a bridge which connects such phenomenologies and the basic equations.

Numerous attempts to attack this problem have been made so far by many researchers. Among others, Kraichnan [69,70] applied the abridged LHDIA [37] to a passive scalar field and showed that

the results were consistent with the well-known scaling laws (4.8), (4.10) and (4.14) below, of the passive scalar spectrum. The formulation of the abridged LHDIA is, however, somewhat complicated, and the deduction of the scaling laws from the ALHDIA equations is partly incomplete. Moreover, it cannot predict the wavenumber boundaries of each scaling law, which are important because there are several different phenomenological proposal of boundaries (see e.g. Ref. [71]). Kaneda [50] and Gotoh et al. [51] applied LRA [36] to a passive scalar field with zero diffusivity.

One of the main tasks of this chapter is to determine the universal functional forms in the statistically steady state of the scalar power spectrum with high accuracy. Although such studies have been made [49, 51] based upon closure equations by LHDIA or LRA, the accuracy of their estimations of the functional form determined from a late state in a decaying numerical simulation of the closure equations may be questionable. It is not easy to know the time when it has approached the universal state and there is no guarantee that the functional forms of the spectrum in the decaying and stationary turbulence ever coincide with each other. For example, in Fig.12 of Ref. [49] or in Fig.13 of Ref. [51] we hardly observe the universality of the constants even when an identical closure equation is solved.

This chapter[1] is organized as follows. Phenomenologies on small-scale statistics of the passive scalar fields are reviewed in the rest of this section, and summarized in Fig.4.1. (See Lesieur [22] and Tennekes & Lumley [17] for more detailed discussions.) After describing the basic equations in §4.2, we formulate in §4.3 the Lagrangian DIA for a passive scalar field to derive an integro-differential equation for the correlation function. A detailed analysis of the resultant closure equation is made in §4.4 to find universal forms of the passive scalar spectrum. Three kinds of scaling laws (4.8), (4.10) and (4.14) are shown to be consistent with the solutions to the closure equation and all the universal constants are evaluated. In addition, the universal forms of the function are determined numerically for several finite values of $s$ as well as for two extremes $s \gg 1$ and $s \ll 1$. Section 4.5 is devoted to concluding remarks of this chapter.

### 4.1.1 Characteristic wavenumbers

Recall that there are only two characteristic length scales, the integral scale $L$ and the viscous (Kolmogorov) scale $\eta$, in the turbulent velocity field. Roughly speaking, the integral scale corresponds to the wavenumber $k_v$ at which the energy spectrum takes the maximum. On the other hand, the reciprocal of $\eta$ is the Kolmogorov wavenumber,

$$k_K = 1/\eta = (\epsilon/\nu^3)^{1/4}, \tag{4.1}$$

where the inertial-range turbulent diffusion time $(k^{2/3}\epsilon^{1/3})^{-1}$ and the viscous dissipation time $(\nu k^2)^{-1}$ are comparable. Incidentally, the viscous dissipation time at wavenumbers larger than $k_K$ is smaller than the inertial time. It is interesting that there is no characteristic length scale between the two

[1] This chapter is based upon Ref. [72].

characteristic wavenumbers $k_v$ and $k_K$, and therefore a scale similarity of the velocity field in the statistical sense may be expected. The $k^{-5/3}$ power law of the energy spectrum in the inertial range, for example, results from this property. The ratio $k_K/k_v$ increases with the Reynolds number in proportion to $Re^{3/4}$ (see (1.26)).

In addition to the two wavenumbers $k_v$ and $k_K$, there exist a few more wavenumbers which characterize the statistics of a passive scalar field. The peak wavenumber $k_s$ of the passive scalar spectrum represents the typical length of the large-scale structures. The characteristic wavenumbers for small scales, on the other hand, are different depending on the Schmidt number (or the Prandtl number on speaking of temperature),

$$s = \nu/\kappa \,, \tag{4.2}$$

the ratio of the kinematic viscosity $\nu$ of a fluid and the diffusion coefficient $\kappa$ of a passive scalar. If $s < 1$, it is the Obukhov-Corrsin wavenumber,

$$k_C = (\epsilon/\kappa^3)^{1/4} \ \ (= s^{3/4}\, k_K) \,, \tag{4.3}$$

at which the inertial-range turbulent diffusion time and the scalar dissipation time $(\kappa k^2)^{-1}$ are comparable, whereas, if $s > 1$, it is the Batchelor wavenumber,

$$k_B = (\epsilon/\nu\kappa^2)^{1/4} \ \ (= s^{1/2}\, k_K = s^{-1/4}\, k_C) \,, \tag{4.4}$$

at which the scalar dissipation time and the shearing time $(\nu/\epsilon)^{1/2}$ of vortices of the Kolmogorov scale are comparable. In the cases that

$$\max\{k_v, k_s\} \ll \min\{k_K, k_C, k_B\} \,, \tag{4.5}$$

which we shall consider in the following, there exist a large number of degrees of freedom between the above two groups of wavenumbers, and scaling regions are expected for the scalar spectrum. As will be shown in §§4.1.2—4, there are a variety of scaling laws, depending on the Schmidt number which controls the relative magnitude of the three wavenumbers $k_K$, $k_C$ and $k_B$ as

$$\begin{cases} k_K \le k_B & (k_C \text{ is meaningless}) \qquad (\text{for } s \ge 1), & \text{(4.6a)} \\ k_C \le k_K & (k_B \text{ is meaningless}) \qquad (\text{for } s \le 1). & \text{(4.6b)} \end{cases}$$

It is worthwhile to mention that the largeness of the number of degrees of freedom is one of the validity conditions of DIA (see Chapter 2).

### 4.1.2 Inertial-advective range

The condition (4.5) guarantees the existence of the inertial-advective (inertial-convective) range,

$$\max\{k_v, k_s\} \ll k \ll \min\{k_K, k_C\}, \tag{4.7}$$

irrespective of the Schmidt number, in which neither the molecular viscosity nor the scalar dissipation is effective. By noting that the scalar spectrum function defined by (4.32) in §4.2.3 is independent of $\kappa$ and $\nu$, and by employing a dimensional analysis, we can derive a scaling law in this range as

$$\Theta(k) = C_1\, \chi\, \epsilon^{-1/3}\, k^{-5/3} \,, \tag{4.8}$$

where $\chi$ denotes the mean rate of the scalar fluctuation dissipation. This $k^{-5/3}$ power law in the inertial-advective range was proposed by Obukhov [64] and Corrsin [65] independently, and is supported by many observations (see Ref. [73]). Experimental value of the universal constant $C_1$, called the Obukhov-Corrsin constant, is about $(5/3) \times 0.4 = 0.67$.

### 4.1.3 Viscous-advective range

In smaller scales than the inertial-advective range, if the Schmidt number is large enough ($s \gg 1$), there exists the viscous-advective (viscous-convective) range,

$$k_K \ll k \ll k_B \,, \tag{4.9}$$

in which the scalar field is deformed by shearing motions induced by vortices of the Kolmogorov scale. Batchelor [67] derived a scaling law in this range as

$$\Theta(k) = C_2 \, \chi \, \nu^{1/2} \, \epsilon^{-1/2} \, k^{-1} \,. \tag{4.10}$$

This $k^{-1}$ power law is supported by measurements in the tidal flow by Grant et al. [74] and by Oakey [75], and the experimental values of the universal constant $C_2$, called the Batchelor constant, were found to be $3.9 \pm 1.5$ and $3.7 \pm 1.5$, respectively.

A simple derivation of (4.10) is as follows. In the advective range, the diffusion term in the governing equation (4.17) of the passive scalar is negligible compared with the other terms, and therefore the time derivative and the advection terms may balance. Then, from scalar fluctuation equation (4.33), we obtain

$$\frac{\partial}{\partial t} \int_k^\infty \mathrm{d}k' \, \Theta(k', t) = \Pi_\theta(k, t) \,. \tag{4.11}$$

Here, $\Pi_\theta$ is the flux function for the scalar fluctuations defined by (4.34) in §4.2.3, which may be equal to $\chi$ in the advective range. The left-hand side of (4.11) is roughly estimated as

$$(\text{l.h.s of (4.11)}) \sim \frac{k \, \Theta(k)}{\tau(k)} \,, \tag{4.12}$$

where $\tau(k)$ is the characteristic time scale of eddies that advect the scalar field. In the viscous-advective range, those eddies of the Kolmogorov scale $\eta$ contribute predominantly, the characteristic time scale of which is $(\nu/\epsilon)^{1/2}$. Equation (4.11) then leads to the $k^{-1}$ power law (4.10). By the way, the power law (4.8) is obtained by putting $\tau(k) = k^{-2/3}\epsilon^{-1/3}$, the time scale of eddies of inertial scale.

### 4.1.4 Inertial-diffusive range

If the Schmidt number is small enough ($s \ll 1$), there exists the inertial-diffusive (inertial-conductive) range

$$k_C \ll k \ll k_K \,, \tag{4.13}$$

in which the passive scalar is rapidly diffusing while being mixed by turbulence. Batchelor et al. [66] proposed a scaling law in this range as

$$\Theta(k) = C_3 \, \chi \, \kappa^{-3} \epsilon^{2/3} \, k^{-17/3} \tag{4.14}$$

with $C_3 = \frac{1}{3} K$. Let us describe an intuitive derivation of this scaling law. (See Ref. [66] for a detailed derivation.) Since in the inertial-diffusive range the eddy turnover time $k^{-2/3} \epsilon^{-1/3}$, which is equal to characteristic time scale of the time derivative term in the governing equation (4.17) of the passive scalar, is much larger than the scalar fluctuation dissipation time $(\nu k^2)^{-1}$, the governing equation may be approximated as

$$u_i(\boldsymbol{x}, t) \, \frac{\partial}{\partial x_i} \, \theta(\boldsymbol{x}, t) = \kappa \, \frac{\partial^2}{\partial x_i \partial x_i} \, \theta(\boldsymbol{x}, t) \, . \tag{4.15}$$

Noting that spatial variation of the scalar field in the diffusive range is relatively moderate because of strong molecular diffusivity effects, the mean rate $\chi$ of the scalar fluctuation dissipation may be evaluated, by the use of (4.15), as

$$\chi \sim \kappa \, \overline{\left( \frac{\partial \theta}{\partial x_1} \right)^2} \sim \kappa \left( \frac{\kappa k^2 \sqrt{k \Theta(k)}}{\sqrt{k E(k)}} \right)^2 = \kappa^3 \, k^4 \, \frac{\Theta(k)}{E(k)} \, . \tag{4.16}$$

Then we arrive at the $k^{-17/3}$ power law of the scalar spectrum because $E(k) \propto k^{-5/3}$ in the inertial range.

This $k^{-17/3}$ scaling law with the relation $C_3 = \frac{1}{3} K$ is supported by numerical simulations by Chasnov et al. [76]. The inertial-diffusive range might be observed by experiments of liquid metal. However, the scaling law seems too steep to measure accurately. Different phenomenological theories have also been proposed. Corrsin [77] predicts exponential decay of the scalar spectrum in this wavenumber range (see Tennekes & Lumley [17]). Gibson et al. [71] argued that there exist two scaling regions in the inertial-diffusive range, that is, the $k^{-3}$ power law between $k_{\mathrm{C}}$ and $k_{\mathrm{B}}$ are followed by the $k^{-17/3}$ power law up to $k_{\mathrm{K}}$. They claimed that Clay's experiment [78] supported their theory.

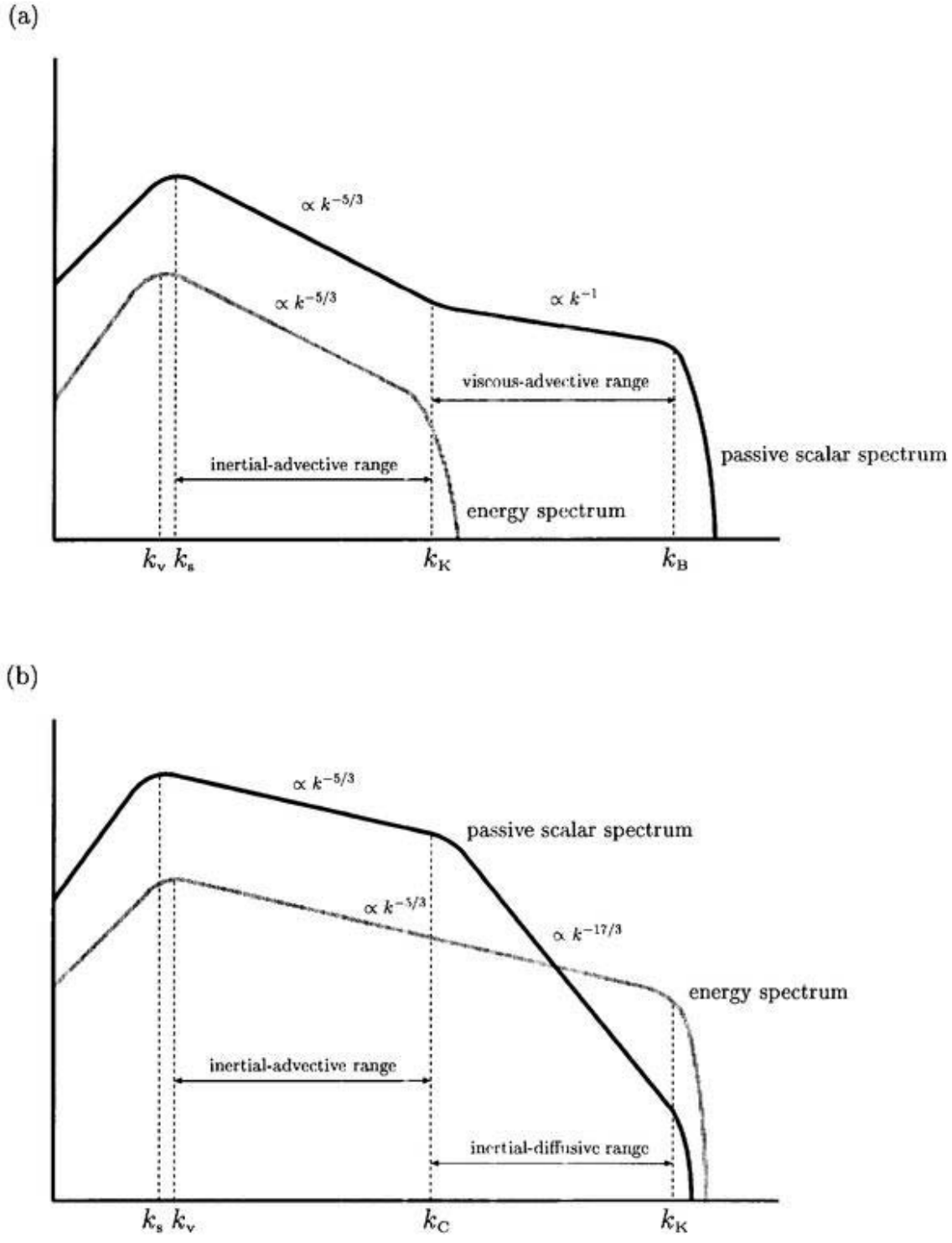


FIGURE 4.1 Schematic sketch of the passive scalar spectra predicted phenomenologically by Obukhov [64], Corrsin [65] (the $k^{-5/3}$ power law in the inertial-advective range), Batchelor [67] (the $k^{-1}$ power law in the viscous-advective range) and Batchelor et al. [66] (the $k^{-17/3}$ power law in the inertial-diffusive range). Figures (a) and (b) correspond to the large and the small Schmidt number limits, respectively. Energy spectrum is also drawn for a comparison. Both horizontal (wavenumber) and vertical (spectra) axes are scaled logarithmically.

## 4.2 Preparations

### 4.2.1 Basic equations

We consider the statistical properties of a passive scalar field $\theta(\boldsymbol{x},t)$ which obeys the advection-diffusion equation,

$$\frac{\partial}{\partial t}\,\theta(\boldsymbol{x},t)+u_i(\boldsymbol{x},t)\,\frac{\partial}{\partial x_i}\,\theta(\boldsymbol{x},t)=\kappa\,\frac{\partial^2}{\partial x_i\partial x_i}\,\theta(\boldsymbol{x},t)\,, \tag{4.17}$$

where $u_i(\boldsymbol{x},t)$ is an incompressible turbulent velocity field governed by the Navier-Stokes equation (3.18) and the equation of continuity (3.19).

### 4.2.2 Lagrangian scalar correlation function

The fundamental variables in the present Lagrangian closure are given by the Lagrangian scalar field and the correlation function of it. Similarly to (3.23) and (3.24), the Lagrangian scalar field $\theta^{(L)}$ is defined by

$$\theta^{(L)}(t|\boldsymbol{x},t')=\int \mathrm{d}^3\boldsymbol{x}'\,\psi(\boldsymbol{x}',t|\boldsymbol{x},t')\,\theta(\boldsymbol{x}',t) \tag{4.18}$$

and

$$\theta(\boldsymbol{x},t)=\int \mathrm{d}^3\boldsymbol{x}'\,\psi(\boldsymbol{x},t|\boldsymbol{x}',t')\,\theta^{(L)}(t|\boldsymbol{x}',t')\,, \tag{4.19}$$

where $\psi$ is the Lagrangian position function [36] defined by (3.20) and governed by (3.21) with initial condition (3.22). The Lagrangian scalar correlation function is then defined by

$$Z(\boldsymbol{r},t,t')=\overline{\theta^{(L)}(t|\boldsymbol{x}+\boldsymbol{r},t')\,\theta^{(L)}(t'|\boldsymbol{x}',t')}=\overline{\theta^{(L)}(t|\boldsymbol{x}+\boldsymbol{r},t')\,\theta(\boldsymbol{x}',t')} \tag{4.20}$$

in the same manner as (3.25).

### 4.2.3 Fourier representation

Just as in Chapter 3, we assume that the fluid is confined in a periodic cube of side $L$ (at the final stage of analysis we shall take the limit $L\to\infty$), and formulate the Lagrangian DIA in the Fourier space. The Eulerian and Lagrangian scalar fields are decomposed into Fourier series as

$$\theta(\boldsymbol{x},t)=\left(\frac{2\pi}{L}\right)^3\sum_{\boldsymbol{k}}\tilde{\theta}(\boldsymbol{k},t)\,\exp\Big[\,\mathrm{i}\boldsymbol{k}\cdot\boldsymbol{x}\,\Big] \tag{4.21}$$

and

$$\theta^{(L)}(\boldsymbol{x},t)=\left(\frac{2\pi}{L}\right)^3\sum_{\boldsymbol{k}}\tilde{\theta}^{(L)}(\boldsymbol{k},t)\,\exp\Big[\,\mathrm{i}\boldsymbol{k}\cdot\boldsymbol{x}\,\Big], \tag{4.22}$$

where $\boldsymbol{k}=(2\pi/L)\,(n_1,n_2,n_3)$, $(\,n_1,n_2,n_3=0,\pm1,\pm2,\cdots\,)$ is the wavenumber vector. The inverse transformations are written as

$$\tilde{\theta}(\boldsymbol{k},t)=\left(\frac{1}{2\pi}\right)^3\int \mathrm{d}^3\boldsymbol{x}\,\theta(\boldsymbol{x},t)\,\exp\Big[\,-\mathrm{i}\boldsymbol{k}\cdot\boldsymbol{x}\,\Big] \tag{4.23}$$

and

$$\widetilde{\theta}^{(L)}(\boldsymbol{k},t) = \left(\frac{1}{2\pi}\right)^3 \int \mathrm{d}^3\boldsymbol{x}\, \theta^{(L)}(\boldsymbol{x},t)\, \exp\Big[-\mathrm{i}\boldsymbol{k}\cdot\boldsymbol{x}\Big]. \tag{4.24}$$

Then, the evolution equation (4.17) of the scalar field and the relations (4.18)—(4.19) are respectively rewritten as

$$\left[\frac{\partial}{\partial t} + \kappa k^2\right] \widetilde{\theta}(\boldsymbol{k},t) = -\mathrm{i}\, k_j \left(\frac{2\pi}{L}\right)^3 \sum_{\substack{\boldsymbol{p}\\(\boldsymbol{k}+\boldsymbol{p}+\boldsymbol{q}=\boldsymbol{o})}} \sum_{\boldsymbol{q}} \widetilde{u}_j(-\boldsymbol{p},t)\, \widetilde{\theta}(-\boldsymbol{q},t) \tag{4.25}$$

and

$$\widetilde{\theta}^{(L)}(t|\boldsymbol{k},t') = \frac{(2\pi)^6}{L^3} \sum_{\boldsymbol{k}'} \widetilde{\psi}(-\boldsymbol{k}',t|\boldsymbol{k},t')\, \widetilde{\theta}(\boldsymbol{k}',t)\,, \tag{4.26}$$

$$\widetilde{\theta}(\boldsymbol{k},t) = \frac{(2\pi)^6}{L^3} \sum_{\boldsymbol{k}'} \widetilde{\psi}(\boldsymbol{k},t|-\boldsymbol{k}',t')\, \widetilde{\theta}^{(L)}(t|\boldsymbol{k}',t')\,. \tag{4.27}$$

Evolution equations for the Fourier transforms of the Lagrangian scalar field $\widetilde{\theta}^{(L)}$ and the correlation function,

$$\widetilde{Z}(\boldsymbol{k},t,t') = \left(\frac{1}{2\pi}\right)^3 \int \mathrm{d}^3\boldsymbol{r}\, Z(\boldsymbol{r},t,t')\, \exp\Big[-\mathrm{i}\boldsymbol{k}\cdot\boldsymbol{r}\Big] = \left(\frac{2\pi}{L}\right)^3 \overline{\widetilde{\theta}^{(L)}(t|\boldsymbol{k},t')\, \widetilde{\theta}(-\boldsymbol{k},t')} \tag{4.28}$$

are derived as follows. The time derivative of (4.26) yields

$$\left[\frac{\partial}{\partial t} + \kappa\, k^2\right] \widetilde{\theta}^{(L)}(t|\boldsymbol{k},t') = 0\,. \tag{4.29}$$

Combination of (4.25) and (4.29) leads to

$$\left[\frac{\partial}{\partial t} + 2\kappa k^2\right] \widetilde{Z}(\boldsymbol{k},t,t) = -\mathrm{i}\, k_j \left(\frac{2\pi}{L}\right)^6 \sum_{\substack{\boldsymbol{p}\\(\boldsymbol{k}+\boldsymbol{p}+\boldsymbol{q}=\boldsymbol{o})}} \sum_{\boldsymbol{q}} \overline{\widetilde{u}_j(-\boldsymbol{p},t)\, \widetilde{\theta}(-\boldsymbol{q},t)\, \widetilde{\theta}(-\boldsymbol{k},t)} + (\boldsymbol{k} \to -\boldsymbol{k}) \tag{4.30}$$

for the single time correlation and to

$$\left[\frac{\partial}{\partial t} + \kappa\, k^2\right] \widetilde{Z}(\boldsymbol{k},t,t') = 0 \tag{4.31}$$

for the two-time correlation.

For a later use, we define here the scalar spectrum,

$$\Theta(k,t) = k^2 \oint \mathrm{d}\Omega\, \widetilde{Z}(\boldsymbol{k},t,t)\,, \tag{4.32}$$

where $\oint \mathrm{d}\Omega$ denotes a solid angle integration in the Fourier space, the transfer functions,

$$T_\theta(k) = \left[\frac{\partial}{\partial t} + 2\kappa k^2\right] \Theta(k,t)\,, \tag{4.33}$$

which is the solid angle integration of the right-hand side of (4.30), and the flux function,

$$\Pi_\theta(k) = \int_k^\infty \mathrm{d}k'\, T_\theta(k')\,. \tag{4.34}$$

### 4.2.4 Response function

The response functions of $\widetilde{\theta}(\boldsymbol{k},t)$ and $\widetilde{\theta}^{(L)}(t|\boldsymbol{k},t')$ are defined by

$$\widetilde{G}_\theta(\boldsymbol{k},t|\boldsymbol{k}',t') = \frac{\delta\widetilde{\theta}(\boldsymbol{k},t)}{\delta\widetilde{\theta}(\boldsymbol{k}',t')} \tag{4.35}$$

and

$$\widetilde{G}_\theta^{(L)}(t|\boldsymbol{k},\boldsymbol{k}',t') = \frac{\delta\widetilde{\theta}^{(L)}(t|\boldsymbol{k},t')}{\delta\widetilde{\theta}(\boldsymbol{k}',t')}\,, \tag{4.36}$$

respectively, where $\delta$ denotes a functional derivative. The evolution equations for these response functions are respectively derived by taking functional derivatives of (4.25) and (4.29) as

$$\left[\frac{\partial}{\partial t} + \kappa k^2\right]\widetilde{G}_\theta(\boldsymbol{k},t|\boldsymbol{k}',t') = -\mathrm{i}\,k_j\left(\frac{2\pi}{L}\right)^3 \sum_{\substack{\boldsymbol{p}}}\sum_{\substack{\boldsymbol{q}\\(\boldsymbol{k}+\boldsymbol{p}+\boldsymbol{q}=\boldsymbol{o})}} \widetilde{u}_j(-\boldsymbol{p},t)\,\widetilde{G}_\theta(-\boldsymbol{q},t|\boldsymbol{k}',t') \tag{4.37}$$

and

$$\left[\frac{\partial}{\partial t} + \kappa k^2\right]\widetilde{G}_\theta^{(L)}(t|\boldsymbol{k},\boldsymbol{k}',t') = 0\,. \tag{4.38}$$

The initial conditions are given by

$$\widetilde{G}_\theta(\boldsymbol{k},t'|\boldsymbol{k}',t') = \widetilde{G}_\theta^{(L)}(t'|\boldsymbol{k},\boldsymbol{k}',t') = \frac{L^3}{(2\pi)^6}\,\delta^3_{\boldsymbol{k}+\boldsymbol{k}'}\,. \tag{4.39}$$

## 4.3 Lagrangian DIA for a passive scalar field

### 4.3.1 Direct-interaction decomposition

In the same manner as in the preceding chapters, we contract a closed set of equations for the scalar two-point correlation and the response functions. Recall that DIA is based upon the direct-interaction decomposition (§2.3.1) [24], in which $\widetilde{\theta}$ and $\widetilde{G}_\theta$ are respectively written as

$$\widetilde{\theta}(\boldsymbol{k},t) = \widetilde{\theta}^{(0)}(\boldsymbol{k},t\|\boldsymbol{k}_0,\boldsymbol{p}_0,\boldsymbol{q}_0) + \widetilde{\theta}^{(1)}(\boldsymbol{k},t\|\boldsymbol{k}_0,\boldsymbol{p}_0,\boldsymbol{q}_0) \tag{4.40}$$

and

$$\widetilde{G}_\theta(\boldsymbol{k},t) = \widetilde{G}_\theta^{(0)}(\boldsymbol{k},t|\boldsymbol{k}',t'\|\boldsymbol{k}_0,\boldsymbol{p}_0,\boldsymbol{q}_0) + \widetilde{G}_\theta^{(1)}(\boldsymbol{k},t|\boldsymbol{k}',t'\|\boldsymbol{k}_0,\boldsymbol{p}_0,\boldsymbol{q}_0)\,, \tag{4.41}$$

where $\boldsymbol{k}_0$, $\boldsymbol{p}_0$ and $\boldsymbol{q}_0$ ($\boldsymbol{k}_0+\boldsymbol{p}_0+\boldsymbol{q}_0=\boldsymbol{o}$) are a triplet of wavenumbers, the direct interaction between which has been removed in the NDI fields $\widetilde{\theta}^{(0)}$ and $\widetilde{G}_\theta^{(0)}$. These decompositions for $\widetilde{\theta}$ and $\widetilde{G}_\theta$ are made after $t_0$ and $t'$, respectively. The initial conditions for $\widetilde{\theta}^{(0)}$, $\widetilde{\theta}^{(1)}$, $\widetilde{G}_\theta^{(0)}$ and $\widetilde{G}_\theta^{(1)}$ are, therefore, given by

$$\widetilde{\theta}^{(0)}(\boldsymbol{k},t_0\|\boldsymbol{k}_0,\boldsymbol{p}_0,\boldsymbol{q}_0) = \widetilde{\theta}(\boldsymbol{k},t_0)\,, \qquad \widetilde{\theta}^{(1)}(\boldsymbol{k},t_0\|\boldsymbol{k}_0,\boldsymbol{p}_0,\boldsymbol{q}_0) = 0\,, \tag{4.42}$$

$$\widetilde{G}_\theta^{(0)}(\boldsymbol{k},t'|\boldsymbol{k}',t'\|\boldsymbol{k}_0,\boldsymbol{p}_0,\boldsymbol{q}_0) = \frac{L^3}{(2\pi)^6}\,\delta^3_{\boldsymbol{k}+\boldsymbol{k}'} \qquad \text{and} \qquad \widetilde{G}_\theta^{(1)}(\boldsymbol{k},t'|\boldsymbol{k}',t'\|\boldsymbol{k}_0,\boldsymbol{p}_0,\boldsymbol{q}_0) = 0\,, \tag{4.43}$$

respectively. By definitions, the NDI fields $\widetilde{\theta}^{(0)}$ and $\widetilde{G}_\theta^{(0)}$ are governed by

$$\left[\frac{\partial}{\partial t}+\kappa k^2\right]\widetilde{\theta}^{(0)}(\boldsymbol{k},t\|\boldsymbol{k}_0,\boldsymbol{p}_0,\boldsymbol{q}_0)=-\mathrm{i}\,k_j\left(\frac{2\pi}{L}\right)^3\sum_{\substack{\boldsymbol{p}\\(\boldsymbol{k}+\boldsymbol{p}+\boldsymbol{q}=\boldsymbol{o})}}\sum_{\boldsymbol{q}}{}'\widetilde{u}_j(-\boldsymbol{p},t)\,\widetilde{\theta}^{(0)}(-\boldsymbol{q},t\|\boldsymbol{k}_0,\boldsymbol{p}_0,\boldsymbol{q}_0) \tag{4.44}$$

and

$$\left[\frac{\partial}{\partial t}+\kappa k^2\right]\widetilde{G}_\theta^{(0)}(\boldsymbol{k},t|\boldsymbol{k}',t'\|\boldsymbol{k}_0,\boldsymbol{p}_0,\boldsymbol{q}_0)=-\mathrm{i}\,k_j\left(\frac{2\pi}{L}\right)^3\sum_{\substack{\boldsymbol{p}\\(\boldsymbol{k}+\boldsymbol{p}+\boldsymbol{q}=\boldsymbol{o})}}\sum_{\boldsymbol{q}}{}'\widetilde{u}_j(-\boldsymbol{p},t)\,\widetilde{G}_\theta^{(0)}(-\boldsymbol{q},t|\boldsymbol{k}',t'\|\boldsymbol{k}_0,\boldsymbol{p}_0,\boldsymbol{q}_0)\,. \tag{4.45}$$

Here, $\sum\sum'$ denotes a summation without direct interactions between the three particular modes of wavenumbers $\boldsymbol{k}_0$, $\boldsymbol{p}_0$ and $\boldsymbol{q}_0$. The evolution equation for the deviation field $\widetilde{\theta}^{(1)}$ is then obtained by subtracting (4.44) from (4.25) as

$$\begin{aligned}\left[\frac{\partial}{\partial t}+\kappa k^2\right]\widetilde{\theta}^{(1)}(\boldsymbol{k},t\|\boldsymbol{k}_0,\boldsymbol{p}_0,\boldsymbol{q}_0)=&-\mathrm{i}\,k_j\left(\frac{2\pi}{L}\right)^3\sum_{\substack{\boldsymbol{p}\\(\boldsymbol{k}+\boldsymbol{p}+\boldsymbol{q}=\boldsymbol{o})}}\sum_{\boldsymbol{q}}{}'\widetilde{u}_j(-\boldsymbol{p},t)\,\widetilde{\theta}^{(1)}(-\boldsymbol{q},t\|\boldsymbol{k}_0,\boldsymbol{p}_0,\boldsymbol{q}_0)\\&-\mathrm{i}\,\delta^3_{\boldsymbol{k}-\boldsymbol{k}_0}\,k_{0j}\,\widetilde{u}_j(-\boldsymbol{p}_0,t)\,\widetilde{\theta}^{(0)}(-\boldsymbol{q}_0,t\|\boldsymbol{k}_0,\boldsymbol{p}_0,\boldsymbol{q}_0)\\&-\mathrm{i}\,\delta^3_{\boldsymbol{k}-\boldsymbol{k}_0}\,k_{0j}\,\widetilde{u}_j(-\boldsymbol{p}_0,t)\,\widetilde{\theta}^{(0)}(-\boldsymbol{q}_0,t\|\boldsymbol{k}_0,\boldsymbol{p}_0,\boldsymbol{q}_0)\\&+\mathrm{i}\,\delta^3_{\boldsymbol{k}+\boldsymbol{k}_0}\,k_{0j}\,\widetilde{u}_j(\boldsymbol{p}_0,t)\,\widetilde{\theta}^{(0)}(\boldsymbol{q}_0,t\|\boldsymbol{k}_0,\boldsymbol{p}_0,\boldsymbol{q}_0)\\&+\mathrm{i}\,\delta^3_{\boldsymbol{k}+\boldsymbol{k}_0}\,k_{0j}\,\widetilde{u}_j(\boldsymbol{q}_0,t)\,\widetilde{\theta}^{(0)}(\boldsymbol{p}_0,t\|\boldsymbol{k}_0,\boldsymbol{p}_0,\boldsymbol{q}_0)\\&+(\boldsymbol{k}_0\to\boldsymbol{p}_0\to\boldsymbol{q}_0\to\boldsymbol{k}_0)\,.\end{aligned} \tag{4.46}$$

It is easily shown from (4.42), (4.45) and (4.46) that the deviation field $\widetilde{\theta}^{(1)}$ is expressed in terms of $\widetilde{G}_\theta^{(0)}$ and $\widetilde{\theta}^{(0)}$ as

$$\begin{aligned}\widetilde{\theta}^{(1)}(\boldsymbol{k},t\|\boldsymbol{k}_0,\boldsymbol{p}_0,\boldsymbol{q}_0)=&-\mathrm{i}\,k_j\,\frac{(2\pi)^9}{L^6}\int_{t_0}^{t}\mathrm{d}t''\,\widetilde{G}_\theta^{(0)}(\boldsymbol{k},t|-\boldsymbol{k},t''\|\boldsymbol{k}_0,\boldsymbol{p}_0,\boldsymbol{q}_0)\\&\times\Big[\delta^3_{\boldsymbol{k}-\boldsymbol{k}_0}\,\widetilde{u}_j(-\boldsymbol{p}_0,t'')\,\widetilde{\theta}^{(0)}(-\boldsymbol{q}_0,t''\|\boldsymbol{k}_0,\boldsymbol{p}_0,\boldsymbol{q}_0)\\&+\delta^3_{\boldsymbol{k}-\boldsymbol{k}_0}\,\widetilde{u}_j(-\boldsymbol{q}_0,t'')\,\widetilde{\theta}^{(0)}(-\boldsymbol{p}_0,t''\|\boldsymbol{k}_0,\boldsymbol{p}_0,\boldsymbol{q}_0)\\&+\delta^3_{\boldsymbol{k}+\boldsymbol{k}_0}\,\widetilde{u}_j(\boldsymbol{p}_0,t'')\,\widetilde{\theta}^{(0)}(\boldsymbol{q}_0,t''\|\boldsymbol{k}_0,\boldsymbol{p}_0,\boldsymbol{q}_0)\\&+\delta^3_{\boldsymbol{k}+\boldsymbol{k}_0}\,\widetilde{u}_j(\boldsymbol{q}_0,t'')\,\widetilde{\theta}^{(0)}(\boldsymbol{p}_0,t''\|\boldsymbol{k}_0,\boldsymbol{p}_0,\boldsymbol{q}_0)\\&+(\boldsymbol{k}_0\to\boldsymbol{p}_0\to\boldsymbol{q}_0\to\boldsymbol{k}_0)\Big].\end{aligned} \tag{4.47}$$

### 4.3.2 Closed equation for passive scalar spectrum

Here, we will derive an approximate expression of the third-order correlation in the evolution equation (4.30) for the scalar correlation function $\widetilde{Z}$ in terms of $\widetilde{Z}$ itself and the Lagrangian velocity correlation function by the Lagrangian DIA. This approximation is based upon the following three assumptions:

**Assumption 1** The deviation filed is much smaller in magnitude than the NDI field as long as $t-t_0$ (for $\widetilde{\theta}$) or $t-t'$ (for $\widetilde{G}_\theta$) is limited within the order of the correlation time scale of the velocity field.

**Assumption 2** Any two Fourier components without their direct interaction are statistically independent of each other. For example, any two of $\widetilde{\theta}^{(0)}(\boldsymbol{k}_0,t\|\boldsymbol{k}_0,\boldsymbol{p}_0,\boldsymbol{q}_0)$, $\widetilde{\theta}^{(0)}(\boldsymbol{p}_0,t'\|\boldsymbol{k}_0,\boldsymbol{p}_0,\boldsymbol{q}_0)$ and $\widetilde{u}_k(\boldsymbol{q}_0,t'')$ are statistically independent (see (4.44)).

**Assumption 3** The NDI field of the position function $\widetilde{\psi}^{(0)}$ is statistically independent of those of the Eulerian quantities such as $\widetilde{\psi}^{(0)}$ itself, $\widetilde{\theta}^{(0)}$, $\widetilde{G}_\theta^{(0)}$ and $\widetilde{u}_i^{(0)}$.

It must be stressed again that although the first and the second assumptions are reasonable and examined in detail for a model equation (chapter 2), the third one is only an assumption for simplification to be checked in future (see §6.3).

First, we consider the one-time scalar correlation function $\widetilde{Z}(\boldsymbol{k},t,t)$ which is governed by (4.30). By substituting the direct-interaction decompositions into the right-hand side of (4.30) and by neglecting the higher-order terms of the deviation fields (Assumption 1), we obtain

$$
\begin{aligned}
&\text{(Nonlinear term of (4.30))}\\
&= -\mathrm{i}\,k_j\left(\frac{2\pi}{L}\right)^6 \sum_{\substack{\boldsymbol{p}\\(\boldsymbol{k}+\boldsymbol{p}+\boldsymbol{q}=\boldsymbol{o})}}\sum_{\boldsymbol{q}} \Bigg[ \overline{\widetilde{u}_j^{(0)}(-\boldsymbol{p},t\|\boldsymbol{k},\boldsymbol{p},\boldsymbol{q})\,\widetilde{\theta}^{(0)}(-\boldsymbol{q},t\|\boldsymbol{k},\boldsymbol{p},\boldsymbol{q})\,\widetilde{\theta}^{(0)}(-\boldsymbol{k},t\|\boldsymbol{k},\boldsymbol{p},\boldsymbol{q})}\\
&\qquad + \overline{\widetilde{u}_j^{(1)}(-\boldsymbol{p},t\|\boldsymbol{k},\boldsymbol{p},\boldsymbol{q})\,\widetilde{\theta}^{(0)}(-\boldsymbol{q},t\|\boldsymbol{k},\boldsymbol{p},\boldsymbol{q})\,\widetilde{\theta}^{(0)}(-\boldsymbol{k},t\|\boldsymbol{k},\boldsymbol{p},\boldsymbol{q})}\\
&\qquad + \overline{\widetilde{u}_j^{(0)}(-\boldsymbol{p},t\|\boldsymbol{k},\boldsymbol{p},\boldsymbol{q})\,\widetilde{\theta}^{(1)}(-\boldsymbol{q},t\|\boldsymbol{k},\boldsymbol{p},\boldsymbol{q})\,\widetilde{\theta}^{(0)}(-\boldsymbol{k},t\|\boldsymbol{k},\boldsymbol{p},\boldsymbol{q})}\\
&\qquad + \overline{\widetilde{u}_j^{(0)}(-\boldsymbol{p},t\|\boldsymbol{k},\boldsymbol{p},\boldsymbol{q})\,\widetilde{\theta}^{(0)}(-\boldsymbol{q},t\|\boldsymbol{k},\boldsymbol{p},\boldsymbol{q})\,\widetilde{\theta}^{(1)}(-\boldsymbol{k},t\|\boldsymbol{k},\boldsymbol{p},\boldsymbol{q})} \Bigg].
\end{aligned}
\tag{4.48}
$$

Note that this approximation is valid as long as $t-t_0$ is within the order of the time-scale of the velocity correlation function. The first term in the above equation vanishes under the assumption that $\widetilde{u}_j^{(0)}(\boldsymbol{p},t\|\boldsymbol{k},\boldsymbol{p},\boldsymbol{q})$, $\widetilde{\theta}^{(0)}(\boldsymbol{p},t\|\boldsymbol{k},\boldsymbol{p},\boldsymbol{q})$ and $\widetilde{\theta}^{(0)}(\boldsymbol{q},t\|\boldsymbol{k},\boldsymbol{p},\boldsymbol{q})$ are statistically independent of each other (Assumption 2). Since the other three terms are evaluated similarly, we describe it here only for the third term. Substitution of the solution (4.47) of $\widetilde{\theta}^{(1)}$ into the third term yields

$$
\begin{aligned}
&\text{(Third term of (4.48))} = -\mathrm{i}\,k_j\left(\frac{2\pi}{L}\right)^6 \sum_{\substack{\boldsymbol{p}\\(\boldsymbol{k}+\boldsymbol{p}+\boldsymbol{q}=\boldsymbol{o})}}\sum_{\boldsymbol{q}} -\mathrm{i}(-q_m)\,\frac{(2\pi)^9}{L^6}\int_{t_0}^{t}\mathrm{d}t''\\
&\times\Bigg[\overline{\widetilde{G}_\theta^{(0)}(-\boldsymbol{q},t|\boldsymbol{q},t''\|\boldsymbol{k},\boldsymbol{p},\boldsymbol{q})\,\widetilde{u}_m^{(0)}(\boldsymbol{p},t''\|\boldsymbol{k},\boldsymbol{p},\boldsymbol{q})\,\widetilde{u}_j^{(0)}(-\boldsymbol{p},t\|\boldsymbol{k},\boldsymbol{p},\boldsymbol{q})\,\widetilde{\theta}^{(0)}(\boldsymbol{k},t''\|\boldsymbol{k},\boldsymbol{p},\boldsymbol{q})\,\widetilde{\theta}^{(0)}(-\boldsymbol{k},t\|\boldsymbol{k},\boldsymbol{p},\boldsymbol{q})}\\
&\quad + \overline{\widetilde{G}_\theta^{(0)}(-\boldsymbol{q},t|\boldsymbol{q},t''\|\boldsymbol{k},\boldsymbol{p},\boldsymbol{q})\,\widetilde{u}_m^{(0)}(\boldsymbol{k},t''\|\boldsymbol{k},\boldsymbol{p},\boldsymbol{q})\,\widetilde{u}_j^{(0)}(-\boldsymbol{p},t\|\boldsymbol{k},\boldsymbol{p},\boldsymbol{q})\,\widetilde{\theta}^{(0)}(\boldsymbol{p},t''\|\boldsymbol{k},\boldsymbol{p},\boldsymbol{q})\,\widetilde{\theta}^{(0)}(-\boldsymbol{k},t\|\boldsymbol{k},\boldsymbol{p},\boldsymbol{q})}\Bigg].
\end{aligned}
\tag{4.49}
$$

The second term in the above equation vanishes because

$$
\overline{\widetilde{\theta}^{(0)}(\boldsymbol{k},t''\|\boldsymbol{k}_0,\boldsymbol{p}_0,\boldsymbol{q}_0)\,\widetilde{u}_i(-\boldsymbol{k},t)} = 0 \tag{4.50}
$$

if the flow field is statistically isotropic.

The first term is converted, under Assumption 2, into

$$\text{(First term of (4.49))} = k_j \frac{(2\pi)^9}{L^6} \sum_{\substack{\boldsymbol{p} \\ (\boldsymbol{k}+\boldsymbol{p}+\boldsymbol{q}=\boldsymbol{o})}} \sum_{\boldsymbol{q}} q_m \int_{t_0}^{t} \mathrm{d}t'' \, \overline{\tilde{G}_\theta^{(L)}(t|-\boldsymbol{q},\boldsymbol{q},t'')} \, \tilde{Q}_{jm}(-\boldsymbol{p},t,t'') \, \tilde{Z}(-\boldsymbol{k},t,t'') \,. \tag{4.51}$$

Here, we have used the relations (3.66),

$$\overline{\tilde{\theta}^{(0)}(\boldsymbol{k},t) \, \tilde{\theta}^{(0)}(-\boldsymbol{k},t')} = \left(\frac{2\pi}{L}\right)^3 \tilde{Z}(\boldsymbol{k},t,t') \tag{4.52}$$

and

$$\overline{\tilde{G}_\theta^{(0)}(\boldsymbol{k},t|-\boldsymbol{k},t')} = \overline{\tilde{G}_\theta^{(L)}(t|\boldsymbol{k},-\boldsymbol{k},t')} \,. \tag{4.53}$$

See Appendix A for derivation of (4.52) and (4.53). Similarly, we can calculate the second and fourth terms on the right-hand side of (4.30) to obtain

$$\begin{aligned}\left[\frac{\partial}{\partial t} + 2\kappa k^2\right] \tilde{Z}(\boldsymbol{k},t,t) = k_j \, k_m \frac{(2\pi)^9}{L^6} \sum_{\substack{\boldsymbol{p} \\ (\boldsymbol{k}+\boldsymbol{p}+\boldsymbol{q}=\boldsymbol{o})}} \sum_{\boldsymbol{q}} \int_{t_0}^{t} \mathrm{d}t'' \, \tilde{Q}_{jm}(-\boldsymbol{p},t,t'') \\ \times \left[ -\overline{\tilde{G}_\theta^{(L)}(t|-\boldsymbol{q},\boldsymbol{q},t'')} \, \tilde{Z}(-\boldsymbol{k},t,t'') + \overline{\tilde{G}_\theta^{(L)}(t|-\boldsymbol{k},\boldsymbol{k},t'')} \, \tilde{Z}(-\boldsymbol{q},t,t'') \right] \\ + (\boldsymbol{k} \to -\boldsymbol{k}) \,,\end{aligned} \tag{4.54}$$

where use has been made of the incompressible condition of the velocity correlation function, i.e., $k_j \tilde{Q}_{ij}(\boldsymbol{k}) = 0$.

Turning now to the two-time correlation function $\tilde{Z}(k,t,t')$ and the response function $\tilde{G}_\theta^{(L)}(k,t,t')$, we integrate the governing equations (4.31) and (4.38) as

$$\tilde{Z}(\boldsymbol{k},t,t') = \tilde{Z}(\boldsymbol{k},t',t') \, \exp\left[ -\kappa k^2 (t-t') \right] \tag{4.55}$$

and

$$\tilde{G}_\theta^{(L)}(t|\boldsymbol{k},-\boldsymbol{k},t') = \frac{L^3}{(2\pi)^6} \, \exp\left[ -\kappa k^2 (t-t') \right] \tag{4.56}$$

under the initial condition (4.39).

A combination of (4.54), (4.55) and (4.56) then yields

$$\begin{aligned}\left[\frac{\partial}{\partial t} + 2\kappa k^2\right] \tilde{Z}(\boldsymbol{k},t,t) = 2 k_j \, k_m \left(\frac{2\pi}{L}\right)^3 \sum_{\substack{\boldsymbol{p} \\ (\boldsymbol{k}+\boldsymbol{p}+\boldsymbol{q}=\boldsymbol{o})}} \sum_{\boldsymbol{q}} \int_{t_0}^{t} \mathrm{d}t'' \, \tilde{Q}_{jm}(-\boldsymbol{p},t,t'') \, \exp\left[ -\kappa (k^2+q^2)(t-t'') \right] \\ \times \left[ -\tilde{Z}(-\boldsymbol{k},t'',t'') + \tilde{Z}(-\boldsymbol{q},t'',t'') \right].\end{aligned} \tag{4.57}$$

By taking the limit $L \to \infty$, we may convert (4.57) into

$$\left[\frac{\partial}{\partial t} + 2\kappa k^2\right] \tilde{Z}(\boldsymbol{k},t,t) = 2\,k_j\,k_m \int \mathrm{d}^3\boldsymbol{p} \int \mathrm{d}^3\boldsymbol{q}\,\delta^3_{\boldsymbol{k}+\boldsymbol{p}+\boldsymbol{q}} \int_{t_0}^{t} \mathrm{d}t''\,\tilde{Q}_{jm}(-\boldsymbol{p},t,t'') \times \exp\Big[-\kappa\,(k^2+q^2)(t-t'')\Big]\Big[-\tilde{Z}(-\boldsymbol{k},t'',t'') + \tilde{Z}(-\boldsymbol{q},t'',t'')\Big]. \tag{4.58}$$

Thus, a closed system of equations for $\tilde{Z}$ and $\tilde{Q}_{ij}$ is obtained by combining this equation and the LRA-DIA equations for $\tilde{Q}_{ij}$ derived in Chapter 3. Let us stress again that the present formulation of the Lagrangian DIA is quite simple and clear.

From now on, the velocity and the scalar fields will be assumed to be statistically stationary and isotropic, so that $\tilde{Z}$ and $\tilde{Q}$ may be expressed as

$$\tilde{Z}(\boldsymbol{k},t,t) = Z^{\dagger}(k)\,, \tag{4.59}$$

$$\tilde{Q}_{ij}(\boldsymbol{k},t,t') = \tfrac{1}{2}\,\tilde{P}_{ij}(\boldsymbol{k})\,\check{Q}(k,t-t')\,. \tag{4.60}$$

Equation (4.58) then reduces to

$$2\kappa\,Z^{\dagger}(k) = \iint_{\triangle_k} \mathrm{d}p\,\mathrm{d}q\,\frac{2\pi pq}{k}\,\sigma(k,p,q)\Big[-Z^{\dagger}(k) + Z^{\dagger}(q)\Big]\int_0^{t-t_0}\mathrm{d}t'\,\check{Q}(p,t')\,\exp\Big[-\kappa\,(k^2+q^2)t'\Big] = T_\theta(k)/4\pi k^4\,, \tag{4.61}$$

where

$$\sigma(k,p,q) = \frac{k_j\,k_m}{k^2}\,\tilde{P}_{jm}(\boldsymbol{p}) = \frac{(k+p+q)(k+p-q)(k-p+q)(-k+p+q)}{4p^2k^2}\,. \tag{4.62}$$

The second equality of (4.61) has followed from (4.32), (4.33) and (4.59). Equation (4.61) describes a balance between the scalar fluctuation transfer and its dissipation. Recall that (4.61) is valid as long as $t - t_0$ does not exceed the order of the velocity correlation time (see a paragraph below (4.48)). However, the exponential decay of $\check{Q}(k,t)$ with respect to $t$ permits us to replace $t - t_0$ by infinity. The resultant closed equation (4.61) for the scalar correlation function may be derived also by LRA [36], although only the LRA equation for $\kappa = 0$ is given in Ref. [50,51]. Note that as discussed in Chapter 2 there is an essential difference between LRA and the Lagrangian DIA in the underlying approximations. In the following, we call (4.61) the LRA-DIA equation.

## 4.4 Universal forms of passive scalar spectrum

We discuss in this section the functional form of the scalar spectrum $\Theta(k)$ in the universal range for arbitrary values of the Schmidt number. To make the following analysis clear, we non-dimensionalize the wavenumber and the time as

$$k = \hat{k}\,k_\kappa \tag{4.63}$$

and

$$t = \tau\,\epsilon^{-1/3}\,k^{-2/3}\,, \tag{4.64}$$

respectively, since the velocity correlation function $\check{Q}(k,t)$ is expressed in terms of these normalized variables as [2]

$$\check{Q}(k,t) = \frac{1}{2\pi} K \epsilon^{2/3} (k_{\rm K}\hat{k})^{-11/3} Q(\hat{k},\tau) \qquad \text{with} \qquad Q(0,0) = 1\,, \tag{4.65}$$

where $K$ denotes the Kolmogorov constant. We define a non-dimensional scalar spectrum $\widehat{\Theta}$ by

$$\Theta(k) = C_1 \chi \epsilon^{-1/3} k_{\rm K}^{-5/3} \widehat{\Theta}(\hat{k})\,. \tag{4.66}$$

It follows from (4.32), (4.59) and (4.66) that

$$Z^{\dagger}(k) = \frac{1}{4\pi k^2}\Theta(k) = \frac{1}{4\pi} C_1 \chi \epsilon^{-1/3} k_{\rm K}^{-11/3} \hat{k}^{-2} \widehat{\Theta}(\hat{k})\,. \tag{4.67}$$

Then, the LRA-DIA equation (4.61) is written as

$$\begin{aligned}\widehat{\Theta}(\hat{k}) = \frac{K}{2} s\hat{k}^{-4/3} \iint_{\triangle_1} {\rm d}p\,{\rm d}q\,\sigma(1,p,q)\,p^{-8/3} q \left[ -\widehat{\Theta}(\hat{k}) + \frac{1}{q^2}\widehat{\Theta}(\hat{k}q)\right] \\ \times \int_0^{\infty} {\rm d}t\, Q(\hat{k}p, tp^{2/3}) \exp\Big[ -s^{-1}\hat{k}^{4/3}(1+q^2)\,t\Big] \\ = T_\theta(k)\Big/[\,2\kappa k^2 C_1 \chi \epsilon^{-1/3} k_{\rm K}^{-5/3}\,],\end{aligned} \tag{4.68}$$

where the second equality follows from (4.33) and (4.66).

In the following subsections we will describe the solution for various values of $k$ and $s$: the $k^{-5/3}$ power spectrum at $k \ll \min\{k_{\rm K}, k_{\rm C}\}$ for arbitrary $s$ in §4.4.1, numerical solutions for finite $s$ in §4.4.2, the asymptotic forms for $s \gg 1$ in §4.4.3, and for $s \ll 1$ in §4.4.4, and bumps in the spectrum at the end of power law regions in §4.4.5.

### 4.4.1 Inertial-advective range

Assuming that both the kinematic viscosity $\nu$ and the scalar diffusivity $\kappa$ are so small that

$$\max\{k_v, k_s\} \ll \min\{k_{\rm K}, k_{\rm C}\}\,, \tag{4.69}$$

we consider the inertial-advective range,

$$\max\{k_v, k_s\} \ll k \ll \min\{k_{\rm K}.\, k_{\rm C}\} \quad \Longrightarrow \quad \hat{k} \ll \min\{1, s^{3/4}\}\,. \tag{4.70}$$

Then, since $s^{-1}\hat{k}^{4/3} \ll 1$ and $\hat{k} \ll 1$, (4.68) may be written as

$$0 = \iint_{\triangle_1} {\rm d}p\,{\rm d}q\,\sigma(1,p,q)\,p^{-10/3} q \left[ -\widehat{\Theta}(\hat{k}) + \frac{1}{q^2}\widehat{\Theta}(\hat{k}q)\right] W_1 \qquad (\forall s,\ k \ll k_{\rm K}, k_{\rm C}) \tag{4.71}$$

[2]The function $Q$ in this chapter relates with $\check{Q}^{\dagger}$ as

$$Q(k,t) = \check{Q}^{\dagger}(K^{-3/8}k, K^{1/2}t)\,,$$

where $K$ is the Kolmogorov constant.

at the leading order, where

$$W_1 = \int_0^\infty \mathrm{d}t\, Q(0,t)\,. \tag{4.72}$$

Since no characteristic scales appear in (4.71). it allows a power form of the spectrum function. Substitution of

$$\widehat{\Theta}(\widehat{k}) \propto \widehat{k}^{-a} \tag{4.73}$$

into (4.71) leads to

$$0 = \left[\int_0^1 \mathrm{d}q \int_{1-q}^{1+q} \mathrm{d}p + \int_1^\infty \mathrm{d}q \int_{q-1}^{q+1} \mathrm{d}p\right] \sigma(1,p,q)\, p^{-10/3}\, q\, (q^{-a-2}-1)\,, \tag{4.74}$$

which is rewritten as

$$0 = \int_0^1 \mathrm{d}q \int_{1-q}^{1+q} \mathrm{d}p\, \sigma(1,p,q)\, p^{-10/3}\, q\, (q^{-a-2}-1)\, (1-q^{a-5/3}) \tag{4.75}$$

by changing the integral variables in the second term on the right-hand side of (4.74) as $p = p'/q'$ and $q = 1/q'$. This equation has two apparent scaling laws of $a = 5/3$ and $-2$. The former corresponds to the Obukhov-Corrsin spectrum (4.8) with finite flux $\Pi_\theta(k) = \chi(\neq 0)$. The latter, on the other hand, represents a state of equipartition of the fluctuation of the passive scalar field with vanishing flux. Since we are interested in a statistically stationary state with finite flux through the advective range toward the diffusive range, we will not consider this solution in the following.

The Obukhov-Corrsin constant $C_1$ in (4.8) is shown to be expressed in terms of $W_1$ and the Kolmogorov constant $K$ as

$$C_1 = \frac{910\sqrt{3}}{729\pi\, K W_1} \tag{4.76}$$

(see Appendix B for derivation). A similar relation was derived in the LHDIA [69, 70]. A numerical integration of (4.72) gives $W_1 = 1.19$ and then $C_1 = 0.34$ [50]. This is about a half of the experimental values which scatter around $(5/3) \times 0.4 = 0.67$ [73]. The reason of this discrepancy is unknown. Incidentally, the abridged LHDIA yields $C_1 = 0.208$ [70].

### 4.4.2 Finite Schmidt number

We describe here numerical solutions of the LRA-DIA equation (4.68) for finite Schmidt numbers. We search for a solution by an iterative method that approaches the $k^{-5/3}$ power form in the inertial-advective range $k \ll \min\{k_\mathrm{K}, k_\mathrm{C}\}$ discussed in the preceding subsection.

The scalar spectra for $s \geq 1$ are shown in Fig.4.2 together with the asymptotic form in the limit $s \gg 1$ (see §4.4.3). The wavenumber is normalized by $k_\mathrm{K}$ in (a) and by $k_\mathrm{B}$ in (b). In these figures we can see that the $k^{-5/3}$ power law range extends up to $k_\mathrm{K}$, which is consistent with the argument in §4.4.1 because $k_\mathrm{K} < k_\mathrm{C}$ if $s > 1$, and that the function obeys the $k^{-1}$ power law in the larger-wavenumber range $k_\mathrm{K} \ll k \ll k_\mathrm{B}$. This $k^{-1}$ power law range widens with increasing Schmidt number, and is followed by an exponential decay at $k \gg k_\mathrm{B}$. These behaviors are consistent with the phenomenology for large Schmidt numbers by Batchelor [67] (see §4.4.3 for detailed discussions). We also observe a bump in the spectrum around $k_\mathrm{B}$, which will be discussed in §4.4.5.

In Fig.4.3, we plot the numerical solutions in the cases of $s \leq 1$ together with the asymptotic form in the small Schmidt number limit (see §4.4.4). Since the upper limit of the inertial-advective range is $k_C$ for $s < 1$ (see (4.7)), the wavenumber is normalized by $k_C$ instead of $k_K$ in (a). The $k^{-5/3}$ power law is actually established at $k \ll k_C$. Moreover we observe that as $s$ decreases the spectrum seems to approach the $k^{-17/3}$ power law at $k \gg k_C$, which was phenomenologically predicted by Batchelor et al. [66]. The wavenumber in (b) is normalized by $k_K$ in order to focus the spectrum around $k_K$. We can see in (a) and (b) that the $k^{-17/3}$ power law range extends between $k_C$ and $k_K$ and widens as $s$ decreases.

### 4.4.3 Large Schmidt number limit

We consider here the universal form of the scalar spectrum in the large Schmidt number limit. To do it we introduce variable normalizations of the wavenumber and the spectrum in such a way that

$$k = \check{k}\, k_K\, s^{\alpha} \tag{4.77}$$

and

$$\Theta(k) = C_1\, \chi\, \epsilon^{-1/3}\, k_K^{-5/3}\, s^{\beta}\, \check{\Theta}(\check{k}) \tag{4.78}$$

with undetermined parameters $\alpha$ and $\beta$. Note that $\alpha$ indicates the reference wavenumber which we focus on. The reference wavenumbers for $\alpha = 0$, $1/2$ and $3/4$, for example, are $k_K$, $k_B$ and $k_C$, respectively. It should be mentioned that in the large (or small) Schmidt number limit the characteristic wavenumbers $\{k_K, k_C, k_B\}$ are separated infinitely far from each other on a logarithmic scale.

On substitution of (4.77) and (4.78) into (4.68), we obtain

$$\begin{aligned}\check{\Xi}(\check{k}) = \frac{K}{2}\, s^{1-4\alpha/3}\, \check{k}^{-4/3} \iint_{\triangle_1} \mathrm{d}p\, \mathrm{d}q\, \sigma(1,p,q)\, p^{-8/3}\, q \left[ -\check{\Xi}(\check{k}) + \check{\Xi}(\check{k}q) \right] \\ \times \int_0^{\infty} \mathrm{d}t\, Q(s^{\alpha}\check{k}p, tp^{2/3}) \exp\Big[ -s^{-(1-4\alpha/3)}\, \check{k}^{4/3}\, (1+q^2)\, t \Big],\end{aligned} \tag{4.79}$$

where

$$\check{\Xi}(\check{k}) = \check{\Theta}(\check{k})/\check{k}^2\,. \tag{4.80}$$

Since this equation depends upon the Schmidt number only through $s^{\alpha}$ and $s^{1-4\alpha/3}$, we consider the cases of $\alpha < 0$, $\alpha = 0$ and $\alpha > 0$ in turn. (It will be shown in subsection [3] below that an apparent critical value $\alpha = 3/4$ is actually irrelevant.)

#### [1] *Inertial-advective range* ($\alpha < 0$)

For $\alpha < 0$ we are in the wavenumber range below $k_K$ because $s^{\alpha} < 1$. Since $s^{\alpha} \ll 1$ and $s^{-(1-4\alpha/3)} \ll 1$, (4.79) leads to

$$0 = \iint_{\triangle_1} \mathrm{d}p\, \mathrm{d}q\, \sigma(1,p,q)\, p^{-10/3}\, q \left[ -\check{\Xi}(\check{k}) + \check{\Xi}(\check{k}q) \right] W_1 \qquad (s \gg 1, \alpha < 0)\,. \tag{4.81}$$

This is identical to the LRA-DIA equation (4.71) in the inertial-advective range, which yields the spectrum $\check{\Theta}(\check{k})$ proportional to $\check{k}^{-5/3}$.

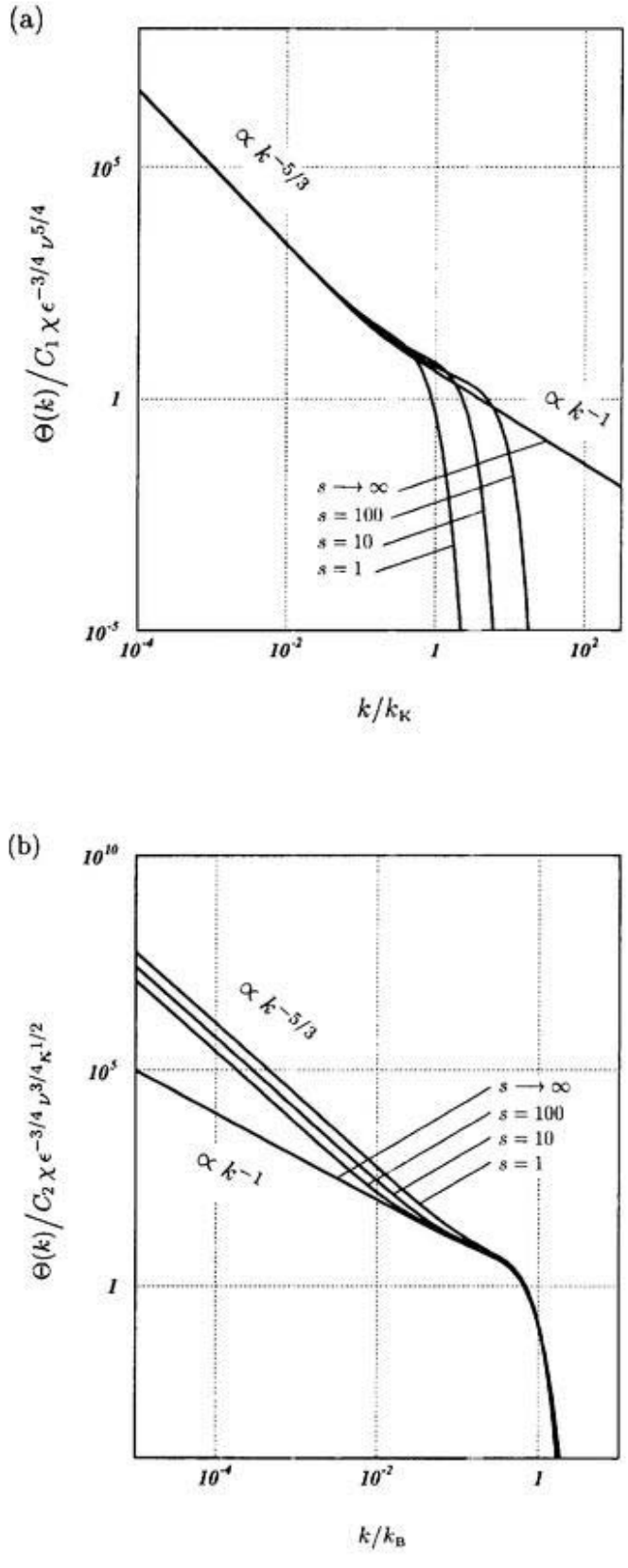


FIGURE 4.2 Passive scalar spectra in stationary isotropic turbulence for $s \geq 1$. The wavenumber is normalized by (a) the Kolmogorov wavenumber $k_K$ and (b) the Batchelor wavenumber $k_B$.

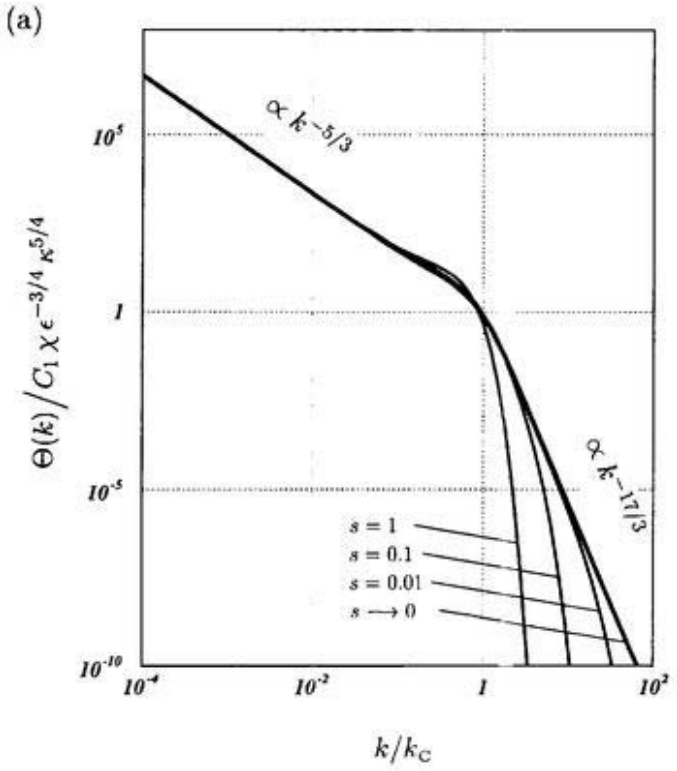


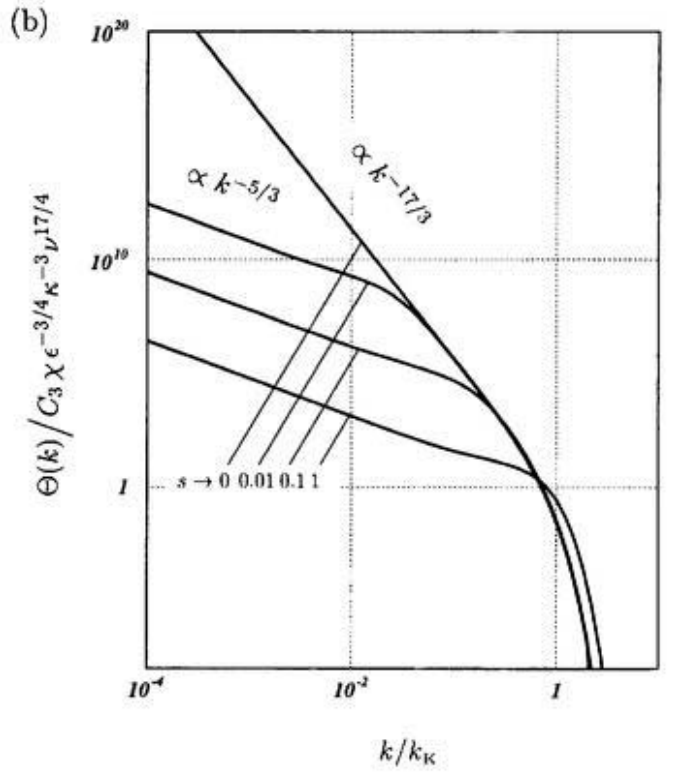


FIGURE 4.3 Same as Fig.4.2 for $s \leq 1$. The wavenumber is normalized by (a) the Obukhov-Corrsin wavenumber $k_C$ and (b) the Kolmogorov wavenumber $k_K$.

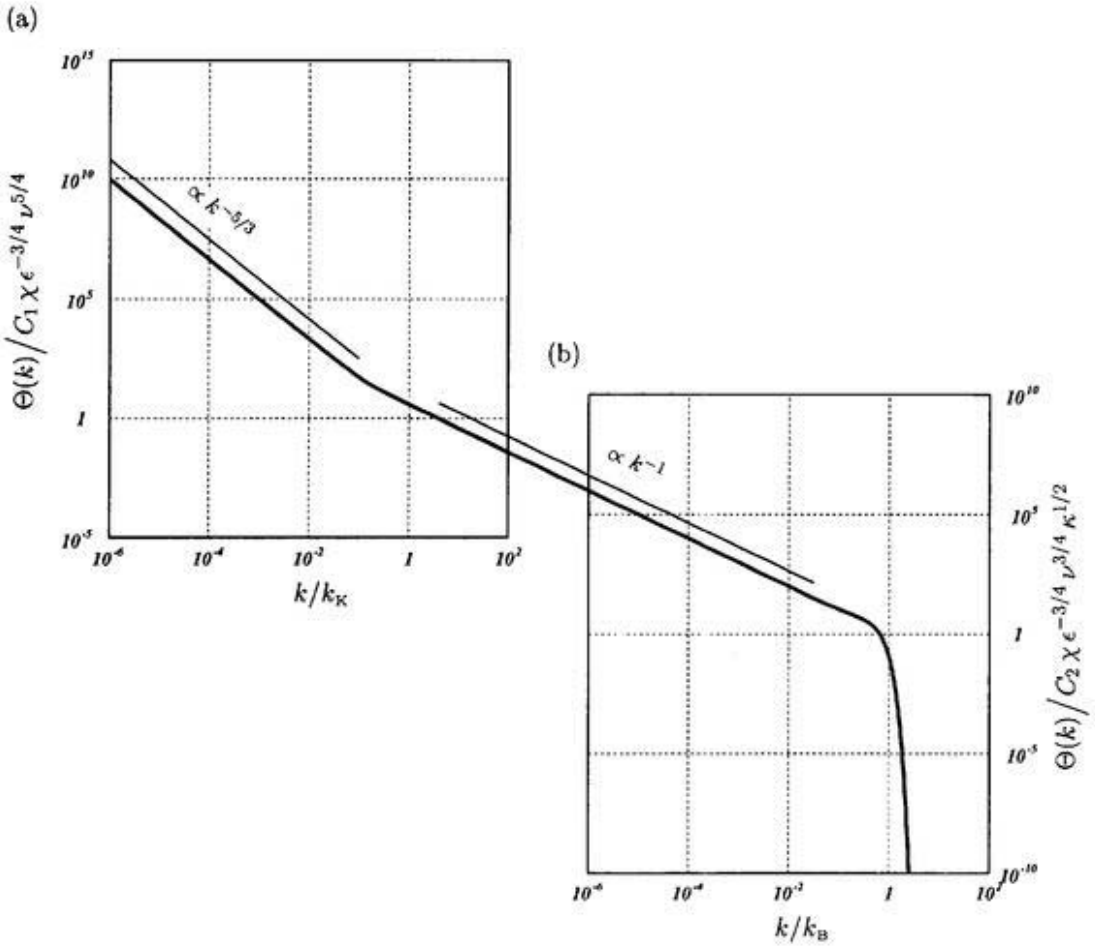


FIGURE 4.4 Passive scalar spectrum in stationary isotropic turbulence around (a) $k_K$ and (b) $k_B$ for $s \gg 1$.

### [2] *Around Kolmogorov wavenumber* ($\alpha = 0$)

For $\alpha = 0$ ($k = O(k_K)$), (4.79) is deduced to

$$0 = \iint_{\triangle_1} \mathrm{d}p\,\mathrm{d}q\,\sigma(1,p,q)\,p^{-10/3}\,q\left[-\check{\Xi}(\check{k}) + \check{\Xi}(\check{k}q)\right]\int_0^\infty \mathrm{d}t\,Q(\check{k}p,t) \qquad (s \gg 1, \alpha = 0)\,. \quad (4.82)$$

This equation has an asymptotic solution proportional to $\check{k}^{-5/3}$ for $\check{k} \ll 1$ because it coincides with (4.71). In the opposite limit $\check{k} \gg 1$, on the other hand, we find that the contribution from the region $p \ll 1$ is dominant in the integral, since $Q(k,t)$ decays exponentially with $k$ as $Q(k,t) \propto \exp(-ck)$ (see a paragraph below (4.126)). Thus, by changing the integral variable as $q = 1 + px$, we may rewrite (4.82) as

$$0 = \int_0^\infty \mathrm{d}p\,p^{-3}\int_{-1}^1 \mathrm{d}x\,\sigma(1,p,1+px)\,(1+px)\left[-\check{\Xi}(\check{k}) + \check{\Xi}(\check{k}(1+px))\right]\int_0^\infty \mathrm{d}t\,Q(\check{k}p,t)\,. \quad (4.83)$$

Substituting the expansions,

$$\sigma(1,p,1+px)\,(1+px) = (1-x^2) + 2\,(1-x^2)\,px + O(p^2) \quad (4.84)$$

and

$$-\check{\Xi}(\check{k}) + \check{\Xi}(\check{k}(1+px)) = \check{k}px\,\frac{\mathrm{d}\check{\Xi}}{\mathrm{d}\check{k}} + \frac{1}{2}\,(\check{k}px)^2\,\frac{\mathrm{d}^2\check{\Xi}}{\mathrm{d}\check{k}^2} + O(p^3) \tag{4.85}$$

into (4.82) and carrying out the integration with respect to $x$, we obtain

$$0 = \int_0^\infty \mathrm{d}p\, p^{-1}\,\frac{\mathrm{d}}{\mathrm{d}\check{k}}\left[\check{k}^4\,\frac{\mathrm{d}\check{\Xi}}{\mathrm{d}\check{k}}\right]\int_0^\infty \mathrm{d}t\, Q(\check{k}p,t) \tag{4.86}$$

at the leading order of $p$. Hence, the leading order of (4.82) for $\check{k} \gg 1$ is

$$\frac{\mathrm{d}}{\mathrm{d}\check{k}}\left[\check{k}^4\,\frac{\mathrm{d}\check{\Xi}}{\mathrm{d}\check{k}}\right] = 0 \qquad (s \gg 1, \alpha = 0, \check{k} \gg 1)\,, \tag{4.87}$$

which gives $\check{\Xi}(\check{k}) \propto \check{k}^{-3}$ (i.e. $\check{\Theta}(\check{k}) \propto \check{k}^{-1}$).

Thus, a solution of (4.82) behaves as $\check{\Theta}(\check{k}) \propto \check{k}^{-5/3}$ for $\check{k} \ll 1$ and $\check{k}^{-1}$ for $\check{k} \gg 1$. We now solve (4.82) numerically so that the solution may satisfy these asymptotic forms. The result is drawn in Fig.4.4(a), in which a transition from the $k^{-5/3}$ to the $k^{-1}$ power laws occurs around the Kolmogorov wavenumber (see also Fig.4.2(a)).

### [3] *Viscous range* ($\alpha > 0$)

In the case of $\alpha > 0$ ($k \gg k_\mathrm{K}$), the contribution from $p \ll 1$ is dominant in the integral of (4.79) because $Q(k,t)$ decays exponentially with $k$ at large $k$. Therefore, we may carry out the integration with respect to $q$ by putting $q = 1 + px$ and by expanding the integrand into power series of $p$ up to $O(p^2)$ (see (4.84) and (4.85)) to obtain

$$\begin{aligned}\check{\Xi}(\check{k}) = \frac{K}{15}\,s^{1-4\alpha/3}\,\check{k}^{-4/3}\int_0^\infty \mathrm{d}p\, p^{1/3}\int_0^\infty \mathrm{d}t\, Q(s^\alpha\check{k}p, tp^{2/3})\,\exp\!\left[-2\,s^{-(1-4\alpha/3)}\,\check{k}^{4/3}\,t\right] \\ \times\left[4\,(\check{k} - \check{k}^{7/3}\,s^{-(1-4\alpha/3)}\,t)\,\frac{\mathrm{d}\check{\Xi}}{\mathrm{d}\check{k}} + \check{k}^2\,\frac{\mathrm{d}^2\check{\Xi}}{\mathrm{d}\check{k}^2}\right]\end{aligned} \tag{4.88}$$

at the leading order. By changing the integral variables as $(p,t) \to (s^{-\alpha}p, s^{2\alpha/3}t)$, this equation is converted into

$$\begin{aligned}\check{\Xi}(\check{k}) = \frac{K}{15}\,s^{1-2\alpha}\,\check{k}^{-4/3}\int_0^\infty \mathrm{d}p\, p^{1/3}\int_0^\infty \mathrm{d}t\, Q(\check{k}p, tp^{2/3})\,\exp\!\left[-2\,s^{-(1-2\alpha)}\,\check{k}^{4/3}\,t\right] \\ \times\left[4\,(\check{k} - \check{k}^{7/3}\,s^{-(1-2\alpha)}\,t)\,\frac{\mathrm{d}\check{\Xi}}{\mathrm{d}\check{k}} + \check{k}^2\,\frac{\mathrm{d}^2\check{\Xi}}{\mathrm{d}\check{k}^2}\right] \qquad (s \gg 1, \alpha > 0)\,.\end{aligned} \tag{4.89}$$

Since this equation depends upon $s$ through only $s^{1-2\alpha}$, we will examine three cases $0 < \alpha < 1/2$, $\alpha = 1/2$ and $1/2 < \alpha$ separately in the following subsections.

### [3-1] *Viscous-advective range* ($0 < \alpha < 1/2$)

If $0 < \alpha < 1/2$ ($k_\mathrm{K} \ll k \ll k_\mathrm{B}$), (4.89) reduces to

$$0 = \frac{K}{15}\,s^{1-2\alpha}\,W_2\,\check{k}^{-1}\left[4\,\frac{\mathrm{d}\check{\Xi}}{\mathrm{d}\check{k}} + \check{k}\,\frac{\mathrm{d}^2\check{\Xi}}{\mathrm{d}\check{k}^2}\right], \tag{4.90}$$

where

$$W_2 = \int_0^\infty \mathrm{d}x \int_0^\infty \mathrm{d}y\, x^{-1/3}\, Q(x,y)\,. \tag{4.91}$$

Since all the factors outside the brackets in (4.90) are non-zero, we have

$$0 = 4\,\frac{\mathrm{d}\check{\Xi}}{\mathrm{d}\check{k}} + \check{k}\,\frac{\mathrm{d}^2\check{\Xi}}{\mathrm{d}\check{k}^2} \qquad (s \gg 1, 0 < \alpha < 1/2)\,, \tag{4.92}$$

which yields a power law solution as $\check{\Xi}(\check{k}) = \propto \check{k}^{-3}$ (that is, $\check{\Theta}(\check{k}) \propto \check{k}^{-1}$). This implies that there is only the $k^{-1}$ power law (4.10) of the spectrum function in the viscous-advective range ($k_\mathrm{K} \ll k \ll k_\mathrm{B}$).

In order to estimate the universal constant $C_2$ in (4.10) we express the transfer function (4.33) in this range in terms of $\Theta(k)$ as

$$T_\theta(k) = \frac{2}{15}\,K\,\nu\,W_2\,k_\mathrm{K}^2\,\frac{\mathrm{d}}{\mathrm{d}k}\left[k^4\,\frac{\mathrm{d}}{\mathrm{d}k}\left[\frac{\Theta(k)}{k^2}\right]\right], \tag{4.93}$$

which follows from (4.33), (4.78), (4.80) and the right-hand side of (4.90). Then, the flux function $\Pi_\theta(k)$, defined by (4.34), is written as

$$\Pi_\theta(k) = -\frac{2}{15}\,K\,\nu\,W_2\,k_\mathrm{K}^2\,k^4\,\frac{\mathrm{d}}{\mathrm{d}k}\left[\frac{\Theta(k)}{k^2}\right], \tag{4.94}$$

since the contribution from the diffusive range to the integration in (4.34) is negligible. By substituting the power law (4.10) into the above equation, we obtain

$$\Pi_\theta(k) = \frac{2}{5}\,\chi\,K\,W_2\,C_2\,, \tag{4.95}$$

which yields

$$C_2 = \frac{5}{2\,K\,W_2} = 1.30\,, \tag{4.96}$$

because $\Pi_\theta(k) = \chi$ in the advective range and the numerical value of $W_2$ is 1.11. This value of $C_2$ should be compared with $3.9 \pm 1.5$ [74], $3.7 \pm 1.5$ [75], which were measured in tidal channel flows, as well as $1.5 \sim 2.5$ (LRA-DIA), 1.5 (a modified LRA) [51], $0.6 \sim 1.0$ (abridged LHDIA; the deviation is too large) and $1.9 \sim 2.0$ (strain-based abridged LHDIA) [49], which were determined numerically from various Lagrangian closure equations. All estimations by these closure theories are quite small compared with the experimental data. It should be mentioned here an important difference in the methods of evaluation of $C_2$ used in the above closure theories and the present one; they estimated it from a late state of a freely decaying solution whereas we did it from a stationary solution. This is the reason why the numerical value obtained in Ref. [51] is different from ours, [3] though the same LRA-DIA equation is solved. Since their results themselves show large deviations, such a method may not be appropriate to evaluate the universal form. In the above measurements [74, 75] the universal constant $C_2$ in the viscous-advective range is evaluated by fitting the temperature spectrum function with the Batchelor form ((4.108) below) in the whole viscous range, in which the Schmidt number is about 10. It should be pointed out here a reservation that the $k^{-1}$ power range is not so wide at this value of the Schmidt number (see Fig.4.2(b)).

[3] Factor 2 is missing in section 4.4 of Ref. [51].

A comment on Gibson's bounds [79] may be in order. He derived that $\sqrt{3} \leq C_2 \leq 2\sqrt{3}$ for a homogeneous dissipation field by making use of the Batchelor form (4.108) of the spectrum function with the relation $C_2 = -(\epsilon/\nu)^{1/2}/\gamma$ ($\gamma$ is the least eigenvalue of the rate-of-strain tensor). Since the Batchelor form (and therefore Gibson's bounds) is not a solution to the LRA-DIA equation but a phenomenology, it is not unnatural that the present estimation of $C_2$ violates these bounds.

### [3-2] *Around Batchelor wavenumber* ($\alpha = 1/2$)

For $\alpha = 1/2$ ($k = O(k_{\rm B})$), (4.89) reduces to

$$\check{\Xi}(\check{k}) = 4\Big[\, f_1(\check{k})\check{k}^{-1/3} - f_2(\check{k})\check{k}\,\Big]\,\frac{\mathrm{d}\check{\Xi}}{\mathrm{d}\check{k}} + f_1(\check{k})\check{k}^{2/3}\,\frac{\mathrm{d}^2\check{\Xi}}{\mathrm{d}\check{k}^2} \qquad (s \gg 1, \alpha = 1/2)\,, \tag{4.97}$$

where

$$f_1(k) = \frac{K}{15}\int_0^\infty \mathrm{d}p\, p^{1/3} \int_0^\infty \mathrm{d}t\, Q(kp, tp^{2/3})\, \exp\Big[-2k^{4/3}t\Big] \tag{4.98}$$

and

$$f_2(k) = \frac{K}{15}\int_0^\infty \mathrm{d}p\, p^{1/3} \int_0^\infty \mathrm{d}t\, t\, Q(kp, tp^{2/3})\, \exp\Big[-2k^{4/3}t\Big]. \tag{4.99}$$

It is easy to show that (4.97) has an asymptotic solution of $\check{\Xi}(\check{k}) \propto \check{k}^{-3}$ (i.e. $\check{\Theta}(\check{k}) \propto \check{k}^{-1}$) at $\check{k} \ll 1$ because (4.97) coincides with (4.92) in this limit. (Note that $f_1(\check{k}) \propto \check{k}^{-2/3}$ and $f_2(\check{k}) \propto \log\check{k}$ for $\check{k} \ll 1$.)

In the opposite limit $\check{k} \gg 1$, on the other hand, we have the asymptotic expressions,

$$f_1(\check{k}) = c_1\check{k}^{-8/3} + c_2\check{k}^{-14/3} + O(\check{k}^{-20/3}) \quad \text{and} \quad f_2(\check{k}) = \tfrac{1}{2}c_1\check{k}^{-4} + c_2\check{k}^{-6} + O(\check{k}^{-8}) \quad (\check{k} \to \infty), \tag{4.100}$$

where

$$c_1 = \frac{K}{30}\int_0^\infty \mathrm{d}p\, p^{1/3}\, Q(p,0) = \frac{1}{60} \tag{4.101}$$

and

$$c_2 = \frac{K}{60}\int_0^\infty \mathrm{d}p\, p\, \frac{\partial}{\partial t} Q(p,t)\Big|_{t=0} = \frac{7S}{360\sqrt{60}}\,. \tag{4.102}$$

The second equalities of (4.101) and (4.102) are respectively derived from the relation,

$$\epsilon = 2\nu\int_0^\infty \mathrm{d}k\, k^2\, E(k) = 2\nu\, K\, \epsilon^{2/3}\int_0^\infty \mathrm{d}k\, k^{1/3}\, Q(k/k_{\rm K}, 0) \tag{4.103}$$

and the Lagrangian DIA equation for $Q(k,t)$ together with the expression of the skewness factor $S$ of the velocity derivative (see (3.103) and (3.107) in Chapter 3). Hence, in the limit $\check{k} \to \infty$, (4.97) reduces to

$$\check{k}^2\,\check{\Xi}(\check{k}) = 2c_1\check{k}^{-1}\,\frac{\mathrm{d}\check{\Xi}}{\mathrm{d}\check{k}} + \Big[\, c_1 + c_2\,\check{k}^{-2}\,\Big]\,\frac{\mathrm{d}^2\check{\Xi}}{\mathrm{d}\check{k}^2} \tag{4.104}$$

at the leading order, from which the asymptotic form of $\check{\Xi}$ is derived to be

$$\check{\Xi}(\check{k}) \propto \check{k}^a\, \exp\Big[-\check{k}^2/(2\sqrt{c_1})\Big] \qquad (s \gg 1, \alpha = 1/2, \check{k} \gg 1) \tag{4.105}$$

or

$$\Theta(k) \propto k^{a+2} \exp\left[ -\frac{\sqrt{60}}{2} \kappa \left(\frac{\nu}{\epsilon}\right)^{1/2} k^2 \right] \tag{4.106}$$

with

$$a = \frac{1}{2}\left[ \frac{c_2}{(c_1)^{3/2}} - 3 \right] = \frac{7}{12} S - \frac{3}{2} \approx -1.9\,, \tag{4.107}$$

where we have used $S \approx -0.66$ which had been already determined in Chapter 3 (see (3.108)). Thus we have found asymptotic solutions of (4.97) in both of small and large wavenumber limits. The numerical solution to this equation integrated from the large wavenumber limit is shown in Fig.4.4(b), in which we can clearly see the $k^{-1}$ power law and the exponential asymptotes at small and large wavenumbers.

The asymptotic form (4.106) is similar to the one derived phenomenologically by Batchelor [67], which is

$$\Theta(k) = C_2 \chi \nu^{1/2} \epsilon^{-1/2} k^{-1} \exp\left[ -C_2 \kappa \left(\frac{\nu}{\epsilon}\right)^{1/2} k^2 \right]. \tag{4.108}$$

A comparison of the arguments of the exponential function in (4.106) and (4.108) gives $C_2 = \sqrt{60}/2 = 3.87$. This value is in a quite good agreement with experimental values $3.9 \pm 1.5$ [74], $3.7 \pm 1.5$ [75]. Recall that $C_2$ is determined experimentally by the use of the Batchelor form (4.108). Another analytical form of the spectrum in the viscous range,

$$\Theta(k) = C_2 \chi (\epsilon/\nu)^{1/2} \check{k}^{-1}\left[ 1 + \sqrt{6C_2}\,\check{k} \right] \exp\left[ -\sqrt{6C_2}\,\check{k} \right], \tag{4.109}$$

was derived by Mjolsness [80] based upon Kraichnan's LHDIA equation under the assumption that the transfer function is proportional to $\check{k}^{-1}\mathrm{d}\check{\Xi}/\mathrm{d}\check{k} + \mathrm{d}^2\check{\Xi}/\mathrm{d}\check{k}^2$. Recently Bogucki et al. [81] have shown that (4.109) agrees with a direct numerical simulation with a fitting parameter $C_2 = 5.26 \pm 0.25$. However, we would like to note two points to be considered. First, (4.109) should not be precise at wavenumbers larger than $k_B$ because the above expression of the transfer function can be applied only at $k \ll k_B$ under Kraichnan's formulation of Lagrangian DIA just like the present one (see a paragraph below (4.99)). Second, the value of $C_2 = 5.26$ suggested by Bogucki et al. is much larger than the experimental data [74,75].

### [3-3] *Far viscous-diffusive range* ($\alpha > 1/2$)

For $\alpha > 1/2$ ($k \gg k_B$), it follows from (4.89) that

$$\check{\Xi}(\check{k}) = 0 \qquad (s \gg 1, \alpha > 1/2)\,. \tag{4.110}$$

This is consistent with an exponential decay of the spectrum function at wavenumbers larger than $k_B$ discussed in the preceding subsection.

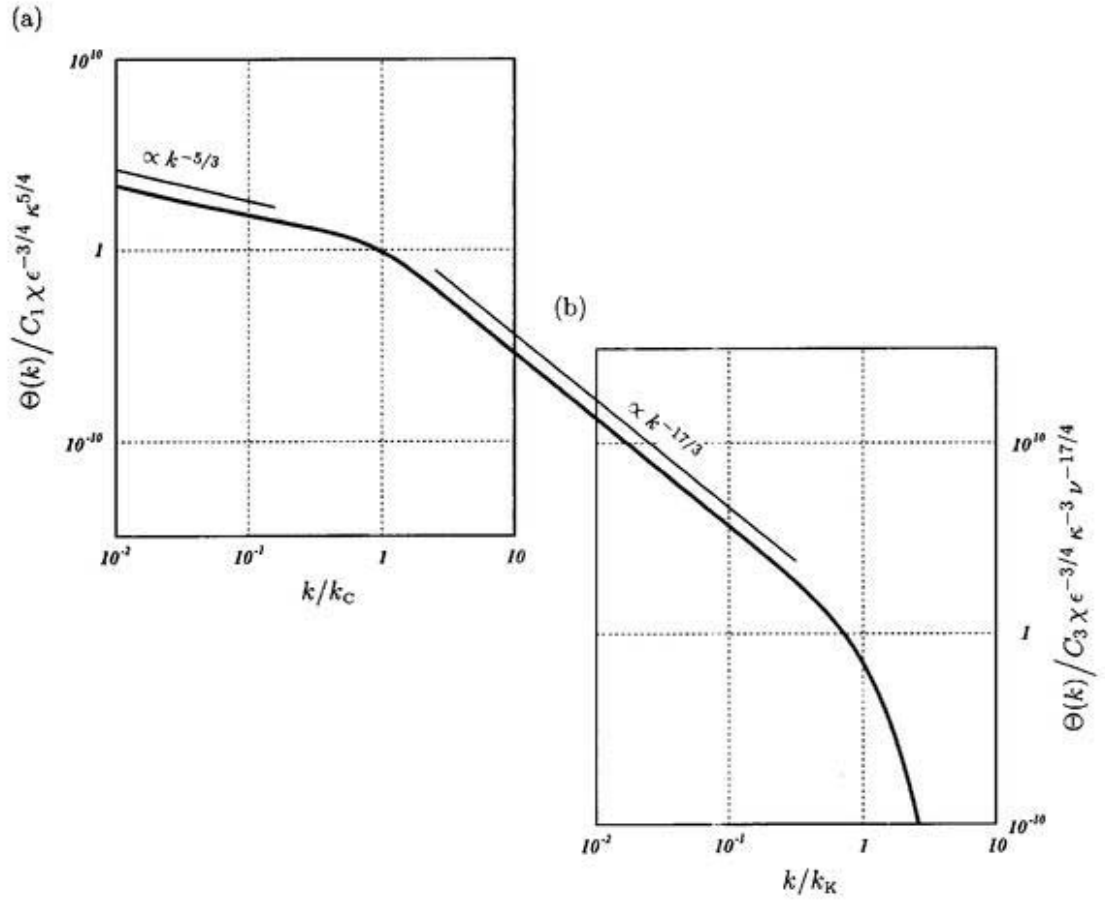


FIGURE 4.5 Passive scalar spectrum in stationary isotropic turbulence around (a) $k_C$ and (b) $k_K$ for $s \ll 1$.

### 4.4.4 Small Schmidt number limit

In order to examine the small Schmidt number limit we write the LRA-DIA equation in terms of the normalized wavenumber $\check{k}$ and the spectrum $\check{\Theta}$ as

$$\check{\Theta}(\check{k}) = \frac{K}{2}\, s^{1-4\alpha/3}\, \check{k}^{-4/3} \iint_{\triangle_1} \mathrm{d}p\, \mathrm{d}q\, \sigma(1,p,q)\, p^{-8/3}\, q \left[ -\check{\Theta}(\check{k}) + \frac{1}{q^2}\, \check{\Theta}(\check{k}q) \right] \times \int_0^\infty \mathrm{d}t\, Q(s^\alpha \check{k}p, tp^{2/3}) \exp\left[ -s^{-(1-4\alpha/3)}\, \check{k}^{4/3}\, (1+q^2)\, t \right]. \quad (4.111)$$

This equation, which is equivalent to (4.79), is more convenient in the present subsection because $\check{\Pi}$ is not necessary to be dealt with. Since (4.111) depends upon $s$ only through $s^\alpha$ and $s^{1-4\alpha/3}$, we will examine three cases $\alpha > 3/4$, $\alpha = 3/4$, $0 < \alpha < 3/4$, $\alpha = 0$ and $\alpha < 0$ separately in the following subsections.

[1] *Inertial-advective range* ($\alpha > 3/4$)

For $\alpha > 3/4$ ($k \ll k_C$), since $s^\alpha \ll 1$ and $s^{-(1-4\alpha/3)} \ll 1$, (4.111) reduces to

$$0 = \iint_{\Delta_1} dp\, dq\, \sigma(1,p,q)\, p^{-10/3}\, q \left[ -\check{\Theta}(\check{k}) + \frac{1}{q^2}\, \check{\Theta}(\check{k}q) \right] \qquad (s \ll 1, \alpha > 3/4)\,, \tag{4.112}$$

which is identical to (4.71). Hence, the spectrum obeys the $k^{-5/3}$ power law. This is consistent with the argument in §4.4.1 because $k_C \ll k_K$ for $s \ll 1$.

[2] *Around Obukhov-Corrsin wavenumber* ($\alpha = 3/4$)

In the case of $\alpha = 3/4$ ($k = O(k_C)$), (4.111) leads to

$$\check{\Theta}(\check{k}) = \frac{K}{2}\, \check{k}^{-4/3} \iint_{\Delta_1} dp\, dq\, \sigma(1,p,q)\, p^{-8/3}\, q \left[ -\check{\Theta}(\check{k}) + \frac{1}{q^2}\, \check{\Theta}(\check{k}q) \right] \times \int_0^\infty dt\, Q(0, tp^{2/3})\, \exp\left[ -\check{k}^{4/3}\, (1+q^2)\, t \right] \qquad (s \ll 1, \alpha = 3/4)\,. \tag{4.113}$$

Since this equation coincides with (4.112) at $\check{k} \ll 1$, its asymptotic solution is proportional to $\check{k}^{-5/3}$ in this limit. At $\check{k} \gg 1$, on the other hand, the exponential factor in the integrand allows us to replace $Q(0, tp^{2/3})$ by $Q(0,0) = 1$. Then, we obtain

$$\check{\Theta}(\check{k}) = \frac{K}{2}\, \check{k}^{-8/3} \iint_{\Delta_1} dp\, dq\, \sigma(1,p,q)\, \frac{p^{-8/3}\, q}{1+q^2} \left[ -\check{\Theta}(\check{k}) + \frac{1}{q^2}\, \check{\Theta}(\check{k}q) \right]. \tag{4.114}$$

In order to estimate the limiting behavior for $\check{k} \gg 1$ of this integral we divide it into three parts as

$$\begin{aligned} \check{\Theta}(\check{k}) = {} & \frac{K}{2}\, \check{k}^{-8/3} \int_0^\varepsilon dp \int_{1-p}^{1+p} dq\, \sigma(1,p,q)\, \frac{p^{-8/3}\, q}{1+q^2} \left[ -\check{\Theta}(\check{k}) + \frac{1}{q^2}\, \check{\Theta}(\check{k}q) \right] \\ & - \frac{K}{2}\, \check{k}^{-8/3} \int_\varepsilon^\infty dp \int_{|1-p|}^{1+p} dq\, \sigma(1,p,q)\, \frac{p^{-8/3}\, q}{1+q^2}\, \check{\Theta}(\check{k}) \\ & + \frac{K}{2}\, \check{k}^{-8/3} \int_\varepsilon^\infty dp \int_{|1-p|}^{1+p} dq\, \sigma(1,p,q)\, \frac{p^{-8/3}}{(1+q^2)q}\, \check{\Theta}(\check{k}q)\,, \end{aligned} \tag{4.115}$$

where $\varepsilon$ ($\ll 1$) is a constant. The first and the second terms are respectively proportional to

$$\varepsilon^{4/3}\, \check{k}^{-2/3}\, \frac{d}{d\check{k}} \left[ \check{k}^2\, \frac{d}{d\check{k}} \left[ \frac{\check{\Theta}}{\check{k}^2} \right] \right]$$

and $\varepsilon^{-2/3}\, \check{k}^{-8/3}\, \check{\Theta}(\check{k})$, both of which will be shown to be smaller than the third term (see (4.116) below). The asymptotic behavior of the third term may be obtained by noting that a dominant contribution to the integral comes from the vicinity of $q \approx 0$ if $\check{\Theta}$ is a decreasing function. Thus, we may convert (4.114) into

$$\check{\Theta}(\check{k}) = \frac{2K}{3}\, \check{k}^{-17/3} \int_0^\infty dq\, q^2\, \check{\Theta}(q) \qquad (s \ll 1, \alpha = 3/4, \check{k} \gg 1)\,. \tag{4.116}$$

Hence, the spectrum obeys the $k^{-17/3}$ power law at $\check{k} \gg 1$. The numerical solution of (4.113) shown in Fig.4.5(a) actually exhibits a transition from the $k^{-5/3}$ to the $k^{-17/3}$ power laws around the Obukhov-Corrsin wavenumber $k_C$.

### [3] *Diffusive range* ($\alpha < 3/4$)

For $\alpha < 3/4$ ($k \gg k_C$), since $s^{-1+4\alpha/3} \gg 1$, the exponential factor in (4.111) is a rapidly decreasing function and the contribution from the vicinity of the origin is dominant in the integral with respect to $t$. It then reduces to

$$\check{\Theta}(\check{k}) = \frac{K}{2}\, s^{2(1-4\alpha/3)}\, \check{k}^{-8/3} \iint_{\triangle_1} \mathrm{d}p\, \mathrm{d}q\, \sigma(1,p,q)\, \frac{p^{-8/3} q}{1+q^2} \left[ -\check{\Theta}(\check{k}) + \frac{1}{q^2}\, \check{\Theta}(\check{k}q) \right] Q(s^\alpha \check{k} p, 0)\,. \tag{4.117}$$

This is further simplified by dividing the integral with respect to $q$ into two regions, $I_1$ ($0 \le q \le \varepsilon$) and $I_2$ ($q \ge \varepsilon$), where $\varepsilon$ ($\ll 1$) is a constant independent of $s$. Then, (4.117) is written as

$$\check{\Theta}(\check{k}) = \frac{K}{2}\, s^{2(1-4\alpha/3)}\, \check{k}^{-8/3} \Big[ I_1 + I_2 \Big]. \tag{4.118}$$

It is easy to show that $I_2$ and the first term of $I_1$ are bounded irrespective of the value of $s$. As for the second term of $I_1$, we make a change of integral variables as $p = 1 + qx$, expand the integrand around $q = 0$ and carry out the integration with respect to $x$ to obtain

$$\begin{aligned} (\text{Second term of } I_1) &= \frac{4}{3}\, Q(\check{k} s^\alpha, 0)\, \check{k}^{-3} \left[ \int_0^\infty \mathrm{d}q\, q^2\, \check{\Theta}(q) - \int_\varepsilon^\infty \mathrm{d}q\, q^2\, \check{\Theta}(q) \right] \\ &= \frac{4}{3}\, Q(\check{k} s^\alpha, 0)\, \check{k}^{-3} \left[ \frac{1}{2\,C_1}\, s^{-\beta-3\alpha+1} - \int_\varepsilon^\infty \mathrm{d}q\, q^2\, \check{\Theta}(q) \right], \end{aligned} \tag{4.119}$$

where use has been made of $\chi = 2\kappa \int_0^\infty \mathrm{d}k\, k^2\, \Theta(k)$. The second term of this equation is also bounded and neglected compared with the first term in the limit $s \to 0$ (because (4.121) and $\alpha < 3/4$). On substitution of the first term of (4.119) into (4.118), we find

$$\check{\Theta}(\check{k}) = \frac{K}{3C_1}\, s^{3-17\alpha/3-\beta} \check{k}^{-17/3}\, Q(s^\alpha \check{k}, 0)\,. \tag{4.120}$$

In order that (4.120) may have a nontrivial solution, we must set

$$\beta = 3 - \tfrac{17}{3}\,\alpha \tag{4.121}$$

to obtain

$$\check{\Theta}(\check{k}) = \frac{K}{3C_1}\, \check{k}^{-17/3}\, Q(s^\alpha \check{k}, 0) \qquad (s \ll 1, \alpha < 3/4)\,. \tag{4.122}$$

Since this equation depends upon $s$ through $s^\alpha$, we will examine three cases $0 < \alpha < 3/4$, $\alpha = 0$ and $\alpha < 0$ separately in the following.

### [3-1] *Inertial-diffusive range* ($0 < \alpha < 3/4$)

For $0 < \alpha < 3/4$ ($k_C \ll k \ll k_K$), we find, because of $Q(0,0) = 1$, that

$$\check{\Theta}(\check{k}) = \frac{K}{3C_1}\, \check{k}^{-17/3} \qquad (s \ll 1, 0 < \alpha < 3/4)\,. \tag{4.123}$$

The dimensional form of the scalar spectrum corresponding to (4.123) is written, using (4.78) and (4.121), as

$$\Theta(k) = \tfrac{1}{3}\, K\, \chi\, \epsilon^{2/3}\, \kappa^{-3}\, k^{-17/3}\,. \tag{4.124}$$

Thus, we have obtained the $k^{-17/3}$ power law in the inertial-diffusive range. By comparing it with (4.14), we get

$$C_3 = \tfrac{1}{3}\, K = 0.572\,. \tag{4.125}$$

This relation between two universal constants $C_3$ and $K$ was obtained before by Batchelor et al. [66]. Qian [82] derived $C_3 = 1.2K$ by a statistical mechanical theory, whereas Canuto et al. [83] proposed a relation $C_3 = 8/(27\, C_1^2)$ by a turbulence model. There seems no experimental data available because of difficulty of measurements in the inertial-diffusive range. The direct and kinematic numerical simulations by Chasnov et al. [76] strongly support the relation (4.125).

[3-2] *Around Kolmogorov wavenumber* ($\alpha = 0$)

In the case of $\alpha = 0$ ($k = O(k_{\rm K})$), (4.122) is written as

$$\check{\Theta}(\check{k}) = \frac{K}{3C_1}\, \check{k}^{-17/3}\, Q(\check{k}, 0) \qquad (s \ll 1, \alpha = 0)\,. \tag{4.126}$$

Since the functional form of $Q(\check{k}, 0)$ has already known in Chapter 3, we can draw the scalar spectrum function around $k_{\rm K}$ (Fig.4.5(b)). The asymptotic form of energy spectrum $E(k) = K\epsilon^{2/3}k^{-5/3}Q(k/k_{\rm K}, 0)$ in the large wavenumber limit may be proportional to $k^3 \exp(-ck)$, as shown from the LRA-DIA equation for the velocity correlation function (see Appendix C). Hence, we have

$$\Theta(k) \propto k^{-1}\, \exp(-ck) \qquad (s \ll 1, k \gg k_{\rm K})\,. \tag{4.127}$$

[3-3] *Far viscous-diffusive range* ($\alpha < 0$)

Finally, for $\alpha < 0$ ($k \gg k_{\rm K}$), (4.122) yields

$$\check{\Theta}(\check{k}) = 0 \qquad (s \ll 1, \alpha < 0)\,, \tag{4.128}$$

which is consistent with (4.127) that the spectrum function is exponentially small at $k \gg k_{\rm K}$.

### 4.4.5 Bump in the spectrum

Here, we discuss the bump structure which is observed around the ends of the viscous-advective range for $s \geq 1$ (see Figs.4.2(b) and 4.4(b)) and of the inertial-advective range for $s \leq 1$ (Figs.4.3(a) and 4.5(a)). These may be seen more clearly in their compensated spectra in Figs.4.6(a) and (b). Since the end wavenumbers ($k_{\rm B}$ for $s \geq 1$ and $k_{\rm C}$ for $s \leq 1$) of these advective ranges correspond to the beginning of the scalar dissipation, this may be understood as a bottleneck phenomenon [84] for the scalar fluctuation transfer. The scalar fluctuation cascades down throughout the advective range

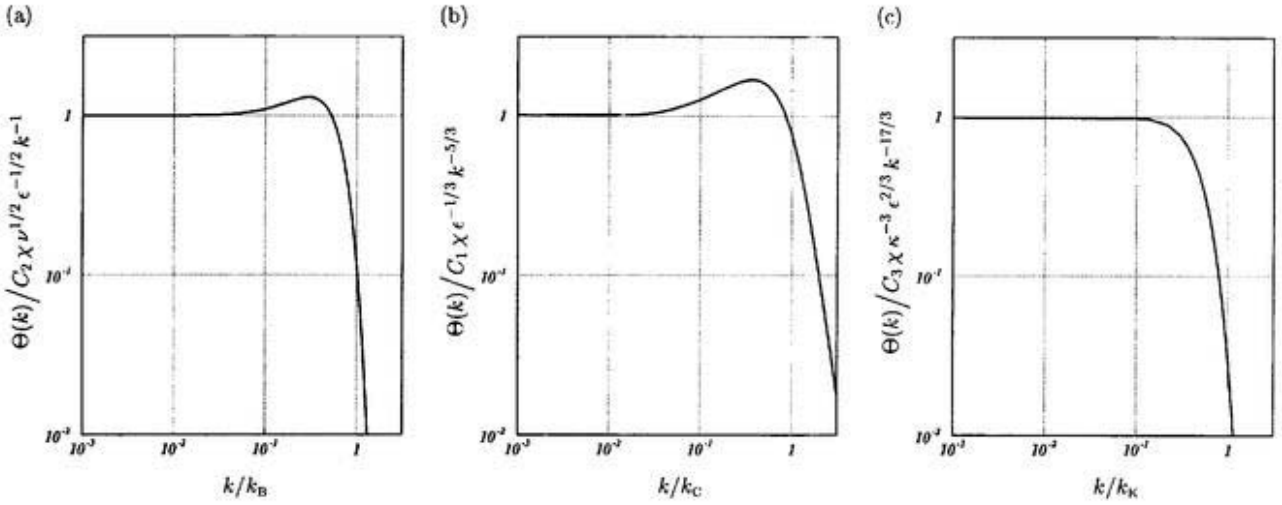


FIGURE 4.6 Compensated passive scalar spectra in stationary isotropic turbulence (a) around $k_B$ for $s \gg 1$, (b) around $k_C$ for $s \ll 1$ and (c) around $k_K$ for $s \ll 1$.

toward smaller scales by the interaction with the turbulent velocity field. The cascade is less effective at the end of this range because the scalar fluctuation damps in the diffusive range. This results in a pile up of the scalar fluctuation around the end of the advective range. Actually, such a bump in the scalar spectrum is observed in measurements of atmospheric boundary layer ($s \sim 0.7$) by Williams and Paulson [85] and Champagne et al. [86], and of tidal flow ($s \sim 9.2$) by Grant et al. [74]; the results of these measurements are collected by Hill [87].

On the other hand, we can hardly observe any bump in the scalar spectrum at the end of the inertial-diffusive range (Fig.4.5(b)) nor in the compensated spectrum (Fig.4.6(c)). Recall that the functional form of the scalar spectrum in this range is similar to that of the energy spectrum in a logarithmic scale (see §4.4.4), and that the end wavenumber $k_K$ represents the beginning of the dissipation range of the velocity field but not of the scalar field. Hence, if there is a bump around $k_K$, it should be due to the bottleneck effect of the energy cascade. A bump in the energy spectrum is, however, not so clearly observed in experiments (see Fig.3.4) if it exists. The bottleneck phenomenon seems to be more effective in the passive scalar fluctuation cascade than in the energy cascade. More detailed quantitative discussions would demand a scrutiny of the three component transfer functions. Anyway, the present results on the bump structures of the spectra are qualitatively consistent with experiments.

It may be worth mentioning, in passing, that the energy spectrum of the system [88] governed by an equation,

$$\frac{\partial}{\partial t}u(x,t) + u(x,t)\frac{\partial}{\partial x}u(x,t) = (-1)^{n+1}\nu\frac{\partial^{2n}}{\partial x^{2n}}u(x,t) + f(x,t) \qquad (n = 1, 2, \cdots) \qquad (4.129)$$

with a random forcing $f(x,t)$ over the whole length scale (wavenumber range) exhibits a clear bump structure. Here, we adopt a hyperviscosity, which enhances the bottleneck effect [84], by putting $n = 6$. By the way, the equation (4.129) with $n = 1$ is the Burgers equation [89]. The numerically evaluated compensated energy spectrum of this system is plotted in Fig.4.7, where we employed the same viscosity $\nu$ and random forcing $f(x,t)$ as those in Ref. [88]. The governing equation of a passive

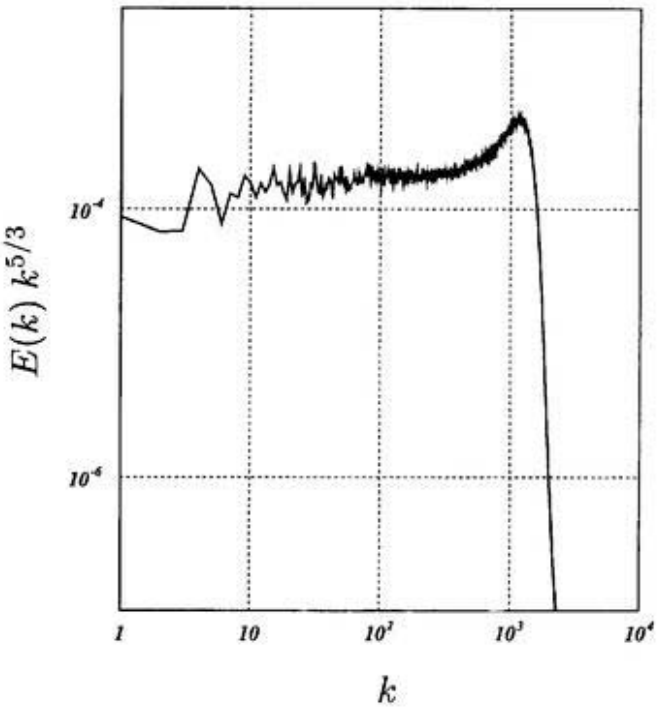


FIGURE 4.7 Compensated energy spectrum of the system governed by the Burgers equation with a random forcing over the whole wavenumber range. Parameters are same to the direct numerical simulation by Chekhlov & Yakhot [88]. A hyperviscosity proportional to $\frac{\partial^{12}u(x)}{\partial x^{12}}$ is employed. The clear bump at the end of the inertial range is observed.

scalar (4.17) and the Burgers equation (4.129) are similar in the sense that they do not have a pressure term.

### 4.4.6 Mixed-derivative skewness

The mixed-derivative skewness factor $S_{u\theta}$ of the scalar and the velocity fields defined by

$$S_{u\theta} = \frac{\overline{\left(\frac{\partial u_1}{\partial x_1}\right)\left(\frac{\partial \theta}{\partial x_1}\right)^2}}{\left[\overline{\left(\frac{\partial u_1}{\partial x_1}\right)^2}\right]^{1/2}\overline{\left(\frac{\partial \theta}{\partial x_1}\right)^2}} \tag{4.130}$$

is a measurable quantity by experiments, and is related to the dissipation rate of the fluctuations of the scalar gradient through the relation

$$S_{u\theta} = -\frac{6}{\sqrt{15}}\,\kappa\left(\frac{\epsilon}{\nu}\right)^{1/2}\frac{\int_0^\infty \mathrm{d}k\, k^4\,\Theta(k)}{\int_0^\infty \mathrm{d}k\, k^2\,\Theta(k)} \tag{4.131}$$

in isotropic stationary fields (see e.g. Ref. [68]). This factor depends upon the Schmidt number $s$, and its asymptotic behaviors in the large and small $s$ limits are described in the framework of the

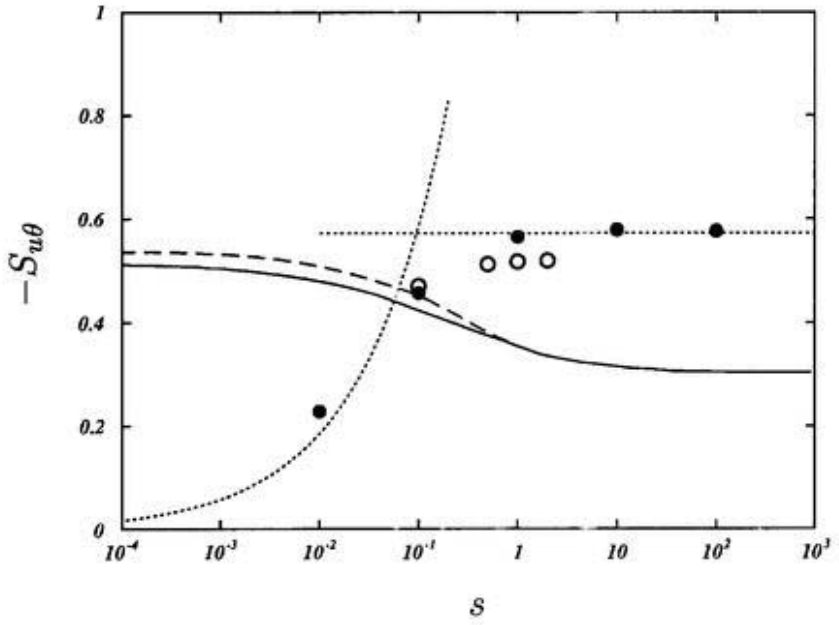


FIGURE 4.8 Mixed-derivative skewness factor defined by (4.130). The present theory (solid circles) with its asymptotic forms $S_{u\theta} \to -1.9\, s^{1/2}$ $(s \to 0)$ and $S_{u\theta} \to -0.57$ $(s \to \infty)$ (dotted lines), direct numerical simulation by Kerr [68] (open circles), Clay's theory [78] (solid line) and Gibson et al.'s theory [71] (dashed line) are plotted.

present theory as follows. In the small $s$ limit, the contribution from the vicinity of $k_C$ is dominant in both of the integrals in (4.131), because the spectrum behaves as drawn in Fig.4.5. Hence, it has an asymptotic form

$$S_{u\theta} \to S_0\, s^{1/2} \quad (s \to 0) \tag{4.132}$$

with

$$S_0 = -\frac{6}{\sqrt{15}} \frac{\displaystyle\int_0^\infty \mathrm{d}k^\dagger\, k^{\dagger 4}\, \Theta(k^\dagger)}{\displaystyle\int_0^\infty \mathrm{d}k^\dagger\, k^{\dagger 2}\, \Theta(k^\dagger)} \approx -1.9\,, \tag{4.133}$$

where $k^\dagger = k/k_C$. The constant $S_0$ is evaluated by the numerical integration of the spectrum given in Fig.4.5(a). In the large Schmidt number limit, on the other hand, the contribution from the vicinity of $k_B$ is dominant in the integrals (see Fig.4.4), and therefore it is shown that

$$S_{u\theta} \to S_\infty \quad (s \to \infty) \tag{4.134}$$

with

$$S_\infty = -\frac{6}{\sqrt{15}} \frac{\displaystyle\int_0^\infty \mathrm{d}k^\ddagger\, k^{\ddagger 4}\, \Theta(k^\ddagger)}{\displaystyle\int_0^\infty \mathrm{d}k^\ddagger\, k^{\ddagger 2}\, \Theta(k^\ddagger)} \approx -0.57\,, \tag{4.135}$$

where $k^\ddagger = k/k_B$, and use has been made of the numerical value of the spectrum shown in Fig.4.4(b).

In Fig.4.8, we plot the mixed-derivative skewness factor (solid circles) obtained numerically through (4.131) for finite Schmidt numbers $s = 0.01, 0.1, 1, 10$ and 100 together with the asymptotic forms (dotted lines). The results by a direct numerical simulation [68] (open circles) and the

prediction by Clay's [78] (solid line) and Gibson et al.'s theory [71] (dashed line) are also shown. The fact that the skewness factors obtained by the numerical simulation for small $s$ around 0.1 remains almost constant led them [68,71] the conclusion that the numerical simulation favored Gibson et al.'s theory rather than Batchelor et al.'s, the latter of which predicts the asymptotic form of the skewness factor similar to (4.132) for $s \to 0$, i.e., $S_{u\theta} \propto s^{1/2}$. On the contrary, however, Fig.4.8 does suggest that the simulation is consistent with our results, i.e., Batchelor et al.'s theory, rather than Gibson et al.'s (or Clay's). An experiment or direct numerical simulation at Schmidt numbers less than $10^{-2}$ is required for more precise comparison.

## 4.5 Concluding remarks

The Lagrangian DIA, which was successful in the application to turbulent velocity field (Chapter 3), has been applied to a scalar field advected passively by isotropic turbulence. The solutions to a closed equation for the scalar correlation function by this theory is shown to be completely consistent with the phenomenological theories for arbitrary Schmidt numbers (Obukhov [64] and Corrsin [65]; Batchelor et al. [66] for small Schmidt number; Batchelor [67] for large Schmidt number), which are well confirmed by experiments and direct numerical simulations. This simple Lagrangian closure is, therefore, excellently successful in making a bridge between the phenomenological theories and the basic equations in describing the power spectra of both the velocity and passive scalar fields in isotropic turbulence. It should be stressed here that the method employed to examine the Schmidt number dependence of the scalar spectrum is systematic.

In addition, the functional forms over the universal range of the scalar spectrum in the statistically stationary state have been determined numerically not only for moderate Schmidt numbers $s$ but also for the large and the small $s$ limits. The numerically evaluated universal forms of the function have a bump at the end of the advective ranges, which was clearly observed in measurements [74,85,86]. Schmidt number dependence of the mixed-derivative skewness factor of the velocity and the scalar fields is also investigated by the integration of the numerically evaluated universal forms of the spectrum, and is shown to be in a good agreement with the direct numerical simulation by Kerr [68]. In summary, the Lagrangian DIA gives predictions consistent with observations at least qualitatively. Although the universal constant in the inertial-diffusive range is in a good agreement with the results of numerical simulations by Chasnov et al. [76], the constants in the inertial- and viscous-advective ranges are only about half the experimental data [73–75]. This is a weak point of the Lagrangian DIA. Recall that this approximation theory is founded on the working assumptions summarized in §4.3.2 (and §3.3.2). As mentioned in that section, the third assumption, i.e., the statistical independency between the position function and the other field quantities, has no physical basis. The failure in the estimation of the universal constants in the advective range may be caused by the this artificial assumption because the position function and passive scalar in the range should be identical. Hence, it seems that we have to take the correlation into account in the formulation of the approximation. This important problem is, however, still open (see §6.3).

# Appendix A

Derivations of (4.52) and (4.53) are described here. By substituting (4.26) into (4.28), we obtain

$$\widetilde{Z}(\boldsymbol{k},t,t') = \frac{(2\pi)^9}{L^6} \sum_{\boldsymbol{k}'} \overline{\widetilde{\theta}(\boldsymbol{k}',t)\,\widetilde{\psi}(-\boldsymbol{k}',t|\boldsymbol{k},t')\,\widetilde{\theta}(-\boldsymbol{k},t')}\,, \tag{4.136}$$

which is further converted, by substitutions of the direct-interaction decompositions, into

$$\widetilde{Z}(\boldsymbol{k},t,t') = \frac{(2\pi)^9}{L^6} \sum_{\boldsymbol{k}'} \overline{\widetilde{\theta}^{(0)}(\boldsymbol{k}',t\|\boldsymbol{k}_0,\boldsymbol{p}_0,\boldsymbol{q}_0)\,\widetilde{\psi}^{(0)}(-\boldsymbol{k}',t|\boldsymbol{k},t'\|\boldsymbol{k}_0,\boldsymbol{p}_0,\boldsymbol{q}_0)\,\widetilde{\theta}^{(0)}(-\boldsymbol{k},t'\|\boldsymbol{k}_0,\boldsymbol{p}_0,\boldsymbol{q}_0)} \tag{4.137}$$

(see Assumption 3 in §4.3.2). A combination of (3.64) and (4.137) yields (4.52). As for (4.53), we take the functional derivative of (4.26) to obtain

$$\overline{\widetilde{G}_\theta^{(L)}(t|\boldsymbol{k},-\boldsymbol{k},t')} = \frac{(2\pi)^6}{L^3} \sum_{\boldsymbol{k}'} \overline{\widetilde{G}_\theta(\boldsymbol{k}',t|-\boldsymbol{k},t')\,\widetilde{\psi}(-\boldsymbol{k}',t|\boldsymbol{k},t')}\,. \tag{4.138}$$

By substituting the direct-interaction decompositions into the right-hand side of the above equation and by taking (3.64) into account, we find (4.53).

# Appendix B

We prove (4.76) based upon the LRA-DIA equation. The right-hand side of (4.71) gives the transfer function (4.33) in the inertial-advective range as

$$T_\theta(k) = KW_1\,\nu\,k_{\mathrm{K}}^{4/3}\,k \iint_{\triangle_k} \mathrm{d}p\,\mathrm{d}q\,\sigma(k,p,q)\,p^{-10/3}\,q\left[-\Theta(k)+\left(\frac{k}{q}\right)^2\Theta(q)\right]. \tag{4.139}$$

The scalar flux function (4.34) is then written as

$$\begin{aligned}\Pi_\theta(k) &= KW_1\,\nu\,k_{\mathrm{K}}^{4/3}\int_k^\infty \mathrm{d}k'k' \iint_{\triangle_{k'}} \mathrm{d}p\,\mathrm{d}q\,\sigma(k',p,q)\,p^{-10/3}\,q\left[-\Theta(k')+\left(\frac{k'}{q}\right)^2\Theta(q)\right] \\ &= KW_1\,\nu\,k_{\mathrm{K}}^{4/3}\int_k^\infty \mathrm{d}k'k' \iint_{\substack{\triangle_{k'} \\ p<k \text{ or } q<k}} \mathrm{d}p\,\mathrm{d}q\,\sigma(k',p,q)\,p^{-10/3}\,q\left[-\Theta(k')+\left(\frac{k'}{q}\right)^2\Theta(q)\right],\end{aligned} \tag{4.140}$$

where we have used the property of the detailed balance of the nonlinear transfer of the scalar fluctuation, i.e.,

$$\int_k^\infty \mathrm{d}k'k' \iint_{\substack{\triangle_{k'} \\ p,q>k}} \mathrm{d}p\,\mathrm{d}q\,\sigma(k',p,q)\,p^{-10/3}\,q\left[-\Theta(k')+\left(\frac{k'}{q}\right)^2\Theta(q)\right] = 0\,. \tag{4.141}$$

Substitution of the inertial-advective power spectrum (4.8) into (4.140) gives

$$\begin{aligned}\Pi_\theta(k) &= KW_1 C_1 \chi \int_k^\infty \mathrm{d}k' \iint_{\substack{\triangle_{k'} \\ p<k \text{ or } q<k}} \mathrm{d}p\,\mathrm{d}q\, \sigma(k',p,q)\, k'\, p^{-10/3}\, q \left[ k'^{-5/3} - k'^2\, q^{-11/3} \right] \\ &= KW_1 C_1 \chi \int_1^\infty \mathrm{d}k' \iint_{\substack{\triangle_{k'} \\ p<1 \text{ or } q<1}} \mathrm{d}p\,\mathrm{d}q\, \sigma(k',p,q)\, k'\, p^{-10/3}\, q \left[ k'^{-5/3} - k'^2\, q^{-11/3} \right] \\ &= KW_1 C_1 \chi\, I\,, \end{aligned} \tag{4.142}$$

where

$$\begin{aligned} I = &\left[ \int_1^\infty \mathrm{d}k' \int_0^1 \mathrm{d}p \int_{k'-p}^{k'+p} \mathrm{d}q - \int_1^2 \mathrm{d}k' \int_{k'/2}^1 \mathrm{d}p \int_{k'-p}^{p} \mathrm{d}q \right] \\ &\times \left[ \sigma(k',p,q)\, k'\, p^{-10/3}\, q \left[ k'^{-5/3} - k'^2\, q^{-11/3} \right] + (\text{similar term } p \leftrightarrow q) \right] \\ = &\frac{729}{910} \int_0^\infty \frac{\mathrm{d}x}{x^{1/3}(x+1)} - \frac{2187}{910} \int_0^1 \frac{\mathrm{d}x}{x^2+x+1} = \frac{729\pi}{910\sqrt{3}}\,. \end{aligned} \tag{4.143}$$

Since $\Pi_\theta = \chi$ in the advective range, we obtain (4.76).

## Appendix C

We show by the procedure described in Ref. [90] that the asymptotic form of the energy spectrum for large wavenumber,

$$E(k) \propto k^3 \exp(-ck) \qquad k \to \infty \tag{4.144}$$

is a solution to the LRA-DIA equation for the velocity correlation function. For simplicity of notations, we write the LRA-DIA equation (3.104) in the statistically stationary state in terms of $\mathcal{Q}$ and $\mathcal{G}$ defined by

$$\check{Q}^{\mathrm{I}}(k,t) = \mathcal{Q}(k)\, \mathcal{G}(k,t) \tag{4.145}$$

with

$$\mathcal{G}(k,0) = 1 \tag{4.146}$$

as

$$\begin{aligned}\mathcal{Q}(k) = \frac{1}{2}\, k^{-1} &\iint_{\triangle_k} \mathrm{d}p\mathrm{d}q\, (pq)^{-8/3}\, \widehat{b}(k,p,q) \left[ k^{11/3}\, \mathcal{Q}(p) - p^{11/3}\, \mathcal{Q}(k) \right] \mathcal{Q}(q) \\ &\times \int_0^\infty \mathrm{d}t\, \mathcal{G}(k,k^{2/3}t)\, \mathcal{G}(p,p^{2/3}t)\, \mathcal{G}(q,q^{2/3}t)\,. \end{aligned} \tag{4.147}$$

Since in the limit $k \to \infty$ the integration with respect to $t$ is evaluated as

$$\int_0^\infty \mathrm{d}t\, \mathcal{G}(k,k^{2/3}t)\, \mathcal{G}(p,p^{2/3}t)\, \mathcal{G}(q,q^{2/3}t) = \frac{C}{k^2} \qquad (C = \text{constant})\,, \tag{4.148}$$

the LRA-DIA equation (4.147) reduces to

$$\mathcal{Q}(k) = \frac{C}{2}\, k^{2/3} \iint_{\triangle_k} \mathrm{d}p\mathrm{d}q\, (pq)^{-8/3}\, \widehat{b}(k,p,q)\, \mathcal{Q}(p)\, \mathcal{Q}(q)\,. \tag{4.149}$$

Furthermore, by changing integral variables from $(p, q)$ to $(\xi, \eta)$ by

$$p + q = k\xi \tag{4.150}$$

$$p - q = k\eta\,, \tag{4.151}$$

we obtain

$$\mathcal{Q}(k) = \frac{C}{4}\, k^{-8/3} \int_1^\infty \mathrm{d}\xi \int_{-1}^1 \mathrm{d}\eta\, \mathcal{Q}\left(\frac{k(\xi+\eta)}{2}\right) \mathcal{Q}\left(\frac{k(\xi-\eta)}{2}\right) \times \left[\frac{\xi^2-\eta^2}{4}\right]^{-8/3} \frac{(1-\eta^2)\,(\xi^2-1)\left[(\xi+\eta)^2+\xi\eta\,(\xi-\eta)^2+4\xi\eta\right]}{2(\xi^2-\eta^2)^2}\,, \tag{4.152}$$

where we have used the definition (3.80) of $\widehat{b}(k,p,q)$. The contribution from the vicinity of $\xi \sim 1$ to the integration is dominant in the large $k$ limit, therefore this equation is further rewritten as

$$\mathcal{Q}(k) = \frac{C}{4}\, k^{-8/3} \int_1^\infty \mathrm{d}\xi \int_{-1}^1 \mathrm{d}\eta\, \mathcal{Q}\left(\frac{k(\xi+\eta)}{2}\right) \mathcal{Q}\left(\frac{k(\xi-\eta)}{2}\right) \times \left[\frac{1-\eta^2}{4}\right]^{-8/3} \frac{(\xi-1)\left[(1+\eta)^2+\eta\,(1-\eta)^2+4\eta\right]}{(1-\eta^2)}\,. \tag{4.153}$$

Then, it is easy to show that

$$\mathcal{Q}(k) \propto k^a \exp(-ck)\,, \tag{4.154}$$

$a$ and $c$ being constants, is a solution to (4.147) if we choose $a$ as

$$a = \frac{14}{3}\,. \tag{4.155}$$

Remembering the relation (3.105) between the energy spectrum $E$ and $\check{Q}^\dagger$, we arrive at (4.144).

# Chapter 5

# Strength of Nonlinear Couplings

We deal with two problems on the strength of the nonlinear couplings. First, defining the strength $s$ of the nonlinear couplings by the average number of direct interactions between a pair of modes, we consider again the applicability of DIA by the use of a model equation introduced in Chapter 2. It is shown both numerically and by a simple argument that DIA gives a good approximation if $s$ is much less than the square root of the number of degrees of freedom of the system. Next, we suggest a reason why the closure equations derived both by DIA and RRE, the latter of which should be valid for low Reynolds-number systems, are applicable to strong nonlinear systems. It is concluded that RRE can be regarded as an approximation under which the nonlinear terms are replaced by independent Gaussian random variables.

## 5.1 Introduction

We have been considering applications of DIA to systems with very weak nonlinear couplings such as the Navier-Stokes turbulence, in which there is only a single direct interaction between each pair of modes. It should be emphasized that DIA is based upon this weakness of nonlinear couplings. In weak coupling systems, if we remove the direct interaction between a particular triplet of modes, there is no direct interaction between any two of these three modes. Furthermore, since many other modes are coupled with them indirectly if the number of degree of freedom is large enough, contributions from indirect interactions to correlation between them are randomized and negligible. Hence, we suppose that the three mode are statistically independent of each other (DIA assumption 2, in §2.3) in the NDI (non-direct-interaction) field in which the direct interaction between them is absent. Actually, in Chapter 2, it was shown that this assumption is well satisfied for a very weak nonlinear coupling system, if the number of degrees of freedom is large. On the other hand, when there are more direct interactions between a pair of modes, this assumption deteriorates even if the number of degrees of freedom is large. In §5.3 of Ref. [34], we investigated a model system with very strong nonlinear couplings, in which a pair of modes directly interact through all the other modes, and showed that the assumption failed and the prediction of the auto-correlation function by the DIA-RRE equations

was inconsistent with numerical results by direct integration of the model equation. In this chapter, we shall examine the relationship between validity of DIA and the strength of nonlinear couplings quantitatively.

Another problem we shall consider is on an explanation of RRE (the Reynolds-number reversed expansion, §2.4). As shown in §2.4.4, the closure equations derived by DIA are also obtained by RRE. It was also shown in Chapter 2 that DIA is valid for systems with weak nonlinear couplings and a large number of degrees of freedom even if the Reynolds number of the systems is large. Therefore the closure equations derived by RRE are applicable to such systems at large Reynolds number. This is surprising because RRE is formulated under the assumption that the Reynolds number is small. We shall solve this inconsistency by noting that the joint-Gaussianity of nonlinear terms is strongly related with the strength of nonlinear couplings and the number of degrees of freedom.

This chapter is organized as follows. By using a model equation with stronger nonlinear couplings introduced in the next section, we examine in detail the validity condition of DIA in §5.3, and suggest an alternative explanation of RRE by considering an approximation based upon the joint-Gaussianity of nonlinear terms in §5.4.

## 5.2 Model equation with stronger nonlinear couplings

We use again the model equation, introduced in Chapter 2, for a set of real variables $\{X_i | i = 1, 2, \cdots, N\}$,

$$\frac{\mathrm{d}}{\mathrm{d}t} X_i(t) = \sum_{j=1}^{N} \sum_{k=1}^{N} C_{ijk}\, X_j(t)\, X_k(t) - \nu\, X_i(t) + F_i(t)\,, \tag{5.1}$$

where constant coefficients $C_{ijk}$ satisfy the following three conditions:

$$C_{ijk} = C_{ikj} \qquad \text{(symmetry)} \tag{5.2}$$

$$C_{ijk} + C_{jki} + C_{kij} = 0 \qquad \text{(detailed balance of energy)} \tag{5.3}$$

$$C_{ijk} = 0 \qquad \text{for } i = j,\ j = k \text{ or } k = i \qquad \text{(absence of self-interaction)}\,. \tag{5.4}$$

The random forcing $F_i$ is assumed to be a Gaussian with zero mean and variance,

$$\sigma^2 = \frac{2\nu}{N \Delta t}\,, \tag{5.5}$$

where $\Delta t$ is a time increment in numerical integration of (5.1).

One of the advantages of this model equation is that we can easily construct nonlinear systems with either weak or strong couplings by changing coefficients $C_{ijk}$. We studied in Chapter 2 only a very weak nonlinear coupling case, that is, there is only a single, at the most, direct interaction between an arbitrary pair of modes. Here, we shall deal with systems with stronger nonlinear couplings. The strength $s$ of the nonlinear couplings is quantitatively defined by the average number of direct

interactions between arbitrary pairs of modes. For example, $s$ is estimated as $s \sim 1$ for the systems used in Chapter 2, and $s = 1$ for the Navier-Stokes system in Chapters 3 and 4. (Because of the restriction of symmetry with respect to subscript $i$ of coefficients $C_{ijk}$ we may not be able to construct this model system (5.1) with $s$ exactly equal to unity.) See also Fig.5.1 in which direct interactions between $X_1$ and the other modes in several cases of coupling strength are schematically depicted. Since there is arbitrariness in the choice of coefficients even if we set $s$ an approximately fixed value, we shall examine numerically several cases with almost same strength of couplings. We choose the coefficients $C_{ijk}$ so that the system can be homogeneous with respect to subscripts $i$, and that the maximum number of the direct interactions between an arbitrary pair of modes cannot exceed $[s]+1$. The latter condition is imposed in order that the strength of nonlinear couplings may also be homogeneous.

The model equation (5.1) has three parameters, that is, the viscosity $\nu$ (or the Reynolds number $\mathcal{R} = 1/\nu$), the number $N$ of degrees of freedom and the strength $s$ of the nonlinear couplings. In the following, we restrict ourselves in the strong nonlinearity limit that

$$\mathcal{R} \to \infty \quad \Longleftrightarrow \quad \nu \to 0\,. \tag{5.6}$$

In this limit both the dissipative and the forcing terms in (5.1) vanish (see (5.5)).

## 5.3 Validity condition of DIA

It was shown in Chapter 2 that DIA was valid for systems with weak nonlinear couplings and a large number of degrees of freedom. However it has not yet considered how large the number of degrees of freedom should be, or how weak the strength of nonlinear couplings should be so that DIA may be accurate. In this section, we investigate such a quantitative evaluation of validity condition of DIA.

In Fig.5.2, we plot the prediction $\mathcal{V}_{\rm DIA}$ of the auto-correlation function by the DIA-RRE equations (2.70)—(2.73) in statistically stationary state and the results $\mathcal{V}_{\rm DNS}$ of the direct numerical simulation of the model equation (5.1) for several combinations $(s, N)$ of the strength of nonlinear couplings and the number of degrees of freedom. When $N$ is large or $s$ is small, the DIA-RRE equations give good results. This is consistent with the conclusion in Chapter 2 that DIA is valid for systems with weak nonlinear couplings and a large number of degree of freedom. Recall that DIA is based upon two assumptions: the smallness of the deviation fields, and the statistical independency between three modes without direct interaction. These two assumptions are valid for large $N$ systems. As for the first assumption, since there are many direct interactions in such systems, the influence of an artificial removal of one direct interaction is small. As for the second assumption, since many modes are coupled with the three modes indirectly if $N$ is large, influence of indirect interaction may be randomized and the contribution to correlation between the modes may be negligible. However, we have to notice that the second assumption requires also weakness of nonlinear couplings because if couplings are stronger there exist indirect interactions between a triplet of modes through a small number of modes (e.g., four-mode indirect interaction shown in Fig.5.3). Since such indirect interactions through a small number of modes are not expected to be randomized, correlation between the three modes is not necessarily small in strong nonlinear coupling systems.

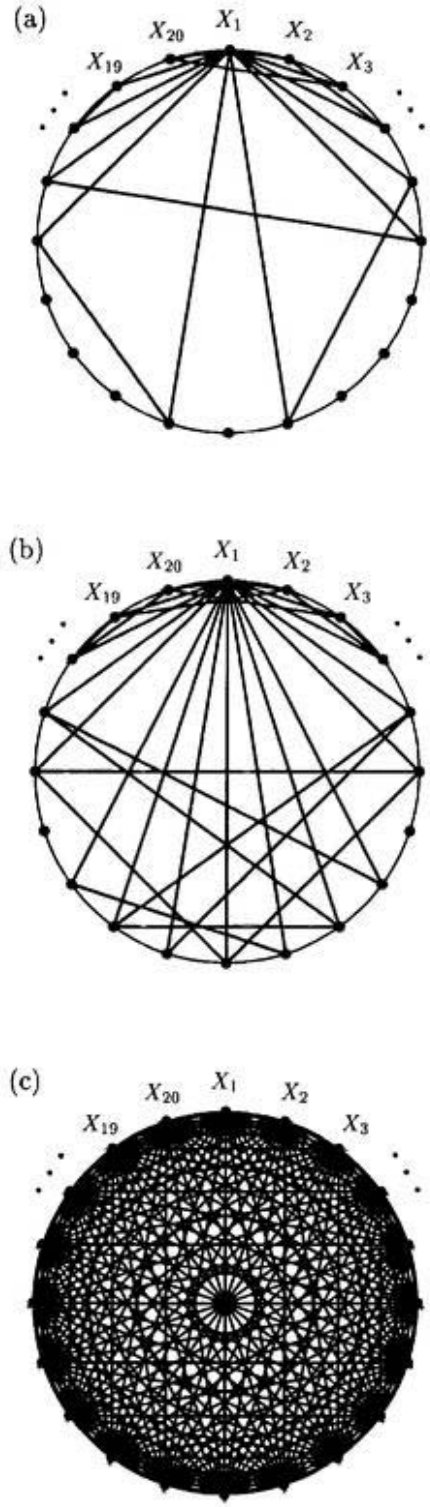


FIGURE 5.1 Direct interactions of the model equation (5.1) between $X_1$ and other modes. The number of degrees of freedom is 20. The cases of (a) $s \sim 1$ (b) 2 and (c) 18 are shown, where the strength of the nonlinear couplings $s$ is defined by the average number of direct interactions between an arbitrary pair of modes. We choose the coefficients $C_{ijk}$ so that the number of direct interactions between a pair of modes may not exceed $[s]+1$ and that the system $\{X_i\}$ may be homogeneous with respect to $i$.

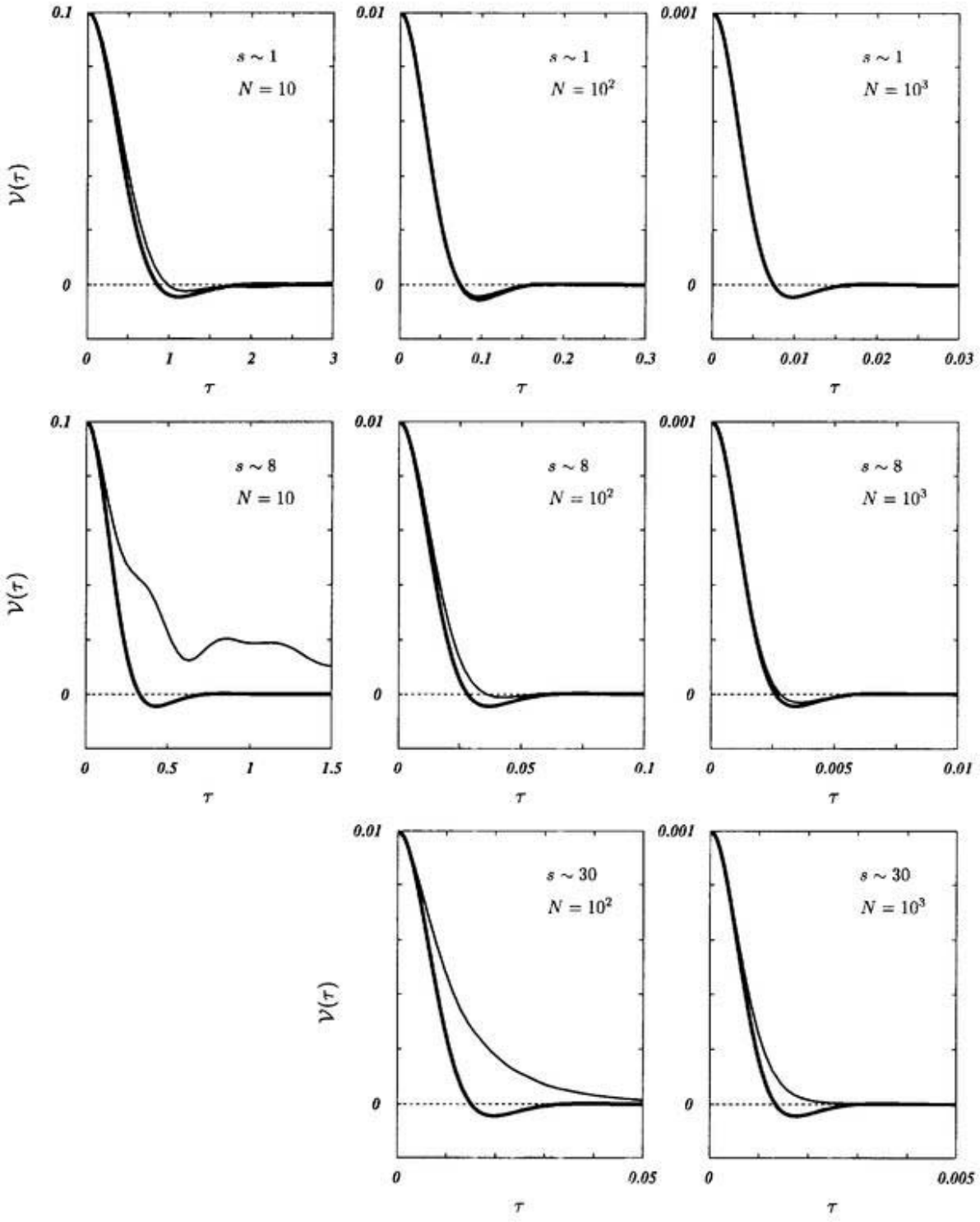


FIGURE 5.2 Auto-correlation function. Thick lines denote predictions by the DIA-RRE equations, and thin lines are results by direct numerical integration of the model equation. Results for various combinations of number $N$ of degrees of freedom and strength $s$ of nonlinear couplings are shown. As $N$ increases or $s$ decreases, the DIA-RRE equations give better results.

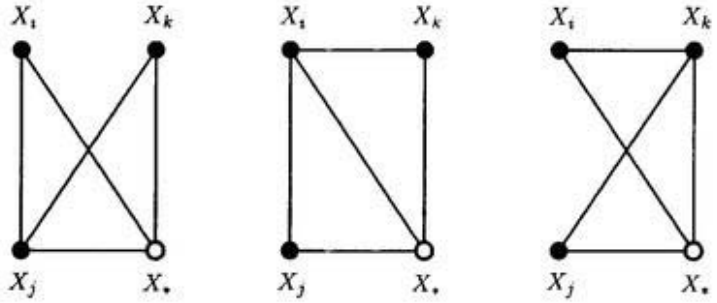


FIGURE 5.3 Four-mode indirect interactions between $X_i$, $X_j$ and $X_k$ through a mode $X_*$.

In order to make a quantitative consideration, we introduce a parameter $\Delta$ by

$$\Delta = \frac{\int_0^\infty d\tau \left| \mathcal{V}_{\mathrm{DIA}}(\tau) - \mathcal{V}_{\mathrm{DNS}}(\tau) \right|}{\int_0^\infty d\tau \left| \mathcal{V}_{\mathrm{DIA}}(\tau) \right|}, \tag{5.7}$$

which denotes a deviation from direct numerical simulation of prediction by the DIA-RRE equations, that is, small $\Delta$ implies the validness of the DIA-RRE equations. Numerical results of $\Delta$ evaluated for various strength $s$ ($\ll N$) of nonlinear couplings are plotted in Figs.5.4(a) for $N = 10^2$ and (b) $N = 10^3$. These figures are qualitatively consistent with the above argument, namely, the deviation $\Delta$ of prediction by the DIA-RRE equations is small for larger $N$ and smaller $s$. As shown in Fig.5.4(c), $\Delta$ may be a function of $s/N^{1/2}$. This is understandable by a simple discussion as follows. The simplest indirect interactions between a triplet of modes are four-mode interactions shown in Fig.5.3. We assume that if there exists such a four-mode indirect interaction, which is never randomized in contrast with many-mode indirect interactions, the three modes have a correlation, and the independency assumption (DIA assumption 2) is violated. The probability $p$ of the existence of a four-mode indirect interaction is evaluated as

$$p = \begin{cases} 0 & (s \leq 1)\,, \\ \dfrac{3s(s-1)}{N} & (1 \leq s) \end{cases} \tag{5.8}$$

under the condition,

$$1 \ll N\,. \tag{5.9}$$

Thus, we expect that if $p$ is much less than unity then $\Delta$ is also small. This may be a reason why $\Delta$ is a function of $s/N^{1/2}$.

## 5.4 RRE and NNA

As shown in §2.4.4, when we apply RRE to the model equation (5.1), we obtain the same set of closure equations (the DIA-RRE equations) as those by DIA. It has also been shown that DIA is valid for systems with weak nonlinear couplings and a large number of degrees of freedom even if the Reynolds number of the system is large. These imply that the *DIA*-RRE equations can be valid for

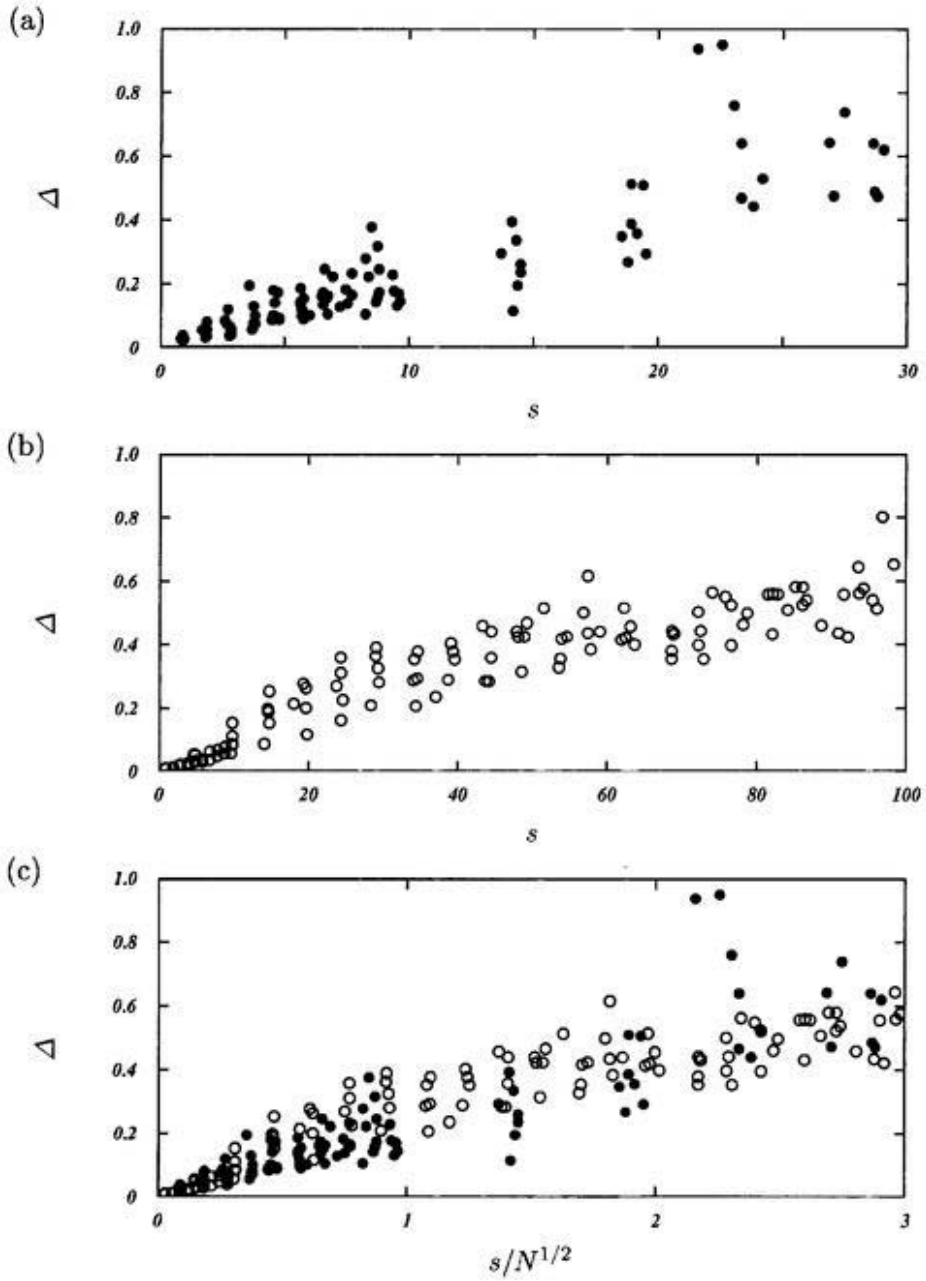


FIGURE 5.4 Deviation of the prediction of the auto-correlation function by the DIA-RRE equations from the results by the direct integration of the model equation for the number of degrees of freedom (a) $N = 100$ (closed circles) and (b) $N = 1000$ (open circles). Parameter $\Delta$ is defined by (5.7) and $s$ is the strength of nonlinear couplings. In (c), $s$ is normalized by $N^{1/2}$.

large Reynolds-number systems. However, it seems strange that the DIA-*RRE* equations give good approximation for such large Reynolds-number systems because RRE is obviously an approximation for small Reynolds-number systems. In this section, we resolve this inconsistency problem from the viewpoint of the joint-Gaussianity of the nonlinear terms.

### 5.4.1 Normal nonlinear term approximation

[1] *Assumptions*

Let us consider an approximation under which the nonlinear terms,

$$\mathcal{N}_i(t) = \sum_j \sum_k C_{ijk}\, X_j(t)\, X_k(t) \tag{5.10}$$

of the model equation (5.1) are replaced by joint-Gaussian random variables without covariance. In the following, we call it the normal nonlinear term approximation (NNA). First, we decompose $X_i(t)$ into

$$X_i(t) = X_i^{(0)}(t) + X_i^{(1)}(t)\,. \tag{5.11}$$

where $X_i^{(0)}$ is governed by (5.1) with the nonlinear terms $\mathcal{N}_i$ replaced by random variables $f_i$ as

$$\frac{\mathrm{d}}{\mathrm{d}t} X_i^{(0)}(t) = f_i(t) - \nu\, X_i^{(0)}(t) + F_i(t)\,, \tag{5.12}$$

and $X_i^{(1)}$ denotes the deviation originating from the replacement. We define $t_0$ as the time when we start this decomposition, i.e.,

$$X_i^{(1)}(t_0) = 0\,. \tag{5.13}$$

In the framework of NNA, we impose the following three assumptions:

**NNA assumption 1** Effective forcing terms $\{f_i | i = 1.2, \cdots, N\}$ are a set of independent random variables with Gaussian distribution.

**NNA assumption 2** Amplitude of $X_i^{(1)}(t)$ $(G_{in}^{(1)}(t|t'))$ is much smaller than that of $X_i^{(0)}(t)$ $(G_{in}^{(0)}(t|t'))$, as long as $t - t_0$ $(t - t')$ is within the order of the time scale of the auto-correlation function of $X_i$.

**NNA assumption 3** Functions $X_i^{(0)}$ and $G_{in}^{(0)}$ are statistically independent of each other.

Here, $G_{in}^{(0)}(t|t')$ and $G_{in}^{(1)}(t|t')$ are defined by (5.16) and (5.20) below. Then, by subtracting (5.12) from (5.1), we obtain the governing equation for $X_i^{(1)}$ as

$$\frac{\mathrm{d}}{\mathrm{d}t} X_i^{(1)}(t) = \sum_j \sum_k C_{ijk}\, X_j^{(0)}(t)\, X_k^{(0)}(t) - f_i(t) - \nu\, X_i^{(1)}(t) \tag{5.14}$$

under NNA assumption 2.

[2] *Response function*

The response functions $G_{in}(t|t')$ and $G^{(0)}_{in}(t|t')$ are respectively defined by

$$G_{in}(t|t') = \frac{\delta X_i(t)}{\delta X_n(t')} \tag{5.15}$$

and

$$G^{(0)}_{in}(t|t') = \frac{\delta X^{(0)}_i(t)}{\delta X^{(0)}_n(t')}\,, \tag{5.16}$$

and are governed by

$$\frac{\partial}{\partial t} G_{in}(t|t') = \sum_j \sum_k 2\, C_{ijk}\, X_j(t)\, G_{kn}(t|t') - \nu\, G_{in}(t|t') \qquad (t > t') \tag{5.17}$$

and

$$\frac{\partial}{\partial t} G^{(0)}_{in}(t|t') = -\nu\, G^{(0)}_{in}(t|t') \qquad (t > t') \tag{5.18}$$

with initial conditions

$$G_{in}(t|t) = G^{(0)}_{in}(t|t) = \delta_{in}\,. \tag{5.19}$$

Then, the governing equation for $G^{(1)}_{in}(t|t')$, defined by

$$G_{in}(t|t') = G^{(0)}_{in}(t|t') + G^{(1)}_{in}(t|t')\,, \tag{5.20}$$

is obtained from (5.17) and (5.18) as

$$\frac{\partial}{\partial t} G^{(1)}_{in}(t|t') = \sum_j \sum_k 2\, C_{ijk}\, X^{(0)}_j(t)\, G^{(0)}_{kn}(t|t') - \nu\, G^{(1)}_{in}(t|t')\,, \tag{5.21}$$

where we have assumed that $|G^{(1)}_{in}| \ll |G^{(0)}_{in}|$ (NNA assumption 2).

By employing $G^{(0)}_{in}(t|t')$ as the Green function, we obtain formal solutions,

$$\begin{aligned} X^{(1)}_i(t) = &\sum_a \sum_b \sum_c \int_{t_0}^{t} \mathrm{d}t'' C_{abc}\, G^{(0)}_{ia}(t|t'')\, X^{(0)}_b(t'')\, X^{(0)}_c(t'') \\ &- \sum_a \int_{t_0}^{t} \mathrm{d}t'' G^{(0)}_{ia}(t|t'')\, f_a(t'') \end{aligned} \tag{5.22}$$

from (5.13), (5.14), (5.18) and (5.19), and

$$G^{(1)}_{in}(t|t') = \sum_a \sum_b \sum_c \int_{t'}^{t} \mathrm{d}t''\, 2\, C_{abc}\, G^{(0)}_{ia}(t|t'')\, X^{(0)}_b(t'')\, G^{(0)}_{cn}(t''|t') \tag{5.23}$$

from (5.18)—(5.21).

## [3] *NNA for correlation functions*

The governing equation for the two-time two-mode correlation function $V_{in}(t,t') = \overline{X_i(t)\,X_n(t')}$ is obtained from (5.1) as

$$\left[\frac{\partial}{\partial t} + \nu\right] V_{in}(t,t') = \sum_j \sum_k C_{ijk}\,\overline{X_j(t)\,X_k(t)\,X_n(t')} \qquad (t > t')\,. \tag{5.24}$$

By substituting the decomposition (5.11) into the nonlinear term of this equation, we obtain under NNA assumption 2 that

$$\begin{aligned}\sum_j \sum_k C_{ijk}\,\overline{X_j(t)\,X_k(t)\,X_n(t')} &= \sum_j \sum_k C_{ijk}\,\overline{X_j^{(0)}(t)\,X_k^{(0)}(t)\,X_n^{(0)}(t')} \\ &\quad + \sum_j \sum_k 2\,C_{ijk}\,\overline{X_j^{(1)}(t)\,X_k^{(0)}(t)\,X_n^{(0)}(t')} \\ &\quad + \sum_j \sum_k C_{ijk}\,\overline{X_j^{(0)}(t)\,X_k^{(0)}(t)\,X_n^{(1)}(t')}\,. \end{aligned} \tag{5.25}$$

The first term of (5.25) vanishes because the solution $X_i^{(0)}$ is expressed, from (5.12), as

$$X_i^{(0)}(t) = \int^t \mathrm{d}t'\, \exp\Big[-\nu\,(t-t')\Big]\,\Big[f_i(t') + F_i(t')\Big], \tag{5.26}$$

and because $\{f_i\}$ and $\{F_i\}$ are Gaussian. Note that $F_i$ can be included into $f_i$ in general, and that the amplitude of $F_i$ is much smaller than that of $f_i$ for high Reynolds-number systems. On the other hand, the second term on the right-hand side of (5.25) is evaluated as

$$\begin{aligned}&\text{(Second term on r.h.s. of (5.25))} \\ &= 2\sum_j\sum_k\sum_a\sum_b\sum_c \int_{t_0}^t \mathrm{d}t''\, C_{abc}\,C_{ijk}\,\overline{G_{ka}^{(0)}(t|t'')\,X_j^{(0)}(t)\,X_n^{(0)}(t')\,X_b^{(0)}(t'')\,X_c^{(0)}(t'')} \\ &\quad - 2\sum_j\sum_k\sum_a \int_{t_0}^t \mathrm{d}t''\, C_{ijk}\,\overline{G_{ka}^{(0)}(t|t'')\,X_j^{(0)}(t)\,X_n^{(0)}(t')}\;\overline{f_a(t'')} \\ &= 2\sum_j\sum_k\sum_a\sum_b\sum_c \int_{t_0}^t \mathrm{d}t''\, C_{abc}\,C_{ijk}\,\overline{G_{ka}^{(0)}(t|t'')\,X_j^{(0)}(t)\,X_n^{(0)}(t')\,X_b^{(0)}(t'')\,X_c^{(0)}(t'')} \\ &= 2\sum_j\sum_k\sum_a\sum_b\sum_c \int_{t_0}^t \mathrm{d}t''\, C_{abc}\,C_{ijk}\,\overline{G_{ka}^{(0)}(t|t'')} \\ &\qquad \times\Big[\;\overline{X_j^{(0)}(t)\,X_n^{(0)}(t')}\;\overline{X_b^{(0)}(t'')\,X_c^{(0)}(t'')} \\ &\qquad\quad + \overline{X_j^{(0)}(t)\,X_b^{(0)}(t'')}\;\overline{X_n^{(0)}(t')\,X_c^{(0)}(t'')} \\ &\qquad\quad + \overline{X_j^{(0)}(t)\,X_c^{(0)}(t'')}\;\overline{X_n^{(0)}(t')\,X_b^{(0)}(t'')}\;\Big] \\ &= 4\sum_j\sum_k \int_{t_0}^t \mathrm{d}t''\, C_{knj}\,C_{ijk}\,\overline{G_{kk}(t|t'')}\,V_{jj}(t,t'')\,V_{nn}(\min\{t',t''\},\max\{t',t''\})\,. \end{aligned} \tag{5.27}$$

Here, we have used condition (5.4) of absence of self-interaction. In a similar manner, we can rewrite the third term as

$$\text{(Third term on r.h.s. of (5.25))} = 2\sum_j\sum_k \int_{t_0}^{t'} \mathrm{d}t''\, C_{njk}\,C_{ijk}\,\overline{G_{nn}(t'|t'')}\;V_{jj}(t,t'')\,V_{kk}(t,t'')\,.$$

(5.28)

Thus, we rewrite the three-mode correlation function on the right-hand side of (5.25) in terms of the two-mode correlation and the response functions, and obtain, from (5.27) and (5.28), that

$$\left[\frac{\partial}{\partial t}+\nu\right] V_{in}(t,t') = 4\sum_j\sum_k \int_{t_0}^{t} \mathrm{d}t''\, C_{knj}\, C_{ijk}\, \overline{G_{kk}(t|t'')}\; V_{jj}(t,t'')\, V_{nn}(\max\{t',t''\},\min\{t',t''\}) + 2\sum_j\sum_k \int_{t_0}^{t'} \mathrm{d}t''\, C_{njk}\, C_{ijk}\, \overline{G_{nn}(t'|t'')}\; V_{jj}(t,t'')\, V_{kk}(t,t'')\,. \tag{5.29}$$

Similarly, the evolution equation for the one-time correlation function,

$$\left[\frac{\mathrm{d}}{\mathrm{d}t}+2\nu\right] V_{in}(t,t) = \sum_j\sum_k C_{ijk}\,\overline{X_j(t)\,X_k(t)\,X_n(t)} + \overline{F_i(t)\,X_n(t)} + \;(i\leftrightarrow n) \tag{5.30}$$

is rewritten under NNA as

$$\left[\frac{\mathrm{d}}{\mathrm{d}t}+2\nu\right] V_{in}(t,t) = 4\sum_j\sum_k \int_{t_0}^{t} \mathrm{d}t'\, C_{knj}\, C_{ijk}\, \overline{G_{kk}(t|t')}\; V_{jj}(t,t')\, V_{nn}(t,t') + 2\sum_j\sum_k \int_{t_0}^{t} \mathrm{d}t'\, C_{njk}\, C_{ijk}\, \overline{G_{nn}(t|t')}\; V_{jj}(t,t')\, V_{kk}(t,t') + \frac{\nu}{N}\,\delta_{in} + (i\leftrightarrow n)\,. \tag{5.31}$$

### [4] *NNA for response function*

The ensemble average of the response function is governed by

$$\frac{\partial}{\partial t}\,\overline{G_{in}(t|t')} = \sum_j\sum_k 2\,C_{ijk}\,\overline{X_j(t)\,G_{kn}(t|t')} - \nu\,\overline{G_{in}(t|t')}\,, \tag{5.32}$$

the nonlinear term of which is rewritten by substituting the decompositions (5.11) and (5.20) as

$$2\sum_j\sum_k C_{ijk}\,\overline{X_j(t)\,G_{kn}(t|t')} = 2\sum_j\sum_k C_{ijk}\,\overline{X_j^{(0)}(t)\,G_{kn}^{(0)}(t|t')} + 2\sum_j\sum_k C_{ijk}\,\overline{X_j^{(1)}(t)\,G_{kn}^{(0)}(t|t')} + 2\sum_j\sum_k C_{ijk}\,\overline{X_j^{(0)}(t)\,G_{kn}^{(1)}(t|t')}\,, \tag{5.33}$$

where we have neglected the higher order term $\sum_{j,k} C_{ijk}\overline{X_j^{(1)}G_{kn}^{(1)}}$ (NNA assumption 2). Then, by using the solutions (5.26) and (5.22) of $X_i^{(0)}$ and $X_i^{(1)}$, it is shown that both the first and the second

terms of (5.33) vanish under NNA assumptions 1 and 3. The third term is evaluated, from (5.23), as

$$\begin{aligned}
&\text{(Third term on r.h.s. of (5.33))} \\
&= 4 \sum_j \sum_k \sum_a \sum_b \sum_c \int_{t'}^{t} \mathrm{d}t''\, C_{ijk}\, C_{abc}\, \overline{X_j^{(0)}(t)\, G_{ka}^{(0)}(t|t'')\, X_b^{(0)}(t'')\, G_{cn}^{(0)}(t''|t')} \\
&= 4 \sum_j \sum_k \int_{t'}^{t} \mathrm{d}t''\, C_{ijk}\, C_{kjn}\, \overline{X_j^{(0)}(t)\, X_j^{(0)}(t'')}\ \overline{G_{kk}^{(0)}(t|t'')}\ \overline{G_{nn}^{(0)}(t''|t')} \\
&= 4 \sum_j \sum_k \int_{t'}^{t} \mathrm{d}t''\, C_{ijk}\, C_{knj}\, V_{jj}(t,t'')\, \overline{G_{kk}(t|t'')}\ \overline{G_{nn}(t''|t')}\,. \qquad (5.34)
\end{aligned}$$

Hence, we obtain

$$\left[\frac{\partial}{\partial t} + \nu\right] \overline{G_{in}(t|t')} = 4 \sum_j \sum_k \int_{t'}^{t} \mathrm{d}t''\, C_{ijk}\, C_{knj}\, V_{jj}(t,t'')\, \overline{G_{kk}(t|t'')}\ \overline{G_{nn}(t''|t')}\,. \qquad (5.35)$$

Equations (5.29), (5.31) and (5.35) constitute a closed set of equations for the two-mode correlation and the response functions. Note that this closure equations are identical to the DIA-RRE equations (2.63), (2.64) and (2.67), which are equivalent to (2.26), (2.28) and (2.32).

### 5.4.2 Similarity between RRE and NNA

It can be seen that the formulation of NNA in the preceding subsection is quite similar to that of RRE in §2.4. In Table 5.1, similarities of RRE and NNA are summarized. Only a mathematical difference is the effective random forcing term $f_i$ appearing in the evolution equations for $X_i^{(0)}$ and $X_i^{(1)}$, and then in the formal solution of $X_i^{(1)}$ (see equations (5.12)(5.14)(5.22)). Since the equation for $X_i^{(0)}$ is only used to justify the Gaussianity of the distribution function of $X_i^{(0)}$ by (5.26), the existence of $f_i$ in the equation does not affect the closure formulation at all. Furthermore, the contribution from $f_i$ in the equation and the formal solution of $X_i^{(1)}$ vanishes by taking an ensemble average (see a paragraph below (5.27), for example).

The RRE described in §2.4 is a Reynolds-number expansion, in which the nonlinear term is treated as a perturbation. On the other hand, in the framework of NNA, the nonlinear term is never dealt with as a perturbation. A reason why, in spite of this great difference, their formulations are mathematically very similar may be due to the fact that the equations for $X_i^{(0)}$ are used only implicitly. In concluding remarks in this chapter, we shall discuss this issue in somewhat detail.

Anyway, since the formulations of RRE and NNA are quite similar from a mathematical point of view, we suggest that RRE should be regarded as NNA. Otherwise, we cannot understand why RRE is applicable to systems at large Reynolds numbers.

### 5.4.3 Joint-Gaussianity of the nonlinear terms

If the nonlinear couplings are weak and the number of degree of freedom is large, then the nonlinear term which consists of a sum of random variables may obey a Gaussian distribution according to the

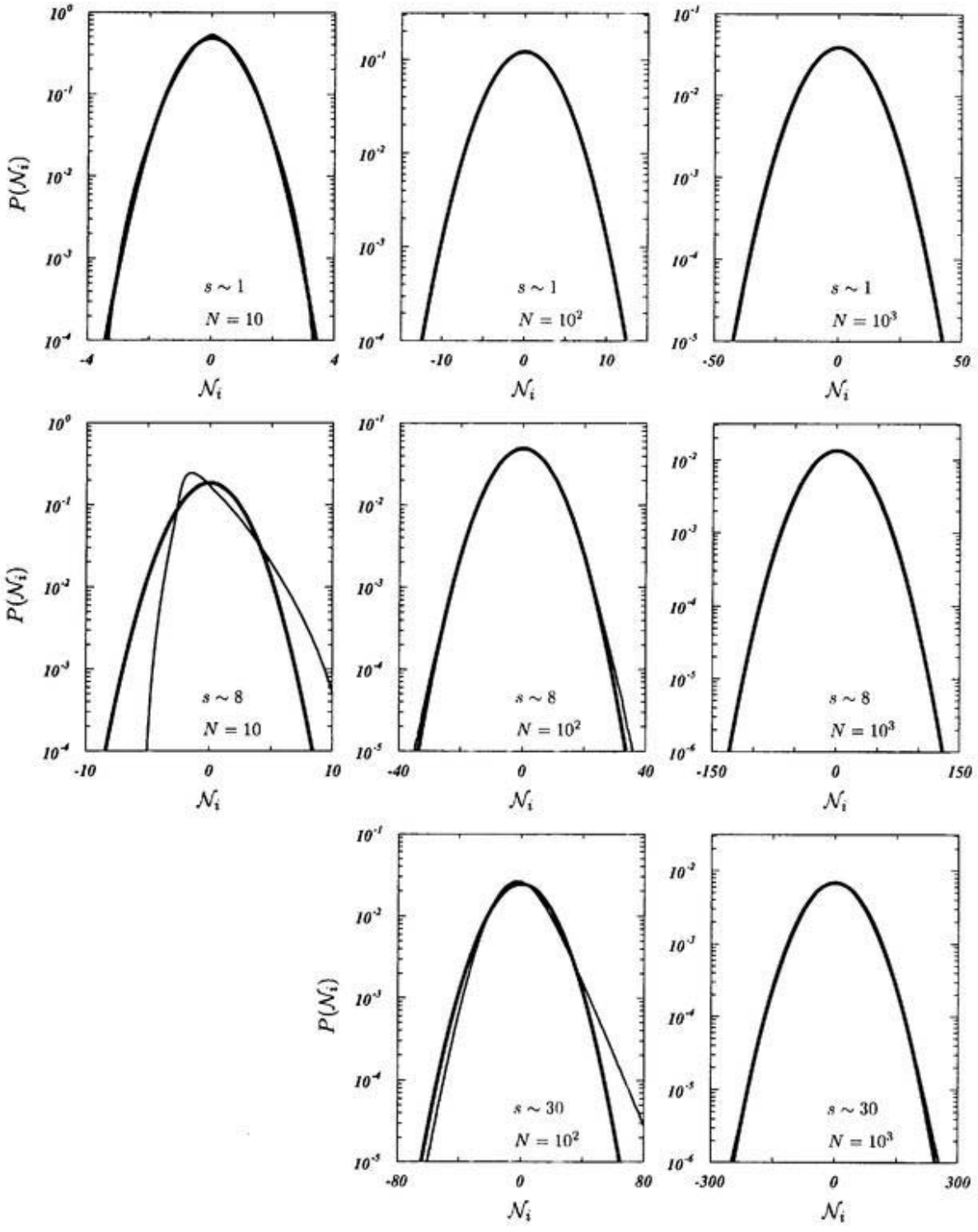


FIGURE 5.5 Probability density function of the nonlinear term $\mathcal{N}_i$ of the model equation (5.1) evaluated by the direct numerical integration of the equation (thin solid lines). Results for various combinations of the number $N$ of degrees of freedom and the strength $s$ of nonlinear couplings are shown. Thick solid lines denote the Gaussian distribution with zero mean and the same variance as the numerical results. As $N$ increases or $s$ decreases, the probability density of the nonlinear term tends to a Gaussian distribution.

| | RRE | NNA | difference |
|---|---|---|---|
| Equation for $X_i^{(0)}$ | (2.41) | (5.12) | effective forcing term $f_i$ |
| $X_i^{(1)}$ | (2.43) | (5.14) | effective forcing term $f_i$ |
| $G_{in}^{(0)}$ | (2.42) | (5.18) | |
| $G_{in}^{(1)}$ | (2.44) | (5.21) | |
| Formal solution of $X_i^{(1)}$ | (2.47) | (5.22) | term originating from $f_i$ |
| $G_{in}^{(1)}$ | (2.48) | (5.23) | |
| Closure equation for $V_{in}(t,t')$ | (2.63) | (5.29) | |
| $V_{in}(t,t)$ | (2.64) | (5.31) | |
| $G_{in}(t\|t')$ | (2.67) | (5.35) | |

TABLE 5.1 Similarity between RRE and NNA.

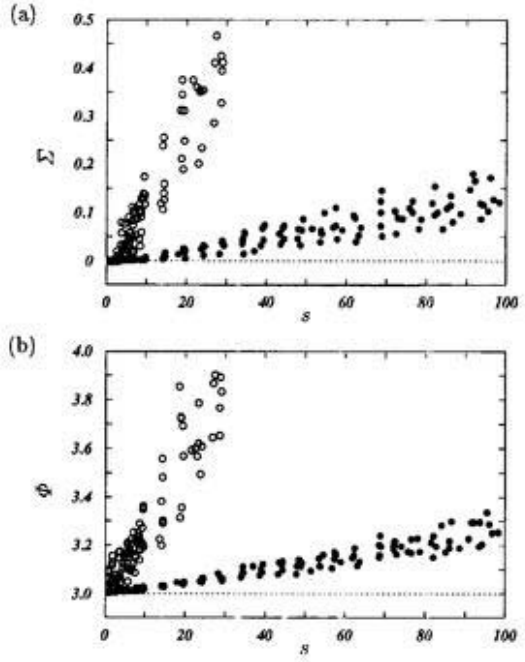


FIGURE 5.6 (a) Skewness factor $\Sigma$ and (b) flatness factor $\Phi$ of the nonlinear terms $\mathcal{N}_i$ of model equation (5.1). The horizontal axis denotes the strength of nonlinear couplings. Open circles for $N$ (the number of degree of freedom) = 100, solid circles for $N = 1000$. $\Sigma = 0$ and $\Phi = 3$ correspond to the Gaussian distribution.

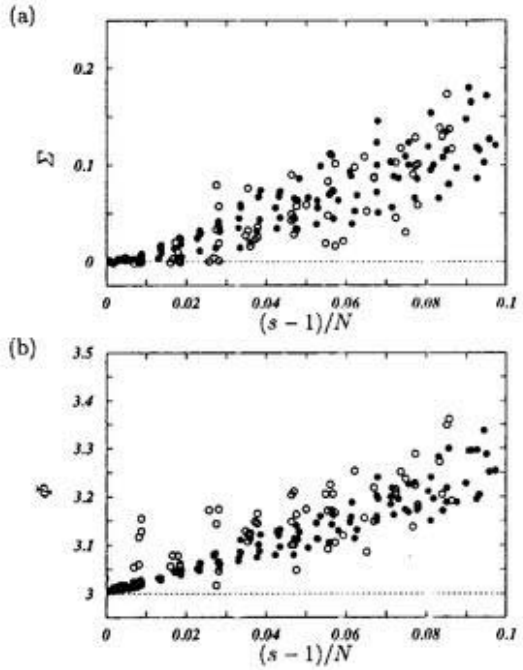


FIGURE 5.7 Same as Fig.5.6. The strength $s$ of nonlinear couplings is normalized by the number of degrees of freedom.

central limit theorem. Indeed, Fig.5.5 supports this conjecture that the probability density function of the nonlinear term is nearly Gaussian for small $s$ or large $N$. For quantitative estimations of Gaussianity, we define the skewness factor $\Sigma$ of the nonlinear term by

$$\Sigma = \frac{\overline{\mathcal{N}_i^3}}{\left(\overline{\mathcal{N}_i^2}\right)^{3/2}}, \tag{5.36}$$

which vanishes for a Gaussian distribution, and the flatness factor $\Phi$ by

$$\Phi = \frac{\overline{\mathcal{N}_i^4}}{\left(\overline{\mathcal{N}_i^2}\right)^2}, \tag{5.37}$$

which is equal to three for a Gaussian. These factors evaluated numerically are plotted in Fig.5.6. These figures suggest that as the number of degrees of freedom increases or the nonlinear couplings get weaker, the probability density tends to a Gaussian distribution.

The parameters $s$ and $N$ examined in Fig.5.6 are the same as in Fig.5.2. It is likely that the deviation of the distribution function of the nonlinear term from the Gaussian corresponds to the deviation of prediction of correlation function by the DIA-RRE(-NNA) equations. However, we should not jump to such a conclusion. We replot the skewness and the flatness factors of $\mathcal{N}_i$ against the strength of nonlinear couplings divided by the number of degrees of freedom in Fig.5.7. This figure tells us that the deviation of the distribution function of $\mathcal{N}_i$ from the Gaussian is a function of $s/N$ rather than $s/N^{1/2}$. Recall that $\Delta$, which denotes the deviation of the prediction of the correlation function by the DIA-RRE(-NNA) equations, is a function of $s/N^{1/2}$ (see Fig.5.4(c)). This scaling $s/N$ is explained as follows. The central limit theorem, due to which the Gaussianity of the distribution

function of $\mathcal{N}_i$ is expected, requires that the summands of the nonlinear term (5.10) are independent of each other. We assume that the dependency between two terms,

$$C_{ij_1k_1} X_{j_1} X_{k_1} \quad \text{and} \quad C_{ij_2k_2} X_{j_2} X_{k_2} ,$$

is produced by direct interactions between $X_{j_1}$, $X_{k_1}$, $X_{j_2}$ and $X_{k_2}$. The probability $p_1$ that there exists one of direct interactions shown in Fig.5.8(a) between them may be evaluated as

$$p_1 = \begin{cases} 0 & (s \leq 1) , \\ \dfrac{4(s-1)}{N} & (1 \leq s) \end{cases} \tag{5.38}$$

for a system with a large number of degrees of freedom. Similarly, the probability $p_2$ that there are two direct interactions between them (Fig.5.8(b)) is

$$p_2 = \begin{cases} 0 & (s \leq 1) , \\ \dfrac{4(s-1)^2}{N^2} & (1 \leq s \leq 2) , \\ \dfrac{2(s-1)(3s-4)}{N^2} & (2 \leq s) \end{cases} \tag{5.39}$$

for $N \gg 1$. It has been checked that the probability of the existence of the direct interactions evaluated by the use of the coefficients $C_{ijk}$ adopted in the numerical calculations are well approximated by (5.38) and (5.39) for $N = 10^2$ and $10^3$ (figures are omitted). Furthermore, the probabilities of the existence of three and four direct interactions between them are $p_3 = O\left((s/N)^3\right)$ and $p_4 = O\left((s/N)^4\right)$ respectively, which are much smaller than $p_1$ for large $N$. If $p_i$ $(i = 1, 2, 3, 4)$ is much smaller than unity, then the distribution function of the nonlinear term $\mathcal{N}_i$ may well approximated by a Gaussian. This is the reason why the skewness and flatness factors of the distribution function are functions of $s/N$.

The condition, $s \ll N$, that probability density function of $\mathcal{N}_i$ is approximated by a Gaussian is much weaker than validity condition, $s \ll N^{1/2}$ of the DIA-RRE(-NNA) equations. This is reasonable because NNA assumption 1 requires that the joint-probability distribution function of the set $\mathcal{N}_i$ is a joint-Gaussian with zero covariance. In other words, the nonlinear terms $\mathcal{N}_i$ and $\mathcal{N}_{i'}$ $(i \neq i')$ must be statistically independent of each other. By estimating the correlation of nonlinear terms, we may explain why the DIA-RRE(-NNA) equations give good approximations when $s \ll N^{1/2}$ (see Ref. [91]).

## 5.5 Concluding remarks

From a viewpoint of the strength of nonlinear couplings we have considered two problems, the validity of DIA for stronger nonlinear coupling systems, and an alternative explanation of RRE.

First, we have introduced the strength $s$ of nonlinear couplings, which represents the average number of direct interactions between a pair of modes, and further investigated the validity conditions of DIA, the largeness of the number $N$ of degrees of freedom and the weakness of nonlinear couplings.

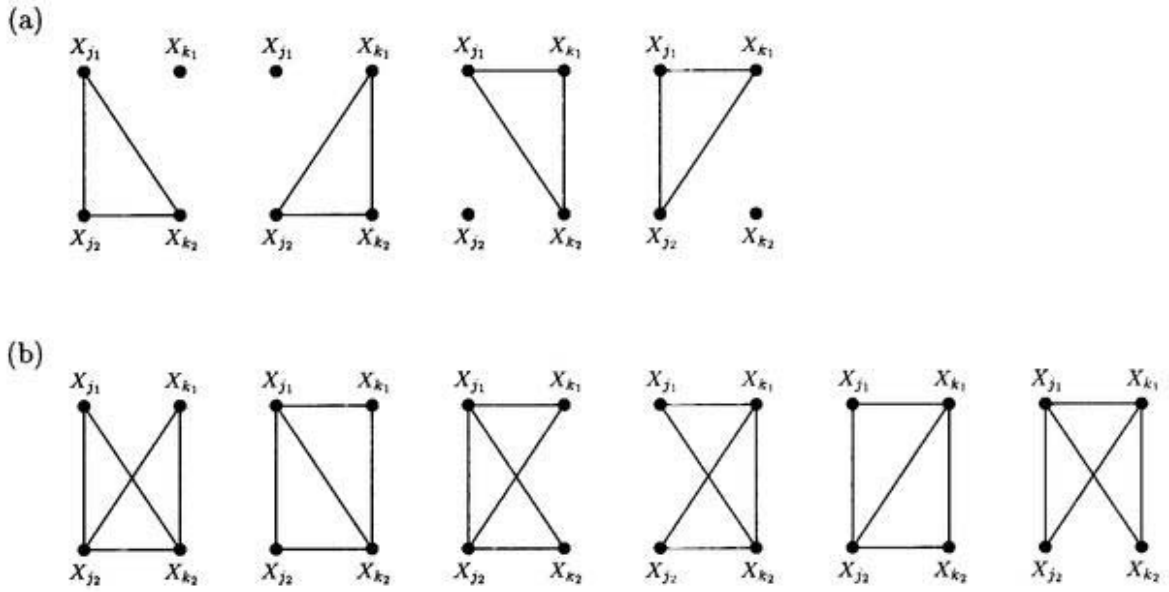


FIGURE 5.8 Direct interactions between four modes $X_{j_1}$, $X_{k_1}$, $X_{j_2}$ and $X_{k_2}$. (a) One and (b) two direct interactions.

By a simple argument based on a relationship between the existence of four-mode indirect interactions between a triplet of modes and a correlation between them, it is shown that DIA is valid for $s \ll N^{1/2}$. This is consistent with deviations, shown in Fig.5.4, of the auto-correlation function by the DIA-RRE equations from the results of direct numerical simulation of the model equation.

Next, we have considered the problem why the DIA-*RRE* equations, which are derived for small Reynolds-number systems in the framework of RRE, are applicable to large Reynolds-number systems if the condition $s \ll N^{1/2}$ is satisfied. The joint-Gaussianity of the set of nonlinear terms is a key. If the nonlinear couplings between the modes $X_i$ are weak, the nonlinear term $\mathcal{N}_i$ is regarded as a sum of independent random variables. Then, according to the central limit theorem, the distribution function of the nonlinear term is nearly Gaussian if $N$ is large. Furthermore, in such systems, a correlation between the nonlinear terms is also expected to be small. It is emphasized that the formulation of RRE is almost identical to that of NNA in which the nonlinear terms are replaced by independent Gaussian random variables. This is a reason why the equations by RRE are valid for large Reynolds-number systems with weak nonlinear couplings and a large number of degrees of freedom.

Let us further consider a relationship between RRE and NNA. [1] The evolution equations of the zeroth order variable $X_i^{(0)}$ are expressed in RRE as

$$\frac{\mathrm{d}}{\mathrm{d}t} X_i^{(0)}(t) = -\nu X_i^{(0)}(t) + F_i(t) \qquad \text{(RRE, see (2.41))}\,,$$

where the nonlinear term is neglected and the external force should exist to prevent the system from

[1] Please sift four letters in the alphabetical order.

an exponential decay by the viscous term. On the other hand, in NNA, it is

$$\frac{\mathrm{d}}{\mathrm{d}t} X_i^{(0)}(t) = f_i(t) - \nu X_i^{(0)}(t) \qquad \text{(NNA, see (5.12))}\,,$$

where the nonlinear term is replaced by an effective random forcing and the external forcing is included into $f_i$. We can see that, in both approximations, the evolution equation takes a form like

$$\text{(time derivative term)} = \text{(random forcing term)} - \text{(dissipative term)}\,. \tag{5.40}$$

The origin of random forcing is, however, completely different. Let us consider a variable $z$ defined by

$$z = \frac{\mathcal{R}}{\sqrt{N}} \sum_{i=1}^{N} x_i + f\,, \tag{5.41}$$

where $\{x_i | i = 1, 2, \cdots, N\}$ is a set of random variables with finite variances and vanishing covariances, and $f$ is a Gaussian random variable. There are two parameters $\mathcal{R}$ and $N$ similarly to the system we have considered. Probability density function of the variable $z$ is well approximated to be Gaussian distribution in the cases that $\mathcal{R}$ is small or $N$ is large. The former corresponds to RRE, and the latter to NNA. In statistical theories for strong nonlinear systems, e.g., turbulence, it is meaningless to treat the nonlinear term as a perturbation as done in RRE. Hence, in this sense, RRE should be explained as NNA, when we apply it to strong nonlinearity systems.

Finally, we mention a relation between NNA and DIA. As shown in this chapter, these two approximations have the same validity conditions, i.e., weakness of nonlinear couplings and largeness of degrees of freedom, and they yield an identical set of equations for the two-mode correlation and the response function of the model system (5.1). However, this does not necessarily imply that DIA and NNA are identical as approximation. First of all, these two are based on different working assumptions described in §2.3 for DIA, and in §5.4 for NNA. Furthermore, in general, DIA and NNA lead different closure equations for some systems, for example the model system (5.1) without the condition (5.4) of the absence of self-interaction. Details of this point will be seen elsewhere in the near future.

# Chapter 6

# Concluding Remarks

## 6.1 Summary

In Chapter 2, we introduced a model equation the mathematical structures of which were similar to those of the Navier-Stokes equation, namely, quadratic nonlinear term with weak nonlinear couplings and linear dissipative term. We formulated the direct-interaction approximation (DIA) and the Reynolds-number reversed expansion (RRE) for this model system. By comparing numerically solutions to the resultant closure equations by these two approximations and to the model equation itself, we obtained the following results.

1. The DIA is applicable to systems with weak nonlinear couplings and a large number of degrees of freedom.
2. The two approximations, DIA and RRE, should be distinguished, although they yield an identical set of equations for the two-mode correlation and the response functions of this model system. They are based upon completely different ideas and working assumptions, and therefore have different validity conditions and applicability.

In Chapter 3, we applied DIA to the Lagrangian velocity correlation and the Lagrangian velocity response functions of incompressible fluid turbulence which was assumed to be governed by the Navier-Stokes equation. Then, we obtained the following results.

1. The resultant closure equations for the correlation and the response functions are identical to those by the Lagrangian renormalized approximation [36], which is a kind of RRE.
2. A solution to the closure equations derived by the Lagrangian DIA is consistent with the $k^{-3/5}$ law of the energy spectrum $E(k)$ predicted by Kolmogorov's phenomenology [1].

3. The universal form of the energy spectrum, which is common both in stationary and in freely decaying cases, numerically evaluated by the closure equations is in an excellent agreement with measurements (see Fig.1.1).

4. The skewness factor of the velocity derivative, which is a third order moment, is also consistent with experimental data [53].

5. By evaluating the energy transfer and the flux functions in the wavenumber space, it is shown that although strong nonlocal interactions are observed, the energy transfer takes place locally in the wavenumber space. This is consistent with the results by direct numerical simulations [4].

6. Wavenumber dependence of eddy viscosity, which is a basis of a turbulent model so-called the large-eddy simulation, was determined.

7. In the framework of the Lagrangian DIA, the Birkhoff [38] invariance of large-scale structures of turbulence is valid, but the Loitsiansky [39] is not.

In Chapter 4, we formulated the Lagrangian DIA for a passive scalar field advected by homogeneous turbulence. By examining analytically and numerically solutions to the resultant closure equations by the Lagrangian DIA, we obtained the following results.

1. The solutions to the closure equations are completely consistent with the well-known phenomenologies on the passive scalar spectrum by Obukhov [64] and Corrsin [65] in the inertial-advective range, Batchelor, Howells & Townsend [66] in the inertial-diffusive range, and Batchelor [67] in the viscous-advective range.

2. The functional forms of the passive scalar spectrum over the entire universal range are determined numerically for several moderate, and two extreme Schmidt numbers.

3. Schmidt number dependence of mixed-derivative skewness factor of the passive scalar and the velocity fields is evaluated, which is also consistent with a direct numerical simulation by Kerr [68].

In Chapter 5, we extended the model equation introduced in Chapter 2. By the use of this model equation, we further investigated validity conditions of DIA and relationships between DIA and RRE from a viewpoint of strength of nonlinear couplings. Then, we obtained the following results.

1. The DIA is valid if the average number of the direct interactions between a pair of modes is much smaller than the square root of the number of degrees of freedom.

2. The RRE may be regarded as an approximation, called the normal nonlinear term approximation (NNA), of a replacement of the set of nonlinear terms by joint-Gaussian random variables without covariance.

3. The NNA has the same validity condition as DIA, i.e., the weakness of nonlinear couplings and the largeness of the number of degrees of freedom. This result together with the above 2. is consistent with the fact that DIA and RRE-NNA yield identical closure equations for this model system.

## 6.2 Conclusion

The DIA is an appropriate approximation for strong nonlinear systems. This approximation is valid if the number of degrees of freedom is large enough, and if the strength of nonlinear couplings is weak. Fortunately, these two conditions are well satisfied by high Reynolds-number homogeneous turbulence of incompressible fluids governed by the Navier-Stokes equation. Actually, the applications of DIA to the Navier-Stokes turbulence by the use of Lagrangian variables are extremely successful.

## 6.3 Future works

[1] Check of Lagrangian DIA assumptions

The DIA is formulated under two assumptions described in §2.3.1. Validity conditions of them have been checked by the use of the model equation (2.1) in detail in Chapters 2 and 5. However, recall that we have to impose an additional assumption of statistical independency between the position function and the other Eulerian quantities in the formulation of the Lagrangian DIA for actual turbulent fields (see §§3.3.2 and 4.3.2). This third assumption is introduced only for simplification of the formulation, and there seems to be no physical or mathematical reason to justify it.

On the other hand, as shown in Chapter 4, quantitative estimations by the Lagrangian DIA of the statistical properties of passive scalar in the advective range are not necessarily satisfiable. The universal constants $C_1$ and $C_2$ in (4.8) and (4.10) of the passive scalar spectrum in the inertial- and viscous-advective ranges are evaluated as about a half of experimental data. In the advective range, the molecular diffusion is ineffective comparing with the turbulent advection. Note that the governing equation (3.21) for the passive scalar with neglecting the molecular diffusivity, $\kappa \to 0$, is exactly identical to the evolution equation (4.17) for the position function. Hence, the failure of the estimation of the universal constants in the advective range may be caused by the third assumption of the statistical independency between the position function and the other quantities including the passive scalar field.

We have not yet checked the validity of not only the third assumption but also the first and the second ones for the Navier-Stokes system. A systematic check of the Lagrangian DIA assumptions is one of the most important future works because such a study may lead to an improvement of the approximation. However, since there are many kinds of triplets of wavenumbers in contrast with the case of the model equation, such a systematic consideration is not easy to achieve, even though it may be relatively easy to construct the non-direct-interaction field by direct numerical simulations by the use of a spectral method.

### [2] Eulerian and Lagrangian formulations

As shown in Chapters 3 and 4, the applications of DIA to the Lagrangian correlation and the Lagrangian response functions are quite successful. It is well known, however, that the application of DIA to the Eulerian correlation and the Eulerian response functions meets with failure that it predicts the energy spectrum to be proportional to the $-3/2$ power of the wavenumber in the inertial range.

This misprediction of behavior of the energy spectrum by the Eulerian DIA is sometimes understood from the viewpoint of time scale of correlation functions. Time scale of the Eulerian velocity correlation function in the inertial range may be estimated as $\tau_{\rm E} = (u_m k)^{-1}$, which is the sweeping time scale of eddies of the length scale $k^{-1}$ by large-scale motions with characteristic velocity $u_m$, while that of the Lagrangian correlation function may be $\tau_{\rm L} = k^{-2/3}\epsilon^{-1/3}$, which is the eddy turnover time at scale $k^{-1}$. The energy equation by DIA gives $\epsilon \sim k^4 E(k)^2 \tau$ (see (3.84) with (3.74) in the present formulation). Then, we obtain the $k^{-5/3}$ spectrum by putting $\tau = \tau_{\rm L}$, but $k^{-3/2}$ by $\tau = \tau_{\rm E}$. However, this is only an explanation of the reason why the Eulerian DIA predicts $k^{-2/3}$ energy spectrum in the inertial range, and is not a reason why Eulerian formulation is inappropriate. In addition, McComb et al. [45] numerically showed that time scale of Eulerian velocity correlation function evaluated by the Eulerian DIA equations was the inertial time scale $k^{-2/3}\epsilon^{-1/3}$ rather than the sweeping time $(u_m k)^{-1}$.

Kraichnan [37, 92] introduced the notion of random Galilean invariance in order to explain this Eulerian-Lagrangian problem. Although the Navier-Stokes equation and closure equations derived by Lagrangian versions of DIA, e.g., the LRA-DIA equations, satisfy this invariance, the Eulerian DIA equations do not. McComb et al. [45] showed, however, that the random Galilean invariance was too strong, and it was inconsistent with ergodicity. Moreover, even though the Eulerian DIA equations are not random Galilean invariant, they are Galilean invariant in the usual sense. Thus, it is not easy to understand why the Eulerian formulation is inappropriate from the viewpoint of Galilean invariance.

The Lagrangian formulation seems to be just pragmatic at the present. We should understand why Lagrangian formulations are more appropriate than Eulerian ones before developing the Lagrangian closures further.

### [3] Higher-order moments and intermittency

Since §1.2, we have focused only on lower-order moments of the probability density function such as mean velocity or the two-point velocity correlation function. However, we have to confess that the main result that we obtain in this thesis is just to bridge the Navier-Stokes equation and the excellent phenomenology by Kolmogorov [1] in fifty years ago, which properly predicts the behavior of the second order moment of velocity in the inertial range by a simple argument.

Kolmogorov's phenomenology is not applicable to higher-order moments. In his theory, statistical properties of inertial-scale turbulence are characterized only by the mean dissipation rate of energy

per unit mass. However, it is pointed out by Landau [93] that strong energy dissipation takes place in small regions, and this (spatial) intermittency of turbulence (see Chapter 8 of Ref. [21]) is widely supported by measurements [94, 95] and direct numerical simulations [96]. This intermittency of turbulence implies that large deviations from the average occurs with relatively large probability, in other words, the probability density function of the energy dissipation rate has long tails. Hence, the Kolmogorov theory, which can be regarded as a kind of mean field theory, may not be able to predict appropriately the behavior of higher-order moments, which is more significantly affected by the long tails of the distribution function. Indeed, measurements by Anselmet et al. [95] exhibit deviations of exponents of the higher-order velocity structure functions predicted by a naive extension of the Kolmogorov theory.

Then, in order to evaluate the behavior of higher-order moments, we have to take spatial distribution of the energy dissipation rate into account. Kolmogorov [97] introduced locally averaged energy dissipation rate $\epsilon_r$ in a sphere of radius $r$, and considering the effect of intermittency to higher-order moments by assuming that the probability density of $\epsilon_r/\epsilon_{r'}$ is a log-normal distribution. However, it has been pointed out [98–100] that this phenomenological theory has some problems. Since this log-normal theory, a numerous number of theories, e.g., an extension of the log-normal theory from the viewpoint of the central limit theorem [101], $\beta$-models [102,103] based upon the cascade picture, multifractal models based on the scale invariance of turbulence [104–106], the log-Poisson model [107,108] constructed under a reasonable assumption that the most singular structure is filament, etc., have been proposed. However, all of these are based upon ad hoc assumptions, and except the log-Poisson model, they have one or more adjustable parameters.

On the other hand, although there are a few analytical theories, e.g., the mapping closure approximation [109,110], to deal with the higher-order moments or the distribution function itself, they are controversial. Incidentally, in the present formulation of DIA, we do not treat effects of intermittency at all.

Both phenomenology and analytical theory based on the Navier-Stokes equation on the higher-order moments or the probability density function are not conclusive up to the present. This problem is one of the most interesting and challenging problems in the statistical theory of *isotropic* turbulence. —— Finally, we, theorists of turbulence, must not forget that our theories cannot predict even the mean velocity profile of turbulence of an incompressible fluid in a pipe.

## Acknowledgements

I would like to thank Prof. Shigeo Kida for inviting me to the turbulent world, and for guiding me with great patience.

Great thanks are due to all researchers and students, friends, my parents and sister who have provided comments on my study, discussed various topics with me, encouraged and supported me in both study and day-to-day lives in Kyoto and Toki.

# References


[1] A. N. Kolmogorov, "The local structure of turbulence in incompressible viscous fluid for very large Reynolds numbers," Dokl. Akad. Nauk SSSR **30,** 301–305 (1941), English translation in Proc. R. Soc. London, Ser.A **434**, 9–13 (1991).

[2] G. I. Taylor, "Statistical theory of turbulence," Proc. Roy. Soc. A **151,** 421–444 (1935).

[3] G. I. Taylor, "Statistical theory of turbulence II," Proc. Roy. Soc. A **151,** 444–454 (1935).

[4] K. Ohkitani and S. Kida, "Triad interactions in a forced turbulence," Phys. Fluids A **4,** 794–802 (1992).

[5] E. Hopf, "Statistical hydrodynamics and functional calculus," J. Ratl. Mech. Anal. **1,** 87–123 (1952).

[6] M. Millionshtchikov, "On the theory of homogeneous isotropic turbulence," Dokl. Akad. Nauk SSSR **32,** 615–618 (1941).

[7] I. Proudman and W. H. Reid, "On the decay of normally distributed and homogeneous turbulent velocity fields," Phil. Trans. Roy. Soc. A **247,** 163 189 (1954).

[8] T. Tatsumi, "The theory of decay process of incompressible isotropic turbulence," Proc. Roy. Soc. A **239,** 16-45 (1957).

[9] Y. Ogura, "A consequence of the zero-fourth-cumulant approximation in the decay of isotropic turbulence," J. Fluid Mech. **16,** 38–41 (1963).

[10] T. Tatsumi, S. Kida, and J. Mizushima, "The multiple-scale cumulant expansion for isotropic turbulence," J. Fluid Mech. **85,** 97–142 (1978).

[11] U. Frisch, M. Lesieur, and D. Schertzer, "Comments on the quasi-normal Markovian approximation for fully-developed turbulence," J. Fluid Mech. **97,** 181–192 (1980).

[12] S. A. Orszag, "Statistical theory of turbulence," In *Fluid Dynamics* Les Houches 1973, R. Balian and J. L. Peube, eds., pp. 237–374 (Gordon and Breach, New York, 1977).

[13] H. Lamb, *Hydrodynamics, (sixth edition)* (Dover, New York, 1932).

[14] G. K. Batchelor, *An introduction to fluid dynamics* (Cambridge Univ. Press., 1967).

[15] G. K. Batchelor, *The theory of homogeneous turbulence* (Cambridge Univ. Press., 1953).

[16] von J. C. Rotta, *Turbulente Strömungen* (B. G. Teubner, Stuttgart, 1972).

[17] H. Tennekes and J. L. Lumley, *A First Course in Turbulence* (M.I.T. Press, Cambridge, Mass., 1972).

[18] D. C. Leslie, *Developments in the theory of turbulence* (Clarendon Press, Oxford, 1973).

[19] A. S. Moin and A. M. Yaglom, *Statistical fluid mechanics, Vol. 2* (MIT press, Cambridge, Massachusetts, 1975).

[20] W. D. McComb, *The physics of fluid turbulence* (Oxford Univ. Press, 1990).

[21] U. Frisch, *Turbulence, The Legacy of A. N. Kolmogorov* (Cambridge Univ. Press., 1995).

[22] M. Lesieur, *Turbulence in Fluids, third revised and enlarged edition* (Kluwer, 1997).

[23] K. R. Sreenivasan and P. J. Strykowski, "On analogies between turbulence in open flows and chaotic dynamical systems," In *Turbulence and chaotic phenomena in fluids*, T. Tatsumi, ed., pp. 191–196 (Elsevier Science Publishers B. V., North-Holland, 1984).

[24] R. H. Kraichnan, "The structure of isotropic turbulence at very high Reynolds number," J. Fluid Mech. **5,** 497–543 (1959).

[25] R. H. Kraichnan, "Eulerian and Lagrangian renormalization in turbulence theory," J. Fluid Mech. **83,** 349–374 (1977).

[26] J. H. W. Wyld, "Formulation of the theory of turbulence in an incompressible fluid," Ann. Phys., N.Y. **14,** 143–165 (1961).

[27] P. C. Martin, E. D. Siggia, and H. A. Rose, "Statistical dynamics of classical systems," Phys. Rev. A **8,** 423–437 (1973).

[28] R. H. Kraichnan, "Dynamics of nonlinear stochastic systems," J. Math. Phys **2,** 124–148 (1961).

[29] J. R. Herring and R. H. Kraichnan, "Comparison of some approximations for isotropic turbulence," In *Statistical models and turbulence*, M. Rosenblatt and C. V. Atta, eds., pp. 148–194 (Springer Verlog, 1972).

[30] U. Frisch, M. Lesieur, and A. Brissaud, "A Markovian random coupling model for turbulence," J. Fluid Mech. **65,** 145–152 (1974).

[31] C.-Y. Mou and P. B. Weichman, "Spherical model for turbulence," Phys. Rev. Lett. **70,** 1101–1104 (1993).

[32] G. I. Eyink, "Large-$N$ limit of the "spherical model" of turbulence," Phys. Rev. E **49,** 3990–4002 (1994).

[33] R. Betchov, "Introduction to the Kraichnan theory of turbulence," In *Dynamics of Fluids and Plasmas*, S. I. Pai, ed., pp. 215–237 (Academic Press, New York, 1966).

[34] S. Goto and S. Kida, "Direct-interaction approximation and Reynolds-number reversed expansion for a dynamical system," Physica D **117,** 191–214 (1998).

[35] S. Kida and S. Goto, "A Lagrangian direct-interaction approximation for homogeneous isotropic turbulence," J. Fluid Mech. **345,** 307–346 (1997).

[36] Y. Kaneda, "Renormalized expansions in the theory of turbulence with the use of the Lagrangian position function," J. Fluid Mech. **107,** 131–145 (1981).

[37] R. H. Kraichnan, "Lagrangian-history closure approximation for turbulence," Phys. Fluids **8,** 575–598 (1965), (erratum 1966, *ibid.*, 1884).

[38] G. Birkhoff, "Fourier synthesis of homogeneous turbulence," Comm. Pure Appl. Math. **7,** 19–44 (1954).

[39] L. G. Loitsiansky, "Some basic laws of isotropic turbulent flow," Rep. Cent. Aero-Hedrodyn. Inst., Moscow 440 (1939).

[40] K. R. Sreenivasan, "On the universality of the Kolmogorov constant," Phys. Fluids **7,** 2778–2784 (1995).

[41] T. von Kármán and L. Howarth, "On the statistical theory of isotropic turbulence," Proc. Roy. Soc. London A **164,** 192–215 (1938).

[42] G. K. Batchelor and I. Proudman, "The large-scale structure of homogeneous turbulence," Phil. Trans. Roy. Soc. London A **248,** 369–405 (1956).

[43] W. D. McComb, "A theory of time-dependent, isotropic turublence," J. Phys. A: Math. Gen. **11,** 613–632 (1978).

[44] W. D. McComb and V. Shanmugasundaram, "Numerical calculation of decaying isotropic turbulence using the LET theory," J. Fluid Mech. **143,** 95–123 (1984).

[45] W. D. McComb, V. Shanmugasundaram, and P. Hutchinson, "Velocity-derivative skewness and two-time velocity correlations of isotropic turbulence as predicted by the LET theory," J. Fluid Mech. **208,** 91–114 (1989).

[46] W. D. McComb, M. J. Filipiak, and V. Shanmugasundaram, "Rederivation and further assessment of the LET theory of isotropic turbulence, as applied to passive scalar convection," J. Fluid Mech. **245,** 279–300 (1992).

[47] R. H. Kraichnan and J. R. Herring, "A strain-based Lagrangian-history turbulence theory," J. Fluid Mech. **88,** 355–367 (1978).

[48] R. H. Kraichnan, "Isotropic turbulence and inertial range structure," Phys. Fluids **9,** 1728–1752 (1966).

[49] J. R. Herring and R. H. Kraichnan, "A numerical comparison of velocity-based and strain-based Lagrangian-history turbulence approximations," J. Fluid Mech. **91,** 581–597 (1979).

[50] Y. Kaneda, "Inertial range structure of turbulent velocity and scalar fields in a Lagrangian renormalized approximation," Phys. Fluids **29,** 701–708 (1986).

[51] T. Gotoh, Y. Kaneda, and N. Bekki, "Numerical integration of the Lagrangian renormalized approximation," J. Phys. Soc. Japan **57,** 866–880 (1988).

[52] Y. Kaneda, "Lagrangian and Eulerian time correlation in turbulence," Phys. Fluids A **11,** 2835–2845 (1993).

[53] C. W. V. Atta and R. A. Antonia, "Reynolds number dependence of skewness and flatness of turbulent velocity derivatives," Phys. Fluids **23,** 252–257 (1980).

[54] J. A. Domaradzki, "Analysis of energy transfer in direct numerical simulations of isotropic turbulence," Phys. Fluids **31,** 2747–2749 (1988).

[55] J. A. Domaradzki and R. S. Rogallo, "Local energy transfer and nonlocal interactions in homogeneous, isotropic turbulence," Phys. Fluids A **2,** 413–426 (1990).

[56] R. H. Kraichnan, "Inertial-range transfer in two- and three-dimensional turbulence," J. Fluid Mech. **47,** 525–535 (1971).

[57] M. Lesieur and O. Métais, "New trends in large-eddy simulations of turbulence," Annu. Rev. Fluid. Mech. **28,** 45–82 (1996).

[58] R. H. Kraichnan, "Eddy viscosity in two and three dimensions," J. Atoms. Sci. **33,** 1521–1536 (1976).

[59] M. Lesieur and R. Rogallo, "Large-eddy simulation of passive scalar diffusion in isotropic turbulence," Phys. Fluids A **1,** 719–722 (1989).

[60] J. A. Domaradzki, W. Liu, and M. E. Brachet, "An analysis of subgrid-scale interactions in numerically simulated isotropic turbulence," Phys. Fluids A **5,** 1747–1759 (1993).

[61] S. Kida, "Similar solutions in modified cumulant expansion," Phys. Fluids **24,** 604–614 (1981).

[62] M. Lesieur and D. Schertzer, "Amortissement auto similaire d'une turbulence à grand nombre de Reynolds," J. Méc. **17,** 609–646 (1978).

[63] M. Nelkin, "Universality and scaling in fully developed turbulence," Adv. Phys. **43,** 143–181 (1994).

[64] A. M. Obukhov, "Structure of the temperature field in turbulent flows," Isv. Geogr. Geophys. Ser. **13,** 58–69 (1949).

[65] S. Corrsin, "On the spectrum of isotropic temperature fluctuations in an isotropic turbulence," J. Appl. Phys. **22,** 469–473 (1951).

[66] G. K. Batchelor, I. D. Howells, and A. A. Townsend, "Small-scale variation of convected quantities like temperature in turbulent fluid Part 2 The case of large conductivity," J. Fluid Mech. **5,** 134–139 (1959).

[67] G. K. Batchelor, "Small-scale variation of convected quantities like temperature in turbulent fluid Part 1 General discussion and the case of small conductivity," J. Fluid Mech. **5,** 113–133 (1959).

[68] R. M. Kerr, "Higher-order derivative correlations and the alignment of small-scale structures in isotropic numerical turbulence," J. Fluid Mech. **153,** 31–58 (1985).

[69] R. H. Kraichnan, "Small-scale structure of a scalar field convected by turbulence," Phys. Fluids **11,** 945–953 (1968).

[70] R. H. Kraichnan, "Dispersion of particle pairs in homogeneous turbulence," Phys. Fluids **9,** 1937–1943 (1966).

[71] C. H. Gibson, W. T. Ashurst, and A. R. Kerstein, "Mixing of strongly diffusive passive scalars like temperature by turbulence," J. Fluid Mech. **194,** 261–293 (1988).

[72] S. Goto and S. Kida, "Passive scalar spectrum in isotropic turbulence: Prediction by the Lagrangian direct-interaction approximation," Phys. Fluids (1999), (in press).

[73] K. R. Sreenivasan, "The passive scalar spectrum and the Obukhov-Corrsin constant," Phys. Fluids **8,** 189–196 (1996).

[74] H. L. Grant, B. A. Hughes, R. B. Williams, and A. Moillient, "The spectrum of temperature fluctuations in turbulent flow," J. Fluid Mech. **34,** 423–442 (1968).

[75] N. S. Oakey, "Determination of the rate of dissipation of turbulent energy from simultaneous temperature and velocity shear microstructure measurements," J. Phys. Oceanogr. **12,** 256–271 (1982).

[76] J. Chasnov, V. M. Canuto, and R. S. Rogallo, "Turbulence spectrum of a passive temperature field: Results of a numerical simulation," Phys. Fluids **31,** 2065–2067 (1988).

[77] S. Corrsin, "Further generalization of Onsager's cascade model for turbulent spectra," Phys. Fluids **7,** 1156–1159 (1964).

[78] J. P. Clay, Ph.D. thesis, University of California at San Diego, 1973.

[79] C. H. Gibson, "Fine structure of scalar fields mixed by turbulence. II. Spectral theory," Phys. Fluids **11,** 2316–2327 (1968).

[80] R. C. Mjolsness, "Diffusion of a passive scalar at large Prandtl number according to the abridged Lagrangian interaction theory," Phys. Fluids **18,** 1393–1394 (1975).

[81] D. Bogucki, J. A. Domaradzki, and P. K. Yeung, "Direct numerical simulations of passive scalars with $Pr > 1$ advected by turbulent flow," J. Fluid Mech. **343,** 111–130 (1997).

[82] J. Qian, "Turbulent passive scalar field of a small Prandtl number," Phys. Fluids **29,** 3586–3589 (1986).

[83] V. M. Canuto, I. Goldman, and J. Chasnov, "A model for fully developed turbulence," Phys. Fluids **30,** 3391–3418 (1987).

[84] G. Falkovich, "Bottleneck phenomenon in developed turbulence," Phys. Fluids **6,** 1411–1414 (1994).

[85] R. M. Williams and C. A. Paulson, "Microscale temperature and velocity spectra in the atmospheric boundary layer," J. Fluid Mech. **83,** 547–567 (1977).

[86] F. H. Champagne, C. A. Friehe, J. C. LaRue, and J. C. Wyngaard, "Flux measurements, flux estimation techniques, and fine-scale turbulence measurements in the unstable surface layer over land," J. Atomos. Sci. **34,** 515–530 (1977).

[87] R. J. Hill, "Models of the scalar spectrum for turbulent advection," J. Fluid Mech. **88,** 541–662 (1978).

[88] A. Chekhlov and V. Yakhot, "Kolmogorov turbulence in a random-force-driven Burgers equation," Phys. Rev. E **51,** R2739–2742 (1995).

[89] J. M. Burgers, *The nonlinear diffusion equation. Asymptotic solutions and statistical problems* (Reidel, Dordrecht, 1974).

[90] T. Tatsumi, "Theory of homogeneous turbulence," Adv. Appl. Mech. **20,** 39–133 (1980).

[91] S. Goto and S. Kida, "Statistical closure theories and strength of nonlinear couplings," (1999), (in preparation).

[92] R. H. Kraichnan, "Kolmogorov's hypotheses and Eulerian turbulence theory," Phys. Fluids **7,** 1723–1734 (1964).

[93] L. D. Landau and E. M. Lifshitz, *Fluid Mechanics, (second edition)* (Pergamon, Oxford, 1987).

[94] R. A. Antonia, B. R. Satyaprakash, and A. K. M. F. Hussain, "Statistics of fine-scale velocity in turbulent plane and circular jets," J. Fluid Mech. **119,** 55–89 (1982).

[95] F. Anselmet, Y. Gagne, E. J. Hopfinger, and R. A. Antonia, "High-order velocity structure functions in turbulent shear flow," J. Fluid Mech. **140,** 63–89 (1984).

[96] I. Hosokawa and K. Yamamoto, "Fine structure of a directly simulated isotropic turbulence," J. Phys. Soc. Japan **58,** 20–23 (1989).

[97] A. N. Kolmogorov, "A refinement of previous hypotheses concerning the local structure of turbulence in a viscous incompressible fluid at high Reynolds number," J. Fluid Mech. **13,** 82–85 (1962).

[98] B. B. Mandelbrot, "Intermittent turbulence in self-similar cascades: divergence of high moments and dimension of the carrier," J. Fluid Mech. **62,** 331–358 (1974).

[99] S. A. Orszag, "Indeterminacy of the moment problem for intermittent turbulence," Phys. Fluids **13,** 2211–2212 (1970).

[100] S. Kida, "Limitation of log-normal theory of turbulence," J. Phys. Soc. Japan **60,** 477–480 (1991).

[101] S. Kida, "Log-stable distribution and intermittency of turbulence," J. Phys. Soc. Japan **60,** 5–8 (1991).

[102] E. A. Novikov and R. W. Stewart, "The intermittency of turbulence and specrum of energy dissipation," Isv. Akad. Nauk Ser. Geophys. **3,** 408–413 (1964).

[103] U. Frisch, P. L. Sulem, and M. Nelkin, "A simple dynamical model of intermittent fully developed turbulence," J. Fluid Mech. **87,** 719–736 (1978).

[104] G. Parisi and U. Frisch, "On the singularity structure of fully developed turbulence," In *Turbulence and Predictability in Geophysical Fluid Dynamics*, M. Ghil, R. Benzi, and G. Parisi, eds., pp. 84–87 (North-Holland, 1985).

[105] U. Frisch, "From global scaling, a la Kolmogorov, to local multifractal scaling in fully developed turbulence," Proc. Roy. Soc. London A **434,** 89–99 (1991).

[106] C. M. Meneveau and K. R. Sreenivasan, "The multifractal nature of turbulent energy dissipation," J. Fluid Mech. **224,** 429–484 (1991).

[107] Z. She and E. Leveque, "Universal scaling laws in fully developed turbulence," Phys. Rev. Lett. **72,** 336–339 (1994).

[108] B. Dubrulle, "Intermittency in fully developed turbulence: log-Poisson statistics and generalized scale covariance," Phys. Rev. Lett. **73,** 959–962 (1994).

[109] H. Chen, S. Chen, and R. H. Kraichnan, "Probability distribution of a stochastically advected scalar field," Phys. Rev. Lett. **63,** 2657–2660 (1989).

[110] R. H. Kraichnan, "Models of intermittency in hydrodynamic turbulence," Phys. Rev. Lett. **65,** 575–578 (1990).